The Development of a Clinical Trial Protocol and Functional Biomarkers for Age-Related Macular Degeneration

Claire McKeague

A thesis submitted to Cardiff University for the degree of Master of Philosophy

SCHOOL OF OPTOMETRY AND VISION SCIENCES, CARDIFF UNIVERSITY

2014

SUPERVISED BY DR ALISON BINNS & DR TOM MARGRAIN

Summary

Age-related macular degeneration (AMD) is the leading cause of blindness amongst older adults in the developed world. With the predicted rise in the ageing population over the next decades, the prevalence of this debilitating disease will simply continue to increase. The only treatments currently available are for advanced neovascular AMD. The retina is already severely compromised by this stage in disease development. Therefore, there is a pressing need to evaluate potential novel interventions that aim to prevent the development of advanced disease in people with early AMD, to prevent sight loss from occurring. Furthermore, it is necessary to develop tests that are sensitive to subtle changes in visual function in order to evaluate the efficacy of these emerging treatments.

There is a growing body of evidence to suggest that hypoxia contributes to the development of AMD. Hypoxia is most acute at night when the retinal photoreceptors are most metabolically active, due to the demands of the rod dark current. Increasing the light levels at night will cause the oxygen demand, and hence the hypoxia, to be substantially diminished. This leads to the hypothesis that providing low level night time light therapy to people with early AMD may slow disease progression by reducing hypoxia.

In order to evaluate the potential effectiveness of such an intervention, it is necessary to select appropriate outcome measures. The inherent variability of the standard test of visual function, visual acuity, renders it inappropriate for use as a primary outcome measure in proof of concept clinical trials. Therefore, the first aim of this thesis was to evaluate the diagnostic validity and repeatability of alternative functional tests that may be used as biomarkers for early macular disease.

Dark adaptation was evaluated using three stimuli, a spot of 2^o radius and annuli of 7^o and 12^o radii, in 21 healthy adults (on two occasions) and in 11 participants with early AMD. All stimuli were found to be highly diagnostic for early AMD. The spot of 2^o radius provided the best separation between groups with respect to the time constant of cone recovery (area under the ROC curve 0.91). The repeatability of chromatic and flicker thresholds were also assessed in 30 healthy adults. The coefficient of repeatability, expressed as a percentage of the mean threshold, was 17.1% for red-green chromatic thresholds, 31.1% for blue-yellow, 53.4% for 14Hz flicker thresholds, and ranged between 36.4%-53.3% for parameters of dark adaptation. A small learning

effect was found for both chromatic thresholds and the 14-Hz flicker test, indicating that a control group is needed in studies of new therapeutic interventions.

The second aim of this thesis was to develop a protocol for a clinical trial that seeks to determine if low level night time light therapy can prevent the progression of early AMD. The level of retinal illuminance required to suppress the rod dark current, the maximum retinal illuminance which prevents substantial suppression of melatonin secretion, and the most appropriate means of delivering the dose of retinal illumination were evaluated. The final protocol employed an organic LED illuminated light mask, worn during hours of sleep, as the mode of intervention.

In conclusion, this thesis has confirmed that cone dark adaptation is a sensitive functional biomarker for AMD, and that all three functional tests have a good inter-session repeatability. These biomarkers will be validated in the prospective clinical trial of low-level light therapy to confirm their prognostic and predictive capabilities. The proposed trial will also evaluate the effectiveness of the low level night time light therapy, delivered by means of an illuminated light mask, at slowing the progression of early AMD.

Acknowledgements

First and foremost, I give thanks to my Saviour Jesus Christ for giving me the knowledge, understanding and strength to undertake and complete this research project. Having spent two years studying just one aspect of the human eye, I have only begun to scratch the surface in understanding its intricate design, and am in awe of the power and wisdom of God and His amazing creation!

I would also like to express my deepest gratitude to my wonderful supervisors, Dr Alison Binns and Dr Tom Margrain, for their continual guidance and support at all stages of this research project. I am greatly indebted to them for all the time they have devoted to helping me, and feel honoured to have worked with them over the past two years.

I am grateful to all the lovely participants in my studies that have given up their time to provide the data presented in this thesis, with only the promise of a cup of tea and a light at the end of the tunnel!

Thank you to all my friends in room 2.10 for helping me perfect the art of procrastination. Thank you to the Eye Clinic staff for all their help throughout this time. Furthermore, a special thank you to Sue and all the lovely staff in the Optometry building for all their help and support. They put a smile on my face every day!

Lastly, I would like to thank my family for their constant love, support and encouragement over the past two years. Without them, this work would not have been accomplished.

Amazing grace, how sweet the sound
That saved a wretch like me.
I once was lost but now am found,
Was blind but now I see.

Table of Contents

List of Figures

List of Tables

List of Equations

1. Introduction

1.1 General Introduction

Age-related macular degeneration (AMD) is a degenerative disease of the central retina that leads to a progressive loss of central vision. Despite being the leading cause of blindness among older adults in the developed world (Bunce et al. 2010; Klein et al. 2011) and the cause of approximately 50% of registrations as sight impaired or severely sight impaired in the UK (Bunce et al. 2010), treatments are currently limited. Indeed, for the 85% of people suffering from the dry form of the condition, the only 'treatment' is vitamin supplementation and lifestyle modification. Therefore, there is a pressing need to evaluate potential new therapies to prevent the progression of this debilitating disease.

The overall objective of this thesis is to investigate the repeatability and diagnostic validity of functional biomarkers in AMD, and to develop a protocol for a clinical trial investigating the impact of low-level light therapy on disease progression in AMD. The introductory chapter of this thesis will comprise the necessary background information on the structure of the healthy retina, before providing an overview of the epidemiology, pathogenesis and classification of AMD and a detailed review of the literature on the role of hypoxia in the progression of AMD. This will be followed by a literature review of the current biomarkers used to detect the disease and monitor its progression. The next chapters will describe the studies into the repeatability and diagnostic validity of three functional biomarkers. Following this, the development of a clinical trial protocol investigating the impact of light therapy in AMD will be outlined, and a final chapter will summarise the conclusions of the thesis and discuss further work.

1.2 The Healthy Retina

1.2.1 Overview of the Retina

The retina is a thin piece of tissue lining the back of the eyeball that is responsible for the first stage of image processing: here, light energy is converted to an electrical signal by photochemical transduction. This signal then travels to the brain via the optic nerve for further processing. Situated between the choroid and the vitreous humour, the retina

extends from the optic nerve head to the ora serrata. It is composed of a number of distinct layers, including three layers of neuron cell bodies, two synaptic layers and an outer, pigmented layer, as depicted in Figure 1 below.

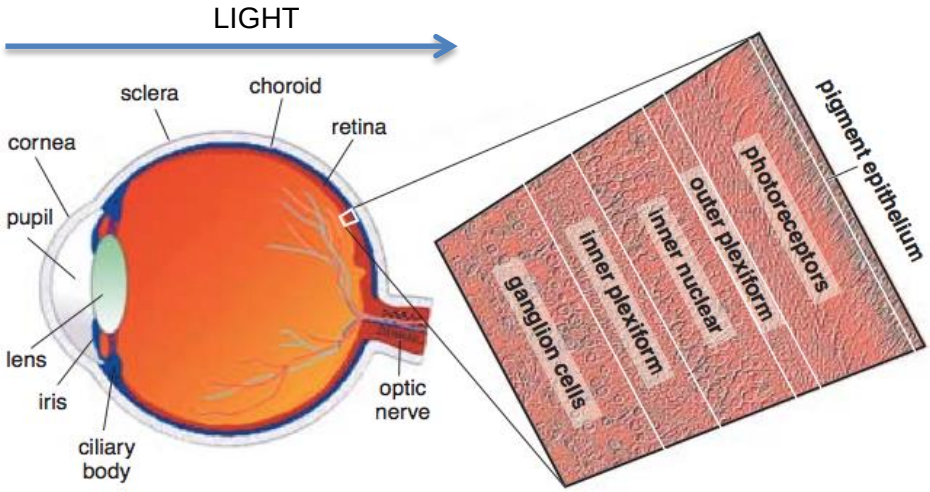

Figure 1. A cross-sectional schematic diagram of a human eye with its various structures (left). A small section of retina is magnified (right), outlining its layers. The photoreceptors lie against a layer of pigmented cells known as the retinal pigment epithelium (Kolb 2003).

Knowledge of the retinal anatomy is vital for a proper understanding of its function and associated pathology. Light is transmitted through the full thickness of the retina to activate the rod and cone photoreceptor cells. Following the absorption of a photon of light by the visual pigment in the photoreceptors, an electrical signal is generated which then stimulates the remaining retinal cells. A schematic of these major cell types in the retina is shown in Figure 2.

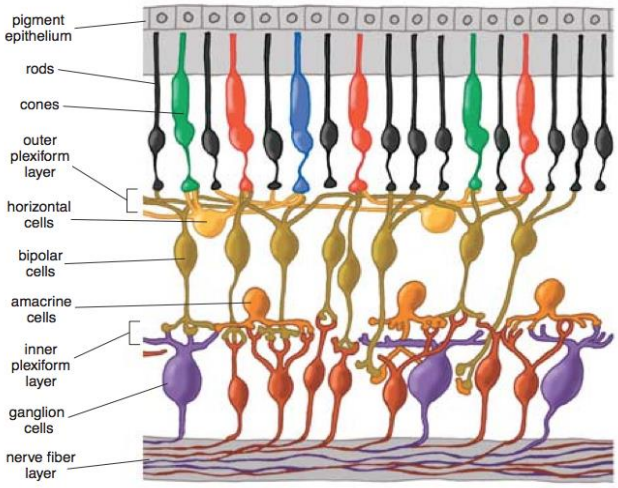

Figure 2. The arrangement of the major cells in the retina. In this rendering, light enters the eye from bottom to top (Kolb 2003).

The first neurophil area is the outer plexiform layer where the rod and cone cells synapse with the vertically orientated bipolar cells, of which there are 11 types, and the horizontally running horizontal cells. The second region of neurophil is the inner plexiform layer, the site where bipolar cells transfer their information to the 20 different types of ganglion cells. Additionally, there are 22 to 30 varieties of amacrine cell present in this region, which integrate and modulate the visual information for the retinal ganglion cells to transmit along the optic nerve to the brain (Kolb 2003). For further information on this subject, the reader is referred to an excellent review by Kolb (2003). AMD is a condition affecting the outer retina and associated structures, targeting the macular region (Ambati et al. 2003). Therefore, the following sections will concentrate on these structures.

1.2.2 Bruch's Membrane

Although Bruch's membrane (BM) is not considered a part of the retina, it is closely attached to it via the basement membrane of the RPE and plays a vital role in normal retinal function. According to Hogan's classification, BM consists of five distinct layers: the RPE basement membrane, the inner collagenous layer, the elastin layer, the outer collagenous layer and the basement membrane of the choriocapillaris (Hogan 1961). The inner and outer collagenous layers are composed of striated collagen fibres, organised in a multi-layered grid-like structure embedded in a number of biomolecules, such as heparin sulphate and chondroitin sulphate (Booij et al. 2010).

In addition to its role in providing physical support for RPE cell adhesion, it also serves as a semi-permeable filtration barrier for metabolic exchange between the choroid and the retina and a diffusion barrier for cell migration (Booij et al. 2010; Guymer et al. 1999). The pentalaminar BM undergoes age-related changes throughout life, including an overall increase in thickness and a reduced capacity to facilitate macromolecular exchange (Moore and Clover 2001) due to a reduction in membrane elasticity, increased hydrophobicity and accumulation of cellular debris (Pauleikhoff et al. 1990; Bird 1992). In particular, the presence of lipid deposits has been shown to play a small but significant role in this decline in the hydraulic conductivity of Bruch's membrane (Sheraidah et al. 1993; Moore and Clover 2001).

1.2.3 The Retinal Pigment Epithelium

The retinal pigment epithelium (RPE), the outermost layer of the retina, forms part of the blood-retinal barrier (Bok 1993; Strauss 2005). It is a single layer of pigmented, hexagonal cells that are connected by tight junctions. The basement membrane of the RPE forms part of Bruch's membrane. Its apical membrane contains numerous microvilli that project towards the neural retina and enclose the photoreceptor outer segment tips. An adhesion between the RPE and the retina is provided by a variety of factors such as osmotic pressure and water transport (Kita and Marmor 1992), and adhesive forces from extracellular material in the sub-retinal space (Hageman et al. 1995).

The RPE has a number of essential functions, including:

1) **Absorption of Light.** The melanin-containing melanosomes in the RPE help to prevent light scatter, improving visual acuity (Strauss 2005).
2) **Transport of Metabolites and Ions.** The RPE transports ions and water from the subretinal space to the blood (Hamann 2002) and so has the structural characteristics of an ion transporting epithelium. Gap junctions between cells enable the controlled transport of nutrients and ions between photoreceptors and choriocapillaris, which also prevents retinal oedema (Steinberg 1985; Miller and Steinberg 1977; Hamann 2002).
3) **Blood-retinal Barrier.** The zonular adherens and zonular occludens that bind adjacent RPE cells together allow the RPE to act as a blood-retinal barrier between the choriocapillaris and the neural retina (Steinberg 1985).
4) **Phagocytosis of Photoreceptor Outer Membranes.** The RPE diurnally regulates the phagocytosis of the tips of the photoreceptor outer segments to maintain vision. With increasing age, incomplete digestion of these tips leads to an accumulation of lipofuscin in the RPE (Beatty et al. 2000).
5) **Photopigment Regeneration**. The RPE is the site of the re-isomerisation of 11-*cis* retinal following phototransduction (Lamb and Pugh 2004).
6) **Immune Privilege**. The RPE aids immune privilege by the tight barrier separating the neural retina from the blood circulation, and by secreting immune modulatory factors, such as complement factor H, to activate or disable the eye's immune response (Kim et al. 2009).

1.2.4 Photoreceptor cells

The human retina contains four types of photoreceptor cells, which have been designed to absorb photons of light and convert them into nervous impulses i.e. to intitate phototransduction. The rod photoreceptors responsible for scotopic vision are sensitive to low levels of illumination, whereas cone photoreceptors, which mediate photopic vision, optimally function at higher illumination levels. There are three classes of cones, each containing a different photopigment: short-wavelength sensitive cones (S-cones) contain cyanolabe, middle-wavelength sensitive cones (M-cones) contain chlorolabe and long-wavelength sensitive cones (L-cones) contain erythrolabe. Normal colour vision is dependent upon these three cone mechanisms (Schwartz 2009).

The relative density of the different classes of photoreceptors varies with retinal eccentricity. Cone density peaks at the fovea (199,000 cells/mm) and falls rapidly with increasing eccentricity (Figure 3). In contrast, rod photoreceptors are absent from the fovea and peak in density (150,000 cells/mm) between 12-18 degrees from fixation. However, the total number of rods far exceeds that of cones. Indeed, the average human retina contains 92 millions rod photoreceptors, as opposed to only 4.6 million cones (Curcio et al. 1990).

A further distinction between these two classes of cells is their physical structure. Cones are so-called because of their conical shape, with their inner and outer segments pointing towards the retinal pigment epithelium. Rods, on the other hand, have slim rod-shaped bodies with thinner outer and inner segments than cones, except at the fovea (Anderson and Fisher 1976). Both classes of cell, however, do consist of the same basic elements: an outer segment containing stacks of membranous discs in which the photopigment is embedded; an inner segment containing mitochondria, a cell body containing the nucleus and a synaptic terminal where the cell can transmit information to other neurons (Young 1971).

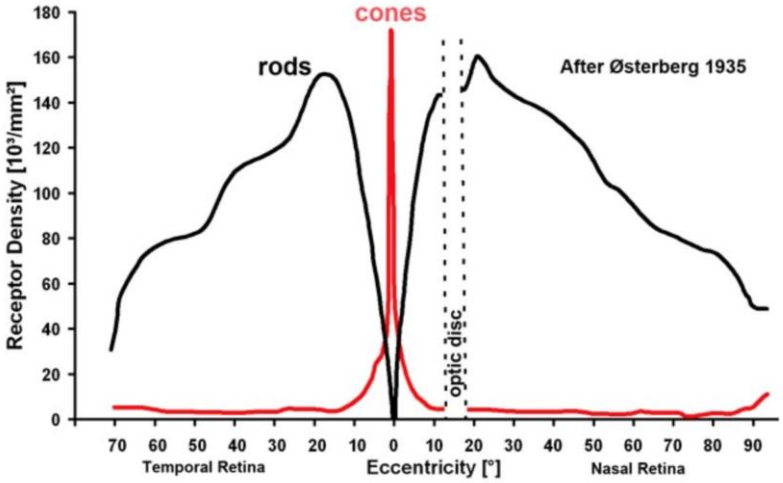

Figure 3. Graph illustrating the rod and cone densities as a function of retinal eccentricity (Kalloniatis and Luu 2011a).

1.2.5 The Macula

The macula is the central region of the retina that is responsible for high acuity vision. It is often called the macula lutea, or yellow spot, due to its high density of yellow xanthophylls such as lutein and zeazanthin, which comprise macular pigment (Snodderly 1995). Macular pigment peaks in concentration in the central 1-2 degrees of the fovea, and rapidly declines to an insignificant level at 5-10 degrees retinal eccentricity (Delori et al. 2006). This pigment is thought to protect the macula by filtering out short wavelength light and by acting as an antioxidant (Snodderly 1995).

Located in the midst of the vascular arcades, the macula is approximately 6mm in diameter, which equates to 15-20 degrees of visual angle (Figure 4) (Hendrickson 2005). In anatomical terms, it is defined as the retinal area where the retinal ganglion cell layer is more than 1 cell thick. The macula can be further organised into four anatomical regions, named in relation to the fovea centralis, as depicted in (Polyak 1941). The foveola, which is the central avascular zone, contains the highest volume of cone photoreceptors and midget pathways, and corresponds to the visual axis (Provis et al. 2005). The foveola is also devoid of all short-wavelength sensitive cones, rods, ganglion cells and inner nuclear layer cells (Neelam et al. 2009). These second and third order neurones are displaced to the surrounding macula by the elongated cone axons which form the fibres of Henle, and are the principal location of macular pigment accumulation. The displaced foveal bipolar cells and retinal ganglion cells result in a

thickening of the macula relative to other retinal locations. The surrounding fovea represents a transition zone between the cone-dominated fovea and the periphery. The perifovea, like the peripheral retina, contain a high density of blood vessels and a preponderance of rod photoreceptors (rod: cone ratio approximately 33-130:1); whereas the parafovea has little retinal vasculature, a large number of ganglion cells and approximately a 4:1 ratio of rods to cones (Provis et al. 2005).

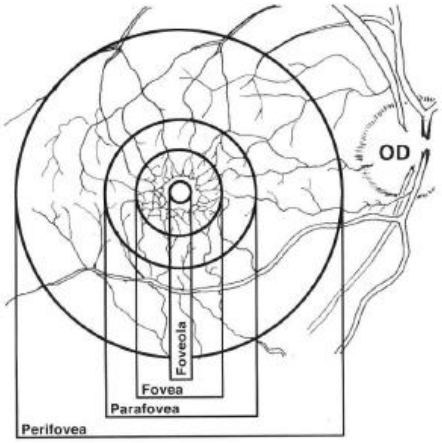

Figure 4. Diagrammatic representation of the human macula showing the anatomical divisions centred on the fovea centralis, or foveola (Hendrickson 2005).

1.2.6 Blood Supply to the Retina

Oxygen is delivered to the retina via two circulatory systems, as shown in Figure 5. The central retinal artery provides oxygen to the inner two thirds of the retina, including the bipolar and ganglion cell layers, and has lower blood flow with higher oxygen extraction ratio than the choroid (Alm and Bill 1973). In contrast to the outer retina, inner retinal blood flow is autoregulated by the secretion of vasoactive factors, such as nitric oxide and prostaglandins, by the vascular endothelium and retinal tissue encapsulating the arteriolar cell wall. This allows a tissue to adjust its blood flow in accordance with its metabolic requirements.

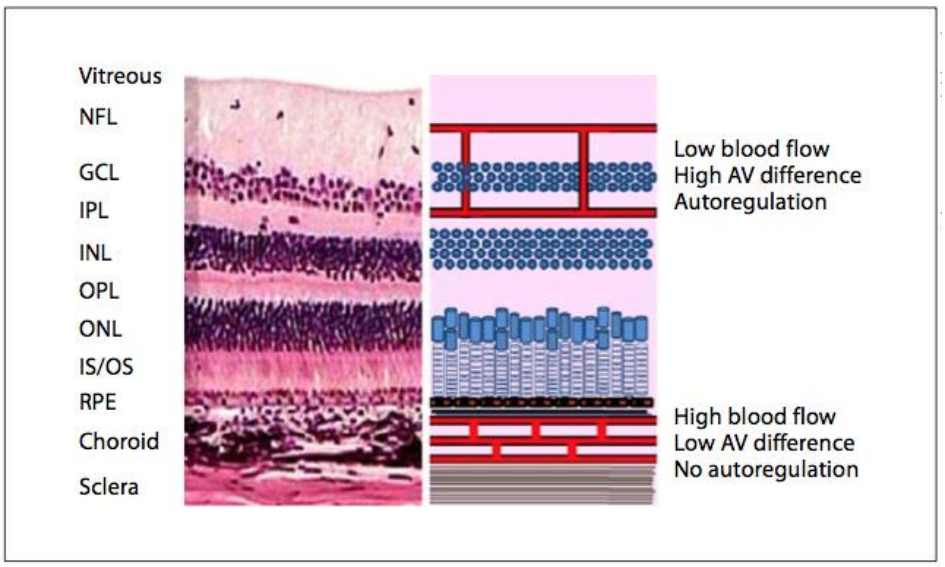

Figure 5. Histology of the human retina and its assciated blood supply. IS/OS = Inner and outer segments; ONL = outer nuclear layer; OPL = outer plexiform layer; INL = inner nuclear layer; IPL = inner plexiform layer; GCL = ganglion cell layer; NFL = nerve fibre layer (Lange and Bainbridge 2012).

The choroidal vasculature supplies the outer retina, which includes the retinal pigment epithelium and photoreceptor layer, and also the avascular macular region (Hendrickson 2005). It has a 20-fold greater blood flow than the inner retina and has a low oxygen extraction ratio, leading to a low arteriovenous difference and increased reserve of oxygen transport (Alm and Bill 1970; Alm and Bill 1972). The choroidal circulation shows less evidence of oxygen regulation than the inner retinal vasculature (Bosch et al. 2009).

In order for cells to function at their best, a tightly regulated environment is necessary. The blood-retinal barrier, with its specialised tissues and extracellular materials, is able to rapidly respond to changes in extracellular conditions to maintain homeostasis and control transport between retinal structures. The inner blood retinal barrier is mediated by the endothelium with its associated pericytes and glial cells. The outer barrier is composed of the endothelium of the choriocapillaris, Bruch's membrane and the RPE (Pournaras et al. 2008).

1.3 Age-Related Macular Degeneration

1.3.1 Background

Age-related macular degeneration (AMD) is a degenerative condition of the macula characterized by dysfunction and death of photoreceptors, which can cause progressive loss of central vision in one or both eyes. This occurs either due to extensive atrophy of the macular area, or because of scarring secondary to a neovascular event.

AMD is the leading cause of visual impairment in the UK. Figures from 2007-2008 estimate that degeneration of the macula and posterior pole account for 58.6% of severe sight impairment (SSI) and 57.2% of sight impairment (SI) certifications in England and Wales (Bunce et al. 2010). Whilst certification figures provide an insight into the proportion of visual impairment in the UK attributable to AMD, they almost certainly underestimate the actual prevalence of the condition since these data exclude those who choose not to be registered and those who are deemed ineligible for certification by the ophthalmologist. A Bayesian meta-analysis of 31 UK population studies from 2007-2009 with a total sample of 57,173 estimated the overall prevalence of late AMD in the UK to be 2.4% in the population aged over 50 years and 12.2% in those aged over 80 years. Furthermore, 71,000 new cases of late AMD were estimated to occur per year (Owen et al. 2012). Similar trends to this are seen in the rest of the developed world. In the United States, AMD has been reported to affect 11.1% of the population over 60 years (Klein et al. 2011) and is the estimated cause of 22.9% of low vision and 54.4% of blindness among white persons (Congdon et al. 2004).

Given the prediction by the Office for National Statistics of a 32% increase in the population of pensionable age, with the number aged over 85 more than doubling to 3.3m by 2033, the prevalence of AMD and its resultant morbidity will continue to escalate (Office for National Statistics 2009). Advanced AMD is not only associated with visual loss, but also depression, social isolation and falls (Dargent-Molina et al. 1996; Margrain et al. 2012). Furthermore, it is a significant financial burden on the NHS, costing the British economy between £1.2B and £3.7B p.a. (Access Economics 2009; Cruess et al. 2008). Given this massive socio-economic burden, there is a great necessity to evaluate potential new therapeutic interventions to prevent the progression of early AMD to the advanced form in which vision is threatened.

1.3.2 Clinical Classification

Practitioners and patients commonly refer to macular degenerative changes as being either dry or wet. The former signifies the absence of neovascularisation, and can either indicate early AMD or the advanced, atrophic form of the disease known as geographic atrophy (GA), as depicted in Figure 6. Wet, or neovascular AMD (nAMD), occurs following an ingrowth of new blood vessels from the choriocapillaris, which penetrate Bruch's membrane to proliferate underneath the RPE and/or the retina. The resultant haemorrhages, exudates, or RPE detachments lead to a rapid reduction and distortion in vision. Neovascular AMD accounts for approximately 10-15% of the total AMD population (Bhutto and Lutty 2012).

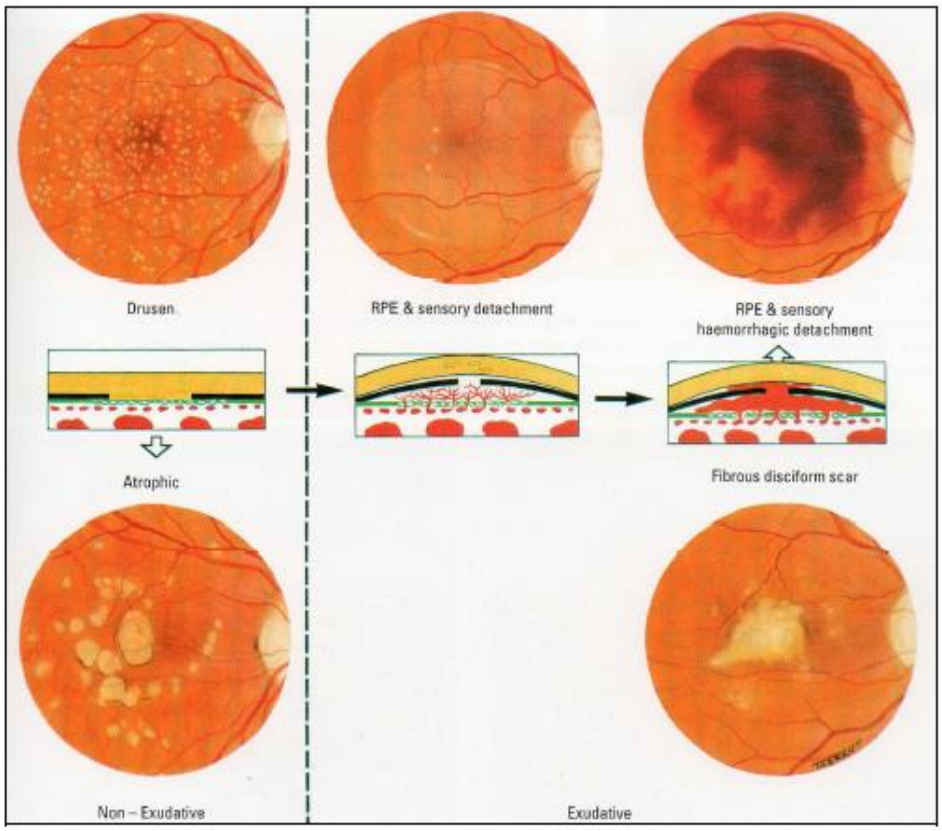

Figure 6. Diagrammatic representation of early AMD (Left, top), geographic atrophy (Left, bottom) and neovascular AMD (Right) (Kanski, 2003).

1.3.3 Clinical features of AMD

1.3.3.1 Drusen

Drusen are deposits of extracellular material that accumulate between the RPE and the

inner collagenous layer of Bruch's membrane (Johnson et al. 2003). They vary greatly in terms of size, number, shape, elevation and distinctness (Kanski and Bowling 2011). Although drusen are the first clinically detectable funduscopic sign of AMD, they can also be found in healthy retinas. Those drusen associated with AMD can be divided into two main phenotypes, hard and soft (Figure 7).

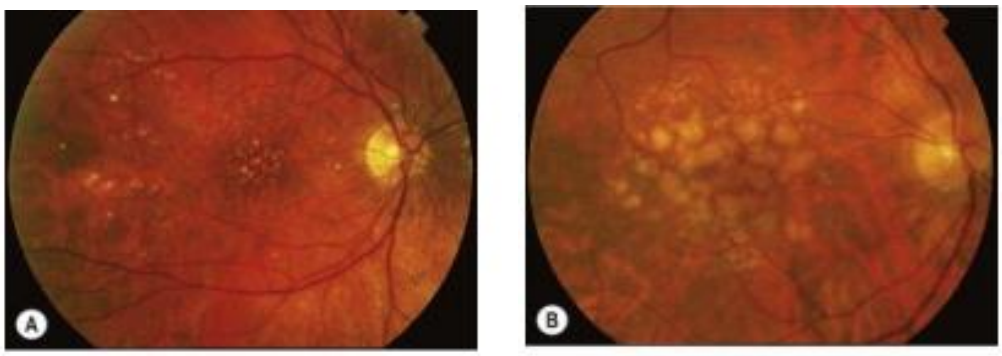

Figure 7. Drusen. Hard drusen (A), Soft drusen (B). (Kanski 2011).

Hard drusen are small (≤63μm), round, discrete yellow-white deposits associated with local RPE dysfunction. Although they are not considered to be indicative of AMD in isolation (Bird et al. 1995), large numbers (8 or more) of hard drusen are associated with an increased risk of developing both soft drusen and pigmentary abnormalities (Klein et al. 2002). Soft drusen are larger with indistinct margins, and may enlarge and coalesce to form confluent drusen, a common precursor to the development of advanced AMD (Holz et al. 1994). Unlike with hard drusen, the presence of soft drusen alone is indicative of AMD (Bird et al. 1995; Davis et al. 2005; Ferris et al. 2005).

1.3.3.2 Pigmentary abnormalities

Another characteristic indication of AMD is the presence of focal regions of RPE hypo- or hyperpigmentation (AREDS 2001b). Focal hyperpigmentation is an area of pigment clumping, due to an increase in melanin concentration in the RPE cells (Bressler et al. 1994). Focal hypopigmentation may be caused by RPE atrophy, RPE thinning or a reduction in melanin concentration in RPE cells. Eyes with these retinal pigmentary abnormalities are more at risk of developing advanced AMD over time compared to eyes without these lesions (Klein et al. 2002; Ferris et al. 2005).

1.3.3.3 Geographic Atrophy

Geographic atrophy is a sharply delineated area of partial or complete depigmentation of the RPE of at least 175μm in diameter, often with exposure of the underlying

choroidal vasculature (Bird et al. 1995; AREDS 2001b). The atrophy often begins near, but not in, the foveal region, thus sparing the central vision. Over time, foveal atrophy develops and the patient must take up eccentric fixation to view objects of interest (Sarks et al. 1988; Sunness et al. 2008).

1.3.3.4 Choroidal neovascularisation (CNV)

Neovascular AMD is caused by choroidal neovascularisation (CNV) originating from the choriocapillaris that grows through defects in Bruch's membrane. The new vessels either remain in the sub-RPE space ("occult" CNV) or may extend anteriorly into the subretinal space ("classic" CNV) (Roth et al. 2004). This neovascularisation is thought to be due to a local imbalance of growth factors such as VEGF-A, which stimulate the inward growth of blood vessels from the choroid. If left untreated, it will lead to the formation of a fibrous disciform scar at the fovea with permanent loss of central vision (Penfold et al. 2001).

1.3.3.5 Retinal pigment epithelial detachment (PED)

Pigment epithelial detachments (PED) are clinically detectable as round, sharply demarcated elevations of the retina. They occur between the inner collagenous layer of Bruch's membrane and the RPE basal lamina, and are often associated with CNV (Murphy et al. 1985). They are either inflammatory, ischaemic, idiopathic or degenerative in aetiology, the latter of which is associated with AMD (Zayit-Soudry et al. 2007). The three types of PED that occur in AMD (serous, fibrovascular and drusenoid) can be distinguished using fluorescein angiography (Pauleikhoff et al. 2002). Although PEDs may spontaneously resolve, the course is variable and they can potentially lead to detachment of the sensory retina, RPE tear formation or geographic atrophy (Pauleikhoff et al. 2002).

1.3.4 Grading scales for severity of AMD

A number of grading systems have been developed to describe and characterise AMD-associated lesions in epidemiologic and clinical studies. In 1980, the Framingham Eye Study relied solely on ophthalmological opinion and visual acuity to rank disease severity (Milton 1979). Later, the 'Wisconsin Age-Related Maculopathy Grading System' (Klein et al. 1991) was developed as an observer-based, photographic grading method for the Beaver Dam study, a large population-based cohort study examining the 15-year incidence and progression of AMD (Klein et al. 2007). This formed the basis

for the standardised 'International Classification and Grading System' (Bird et al. 1995) and the 'Age-related Eye Disease Study System' (AREDS 2001b; Davis et al. 2005; Ferris et al. 2005), the two most commonly used grading scales to date. They both classify AMD on the basis of fundus appearance alone, as assessed by stereo photography. A summary of the diagnostic criteria used in the former is outlined in Table 1 below.

AMD Status	Diagnostic Criteria
Early AMD/ ARM	Soft drusen (≥63μm) with or without associated hyperpigmentation or hypopigmentation of the RPE
Advanced dry AMD	Area of geographic atrophy >175μm in diameter
Advanced wet AMD	At least one of the following: • RPE detachment • SubRPE/ subretinal neovascular membrane • Subretinal haemmhorage • Hard exudates • Disciform scar

Table 1. AMD Classification according to the International Classification and Grading System (Bird et al. 1995).

The AREDS grading scale outlines 9 sub-classifications of increasing overall severity of non-advanced AMD, including a 6-step drusen area scale and a 5-step pigmentary abnormality scale, based on the risk of developing advanced AMD involving the central macula within 5 years (AREDS 2001b; Davis et al. 2005). A more simplified scale was later developed for use in clinical practice (Ferris et al. 2005). The scoring system assigns to each eye 1 risk factor for the presence of 1 or more large (≥125μm) drusen and 1 risk factor for any pigmentary changes. Risk factors are summed across both eyes, resulting in a 5-step severity scale (0-4) on which the 5-year risk of developing advanced AMD increases progressively: 0 factors, 0.5%; 1 factor, 3%; 2 factors, 12%; 3 factors, 25%; 4 factors, 50%. Two risk factors are assigned when one has advanced AMD one eye.

1.3.5 Risk Factors for the Development of AMD

AMD is a multifactorial condition involving a complex interaction between both genetic and environmental risk factors. A summary of the main risk factors associated with AMD is presented below. For further information, the reader is referred to excellent reviews by Evans 2001 and Chakravarthy et al. 2010.

1.3.5.1 Age

Given that it is a disease of the ageing eye, it is not surprising that the predominant risk factor for the development and progression of AMD is increasing age (Evans 2001). In a 10-year study of the incidence and progression of AMD, persons aged 75 or older were 5.2 times more likely to develop early AMD than persons aged 43 to 54 years (Klein et al. 2002).

1.3.5.2 Smoking

There is strong evidence to suggest a causal relationship between current smoking and the progression of AMD (Thornton et al. 2005; Khan et al. 2006; Klein et al. 2008b; Cong et al. 2008; Chakravarthy et al. 2010). Indeed, those who currently smoke have up to five times greater chance of developing AMD compared with a non-smoker (Smith et al. 1996), which increases with increased consumption of cigarettes and number of years of smoking (Khan et al. 2006). It has been calculated that approximately one quarter of AMD cases may be attributable to cigarette smoking in persons over 69 years of age (Kelly et al. 2004). Several studies have examined the reversibility of the damage caused by smoking. A systematic review of 11 studies carried out a pooled analysis, and determined that ex-smokers had only a slightly increased risk of developing AMD compared with never-smokers, which was greater for those who smoked more than 25 cigarettes a day (Thornton et al. 2005).

1.3.5.3 Genetics

Current research suggests that there may be a strong genetic factor in the pathogenesis of AMD. Indeed, people with a family history of AMD are at increased risk of developing the disease (Heiba et al. 1994; Smith et al. 1998). It has been estimated that siblings of an affected person have an almost 20 times greater risk of developing AMD compared to a control sibling (Silvestri et al. 1994). In addition, a US study of 840 elderly male twins found that genetic factors contributed to between 46% and 71% of

the variation in disease severity (Seddon et al. 2005). Studies of twins have shown a greater concordance for AMD in monozygotic (identical) than dizygotic (non-identical) twins (Hammond et al. 2002).

Genetic factors, mainly in the complement factor H (CFH) gene and on the 10q26 locus are now thought to be reliable biomarkers to characterise the risk of AMD onset (Leveziel et al. 2011). Certainly, the development of AMD has been linked to polymorphisms on chromosome 1 of CFH (Haines et al. 2005), complement 2 (C2) (Gold et al. 2006), complement factor B (CFB) (Gold et al. 2006), complement 3 (C3) (Maller et al. 2007) and complement factor H-related gene (CFHR1 and CFHR3) (Spencer et al. 2008). Additionally, there is thought to be an association between the development of wet AMD and polymorphisms on chromosome 10 in the Age-Related Maculopathy Susceptibility 2 (ARMS2) and the HTR1A serine peptidase 1 (HTRA1) genes (Edwards et al. 2005; DeWan et al. 2006). These genetic factors lead to varying degrees of susceptibility to the development of AMD, which is influenced by modifiable environmental factors (Seddon 2013).

1.3.5.4 Race

A number of studies have demonstrated that white people have a greater risk of development and progression of AMD than black people (Klein et al. 2006; Klein 2011; Klein et al. 2011). For example, a population-based study involving 6176 older adults determined the prevalence of AMD to be 2.4% in blacks compared with 5.4% in whites (Klein et al. 2006). Assuming that the data in these studies are an accurate reflection of the wider population, the reasons for these racial differences are not known. It has been speculated that the higher melanin concentration in the RPE of people with darker skin may act as a barrier to oxidative damage to the RPE, Bruch's membrane and choroid (Jampol and Tielsch 1992). An alternative theory is that different ethnic groups have different distributions of protective and deleterious genes such as complement factor H, which may increase susceptibility to disease progression in certain races (Klein et al. 2008a; Klein 2011).

1.3.5.5 Diet

Throughout life, the photoreceptors in the retina are susceptible to oxidative stress caused by long-term light and oxygen exposure. Anti-oxidant vitamin and mineral supplements are thought to minimise the cellular damage caused by these

environmental influences and, hence, lower the risk of AMD progression (Evans 2008). The most robust evidence comes from the Age-Related Eye Disease Study (AREDS), a randomised controlled trial which assigned 4757 participants to one of four treatment groups, receiving: (i) high dose antioxidants only (vitamin C 500mg, vitamin E 400IU and beta-carotene 15mg); (ii) zinc only (zinc oxide 80mg and cupric oxide 2mg); (iii) antioxidants plus zinc; (iv) a placebo tablet (AREDS 2001a; Chew et al. 2009). The results demonstrated a 25% reduction in the risk of progression to advanced AMD in participants with extensive intermediate drusen, large drusen or advanced unilateral AMD who were taking the antioxidant plus zinc formulation. Therefore, they suggested that AREDS-type supplements should be recommended to patients at a high risk of developing advanced AMD.

More recently, the National Institute of Health commissioned the Age-Related Eye Disease Study 2 (AREDS2), to determine the effect of lutein, zeaxanthin and the omega-3 polyunsaturated fatty acids (docosahexaenoic acid, DHA, and eicosapentaenoic acid, EPA) on the risk of developing advanced AMD (AREDS2 2013). Docosahexaenoic acid (DHA) is a long-chain omega-3 fatty acid present in photoreceptor outer segments, and is not synthesised by the human body (Krishnadev et al. 2010). EPA may have the potential to affect signalling molecules implicated in abnormal retinal neovascularisation (SanGiovanni and Chew 2005). Since DHA and other fatty acids are thought to help prevent AMD-related oxidative and inflammatory damage, it has been postulated that a deficiency in this nutrient is related to the development of AMD (SanGiovanni and Chew 2005). Indeed, in a 10-year longitudinal study of 2454 participants, one serving of fish every week was associated with a reduction in the risk of developing early AMD (Tan et al. 2009). In a separate study, the 12-year incidence of wet AMD in moderate to high risk individuals was found to be lowest for those who reported the highest intake of omega-3 fatty acids (SanGiovanni et al. 2009). The AREDS 2 trial, however, found that omega-3 fatty acid supplementation had no significant effect on disease progression (AREDS2 2013)

Macular pigment is comprised of the antioxidant carotenoids lutein, zeaxanthin and meso-zeaxanthin, which play a critical role in protecting the retina from the harmful effects of short wavelength light and are obtained solely from dietary sources such as green, leafy vegetables (Ahmed et al. 2005). Indeed, there is evidence to suggest that a diet rich in these nutrients may reduce the risk of developing AMD (Tan et al. 2008).

The AREDS group tried adding the xanthophylls lutein and zeaxanthin to their original formulation as part of the AREDS 2 trial. Despite the primary analysis showing no evidence of an improved overall effect, those individuals with the lowest levels of serum carotenoids at baseline did show a significant reduction in rate of progression when xanthophylls were added to the formula. Another notable finding of the AREDS 2 study was that the effectiveness of the supplement was not reduced when beta carotene was removed, which is important as beta-carotene may increase the risk of lung cancer among current smokers (AREDS2 2013). Hence the authors of AREDS 2 recommend the substitution of beta carotene for lutein and zeaxanthin in the supplement.

The AREDS 1 and 2 supplements are the only nutritional supplements which have been shown in robust randomized controlled trials to reduce the risk of progression of AMD. It should be noted, however, that a systematic review by the Cochrane Collaboration indicated that individuals taking vitamin E and beta carotene supplementation may be at an increased risk of mortality (Evans and Lawrenson 2012).

Other dietary factors which have been implicated in the increased risk of development of AMD include high saturated fat intake (Mares-Perlman et al. 1995) and alcohol consumption (Cho et al. 2000; Ritter et al. 1995). However, the evidence is currently inconclusive.

1.3.5.6 General Health

A recent meta-analysis of the clinical risk factors for AMD found that in case control studies the risk of developing late AMD is doubled in individuals with cardiovascular disease (OR 2.20; 95% CI 1.48 – 3.26). Other significant risk factors with a lower strength of association (OR $\leq$ 1.5) include BMI, hypertension and plasma fibrinogen (Chakravarthy et al. 2010).

1.3.6 Clinical Assessment of AMD

In optometric practice, AMD is currently diagnosed and monitored using a variety of conventional tests such as visual acuity, ophthalmoscopy, fundus photography and Amsler chart evaluation. Increasingly, optical coherence tomography (OCT) is a technology that is also found in optometric practice. Ophthalmological investigation of

AMD involves more sophisticated imaging technology such as fundus fluorescein angiography (FFA) and fundus autofluorescence (FAF), which are better able to detect subtle structural changes at the macula before they are evident ophthalmoscopically.

1.3.6.1 Fundus Photography

Fundus photography has been widely used to screen for retinal pathological conditions such as diabetic retinopathy (Williamson and Keating 1998) and is the primary imaging technique used to document the presence and severity of AMD in clinical practice (Jain et al. 2006). A recent investigation into the necessity of retinal photography in conjunction with OCT in Lucentis clinics claimed that retinal colour photographs were indispensable for ophthalmologists making informed retreatment decisions (Hibbs et al. 2011). A number of studies have examined the validity of fundus photographs for the identification of various features of AMD. For example, the AREDS study reported that stereoscopic colour fundus photography had moderate to high inter-rater reliability and reproducibility for the identification of features of advanced AMD (AREDS 2001b). However, the authors acknowledged that using fundus photographs without FFA to identify advanced AMD might delay its identification and underestimate its incidence. Nevertheless, high-quality, stereoscopic colour fundus photographs have been the gold standard in monitoring disease severity and progression in major epidemiological studies (AREDS 2001b; AREDS2 2013).

1.3.6.2 Fundus Fluorescein Angiography (FFA)

Fluorescein angiography is the principal method used to image superficial retinal vasculature and identify abnormalities in vascular perfusion, permeability and proliferation, as depicted in Figure 8. Despite the growing importance of OCT imaging, FFA remains the gold standard technique for diagnosing nAMD, with fluorescein leakage being the major sign of neovascular activity (Yannuzzi 2011). The technique involves intravenous injection of yellow fluorescein dye followed by sequential photographs assessing choroidal and retinal blood flow properties (Lim et al. 2012). Hyperfluorescence, i.e. leakage of dye, is an indication of neovascular AMD. This leakage can be described by type (classic, occult or mixed) or location (subfoveal, juxtafoveal or extrafoveal). Classic choroidal neovascularisation (CNV) lesions break through the RPE, whereas occult CNV lesions remain underneath the RPE. For this reason, classic lesions cause more sudden and severe vision loss, but respond better to

treatment with photodynamic therapy (Lim et al. 2012).

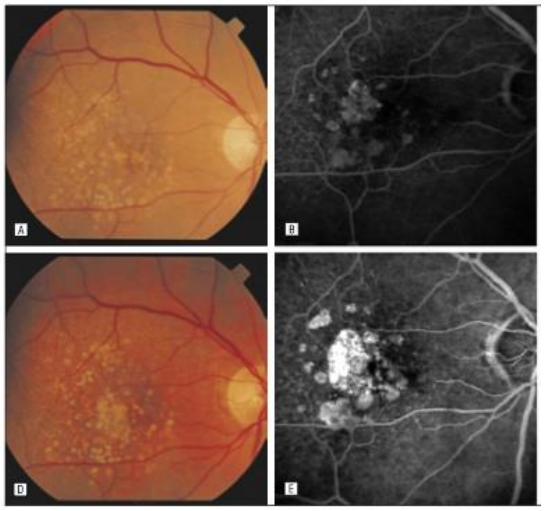

Figure 8. Fundus photograph (A) and fluorescein angiogram (B) of a 76-year-old patient with early age-related macular degeneration, RPE atrophic spots and a central area of prolonged choroidal filling phase. There is an increase of the RPE atrophy in the area of prolonged choroidal filling after 12 months (D and E) (Pauleikhoff et al. 1999).

1.3.6.3 Optical Coherence Tomography (OCT)

During the past two decades, optical coherence tomography (OCT) has been established as a non-invasive, high-resolution, cross-sectional retinal imaging technique (Drexler 2004). The system uses the principle of interferometry, which involves superimposing two light waves to create a 3-D representation of retinal microstructure. Cross-sectional images of the retina (B-scans) are created by performing multiple axial measurements of echo time delay (A-scans). Three-dimensional images can then be acquired by scanning the incident optical beam in a raster pattern, thus producing sequential cross-sectional images (Drexler and Fujimoto 2008). OCT is now a standard clinical device in hospital ophthalmological clinics. However, a prospective analysis of 14 patients revealed that although OCT showed a good sensitivity at detecting active nAMD, specificity was only moderate. Furthermore, since FFA and OCT may not reflect the same structural changes caused by active neovascularisation, the authors concluded that OCT should be used in conjunction with FFA, not as a substitute technique (Henschel et al. 2009). The spectral domain OCT (SD-OCT), with its 40-fold increase in imaging speed and higher resolution compared

with time-domain scanning, is able to capture high-quality B-scans of drusen ultrastructure in vivo in better detail (Khanifar et al. 2008).

The introduction of the SD-OCT has led to the development of algorithms that produce fully automated, quantitative information on the 3-dimensional geometry of the RPE. One particular algorithm has been shown to produce highly reproducible measurements of drusen volume and area (Gregori et al. 2011), which could assess disease progression and be used as a surrogate clinical trial end point (Yehoshua et al. 2011a). See Section 1.6.1 for a detailed discussion of drusen volume analysis.

1.3.6.4 Fundus Autofluorescence (FAF)

Autofluorescent imaging of the retina relies on the stimulated emission of light from predominately lipofuscin molecules found in the RPE (von Rückmann et al. 1997; Solbach et al. 1997). Lipofuscin is a yellow-brown colour and its autofluorescent phosphors emit a typical yellow fluorescence when excited by blue light (Lamb and Simon 2004). It is produced from the oxidative decomposition of fatty acids, proteins and retinoids (Spaide 2003) and is thought to induce RPE apoptosis (Suter et al. 2000). The intensity of the FAF is correlated with the proportion of lipofuscin present in the retina, and hence indicates previous and possible imminent oxidative damage (Spaide 2003). The introduction of the scanning laser ophthalmoscope allows FAF to be imaged over larger retinal areas and minimises autofluorescence from other retinal structures such as the lens (Schmitz-Valckenberg et al. 2009). Abnormalities in FAF have been associated with areas of drusen (von Rückmann et al. 1997; Roth et al. 2004), choroidal neovascularisation (von Rückmann et al. 1997; Spaide 2003), geographic atrophy (von Rückmann et al. 1997; Holz et al. 2001; Holz et al. 2007) and losses in macular sensitivity as assessed by microperimetry (Midena et al. 2007).

1.3.6.5 Visual Acuity (VA)

Visual acuity is the most widely used measure of visual function in both optometric and ophthalmological clinics. However, it is not a strong predictor of visual performance in everyday tasks such as mobility and face recognition (Bullimore et al. 1991; Hassan et al. 2002). Lesions associated with early AMD cause a reduction in VA of approximately two letters or fewer (Klein et al. 1995). Although statistically significant, this level of visual defect is clinically undetectable given that the test-retest variability of Log MAR charts is between one and two lines (Lovie-Kitchin and Brown 2000).

Furthermore, patients with AMD often show considerable between-subject variability in VA measurement because of the heterogeneity of their associated lesions (Sunness et al. 2008). Since VA is relatively unaffected until the later stages of the disease, its diagnostic utility is questionable (Sunness et al. 2008).

1.3.6.6 Amsler Chart

The Amsler chart, a simple square matrix, was developed in 1947 as a screening tool for macular disease (Marmor 2000). Despite being regularly used as a surveillance tool for progression to neovascular AMD, the sensitivity of the Amsler chart has been shown to be as poor as 56% in detecting scotomas (Schuchard 1993). Since symptoms of distortion may precede scotomas, the Amsler chart must be sensitive to detecting new distortion (Crossland and Rubin 2007). In a study of 49 patients with recent nAMD who were regularly observing Amsler charts, just 5 patients had reported Amsler chart distortion as their first visual symptom. However, when the Amsler test was performed on the same patients by an experienced clinician, only 5 of the 49 patients failed to notice any abnormality on the Amsler chart, thus highlighting the importance of thorough patient education (Fine et al. 1986).

Some modifications have been made to the traditional Amsler chart in a bid to improve test sensitivity, such as threshold testing using cross-polarising filters to reduce the grid luminance (Wall and Sadun 1986) and presenting it as a blue grid on a yellow background (Mutlukan 2006). However, no peer-reviewed data on the sensitivity and specificity of these tests is available. The Preferential Hyperacuity Perimeter (PHP) is a computer-based alternative to the Amsler chart that involves a tachistoscopic presentation of a ‘virtual line’ of dots. However, its specificity has been found to be poorer than the Amsler chart (Loewenstein et al. 2003). A scanning laser device and virtual reality display which implements dynamic visual noise (Plummer et al. 2000), is reported to have a sensitivity and specificity of 82% and 100% respectively for the detection of AMD (Freeman et al. 2004). The ForseeHome device, which uses hyperacuity techniques and telemonitoring, has recently been shown in a randomised, controlled trial of 1997 participants to increase the likelihood of better VA after anti-VEGF therapy, compared to standard care (AREDS2-HOME Study Research Group 2014). However, these two devices are expensive and require additional training,

limiting their general applicability amongst the AMD population. Therefore, since the Amsler chart is still an inexpensive, simple and rudimentary screening tool, it should not be completely disregarded.

1.3.7 Pathogenesis of AMD

The pathogenesis of AMD is complex, multi-factorial and not fully understood at present. The current literature indicates that a number of processes including oxidative stress, choroidal vascular changes, hypoxia and local inflammation all contribute to the development and progression of the disease, as depicted in Figure 9.

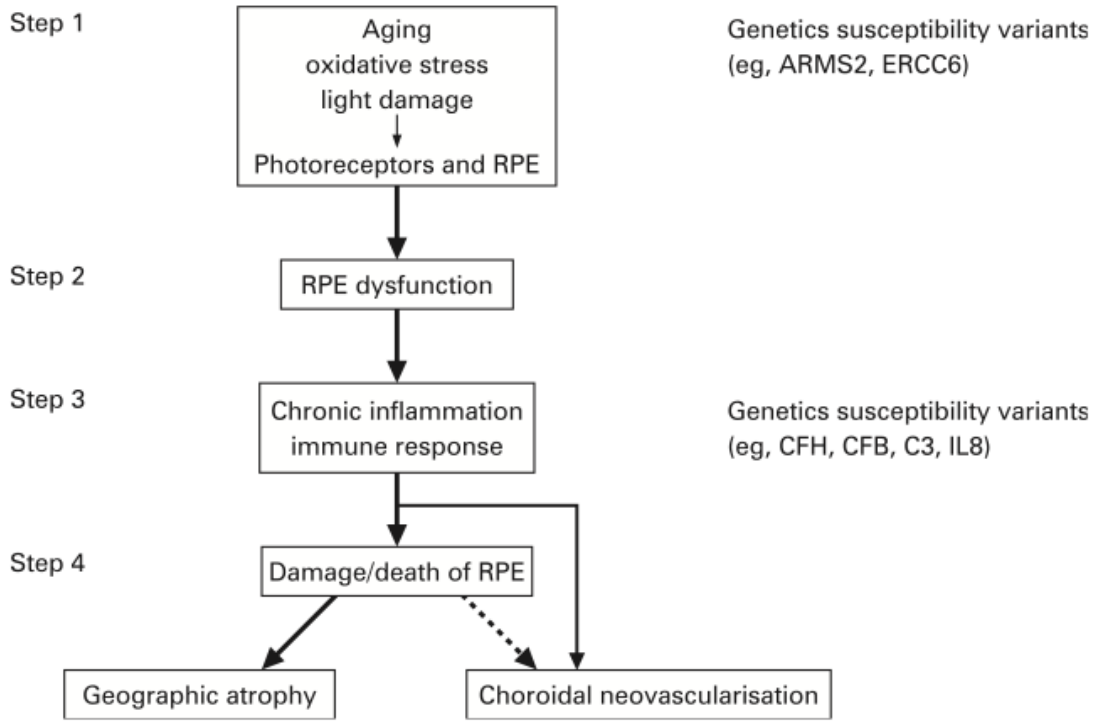

Figure 9. Proposed steps in the pathogenesis of AMD describing the possible relationship between oxidative, inflammatory and genetic factors (Kanda et al. 2008).

Several literature reviews have attempted to describe the disease pathogenesis based upon the current evidence available (Roth et al. 2004; Tezel et al. 2004; Nowak 2006; Ambati and Fowler 2012; Ambati et al. 2013).

1.3.7.1 Oxidative Stress

Both experimental and clinical findings suggest that oxidative stress, i.e. cellular damage caused by reactive oxygen intermediates (ROIs), plays a role in the pathogenesis of AMD (Roth et al. 2004). These ROIs include free radicals and

hydrogen peroxide, and are commonly the by-products of oxygen metabolism. Due to the high level of metabolic activity, the presence of polyunsaturated fatty acids and the high exposure to visible light, the retina is particularly susceptible to oxidative stress (Beatty et al. 2000). A number of factors such as ageing, inflammation, cigarette smoke and air and light pollutants encourage the formation of ROIs which, in turn, cause oxidative damage to cytoplasmic and nuclear components of cells and disrupt the extracellular matrix (Thornton et al. 2005; Zarbin 2004; Khan et al. 2006; Klein et al. 2008b; Cong et al. 2008).

The human retina is protected against the harmful effects of these ROIs by antioxidant enzymes such as catalase, superoxide dismutase and glutathione peroxidase, and carotenoids in the form of macular pigment (Beatty et al. 2000). Macular pigment not only acts as an antioxidant, but also absorbs short wavelength light, a potent mediator of photo-oxidative damage (Beatty et al. 1999). Consequently, the reduction in macular pigment density with ageing further promotes photo-oxidative damage. Recent evidence suggests that increased oxidative stress and reduced anti-oxidant defence may play a synergistic role in the development of AMD (Uğurlu et al. 2013).

Oxidative stress not only leads to disruption of RPE cell junctions (Bailey et al. 2004) and RPE apoptosis (Jiang et al. 2005), but it also may contribute to an accumulation of lipofuscin in the RPE (Roth et al. 2004). Lipofuscin describes a group of autofluorescent lipid granules present in neuronal and non-neuronal tissues. With ageing, there is an accumulation of lipofuscin in RPE cells, which may compromise phagocytosis leading to cell death (Wing et al. 1978; Terman and Brunk 2006). Ma and colleagues have recently demonstrated that accumulation of A2E, a key component of ocular lipofuscin, resulted in microglia activation, reduced microglial protection of photoreceptors and altered complement regulation (Ma et al. 2013). However, Grey and colleagues observed that oxidised A2E does not, in fact, accumulate over time (Grey et al. 2011). Furthermore, it has recently been discovered that there is little correlation between the spatial distribution of A2E and lipofuscin fluorescence in the human RPE (Ablonczy et al. 2013), leading Smith and colleagues to conclude that A2E does not play a significant role in the development of AMD (Smith et al. 2013). However, it has been found that the oxidised A2E bisretinoids degrade into smaller, more damaging fragments such as methylglyoxal (Wu et al. 2010). Therefore, lower A2E levels may

be the result of greater lipofuscin photo-oxidation in the central RPE, and so A2E could still be a contributing factor in the pathogenesis of AMD (Sparrow et al. 2013).

Since the RPE plays a vital role in metabolic and supportive functions for the photoreceptor cells, an impairment in RPE function could lead to the development of advanced AMD (Sparrow and Boulton 2005). There is a range of evidence consistent with this theory. Smoking, the chief modifiable risk factor for the development of AMD, is known to aggravate oxidative stress (Khan et al. 2006; Espinosa-Heidmann et al. 2006; Khandhadia and Lotery 2010). Furthermore, antioxidant supplementation has been shown to reduce the development of AMD (AREDS 2001a; Ho et al. 2011; AREDS2 2013). It has also been shown that patients with AMD have a higher level of systemic homocysteine, an amino acid that oxidises rapidly to produce ROIs (Rochtchina et al. 2007). RPE lipofuscin molecules, detected in vivo with fundus autofluorescence (FAF), have been linked topographically to regions of geographic atrophy (Delori et al. 1995). Several studies have suggested that increased autofluorescence may precede the development or progression of RPE atrophy (Holz et al. 2001; Schmitz-Valckenberg et al. 2006; Holz et al. 2007). However, Hwang and colleagues found no correlation between the area of geographic atrophy enlargement and the area of increased FAF (Hwang et al. 2006). Whilst the exact locations may not correspond, it does appear to be the case that an overall increase in the amount of FAF relates to the rate of geographic atrophy progression (Bearelly 2011), and may be used in future to predict the rate of progression of geographic atrophy.

1.3.7.2 Inflammation and the Immune Response

Inflammation was first implicated in the pathophysiology of AMD from the discovery of immune response proteins present in drusen in post-mortem eyes from people with AMD (Hageman 2001). These and other inflammatory cells may cause microvascular assault through the release of oxidants and proteolytic enzymes that damage Bruch's membrane. Subsequent genetic studies discovered statistically significant correlations between AMD and complement pathway polymorphisms in genes such as CFH (Edwards et al. 2005; Seddon et al. 2007; Despriet et al. 2009). The trigger for this immune response appears to be the cellular damage caused by age-related changes together with oxidative stress (Kanda et al. 2008). The cellular debris produced by compromised RPE cells is then thought to generate a pro-inflammatory signal, up-

regulating cytokines and pro-inflammatory mediators and activating the complement cascade (Roth et al. 2004). Genetic susceptibility variants modulating this inflammatory process may consequently determine the clinical presentation of the disease. For example, genetic polymorphisms in the CFH gene and other complement-related genes have been associated with the development and progression of AMD, altering the cellular response of the retina to insult (Bergeron-Sawitzke et al. 2009; Farwick et al. 2009; van de Ven et al. 2013; Yu et al. 2011).

The dysregulation of retinal microglial cells and their interaction with macrophages derived from monocytes have been postulated to be involved in the pathogenesis of AMD (Ma et al. 2009; Raoul et al. 2010). These microglia are the immune cells of the retina, playing an important role in neuronal protection and tissue regeneration (Langmann 2007). The accumulation of debris in the retina can lead to continuous activation of the microglial cells, leading to the secretion of pro-inflammatory cytokines and chemokines (Langmann 2007). Recently, increased expression of the membrane protein CD200, a regulator of microglial activity, has been found in eyes with wet AMD (Singh et al. 2013). This is surprising, and led the authors to suggest that despite increased expression of CD200, the mechanisms controlling the retinal microglia fail to inhibit the inflammatory response in eyes with wet AMD. Altered regulation of the immune response could play an important role in AMD pathogenesis, and further research needs to be carried out to determine the mechanisms responsible for retinal microglial dysregulation. Despite the evidence showing that inflammatory cells are present in areas of Bruch's membrane damage, RPE atrophy and CNV lesions in AMD, it is still not certain whether they play a causative or protective role (Ozaki et al. 2014). For comprehensive reviews of the evidence for immunological pathogenesis, the reader is referred to Ambati et al. (2013) and Ozaki et al. (2014).

1.3.7.3 Hypoxia

Normal choroidal circulation is upheld by an equilibrium between pro-angiogenic (e.g. VEGF) and anti-angiogenic (e.g. PEDF) growth factors. However, when the retina is in a hypoxic state, it triggers the upregulation of VEGF (Aiello et al. 1995; Blaauwgeers et al. 1999), thus stimulating choroidal angiogenesis. The evidence for this is largely based on signals for the overproduction of VEGF from hypoxia-inducible factors (HIF-

1α and HIF-2α) which have been found in active CNV lesions (Inoue et al. 2007; Sheridan et al. 2009).

It has been found that the choroidal circulation in the healthy retina is barely able to meet the oxygen demand in the dark adapted eye (Wangsa-Wirawan and Linsenmeier 2003). Furthermore, the macular choroid is more sensitive to ischaemia due to the numerous watershed zones present there. Therefore, the alterations in choroidal blood flow and changes in Bruch's membrane that occur in AMD are thought to lead to outer retinal hypoxia (Feigl 2009; Stefánsson et al. 2011). For more information on hypoxia and AMD, the reader is referred to section 1.4.

1.3.8 Management

The current management for patients with early AMD involves advising on lifestyle changes, for example, cessation of smoking, adopting a healthy diet and the consumption of nutritional supplements (see sections 1.3.5.2 and 1.3.5.5 for details). These changes may reduce AMD progression, but there are currently no treatments for early AMD. For those patients with progressive central visual loss resulting from dry, atrophic changes, the only management is the provision of low vision aids. Therefore, there is an urgent need to evaluate potential new interventions. At present, the medical treatments available for AMD target the neovascular form of the disease.

1.3.8.2 Laser photocoagulation

In thermal laser photocoagulation, a laser beam is used to occlude leaking blood vessels arising from choroidal neovascularisation (Chakravarthy et al. 2006). In the 1980s, the Macular Photocoagulation Studies (MPS) reported a favourable outcome in 20% of eyes with a well-defined extrafoveal CNVM (Macular Photocoagulation Study Group 1991). However, approximately 50% of thermal laser treated eyes had persistent or recurrent CNV within 3 years of treatment. Furthermore, thermal laser damage to the overlying retinal tissue can often lead to significant vision loss (Macular Photocoagulation Study Group 1994). Thus, the treatment should only be considered for small extrafoveal lesions away from the foveal avascular zone (Chakravarthy et al. 2006). This is reflected in the steady decline of patients receiving this therapy for the treatment of CNV. Indeed, between 2006 and 2008, the proportion of newly diagnosed patients with nAMD on the Medicare claims database receiving laser treatment

decreased from 5.5% to 3.2% (Curtis et al. 2012).

1.3.8.3 Photodynamic therapy

Photodynamic therapy (PDT) is a two-stage procedure involving the intravenous administration of verteporfin, a green dye that accumulates within endothelial cells of blood vessels, and subsequent activation of the dye with infrared light using a non-thermal laser (Chakravarthy et al. 2006; Lim et al. 2012). This generates free radicals that damage the CNV endothelium, leading to occlusion of the newly formed vessels (Chakravarthy et al. 2006; Cruess et al. 2009). It is deemed to be superior to laser photocoagulation due to the protection of the overlying retinal surface. Several randomised controlled clinical trials of patients with subfoveal CNV have reported PDT to be a 'successful' treatment option for classic lesions, but was less effective for occult CNV lesions, with success being defined as slowed loss of VA, rather than an improvement in VA (Schmidt-Erfurth et al. 1999; Bressler 2001; Azab et al. 2005; Cruess et al. 2009). The main side-effects reported with the use of PDT include back pain, headaches and photosensitivity (Borodoker et al. 2002). The most serious ocular side effect is a sudden, severe decrease in VA within 7 days of PDT due to choroidal infarction (Klais et al. 2005), which in some causes may be permanent (Axer-Siegel et al. 2004). For this reason, PDT is much less frequently used as a treatment for CNV. Only 5.3% of patients receiving treatment for CNV were given this route of therapy in 2008 (Curtis et al. 2012).

1.3.8.4 Anti-VEGF therapy

The discovery of the key role that VEGF plays in the pathogenesis of choroidal neovascularisation has led to the development of drugs inhibiting its secretion. Intraocular injections of anti-VEGF have therefore been established as a standard of care for neovascular AMD since the mid-2000s (Wong et al. 2007; Rosenfeld et al. 2006). Pegatanib sodium (Macugen, EyeTech), a selective antagonist of the 165 isoform of VEGF-A, was the first anti-VEGF drug to be approved by the US Food and Drug Administration (FDA) for treatment of nAMD (Gragoudas et al. 2004). The second to be approved by the FDA was ranibizumab (Lucentis, Novartis), a humanised monoclonal antibody fragment that binds all VEGF-A isoforms (Chakravarthy et al. 2006). Both drugs were approved for use in the treatment of nAMD in the UK by the NHS National Institute for Health and Clinical Excellence (NICE) in 2008. Landmark clinical trials using ranibizumab showed for the first time not only visual stabilisation

but also significant improvements in VA, as shown in Figure 10 below (Rosenfeld et al. 2006; Brown et al. 2006; Brown et al. 2009). The most significant improvement in acuity has been found to occur after the first injection, and this is maintained upon monthly injections of the drug. Serious adverse events, such as endophthalmitis, were rare.

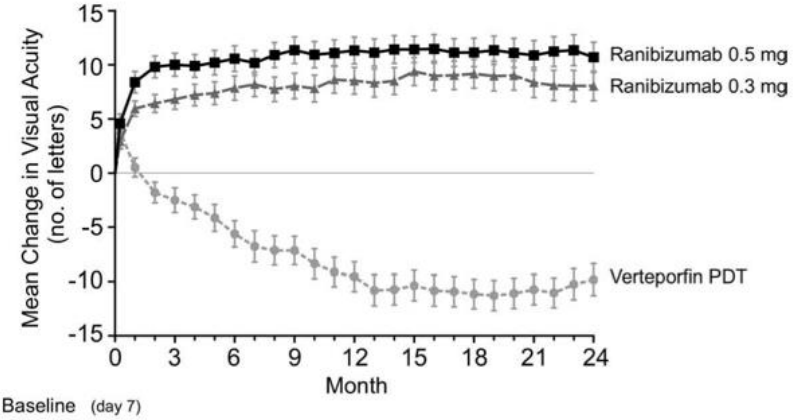

Mean Change from Baseline (day 7)									
Ranibizumab 0.5 mg (n=139)	+4.6	+10.0	+10.6	+11.4	+11.3	+11.4	+11.1	+10.9	+10.7
Ranibizumab 0.3 mg (n=140)	+2.9	+6.8	+7.9	+8.1	+8.5	+9.4	+9.2	+8.4	+8.1
Verteporfin PDT (n=143)	+3.9	-2.5	-5.6	-7.2	-9.6	-10.4	-11.2	-10.7	-9.8

Figure 10. Mean change from baseline VA score (letters) over time, with administration of monthly Ranibizumab injections compared with verteporfin PDT. Vertical bars represent +/- 1 standard error of the mean (Brown et al. 2009).

Bevacizumab (Avastin, Genentech), a third anti-VEGF drug, is an off-label alternative treatment (Martin et al. 2011). Originally manufactured for the treatment of colourectal cancer, it is a full-length monoclonal antibody that also binds all VEGF-A isoforms (Chakravarthy et al. 2006). The recent IVAN randomised controlled trial found a similar efficacy between bevacizumab and ranibizumab (Chakravarthy et al. 2013). Despite this, the uncertainty about systemic safety means that policy makers are unlikely to mandate a switch to the cheaper alternative (Cheung and Wong 2013). Interestingly, the IVAN trial showed that a reduction in injection frequency seems to be associated with a reduction in treatment efficacy. The current advised treatment schedule comprises an initial loading phase with monthly injections for the first three months. This is followed by a maintenance phase, during which the patient is monitored on a monthly basis and given treatment as required (Mitchell et al. 2010). It remains to be seen whether the results from the recent IVAN trial will lead to a change in these guidelines.

The IVAN trial did, however, fail to examine the newest VEGF-binding drug, aflibercept. This fusion protein is given every 2 months after the initial loading phase, and has been approved by both the FDA and NICE after recent clinical trials showed that it had a comparable efficacy and safety to ranibizumab (Cheung and Wong 2013).

1.3.8.5 Stem Cell Therapy

Since the development of human embryonic stem cells and induced pluripotent stem (iPS) cells, there is been great interest in the potential of these cells to treat AMD (Li et al. 2012; Kokkinaki et al. 2011). Recent progress in iPS cells provides a promising therapy for geographic atrophy (Du et al. 2011). Indeed, it has been found that human RPE cells and photoreceptors can be derived from these cells by defined factors (Osakada et al. 2009). This will facilitate the development of transplantation therapies for AMD and will improve our understanding of AMD pathophysiology. Indeed, the first clinical trial transplanting human embryonic stem cell-derived RPE in a patient with dry AMD has recently been undertaken. (Schwartz et al. 2012). After 4 months, the transplanted RPE cells showed no signs of hyperproliferation, tumourigenicity or rejection, and the patient had a functional improvement in VA. Cone photoreceptor transplantation is a challenge yet to be addressed. Whilst cones are similar to rods in that must be post-mitotic in order to integrate, they do so at a much slower rate (Lakowski et al. 2010). However, proof-of-principle experiments have shown that cone transplantation is certainly feasible (Lakowski et al. 2010).

1.4 Hypoxia and AMD

1.4.1 Oxygen Demand of the Retina

Even in the healthy retina, the choroidal circulation is barely adequate to supply the 120 million rod photoreceptors which have the highest metabolic rate of any cell in the body (Arden 2001). Although the retinal circulation is able to sufficiently autoregulate blood flow, the choroid is believed to control oxygen tension poorly, and its autoregulative potential is equivocal (Wangsa-Wirawan and Linsenmeier 2003). Maintaining a state of retinal dark adaptation is a metabolically demanding activity in which photoreceptors are constantly depolarised, causing elevated neurotransmitter release at synapses (Wangsa-Wirawan and Linsenmeier 2003). This depolarisation is caused by the continuous flow of ions into and out of the photoreceptors, the so-called ‘dark current’,

which requires the activity of an ATP-driven sodium-potassium pump in the photoreceptor cell membrane. Intra retinal oxygen profiles obtained from animals show that, in the dark, the oxygen partial pressure falls to almost zero at the proximal side of the photoreceptor inner segments, as depicted in Figure 11A. This reflects the high rate of oxygen consumption required to maintain the dark current of the 120 million rod photoreceptors. It is necessary for the oxygen tension to be greater in the central retina than peripherally due to the higher metabolic requirements of the macula (Wise et al. 1971). For this reason, the macula is extremely vulnerable to oxygen deficiency (Feigl 2009). Figure 11B compares the oxygen profile across the cat retina in normoxia compared with hyperoxia (inspiration of 100% oxygen). Breathing oxygen is seen to considerably increase oxygen tension, especially in the outer retina due to its higher oxygen demand and the limited autoregulative capacity of the choroidal circulation.

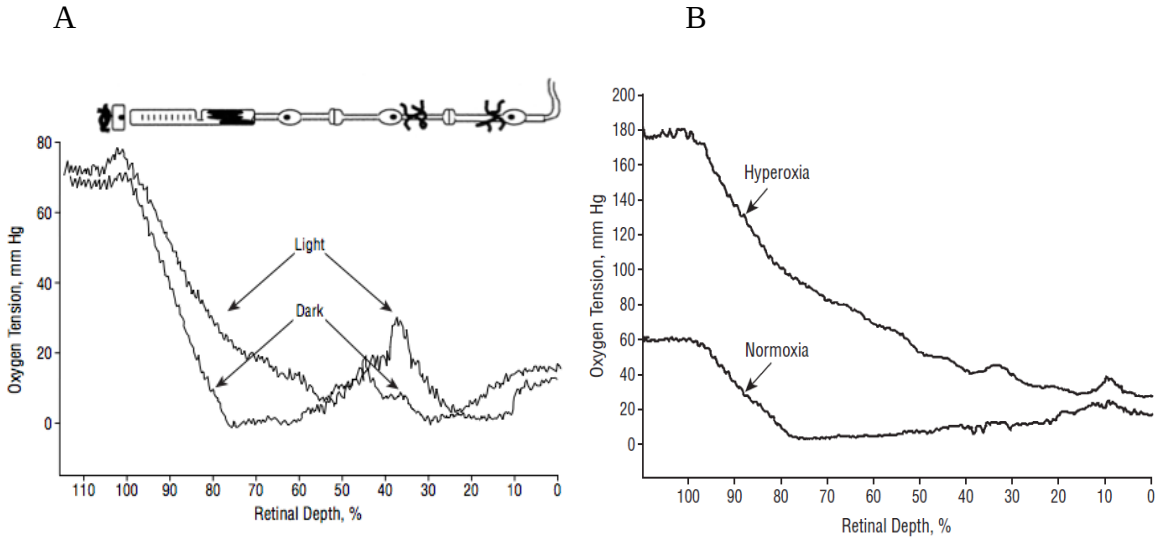

Figure 11. Intraretinal oxygen profiles across cat retina during light and dark adaptation. The retina is shown systematically at the top. The four cell types shown are (from left to right) RPE cells, rod photoreceptors, bipolar cells and ganglion cells (A). Intraretinal oxygen profiles in dark during normoxia and hyperoxia (B) (Wangsa-Wirawan and Linsenmeier 2003).

1.4.2 Oxygen Supply to the Retina

In a healthy eye, the oxygen demand of the retina is met by an efficient blood supply from both the choroidal and the retinal circulation, as previously described in section 1.2.6. The choroid, whose vasculature arises from the short and long posterior ciliary arteries, supplies the outer avascular retina and the macular region. The smooth muscle of the choroidal vessel walls is innervated by a perivascular plexus encompassing both divisions of the autonomic nervous system (Lütjen-Drecoll 2006).

The inner retina receives its nutrients from the vascular plexi arising from the central retinal artery (Lange and Bainbridge 2012). Unlike the choroidal circulation, the retinal vasculature infiltrates the retinal tissue, reducing the diffusion distance from the capillaries to the retinal cells (Kong et al. 2010). The lower rate of blood flow in the retinal circulation is seen in the greater arteriovenous difference in oxygen saturation (Schweitzer et al. 1999). The retinal circulation has been shown to have a greater autoregulative capacity than the choroid (Shakoor et al. 2006). Indeed, retinal blood flow has been shown to increase in response to a flickering light stimulus to support the increased oxygen requirements of the inner retina (Garhöfer et al. 2004; Riva et al. 2005; Shakoor et al. 2006).

1.4.3 Effect of Hypoxia on Visual Function

Psychophysical tests of visual function such as colour vision (Vingrys and Garner 1987; Karakucuk et al. 2004; Connolly et al. 2008), dark adaptation (McFarland and Evans 1939; Connolly and Hosking 2006) and dynamic contrast sensitivity under mesopic conditions (Connolly 2011) are all adversely affected by induced mild systemic hypoxia in healthy humans.

Mild systemic hypoxia has been shown to induce losses in colour discrimination along both the red-green (RG) and yellow-blue (YB) axes in mesopic luminances, with a greater loss occurring along the YB axis (Smith et al. 1976; Connolly 2011). The evidence for a loss of chromatic sensitivity caused by mild hypoxia in photopic conditions is equivocal: certain studies have found YB sensitivity to be marginally diminished (Connolly 2011), whereas others have shown a generalised loss of colour discrimination (Vingrys and Garner 1987). However, Connolly (2011) concluded that the sensitivity of the visual state to induced hypoxia depends fundamentally on light level.

Other types of psychophysical threshold have also been shown to be elevated by mild systemic hypoxia in mesopic conditions. For example, low contrast acuity thresholds in mesopic lighting are consistently elevated by up to 25% in hypoxia compared to hyperoxia (100% oxygen) (Connolly and Serle 2014). When Feigl et al. (2011)

measured retinal luminance thresholds under mesopic conditions on a sample of 3 healthy participants during hypoxia, their thresholds were also significantly elevated for all eccentricities. However, studies using static perimetry in photopic conditions have detected no functional deficits during mild systemic hypoxia (Fulk et al. 1991; Yap et al. 1995). This again indicates that the effect of hypoxia on retinal function is exacerbated by a reduced level of retinal illumination.

Flickering stimuli, such as those used in frequency doubling perimetry, are known to place an increased metabolic demand on the retina. This is illustrated by the compensatory increase in blood flow induced in the inner retinal circulation by flickering lights (Kiryu et al. 1995; Polak et al. 2002; Riva et al. 2001; Riva et al. 2005; Shakoor et al. 2006). Indeed, the blood flow in primate retinal arteries increases by 30% during monochromatic light flicker (Kiryu et al. 1995). It may be expected, therefore, that induced hypoxia will have a greater effect on sensitivity to metabolically demanding flickering stimuli than to static stimuli. Connolly and Hosking (2008) measured visual field sensitivity over 40^{o} of the central field using Frequency Doubling Technology (FDT) under photopic conditions during mild hypoxia (14% oxygen). Hypoxia was found to significantly reduce sensitivity from 5 to 10^{o} eccentricity, but not at more peripheral locations between 10 and 20^{o} (Connolly and Hosking 2008). This is in contrast with a recent study, which found no significant difference in either flicker or static visual field sensitivities between hypoxic and normoxic conditions under photopic illumination (Feigl et al. 2011). The dichotomy in results may be due to methodological differences; FDT uses 10^{o} targets modulated to flicker at 25Hz, whereas the flicker perimeter used by Feigl et al. contained 0.43^{o} diameter targets at temporal frequencies between 9 and 18Hz. The higher rate of flicker employed by Connolly and Hosking (2008) may have increased the effect of systemic hypoxia under photopic conditions. In another study, Connolly (2011) also found that hypoxia reduced dynamic contrast sensitivity (using FDT) by approximately 2dB in mesopic conditions (Connolly 2011). Flicker and chromatic thresholds are mediated by the cone pathways. Therefore, the evidence suggests that in mesopic conditions rod-induced hypoxia may compromise cone function, thus revealing ischaemic abnormalities in cone pathways that are undetected under photopic light levels.

In addition to the elevation of steady state visual thresholds, there is also evidence to suggest that reduced retinal oxygenation affects the kinetics of retinal adaptation (McFarland and Evans 1939; Connolly and Hosking 2006). Dark adaptation, the recovery of visual sensitivity in darkness following a bright flash of light, is affected by compromised arterial circulation. Evidence supporting this is found in an elevated dark adapted threshold in carotid artery disease (Havelius et al. 1997a) which is improved after carotid endarterectomy (Havelius et al. 1997b). Furthermore, healthy subjects have demonstrated delayed rod cone breaks with slower rates of dark adaptation under conditions of mild to moderate induced hypoxia (McFarland and Evans 1939; Connolly and Hosking 2006), suggesting that the compromised oxygen supply to the outer retina impacts on the dynamic process of photopigment regeneration. The impairment in dark adaptation with ageing found by Jackson et al. (1999) was comparable to the prolongation of the dark adaptation function found by Connolly and Hosking (2006) in young healthy controls subjected to hypobaric hypoxia. This similarity may suggest that the delayed dark adaptation observed in older persons is attributable to a localized deficit in oxygen supply to the outer retina.

As well as the substantial psychophysical evidence that visual function is affected in healthy individuals by induced systemic hypoxia, electrophysiological data have also been published (Tinjust et al. 2002; Pavlidis et al. 2005; Feigl 2007b; Feigl et al. 2008). Tinjust et al. (2002) found that humans experiencing mild systemic hypoxia induced by breathing 12% oxygen for 5 minutes had altered full-field ERG b-wave and oscillatory potentials with an unchanged a-wave, which led to the suggestion that the outer retina is more resistant to mild hypoxia than the inner retinal layers. In contrast, Shatz et al. found that 13 healthy volunteers breathing 13.2% oxygen for 45 minutes had significantly reduced a- wave amplitudes and a shallower a-wave slope of combined rod and cone responses (Schatz et al. 2014). This implies that when subjected to longer periods of hypoxia, both inner and outer retinal function are impaired.

The main limitation of the full-field ERG is that it gives little information about localized retinal areas as it represents the summed response across the entire retina, and hence will mask functional alterations to discrete retinal areas. More recent studies have used the multifocal electroretinogram (mfERG) to identify local changes caused by acute hypoxia (Pavlidis et al. 2005; Feigl et al. 2008). The mfERG is especially

pertinent to AMD as it predominately measures bipolar cell activity often described as belonging to the 'outer retina' and because the central retinal area tested (33^{o} diameter) targets the macular region affected by AMD (Hood et al. 2002). In 2008, Feigl et al. found, using the mfERG, that older eyes demonstrate poorer neuroretinal activity in systemic hypoxia (14% oxygen) than younger eyes, as shown in Figure 12, indicating that they may be more susceptible to hypoxia-induced neuroretinal deficits.

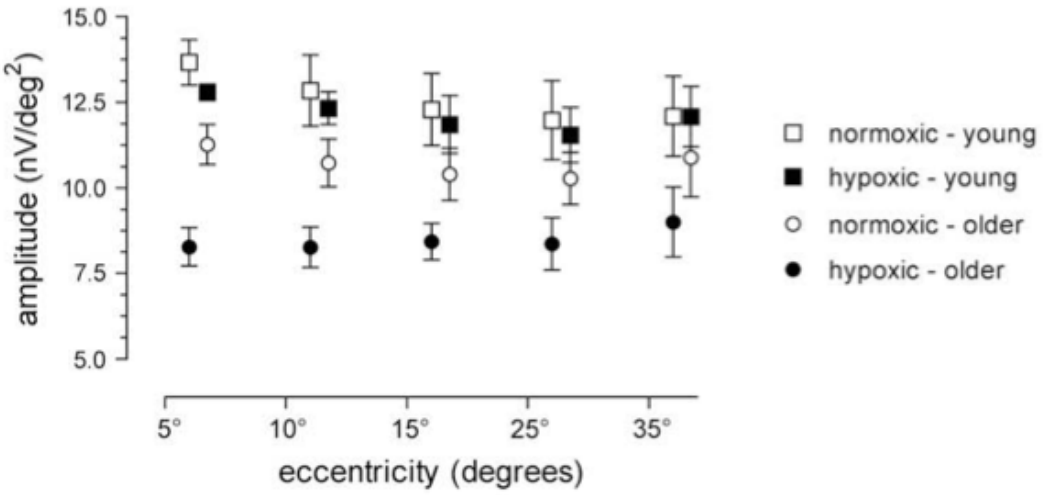

Figure 12. During hypoxia, mfERG response density amplitudes for the central 5 degrees are significantly reduced in the young (squares) and old (circles) groups for all eccentricities, with a more pronounced reduction in the older group ($p<0.01$) (Feigl et al. 2008).

Using the mfERG, ON and OFF bipolar cell function have been found to decline when breathing 10-14% oxygen compared with 21% in normal air at sea level, as shown in Figure 13 (Feigl et al. 2007b). This may be due to a lack of choroidal autoregulation (Shakoor et al. 2006) and a greater metabolic demand induced by the flickering stimuli (Kiryu et al. 1995).

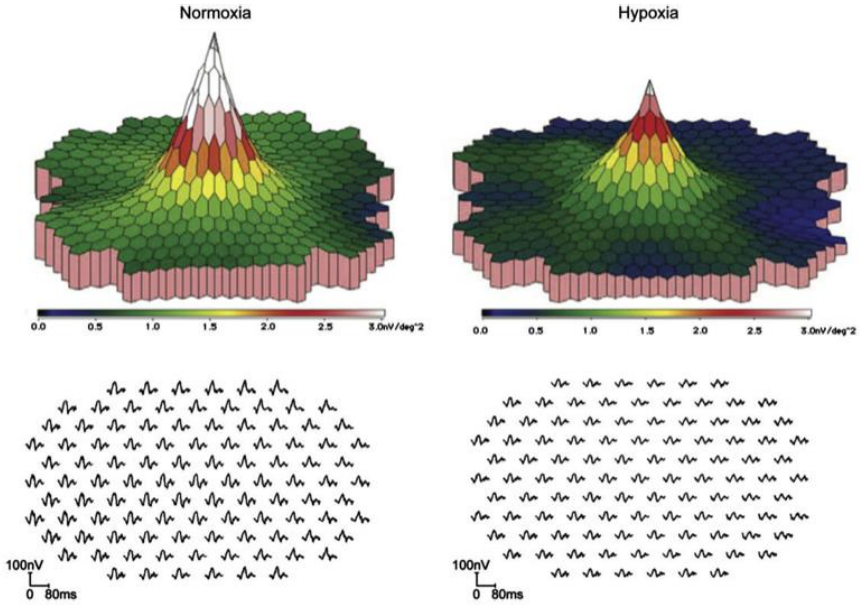

Figure 13. 3D response density plots (above) and the waveform trace array (below) of neuroretinal responses in an individual before (left) and after (right) breathing 14% O_2 shows centrally reduced responses (darker areas) for the standard mfERG (Feigl et al. 2007b).

1.4.4 Hypoxia and AMD

It is notable that the well-reported deficits in visual function seen in people with early AMD, including delayed dark adaptation (Owsley et al. 2001; Owsley et al. 2007; Dimitrov et al. 2008; Gaffney et al. 2011; Dimitrov et al. 2011), reduced flicker sensitivity (Dimitrov et al. 2011; Luu et al. 2013), reduced chromatic sensitivity (O'Neill-Biba et al. 2010) and elevated scotopic thresholds (Owsley et al. 2000), are similar in nature to the impairment recorded in healthy eyes under conditions of induced hypoxia (see section 1.4.3). This supports the hypothesis that the retinal dysfunction reported in early AMD may be, at least in part, attributable to retinal hypoxia. For example, Feigl et al. (2009) suggested that during experimental hypoxia in healthy adults, the metabolic demand induced by flicker could impair neuroretinal responses whilst, in AMD, these impaired responses may be the result of pre-existing hypoxia at

the retinal level. The influence of chronic systemic hypoxia on the aetiology of AMD is still not fully understood. There is, however, a known association between cardiovascular disease and AMD (Eye Disease Case-Control Study Group 1992; van Leeuwen et al. 2003; Chakravarthy et al. 2010), suggesting that this chronic hypoxic condition may have a bearing on the risk of AMD onset. This section will consider the evidence that hypoxia plays a role in the pathogenesis of AMD.

There is substantial evidence demonstrating that changes to the choroidal vasculature play a key role in AMD development (Chen et al. 1992; Friedman et al. 1995; Ciulla et al. 1999; Pauleikhoff et al. 1999; Ciulla et al. 2001; Ciulla et al. 2002). Abnormalities in ocular blood flow have been found in both early and advanced AMD using qualitative and quantitative techniques such as fluorescein and indocyanine green (ICG) angiography (Chen et al. 1992; Pauleikhoff et al. 1999), colour Doppler imaging (Friedman et al. 1995; Ciulla et al. 1999) and laser Doppler flowmetry (Metelitsina et al. 2008; Xu et al. 2010). Indeed, the choroidal blood supply has been suggested to be the initial area of insult in AMD (Ciulla et al. 1999; Seddon et al. 2009). Vascular defects have also been demonstrated by histological evidence reporting a reduced lumen diameter and vessel density in AMD (Sarks 1976). Watershed zones, which represent the anastomoses of the choroidal vessels supplied by the different branches of the posterior ciliary artery, are particularly susceptible to microvascular damage. These regions, as well as angiographic areas of choroidal non-perfusion, are associated with the location of choroidal neovascular growth, suggesting the co-localisation of regions of choroidal ischemia and choroidal neovascularization (Goldberg et al. 1998; Mendrinos and Pournaras 2009). Pauleikhoff et al. also found that it was common for patients with AMD to exhibit prolonged choroidal filling on fluorescein angiography and ICG (Pauleikhoff et al. 1999).

Reduced choroidal blood flow in AMD is also associated with delayed ERG implicit times and scotopic threshold elevation (Chen et al. 1992; Remulla et al. 1995). Chen et al. (1992) measured the scotopic thresholds of 8 eyes showing prolonged choroidal filling on fluorescein angiography and 6 eyes with a similar number of drusen but no perfusion defects using the Humphrey automated perimeter and fine matrix mapping. In 7 out of 8 eyes with delayed perfusion, scotopic thresholds were elevated by up to 3.4 log units compared to the background sensitivity. In contrast, eyes with normal

choroidal filling were not found to have any discrete areas of increased scotopic threshold. Remulla et al. (1995) investigated the foveal cone ERG implicit time (4^o stimulus flickering at 42 Hz) in the fellow eye of 67 patients with unilateral wet AMD. They found that implicit times were on average 1ms slower and were more likely to be delayed in eyes with abnormal choroidal perfusion than in eyes with normal filling, reinforcing the link between choroidal ischaemia and visual dysfunction in early AMD.

In addition to the potential effects of impaired choroidal perfusion on the state of outer retinal oxygenation, changes to Bruch's membrane associated with AMD are also likely to have an impact. The presence of drusen under the RPE and a thickening of Bruch's membrane in AMD increase the distance between the choriocapillaris and the retina, which augments the distance over which oxygen must diffuse. According to Fick's law of diffusion, this will result in a reduced oxygen supply to the retina, stimulating outer retinal hypoxia (Stefánsson et al. 2011). It is possible that the lipid accumulation and thickening of Bruch's membrane in AMD also reduces its permeability to water-soluble nutrients like VEGF-A (Holz et al. 1994). In the normal eye, RPE cells primarily secrete VEGF-A at their basolateral side towards the choriocapillaris. This growth factor is required for vascular permeability, angiogenesis, lymphangiogenesis and has neutrotrophic functions (Witmer et al. 2003), hence, its depletion is likely to lead to atrophy of the choroidal circulation (Sakamoto et al. 1995; Witmer et al. 2003). Choroidal atrophy, in turn, will potentiate choroidal perfusion abnormalities, and drusen and debris accumulation at the level of Bruch's membrane. In turn, this is likely to cause further outer retinal hypoxia (Zarbin 2004; Feigl 2007), leading to a cycle of hypoxic insult.

Although the choroidal circulation is the focus of most research into vascular deficiency in AMD, recently, a non-invasive spectrophotometric retinal oximeter based on a standard fundus camera, the Oxymap Retinal Oximeter T1 (Oxymap, Reykjavik, Iceland), has been developed to enable the direct study of retinal oxygen metabolism by measuring the oxygen saturation in inner retinal arterioles and venules (Geirsdottir et al. 2012). The repeatability of the Oxymap T1 in retinal vasculature oxygenation saturation measurements is approximately 1% (Palsson et al. 2012). Using this instrument, the arteriovenous difference in oxygen saturation in eyes with wet AMD was found to be smaller than in healthy controls, suggesting that less oxygen is being

extracted from the retinal vessels in AMD (Geirsdóttir et al. 2014). This suggests that the inner retinal circulation may also be implicated in the pathogenic mechanism of AMD.

There is also molecular evidence supporting the role of hypoxia in AMD. For example, autopsies have shown that VEGF is expressed in the RPE of eyes with AMD, and VEGF has been identified in surgically removed choroidal neovascular membranes (CNVMs) (Grossniklaus et al. 1992; Frank et al. 1996; Kvanta et al. 1996). Animal models that produce excess VEGF are also associated with the growth of CNVMs (Baffi et al. 2000; Schwesinger et al. 2001). Furthermore, VEGF levels are high in the vitreous of eyes with neovascular AMD (Wells et al. 1996; Holekamp et al. 2002). The upregulation of VEGF expression in response to hypoxia occurs through hypoxia-inducible factor-1 (HIF-1), a transcription factor necessary for the regulation of oxygen homeostasis (Zhang et al. 2007). In normoxia, HIF-1α is rapidly degraded by the von Hippel-Lindau tumour suppressor protein, thus preventing it from heterodimerising with HIF-1β, which consequently prevents VEGF expression (Mole et al. 2001). Under hypoxic conditions, HIF-1α is able to dimerise with HIF-1β, leading to the upregulation of VEGF-A (Klettner et al. 2013).

The evidence suggests that, even in the early stages of AMD, there may be retinal hypoxia as a result of the high metabolic demands of the photoreceptor cells (Arden et al. 2005). The ultimate consequence of outer retinal hypoxia may be an overexpression of VEGF-A in the RPE, triggering choroidal neovascularization (Spilsbury et al. 2000), or cell apoptosis resulting in geographic atrophy of the retina and RPE (Arden et al. 2005). If hypoxia is responsible for the progression of AMD, it follows that most damage will be caused when the retina is most hypoxic, i.e. in darkness (Figure 11A). If the metabolic activity of the outer retina and hence oxygen demand could be reduced, outer retinal hypoxia would be diminished and AMD progression would be potentially prevented.

1.5 Low-level Light Therapy for Retinal Hypoxia

The 120 million rod photoreceptors have the highest metabolic rate of any tissue in the human body, which necessitates a high level of energy (provided by adenosine

triphosphate, ATP) and oxygen consumption (Arden 2001). Okawa et al. (2008) demonstrated that the ATP consumption of mammalian rod photoreceptors is >75% higher in the dark than the light. In the outer segment, the majority of the energy expenditure was required to extrude sodium ions which flow into the cell through cGMP gated ion channels in the dark (maintaining the rod circulating current, or 'dark current'). The inner segment requires energy for the removal of sodium and calcium ions entering voltage-gated channels at the synaptic terminal. It can be seen from Figure 14 that all of these processes are more active at lower light levels (fewer rhodopsin isomerisations per rod per second). Consequently, retinal oxygen consumption decreases by up to 40 to 60% in bright light, as seen in Figure 15.

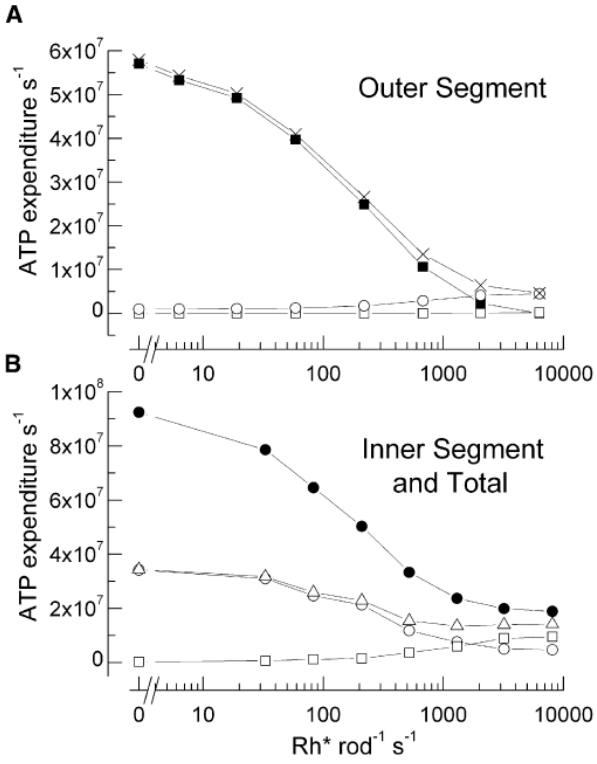

Figure 14. Main contributors to ATP consumption in mammalian rods over the physiological range of steady light intensities. (A) Outer segment. ATP required for extrusion of Na^+ entering cGMP-gated channels (filled square), transducin GTP hydrolysis and rhodopsin phosphorylation (open square), cGMP synthesis (open circle), and sum of these processes (X). (B) Inner segment and total rod ATP consumption. ATP required for extrusion of Na^+ entering through i_h channels (open square), extrusion of Ca^{2+} entering voltage-gated channels at synaptic terminal (open circle), sum of ATP for Na^+ and Ca^{2+} extrusion (open triangle), and sum of ATP turnover in whole rod (closed circle) (Okawa et al. 2008).

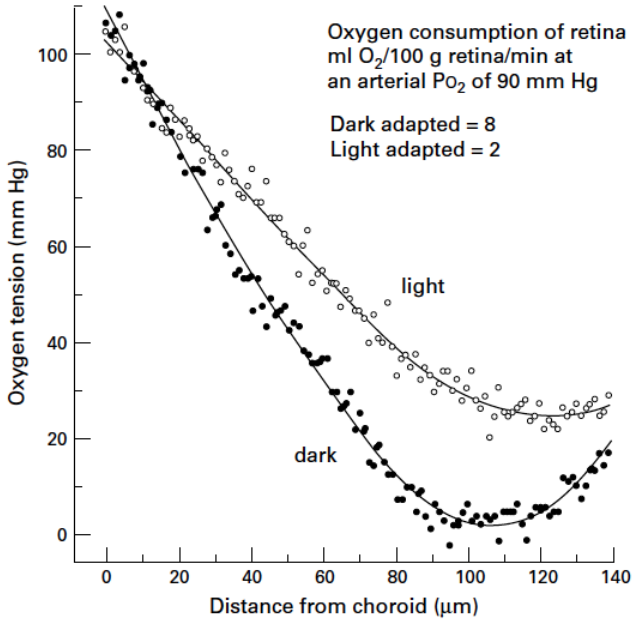

Figure 15. Intraretinal oxygen profiles across cat retina during light and dark adaptation (Arden 2001).

It follows, therefore, that if environmental light levels were increased during the hours of sleep, the metabolic activity of the outer retina and hence the oxygen demand would be reduced, thus providing a potential therapy for conditions with a hypoxic aetiology (Arden 2001).

Diabetes is a disease that selectively damages the retinal vasculature (Wangsa-Wirawan and Linsenmeier 2003), causing capillary dropout, microaneurysms, cellular damage and neovascularisation (Kern and Engerman 1996). For a number of years, hypoxia has been implicated in the progression of diabetic retinopathy (Arden 2001). Because of the retina's vast oxygen requirements, even minor reductions in oxygen availability due to basement membrane thickening (Alder et al. 1997) or increases in oxidative metabolism from hyperglycaemia, could lead to retinal hypoxia (Cao et al. 1998). There is evidence to suggest that hypoxia in diabetes occurs before any capillary dropout (Braun et al. 1995; Linsenmeier et al. 1998; Dean et al. 1997; Harris et al. 1996). In humans, oscillatory potentials are diminished during dark adaptation (Drasdo et al. 2002) and chromatic sensitivity is reduced (Dean et al. 1997) before any vessel damage is observed. Hence, hypoxia may be the stimulus for VEGF upregulation and subsequent macular oedema and retinal neovascularisation. Since outer retinal hypoxia

increases during dark adaptation (Braun et al. 1995), prevention of dark adaptation during sleep should have therapeutic benefits on the progression of diabetic retinopathy.

This hypothesis was tested recently in a phase I clinical trial of 12 diabetic patients (Arden et al. 2010). The light source was provided by a 'glowpatch', i.e. a flat oval sachet (75 x 55mm) containing phthalates and hydrogen peroxide that mix and emit light of peak output 550nm through the lids, secured in place by a light plastic headband. One eye was exposed to local illumination with the fellow eye acting as a control. The intervention was able to prevent complete dark adaptation for up to 12 months without any adverse effects such as sleep disturbances, indicating that this form of treatment is acceptable to patients. Although this was a small pilot study, the results showed that, in the majority of treated eyes, the YB chromatic thresholds were significantly reduced compared to their fellows ($p=0.03$). Furthermore, the areas of microaneurysms and small dot haemorrhages decreased in the treated eyes whilst increasing in the fellow eyes. A limitation of the study was that the light patches did not give a constant output over time, leading to uncertainty as to how long light adaptation was maintained at night, and what light intensity was achieved. It raised the possibility that if higher illumination levels were used for longer periods than the presumed several hours provided by the glowpatch, more significant improvements in treated eyes could be achieved.

In light of this, the same group conducted a further investigation on 34 patients with diabetic macular oedema (Arden et al. 2011). Sleepmasks containing light emitting diodes were enclosed in a cotton cover and held against the eyes by an elastic headband. Four 505nm light emitting diodes were used to provide a constant retinal illuminance in the treated eye of 2 scotopic trolands (allowing for attenuation by the eyelids), which was deemed sufficient to significantly reduce the rod circulating current, and hence the oxygen demand of the retina (Arden et al. 2011). The device was driven by a battery that was recharged every morning. After 6 months, Arden et al. reported a reduction in retinal thickness in the treated eye only, as demonstrated in Figure 16. Furthermore, visual acuity, achromatic sensitivity and microperimetric thresholds significantly improved in study eyes, and deteriorated in fellow eyes.

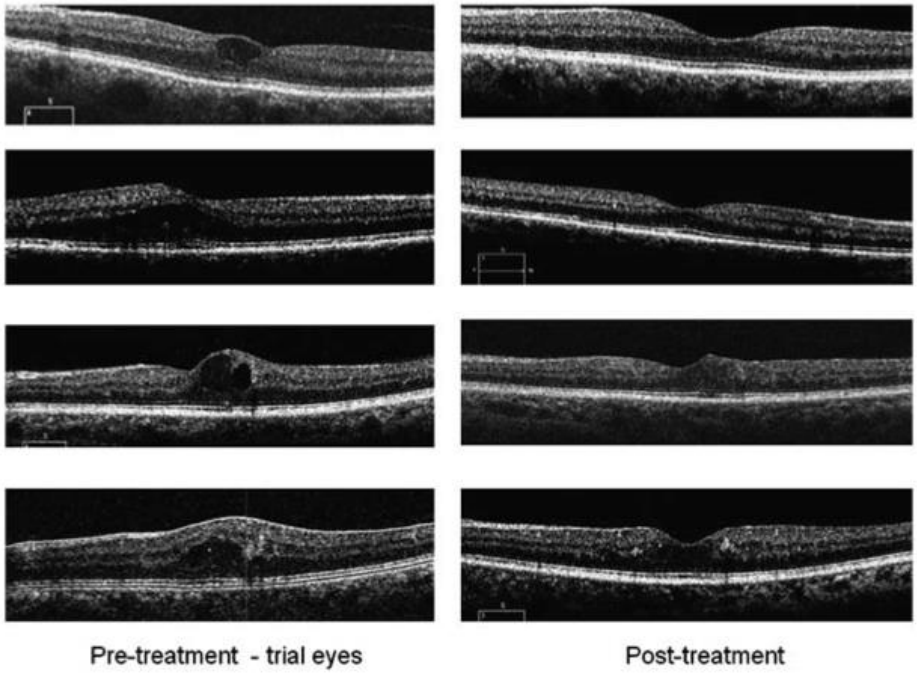

Figure 16. Cross-sectional OCT views horizontally through the macula from some representative patient's study eyes. In every case, the cysts have decreased over 6 months (Arden et al. 2011).

This study provides evidence that significant structural and functional improvements occur in eyes with diabetic macular oedema exposed to light during the night. A limitation of the study is that the masks had a high rate of failure so that patients were not exposed to constant illumination. Furthermore, there was no eye-tracker in the device to ensure that the LEDs were always positioned in front of the pupil. Despite these limitations, trans-lid retinal illumination during the night was found to cause regression of diabetic macular oedema. This was attributed to a reduction in oxygen demand by the dark current. The same therapy could also have significant therapeutic benefits in other conditions of a hypoxic aetiology, such as AMD.

1.6 Biomarkers in AMD

1.6.1 Drusen Volume Analysis

Macular drusen are the hallmark lesions of early and intermediate AMD, and the presence of large soft drusen and retinal pigmentary abnormalities is known to indicate an increased risk of development of neovascular or atrophic AMD (Klaver et al. 2001; Klein et al. 2002; Wang et al. 2003). The natural history of drusen may comprise an increase in size, confluence and area followed by neovascularisation, or a regression leading to atrophy of the RPE and photoreceptors (Gass 1973). The recent Complications of Age-related Macular Degeneration Trial (CAPT), a large, population-based study, found that 1.2% of eyes had a reduction in drusen area greater than 50% after 6 months (Complications of Age-Related Macular Degeneration Prevention Trial Research Group 2006). This proportion increased over time to 31.2% at 5 years, indicating that drusen are not static in nature: the reabsorption of old drusen and formation of new drusen can occur concurrently in the same eye. Although the prognosis for drusen regression is not currently known, there is a possibility that treatments capable of altering drusen morphology could reduce disease progression in AMD (Yehoshua et al. 2011a).

Traditionally, stereoscopic colour fundus photography has been the gold standard objective technique for the manual assessment of drusen to document drusen severity, drusen natural history and the likelihood of disease progression in AMD (Klein et al. 2007). Although these photographs are beneficial in viewing the macular appearance, they do not provide direct information on RPE geometry. Furthermore, there is often considerable variation in drusen measurements between readers, especially at indistinct drusen margins (Jain et al. 2010). Therefore, novel algorithms have been developed for automated and semi-automated drusen analysis (Smith et al. 2005; Jain et al. 2010; Gregori et al. 2011; Yehoshua et al. 2011a; Schlanitz et al. 2011).

The recent development of the SD-OCT has enabled the study of drusen morphology in vivo, due to its faster acquisition speeds and increased image resolution compared with previous time-domain OCT models (Drexler et al. 2003; Srinivasan et al. 2006). It is able to generate high-quality, individual B-scans that provide a cross-sectional view of drusen ultrastructure (Khanifar et al. 2008). Quantitative information about the

3-dimensional RPE deformations can be extracted from the SD-OCT datasets using segmentation algorithms (Yehoshua et al. 2011a). A novel, fully automated algorithm has been developed that is capable of acquiring drusen volume and area from these RPE deformations. This quantitative algorithm has been shown to produce highly repeatable measurements of both drusen volume and area (Gregori et al. 2011). Previously, Szkulmowaski et al had developed a similar algorithm, but their semi-automated method required much operator intervention, and its reliability was limited by the presence of artefacts (Szkulmowski et al. 2007). Later, Yi et al developed a similar strategy to that of Gregori, but it has not been validated, nor has its repeatability been assessed (Yi et al. 2009). Therefore, the most suitable algorithm currently available is that of Gregori et al. (2011). A study of the natural history of drusen morphology using this algorithm has shown that, over a period of 12 months, drusen exhibit a dynamic, undulating growth pattern that is most likely to increase over time (Yehoshua et al. 2011a). Cube root drusen volume was shown to increase significantly (p=0.006) by 0.0016mm (SD=0.059) over 12 months. Irrespective of initial drusen volume, approximately 50% of people with AMD show a significant increase in drusen volume over the 12 month study period i.e. beyond test-retest 95% confidence intervals. Figure 17 shows an example of the images acquired using the SD-OCT and drusen volume analysis algorithm.

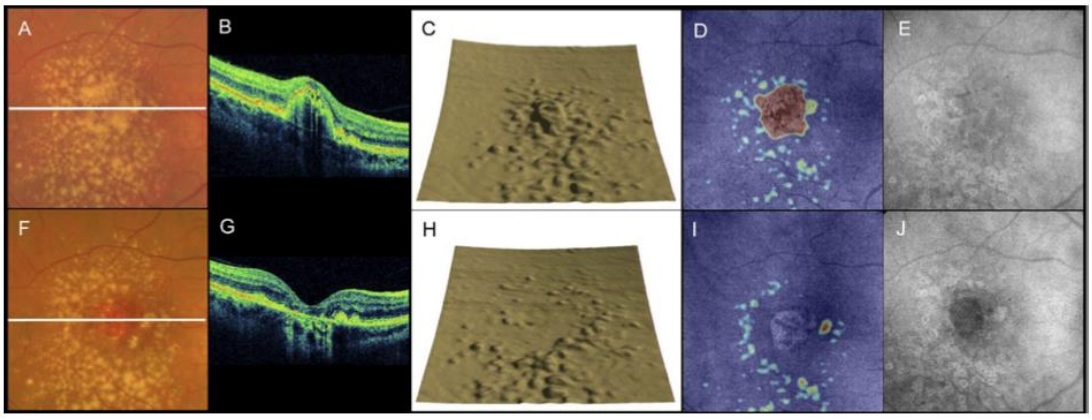

Figure 17. Right eye of a 76-year-old woman followed up over 6 months. Drusen changed to geographic atrophy over 12 months. Colour fundus photograph with a line representing the location of OCT B-Scan (A,F), horizontal B-scan (B,G), RPE segmentation map (C,H), hybrid map made of OCT fundus image and drusen thickness map (D,I), and fundus autofluorescence (E,J). Images are shown at baseline (A-E) and 6 months (F-J). Drusen volume was 0.45mm^3 at baseline and 0.016mm^3 at 12 months (Yehoshua et al. 2011a).

A recent study found that measurements of drusen area from manual segmentation of colour fundus images were typically greater than when measured using SD-OCT imaging and a fully automated algorithm that detects RPE elevations (Yehoshua et al. 2013). The difference in these measurements could be due to the fact that because the algorithm used by the OCT system detects drusen using a threshold to identify significant elevations above the virtual RPE floor and may not detect small, flat drusen and subretinal drusenoid deposits. However, previous studies of drusen measurements using semi-automated segmentation of OCT images correlate well with subjective human grading of fundus images (Jain et al. 2010; Iwama et al. 2012), indicating that it is a potentially useful alternative to drusen assessment by human graders using colour fundus photography.

An exploratory trial using SD-OCT showed a correlation between choroidal thickness and drusen load (volume and area) in patients with dry AMD (Ko et al. 2013). Not surprisingly, patients with greater drusen load also tended to have worse visual acuity, independent of changes to choroidal thickness. Histological studies have also demonstrated that the presence of drusen is associated with underlying diffuse changes to Bruch's membrane (Bressler et al. 1994). This evidence indicates that drusen load or volume may reflect underlying structural changes which occur in early AMD, but which are not visible on clinical examination. This factor, combined with the evidence that drusen volume tends to increase with increasing AMD disease severity, and the fact that the measurement of drusen volume using the SD-OCT is repeatable, objective and easily quantifiable, suggests that this may be a useful outcome measure for future clinical trials of interventions for AMD. Indeed, there is an ongoing clinical trial examining the effects of eculizumab on the progression of geographic atrophy and drusen volume in dry AMD (Yehoshua et al. 2011b). The Age-Related Eye Disease Study 2 is currently conducting an ancillary study to assess the ability of SD-OCT to predict the advancement of AMD, using change in drusen volume and area of geographic atrophy as primary outcome measures (Yehoshua et al. 2011b). As this research is yet to be published, it remains to be seen whether drusen volume will be an effective surrogate clinical study end point when investigating new treatments for AMD.

1.6.2 Dark Adaptation

The human eye is able to operate over an impressive 10 log unit range of luminance levels through a combination of neural, mechanical and photochemical mechanisms. The eye is able to rapidly adapt to moderate changes in luminance. However, it takes approximately 40 minutes to regain maximal visual sensitivity in the dark after viewing a bright or prolonged flash of light, which causes a significant amount of visual pigment to be 'bleached', that is, broken down into its colourless form which is insensitive to light (Lamb & Pugh 2004). This recovery of sensitivity is known as dark adaptation. The dark adaptation curve displays the threshold intensity (logarithmically) needed to detect a visual stimulus against time after extinction of the adapting light. The classical curve, obtained after an almost total bleach, consists of two distinct phases of recovery (Figure 18).

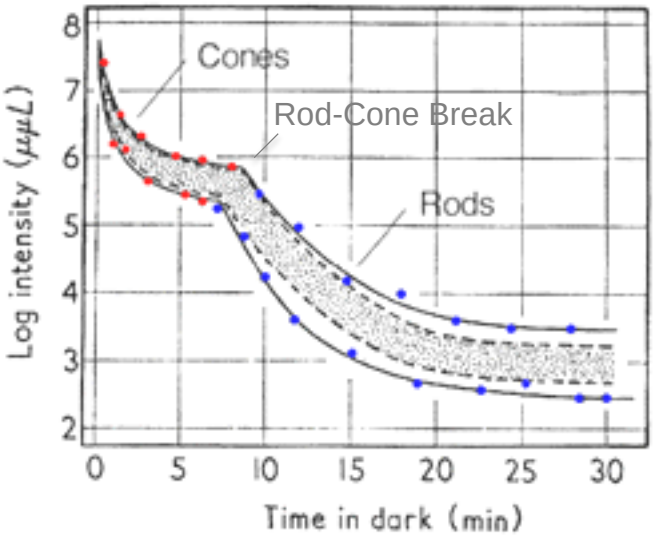

Figure 18. A typical dark adaptation curve. The shaded area represents 80% of the group of subjects. Adapted with permission from Kalloniatis and Luu (2011a).

The first, cone-mediated, phase of recovery shows a rapid reduction in threshold of approximately 2.5 log units and is complete in around 8 minutes, depending on the percentage of photopigment bleached. The second, rod-mediated, phase is associated with a reduction in threshold of over 4 log units. Rod recovery proceeds more slowly so that full rod adaptation can take at least 30 minutes (Hecht et al. 1937). The rod-cone break (RCB) is the point at which cone sensitivity plateaus and the rod system becomes the facilitator of threshold recovery. The recovery of visual sensitivity was previously thought to be a 1st order exponential process, but is now thought to follow rate-limited

kinetics (Lamb and Pugh 2004). Indeed, there is a region of rod recovery following the rod-cone break over which the data exhibits linearity for every bleach level between 0.5% and 98%. This region was termed "component S2" (where "component S1" is masked by cone activity) (Lamb 1981). A third and final component of recovery, S3, can be seen in most subjects as the threshold declines below 1.5 log units after photopigment bleaches greater than 20% (Lamb 1981; Lamb and Pugh 2004).

The shape of the dark adaptation curve is affected by a number of factors, for example, the intensity and duration of the adapting light (Haig 1941; Hecht et al. 1937; Mote and Riopelle 1951; Wald and Clark 1937; Winsor and Clark 1936) . With increasing levels of initial light adaptation, achieved through increasing either the duration or the intensity of the adapting light, the cone branch becomes more prominent whilst the rod branch is delayed. It also takes longer to reach absolute threshold (Figure 19) (Hecht et al. 1937). If the intensity or duration of the pre-adaptation period is low enough, a single rod curve may be acquired. A bi-phasic curve is only seen with a longer duration or more intense period of light adaptation (Wald and Clark 1937).

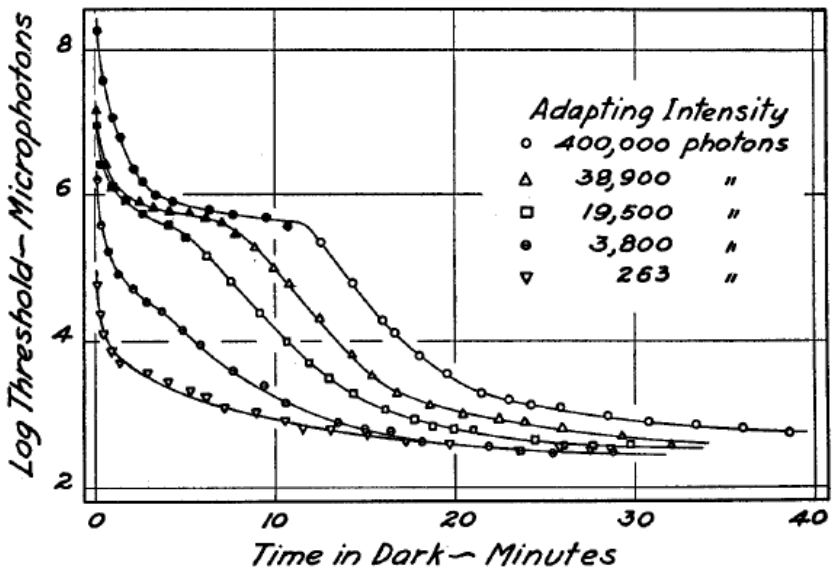

Figure 19. Dark adaptation functions for a normal observer obtained after exposure to five different intensities of adapting light (Hecht et al. 1937).

The dark adaptation function is also affected by the location of retina stimulated by the test spot, due to the topographical arrangement of rods and cones in the retina. In the

left panel of Figure 20, it is seen that in the central 2° test field, dark adaptation is mainly a cone function due to the lack of rods at the fovea. As the stimulus size increases, the absolute threshold decreases due to the increased rod density in the peripheral retina, reaching a peak at approximately 12° eccentricity (Curcio et al. 1990; Osterberg 1935).

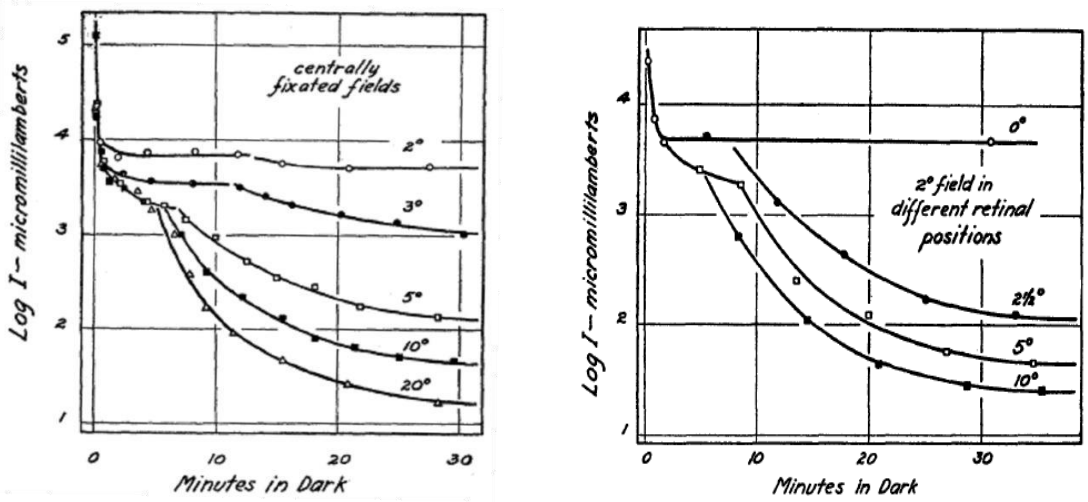

Figure 20. Dark adaptation thresholds measured with centrally fixated stimuli of different size (left panel) and with a 2° stimulus placed at different distances from fixation (right panel) (Hecht et al. 1937).

Similarly, as the position of the stimulus moves from the central retina towards the periphery, the rod branch becomes more prominent (right panel, Figure 20). Lastly, the wavelength of the test stimulus also influences the shape of the dark adaptation curve. Hecht and colleagues (1937) noted that when a long wavelength light stimulus was used, such as deep red, the dark adaptation curve only showed the cone branch of the dark adaptation function. This is because rods and cones have similar sensitivities to longer wavelengths. Conversely, when a short wavelength light is used, to which rods have maximal sensitivity, a more prominent rod branch is produced (Hecht et al. 1937).

1.6.2.1 The Retinoid Cycle

The molecular process underlying the recovery of visual sensitivity in dark adaptation involves resumption of the circulating current in the outer retina and regeneration of visual pigment in the photoreceptors (Neelam et al. 2009). To directly and objectively investigate the kinetics of visual pigment regeneration in a living human eye, fundus reflection densitometry was developed. Using this technique, it was found that the time course of threshold reduction during dark adaptation mirrors that of photopigment regeneration. It was originally hypothesised that the magnitude of visual threshold

recovery was directly proportional to the amount of unbleached photopigment available in the retina (Hecht et al. 1937). However, this was later refuted by the work of Granit and colleagues in 1938, who found that when only 20% of the pigment was bleached, the threshold was elevated by over 1000 fold (Granit et al. 1938). This demonstrates that elevated threshold during dark adaptation is not governed by the absence of unbleached visual pigment, but rather suggests that it is related to the presence of one or more photoproducts from the initial bleach, which actively reduce retinal sensitivity (Lamb and Pugh 2004). In order to examine how the recovery of visual sensitivity is related to the 'retinoid cycle' of photopigment regeneration, it is first necessary to consider the anatomy and biochemistry underlying this process.

The series of biochemical reactions that results in the generation of a visual signal following the absorption of a photon of light is known as the phototransduction cascade (Figure 21). In rods, light isomerizes rhodopsin's 11-*cis* retinal chromophore to the all-*trans* configuration, and the retinal molecule separates from the opsin component of the photopigment (Wald 1968). This activates the G protein transducin, which consequently activates the cGMP PDE, causing a reduction in the intracellular concentration of cGMP, which causes the closure of cation channels in the photoreceptor outer segments and hyperpolarisation of the cell membrane (Burns and Baylor 2001). For a detailed description of the process, the reader is referred to reviews by Burns and Baylor 2001 and Pugh and Lamb 2000.

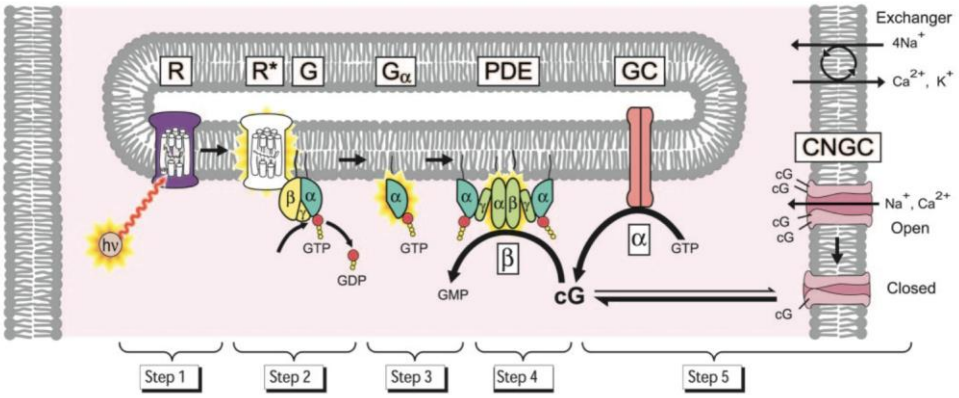

Figure 21. The G-protein cascade of phototransduction (Lamb and Pugh 2006).

The photopigment molecule is quickly inactivated, and can only receive another photon of light when the all-*trans* retinoid has been re-converted to 11-*cis* retinal, and recombined with opsin (Lamb and Pugh 2004). This is achieved through a sequence of biochemical reactions known as the "retinoid cycle" which is outlined below and displayed pictographically in Figure 22. For further information, the reader is directed to Lamb and Pugh (2004).

Photoisomerization in the photoreceptor outer segment

1. 11-*cis* retinal absorbs a photon of light and is isomerised to all-trans retinal, initiating the phototransduction cascade.
2. The all-*trans* retinal and opsin molecule, now called 'metarhodopsin', is converted to metarhodopsin II and is 'bleached'.

Removal of all-trans retinoid from photoreceptor outer segment to RPE

3. Hydrolysis of the covalent bond between opsin and all-*trans* retinal occurs. Some of the retinoid remains non-covalently bound so that the opsin may continue to serve as a chaperone i.e. a binding protein that protects the retinoid, increase its solubility in water and carries it to another location.
4. The all-*trans* retinal that remains bound is then reduced by the enzyme all-*trans* retinol dehydrogenase (RDH) forming Ops-trans ROL.
5. This Ops-trans ROL releases all-*trans* retinol (vitamin A).
6. The retinoid released in step 3 moves across the membrane by ABCR and is reduced by RDH following hydrolysis in the cytoplasm.

7. The all-*trans* retinol is chaperoned from the inter-photoreceptor matrix (IPM) to the RPE using IRBP. Within the RPE cytoplasm, cellular retinol binding protein (CRBP) acts as chaperone molecule.

Reconversion of 11-cis retinal in the RPE

8. In the cytoplasm, the all-trans retinoid is esterified by the enzyme lecithin retinol acyl transferase (LRAT). This all-*trans* retinyl ester is chaperoned by RPE65 protein.

9. Isomerisation by the enzyme retinyl ester isomerohydrolase or 'isomerase' reconfigures the alcohol to 11-*cis* retinol.

10. 11-*cis* retinol dehydrogenase (11-cis RDH) is responsible for the oxidation of 11-*cis* retinol to 11-*cis* retinal, which is then chaperoned by cellular retinaldehyde binding protein (CRALBP).

Transfer of 11-cis retinal to photoreceptor outer segment

11. The 11-cis retinal, possibly chaperoned by IRBP, travels across the IPM to the photoreceptor outer segment by diffusion and traverses the cytoplasmic space to enter the disc membrane.

12. It then forms a non-covalent bond with opsin at an "entry site" forming opsin-11-*cis* retinal (Ops-*cis* RAL).

13. A Schiff-base bond naturally occurs and the protein is transformed to produce rhodopsin or the cone equivalent.

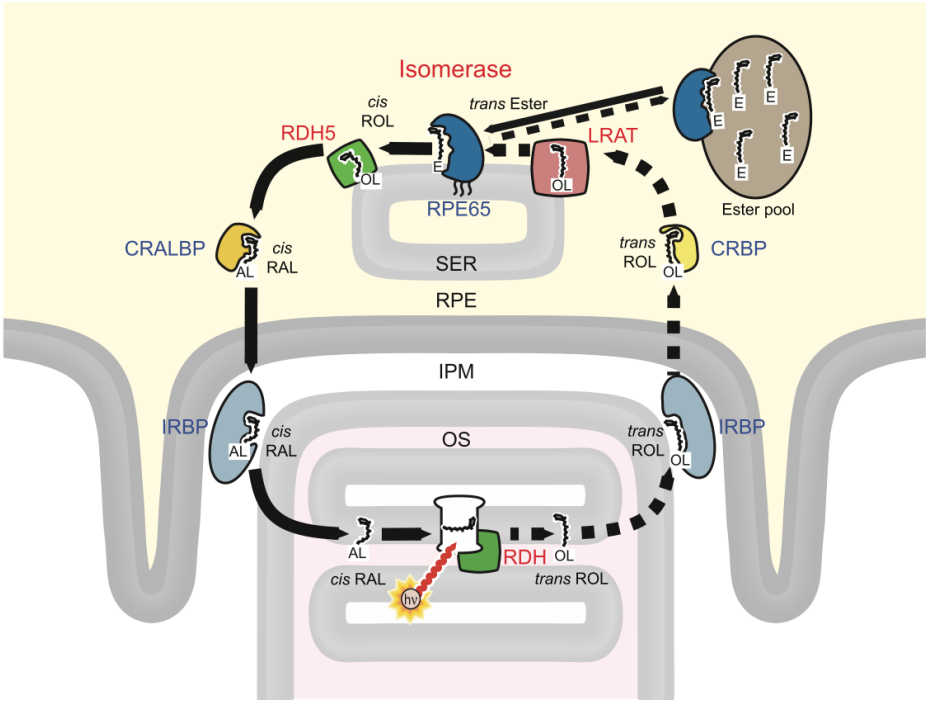

Figure 22. The retinoid cycle of pigment regeneration. The formation and supply of 11-*cis* retinoid is marked by the solid arrows, whereas the removal, conversion and storage of all-*trans*-retinoid is depicted by the dashed arrows (Lamb and Pugh 2006).

It is clear from this cycle that the process of photopigment regeneration relies on healthy photoreceptor and RPE function, as well as the delivery of metabolites and retinal from the choroidal circulation via Bruch's membrane.

1.6.2.2 Dark Adaptation and Rhodopsin Regeneration

It has been known for many decades that the rate of dark adaptation is somehow related to the regeneration of visual pigment, but the underlying cellular mechanisms have remained unclear. In the 1960s, it was thought that there was a linear relationship between the log threshold and the fraction of pigment remaining bleached, i.e. the unregenerated rhodopsin (Dowling 1960). This became known as the Dowling-Rushton relation, shown in Equation 1 below. However, later analyses found this only to be valid for an almost total bleach (Lamb and Pugh 2004; Lamb 1981).

Equation 1 $$\log (E_t/E_\alpha) = \alpha (l - p)$$

E_t is the intensity of a threshold flash at any moment t in the dark after a bleach, E_α is the value of E_t found after full dark adaptation, p is the fraction of pigment present, and α is a constant (Hollins and Alpern 1973).

During dark adaptation, there is an adapting effect consisting of elevated threshold and improved spatial and temporal resolution which has the same effect as a steady light at an intensity known as the 'equivalent background brightness', and which gradually fades with time (Stiles and Crawford 1932). It has been hypothesised that the bleaching photoproduct responsible for the generation of this equivalent background brightness is free opsin (Lamb and Pugh 2004). This follows the discovery that opsin weakly activates phototransduction (Cornwall and Fain 1994) and when combined with 11-cis retinal, opsin's activity is discontinued (Corson et al. 1990; Pepperberg et al. 1978). Lamb and Pugh (2004) gave evidence to support the theory that after a large bleach, the recovery of threshold is a rate-limited process, governed by the removal of a product of bleaching, which they suggest to be opsin. It is the removal of this substance that underlies the regeneration of rhodopsin and recovery of threshold during the second phase of rod adaptation. This model, although effective in linking dark adaptation,

pigment regeneration and retinoid processing together, needs further research to confirm its validity.

1.6.2.3 Alternative Cone Pathway

Since cones are working continuously to facilitate our daytime vision, it is necessary that their visual pigment is able to regenerate quickly. The retinoid cycle through the RPE recycles the chromophore and provides it to both rods and cones. One would assume that cones would be at a disadvantage in the rod-dominant human retina since they would have to compete with a vast number of rods for the 11-*cis* retinal available in the RPE. However, when comparable levels of rod and cone pigment are bleached, cones regain their sensitivity within 5 minutes whereas rods take over 30 minutes to reach absolute threshold (Wald and Clark 1937; Hecht et al. 1937). This implies that cones regenerate their visual pigment significantly faster than rods, and since the rate of photopigment regeneration is limited by the availability of the chromophore to the photoreceptors (Lamb and Pugh 2004), it implies that cones are supplied with chromophore faster than rods with the possible help of a second, cone-specific pathway (Wang and Kefalov 2009; Wang and Kefalov 2011).

Interest in the probable existence of an alternative visual cycle was elicited by the discovery of retinoid derivatives in cone-dominant retinas. Das et al. (1992) found that the cone-dominant chicken retina could produce 11-*cis* retinyl ester, 11-*cis* retinol and all-*trans*-retinyl ester after incubation with all-*trans* retinol, suggesting the presence of at least three retinal enzymatic processes (Das et al. 1992). These processes were identified in chicken and ground squirrel retinas by Mata et al. (2002), thus enabling them to propose a model for a cone- specific visual cycle in cone-dominant retinas (Mata et al. 2002). The first retinal enzymatic process catalyses all-*trans* to 11-*cis* retinol through the activity of isomerase II. The second enzyme is retinyl ester synthase (RES), which converts retinol to retinyl ester. Finally, the third retinal enzyme is retinol dehydrogenase (RDH), which oxidizes 11-*cis* retinol to 11-*cis* retinal and would allow cones to regenerate pigment without involving the RPE.

The expression by Müller cells of the protein CRALBP, which specifically binds 11-*cis* retinol, implies that these cells may be involved in the chromophore visual cycle (Bunt-Milam and Saari 1983; Saari and Bredberg 1987). Indeed, Das et al. (1992) found that Müller cells in cone-dominated chicken retina are able to synthesize 11-*cis* retinol

from all-*trans* retinol. This suggests that Müller cells may be involved in regenerating cone visual pigment. Mata et al. (2002) proposed that the chromophore is recycled in the Müller cells and released into the cytoplasm to be taken up by the cones for the final enzymatic conversion to 11-*cis* retinal. They concluded that this separate pathway could regenerate opsin at a rate 20 times faster than the RPE pathway, which would account for the sustained photosensitivity of vertebrate retinas in daylight.

However, to be of any clinical relevance, this cone-specific pathway must be proven to be functional in human retinas. This was examined by taking ERG recordings from the fovea of freshly removed human retinas whose photoreceptors were initially bleached and then incubated in darkness for 3 hours following enucleation (Wang and Kefalov 2009). It was indeed found that, after dark adaptation, cones recovered their sensitivity whereas rods did not. Furthermore, when Müller cell function was inhibited with gliotoxin, recovery of cone threshold was prevented. These results demonstrate that the neural retinal visual cycle is indeed present in humans and is essential for maintaining cone-mediated daytime vision.

1.6.2.4 The Effect of Age & Pathology on Dark Adaptation

A common visual problem reported among older adults is difficulty seeing under low light levels, even in the absence ocular pathology (McGregor and Chaparro 2005). It has been shown that there is an increase in the scotopic absolute threshold of approximately 0.5 log units with age (Jackson et al. 1998). This is partly attributable to the increased crystalline lens density and senile miosis in the ageing eye (Sturr et al. 1997), but also correlates with histopathological studies reporting a 30% reduction in the density of rod photoreceptors from age 34 to 90 years (Curcio et al. 1993). However, since scotopic sensitivity loss among older adults is seen in peripheral retinal locations where there is minimal rod loss and is not worsened in areas of greater rod loss (Jackson et al. 1998), it follows that rod loss alone cannot account for this age-related decline in scotopic sensitivity. Furthermore, although rod density decreases with age, the remaining rod outer segments are seen to expand to fill any gaps and to maintain the rhodopsin coverage (Curcio et al. 1993). Since the concentration of rhodopsin remains constant throughout life, it cannot be a contributing factor in the reduced retinal sensitivity (Plantner et al. 1988).

Another possible explanation for symptoms of poor night vision in older adults is that

the retinoid cycle responsible for regenerating visual pigment slows with age, resulting in a reduced rate of dark adaptation, since a delay in the visual cycle would be associated with a delay in threshold recovery during dark adaptation. In 1992, the rate of foveal cone dark adaptation was found to decline with age (Coile and Baker 1992). This was confirmed by Gaffney, Binns, & Margrain (2012) who found that the time constant of cone recovery increased by 16.4s/decade of life (Gaffney et al. 2012). In 1999, Jackson and colleagues also found significant delays in rod-mediated dark adaptation with increasing age, particularly in the second and third components of recovery. Indeed, it took 10 minutes longer for 70-year-olds to regain their visual sensitivity than for those in their 20s, as seen in Figure 23 below (Jackson et al. 1999). These findings are consistent with the delay in rhodopsin regeneration with age found using retinal densitometry (Liem et al. 1991).

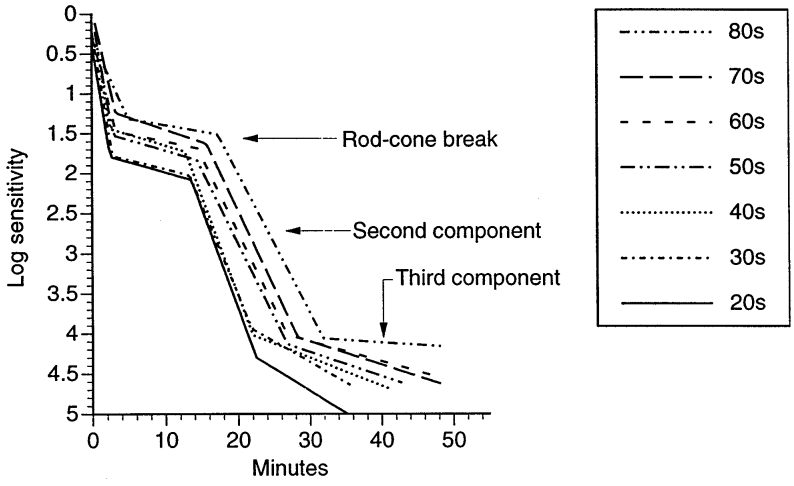

Figure 23. Dark adaptation as a function of decade. Arrows indicate the portion of the function representing the rod-cone break and the second and third components of rod-mediated dark adaptation. Note that with increasing decade, the curve shifts to the right, indicating a slowing of the rate of dark adaptation with increasing age (Jackson et al. 1999).

A likely reason for this slowing of visual pigment regeneration is that, with age, a progressive accumulation of lipids causes a thickening of Bruch's membrane (Newsome et al. 1987; Pauleikhoff et al. 1990; Bird 1992). This could reduce metabolic exchange of vitamin A by creating a diffusion barrier between the photoreceptors and the choroid, thus creating an effective retinol deficiency at the outer retina, and hence delaying rhodopsin regeneration (Bird 1992). Consistent with this hypothesis, psychophysical data show that rod-mediated dark adaptation was faster when older adults with normal retinal health received a high-dose (50,000IU) course of oral retinol

(preformed vitamin A) for 30 days (Owsley et al. 2006).

Since vitamin A is necessary for the retinoid cycle to work efficiently, it is not surprising that systemic deficiency of vitamin A leads to slowed pigment regeneration and dark adaptation (Kemp et al. 1988; Cideciyan et al. 1997). Similar complications are found in other diseases that affect the structures involved in the retinoid cycle, for example, Sorsby fundus dystrophy (Cideciyan et al. 1997; Jacobson et al. 1995), congenital stationary night blindness (Carr 1974), diabetic retinopathy (Greenstein et al. 1993; Henson and North 1979) and age-related macular degeneration (Brown and Kitchin 1983; Owsley et al. 2000; Owsley et al. 2001; Owsley et al. 2007; Dimitrov et al. 2008; Dimitrov et al. 2011; Gaffney et al. 2011).

1.6.2.5 Dark Adaptation and Age-Related Macular Degeneration

There is strong agreement in the literature that rod-mediated dark adaptation delays are a hallmark of early age-related macular degeneration (AMD) (Brown and Kitchin 1983; Owsley et al. 2000; Owsley et al. 2001; Owsley et al. 2007; Dimitrov et al. 2008; Dimitrov et al. 2011; Gaffney et al. 2011). The effect of early AMD on cone adaptation is a matter of debate, with some studies finding little evidence of delayed recovery after a bleach (Owsley et al. 2007) whilst others report a significant delay in cone adaptation (Phipps et al. 2003; Dimitrov et al. 2008; Gaffney et al. 2011; Dimitrov et al. 2011; Dimitrov et al. 2012; Gaffney et al. 2013).

Table 2 (Appendix 1) summarises twenty three studies investigating the effect of early AMD on dark adaptation. The earlier investigations were mainly concerned with the steady-state dark adaptation function, i.e. scotopic (rod-mediated) and photopic (cone-mediated) sensitivity. Scotopic sensitivity refers to the measurement of retinal sensitivity following a period of 30-45 minutes in the dark using a short-wavelength stimulus target (approx. 450-555nm). Conversely, photopic sensitivity measures sensitivity after a pre-adaptation period of 5-10 minutes to light using a long wavelength target (approx. 600-650nm). The kinetic aspect of dark adaptation predominates in latter studies, that is, the recovery of retinal sensitivity to its baseline level following a bright light that bleaches a significant amount of visual pigment, measuring both rod and cone function (Neelam et al. 2009).

Of the ten studies that investigated scotopic retinal sensitivity, the vast majority found a reduction in sensitivity with early AMD (Brown and Kitchin 1983; Brown et al. 1986a; Sunness et al. 1988; Steinmetz et al. 1993; Owsley et al. 2001; Owsley et al. 2000; Haimovici et al. 2002; Scholl et al. 2004), which is consistent with the histopathologic observations of rod vulnerability in this condition (Curcio et al. 1996; Medeiros and Curcio 2001). Scholl et al. (2004) reported a reduction in scotopic sensitivity even in eyes with drusen only. Sunness et al. (1988), found no difference in the scotopic sensitivity of areas overlying drusen compared with non-drusen areas, regardless of the size of drusen, which ranged from 120 to 340μm. This suggests that the sensitivity loss in early AMD is not co-localised to the position of the drusen, perhaps suggesting that it is not the presence of drusen *per se* which causes the elevation of threshold, but rather that the drusen are markers of underlying diffuse changes affecting sensitivity, which are not visible ophthalmoscopically. Sunness et al did, however, find marked sensitivity loss in areas of advanced AMD such as RPE atrophy. Haimovici et al. (2002) found that scotopic sensitivities in their cohort of 31 participants with early AMD were generally good, which in this case may have been because the patients were not selected on the basis of being symptomatic of night vision problems, unlike previous studies. They did, however, find the kinetics of dark adaptation to be dysfunctional in patients from all categories of early AMD. The fact that scotopic sensitivity and dark adaptation are not correlated with each other here suggests that the mechanisms underlying these functions are different. It is, therefore, possible that a person with normal scotopic sensitivity may have abnormal dark adaptation kinetics. Similarly, Owsley et al. (2001) found that out of their 20 early AMD patients, 85% had abnormal rod-mediated dark adaptation, whereas only 25% had reduced scotopic sensitivity. This implies that dark adaptation is better at detecting early functional deficits in AMD.

Indeed, fifteen studies investigating the kinetics of dark adaptation have found significant abnormalities in early AMD. A limitation of the earlier studies is that they did not classify early AMD using a standardised fundus grading system, therefore the subtype or severity or AMD investigated is unknown (Brown et al. 1986b). Furthermore, they tend to have smaller sample sizes, which weaken their diagnostic power (Brown et al. 1986a; Steinmetz et al. 1993). Despite these and other methodological differences in the literature, the general trend shows dark adaptation to

be consistently delayed in AMD. Owsley et al. (2001) measured rod dark adaptation in 20 participants with early AMD. After determining pre-bleach sensitivity following 30 minutes in the dark, subjects were exposed to a 0.25ms adapting light that bleached 98% of photopigment. Recovery was then examined using a 500nm target at 12^{o} inferior eccentricity. Figure 24 displays the dark adaptation plots for three people with AMD plotted alongside an age-matched control.

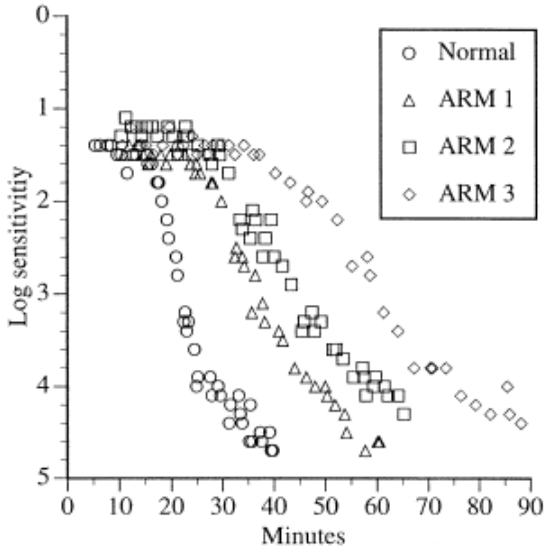

Figure 24. The dark adaptation functions measured in three people with AMD and one older healthy adult. All participants had at least 6/7.5 visual acuity (Owsley et al. 2001).

The rod-cone break was significantly delayed by approximately 10 minutes in AMD, a finding which has been substantiated by further studies (Owsley et al. 2007; Dimitrov et al. 2008; Jackson and Edwards 2008). The AMD group also had a slower recovery during the second component of dark adaptation than the control group. This prolongation of the time constant of rod-mediated dark adaptation demonstrates that AMD impairs the recovery of sensitivity in the visual cycle. In contrast to this, Jackson et al. (2006) did not find abnormalities in dark adaptation in 19 people with early AMD compared with elderly controls using the Scotopic Sensitivity Tester-1 (SST-1, LKC Technologies, Gaithersburg, MD, USA). The same group later designed a novel instrument to measure dark adaptation using a 4^{o} foveal stimulus (AdaptDx, Apeliotus Technologies, Atlanta, GA). The "rod intercept", i.e. the time taken for sensitivity to recover to a stimulus with a 4 log unit intensity, was measured since it reflected rod function only and took just 20 minutes to attain. Using this device, dark adaptation was substantially slower in early AMD compared with old and young controls, and the delay

increased with disease severity, which shows its potential to be used as a clinical outcome measure (Jackson and Edwards 2008). More recently, Jackson et al. found that a reduced testing time of up to 6.5 minutes using the AdaptDx had a diagnostic sensitivity of 90.6% ($P<0.001$) and a specificity of 90.5% ($P<0.027$) in a cohort of 127 AMD patients and 21 normal adults (Jackson et al. 2014). The clear discrepancy in findings between AdaptDx and SST-1 is likely to be due to the fact that the latter uses a full-field test stimulus, which elicits a response from the entire retina. In people with AMD, the sensitivity of the healthy peripheral retina would be likely to mask any small functional deficits at the macula, and thus a full-field stimulus is unlikely to be sensitive to early disease.

There is also evidence that delayed dark adaptation may predict the development of advanced AMD. In a small, 45-month prospective study of 18 patients by Sunness et al. (1989), foveal dark-adapted sensitivity predicted the development of advanced AMD in eyes with drusen with 100% sensitivity and 92% specificity. Haimovici et al. (2002) postulated that the fellow eye of patients with a RPE detachment would have significantly slower dark adaptation than the fellow eye of patients with CNV or drusen only. This hypothesis was based on the pathogenesis of retinal pigment epithelial detachment, and the increased risk of RPE detachment in the second eye of individuals with a unilateral detachment. The deposition of lipids in Bruch's membrane causes it to become hydrophobic. This reduces its hydraulic conductivity, causing retinal fluid to accumulate in the sub-RPE space, causing RPE detachment, and increasing the time taken for the photopigment to regenerate (Bird 1992). Hydraulic conductivity is thought to be more reduced in eyes at risk of RPE detachment than CNV (Bird 1992; Pauleikhoff et al. 1999). Haimovici et al. did find evidence that dark adaptation was more delayed in the fellow eyes of eyes with RPE detachments, although the differences between the groups did not reach statistical significance due to the limited sample size.

Until recently, histopathologic studies on human donor retinas with early AMD have only found rod photoreceptors to be affected in early stages of the disease (Curcio et al. 1996). Consistent with this evidence, Owsley et al. (2007) found disturbances in rod- but not cone- mediated dark adaptation in the parafovea (12^{o} eccentricity). They suggested that cones were unaffected due to the alternative source of retinol from the Müller cells, which allows cone photopigment to regenerate more rapidly than rods (see

section 1.6.2.3). However, in contrast to this, Dimitrov et al. (2008) found abnormal cone recovery dynamics in early AMD, using a 4 degree diameter foveally presented spot stimulus. Furthermore, Gaffney et al. (2011) found the time constant of cone recovery to be significantly impaired in early AMD compared with control subjects, when assessed using an annular target with a radius of 12^{o}. A possible reason for this conflicting evidence is the bleaching method used in the different studies, i.e. the latter study used a steady-state bleach lasting 2 minutes whereas Owsley et al. used an 11-millisecond photoflash. Steady-state bleaches involve prolonged metabolic activity, which could interfere with the Müller cell pathway causing cones to be more dependent on the 11-cis-retinal derived from the RPE, the structure that is damaged in early AMD (Gaffney et al. 2011). Therefore, a steady-state bleach could reveal impairments in cone-mediated dark adaptation that would be otherwise masked. It is also possible that the different stimulus sizes used to monitor threshold recovery could contribute to the discrepancy in results. The smaller the stimulus, the greater the variability in the data, since it will be more affected by focal retinal abnormalities (Gaffney et al. 2011). Indeed, Owsley et al. (2007), who used a small spot stimulus, found large standard deviations in their intermediate AMD cohort whereas Dimitrov et al. (2008), who used a larger spot stimulus, reported little variability in their data. Further studies by Dimitrov and colleagues (Dimitrov et al. 2011; Dimitrov et al. 2012) have confirmed that cone adaptation is just as diagnostic in early AMD as rod-mediated dark adaptation. This may be explained by the fact that rod and cone dark adaptation are both, ultimately, reliant upon the supply of retinal and metabolites from the choroidal circulation via Bruch's membrane and the RPE. Therefore, rod and cone adaptational defects may both reflect the same pathological changes to underlying structures.

In conclusion, patients with early AMD exhibit significant abnormalities in both scotopic sensitivity and the kinetic aspects of dark adaptation. However, the latter appears to be more sensitive in detecting functional impairments in early AMD and since it takes less time to perform, it is more clinically applicable. Both rod- and cone-mediated dark adaptation have been found to be diagnostic of early AMD. For this reason, dark adaptation has the potential to provide a functional measure of disease progression for monitoring the efficacy of potential new therapies in clinical trials.

1.6.3 Photostress Recovery Test (PSRT)

The photostress recovery test (PSRT), also known as glare or macular recovery, is a simple technique that assesses the dynamic response of the retina after exposure to an intense light, and measures the time taken for visual acuity or contrast sensitivity to recover to a pre-determined level (Margrain and Thomson 2002). It can be used to distinguish between macular disease and optic neuropathy when the retinal appearance is equivocal (Glaser et al. 1977). The reduction in sensitivity after intense illumination is primarily attributed to photopigment depletion and the rate of recovery is dependent upon the rate of photopigment regeneration (Margrain and Thomson 2002). Severin et al. (1963) postulated that a higher degree of macular function is required for the recovery of visual acuity than for contrast discrimination, since some patients with macular disease demonstrated prolonged visual acuity with normal contrast sensitivity (Severin et al. 1963).

The PST is an objective technique that takes very little time to perform and can be easily implemented in optometric practice. Why, then, is it seldom used? It must be due to the lack of standardised methodology and the wide variability in the observed recovery time (Neelam et al. 2009). Several studies have investigated the effect of age on PSRT on normal patients; however, the results are equivocal. Sandberg et al. (1995) found that recovery time increased by 0.19 log seconds per decade, whereas other investigators failed to find any effect of ageing on PSRT (Wu et al. 1990; Glaser et al. 1977). This inconsistency is mostly attributed to the lack of standardisation in test protocol. Wood et al (2011) showed that the reliability and repeatability of the ERG PST was improved by using an equilibrium bleach compared to a photoflash. Using this bleaching method, the time constant of recovery increased with age at a rate of 27 seconds per decade (Wood et al. 2011).

The Eger Macular Stressometer (EMS; Gulden Ophthalmics, USA) was developed in attempt to resolve these problems, and three published studies have examined its clinical validity in the assessment of macular disease (see Table 3 in Appendix I for a summary of studies investigating the PSRT in AMD). A pilot study using this device found no difference in EMS recovery time between patients with AMD (n=30) and those with cataract (n=30), diabetic retinopathy (n=16) or glaucoma (n=16) (Schmitt et al. 2003). However, Bartlett and colleagues found that patients with both early (n=17)

and advanced (n=12) AMD had significantly longer photostress recovery times with the EMS compared with age-matched controls. EMS sensitivity was moderate at 29% for early and 50% for advanced AMD, and readings were repeatable to within 7 seconds (Bartlett et al. 2004). Wolffsohn and colleagues found a much larger coefficient of repeatability (10.2 seconds) in their prospective study of 156 AMD patients (Wolffsohn et al. 2006). Furthermore, it was not predictive of those patients whose vision decreased over the following year. They concluded that the EMS with its short photoflash did not sufficiently bleach photopigment and hence was unable to identify people with AMD or to indicate risk of disease progression. Indeed, flash devices require accurate patient fixation and lack of blinking. Exposing the eye to light from a direct ophthalmoscope for 30 seconds has been suggested to be more reliable, since more visual pigment is bleached and pupil size effects are minimized (Margrain and Thomson 2002). Furthermore, a prolonged exposure to a high intensity light will result in an equilibrium being obtained between photopigment bleached and photopigment recovery, such that small losses in fixation or blinks are unlikely to have a substantial impact on the final level of pigment bleach obtained (Hollins and Alpern 1973).

The Macular Automated Photostress (MAP) test uses the Humphrey Field Analyser to evaluate foveal sensitivity before and after a photostress stimulus lasting 5 seconds (Dhalla and Fantin 2005). In a pilot study, foveal sensitivity after the macular photostress and recovery time to baseline sensitivity were significantly delayed in 15 people with AMD compared with 55 controls of varying age. Furthermore, recovery rate was delayed with increasing disease severity (Dhalla et al. 2007). Given that there is currently no published data on the repeatability of this device, its clinical applicability in detecting and monitoring AMD remains to be seen.

Despite the variability in methodology, the majority of studies investigating PSRT in patients with AMD have found a delayed recovery time compared with controls (Chilaris 1962; Severin et al. 1963; Forsius et al. 1964; Glaser et al. 1977; Smiddy and Fine 1984; Wu et al. 1990; Collins and Brown 1989; Cheng and Vingrys 1993; Remulla et al. 1995; Sandberg et al. 1998; Midena et al. 1997; Bartlett et al. 2004; Binns and Margrain 2007; Dhalla et al. 2007; Sandberg and Gaudio 1995). Indeed, Collins and Brown (1989) found significant delays in recovery time in people with early AMD and good visual acuity. The only two studies that failed to detect a significant difference

were likely due to the limitations of the EMS apparatus, as described above (Schmitt et al. 2003; Wolffsohn et al. 2006). There is, however, conflicting evidence regarding the correlation between PSRT and disease severity. Midena and colleagues (1997) found macular recovery function to be the most sensitive test in documenting the progression of AMD, due to the significant increase in PSRT with increasing drusen confluence, focal hyperpigmentation and geographic atrophy. Cheng and Vingrys (1993) also found a correlation between PSRT and pigmentary changes but, contrary to the previous study, they failed to detect any association between drusen confluence and PSRT. Smiddy and Fine (1984), in a prospective study (4.3 years) of 71 patients with bilateral drusen, found no relationship between PSRT and disease severity.

Sandberg et al. (1998) also conducted a prospective study evaluating the predictive value of PSRT in AMD. One hundred and twenty-seven patients with unilateral nAMD were observed for up to 4.5 years. PSRT was measured by recovery of VA in the fellow eye with early AMD (VA 20/20 to 20/60) following a 10 second exposure to a bleaching light. The risk of CNV development was found to increase by a factor of 30% for each additional minute of recovery time. Figure 25 demonstrates how the PSRT may be used to predict neovascularisation in the fellow eyes of patients with unilateral AMD.

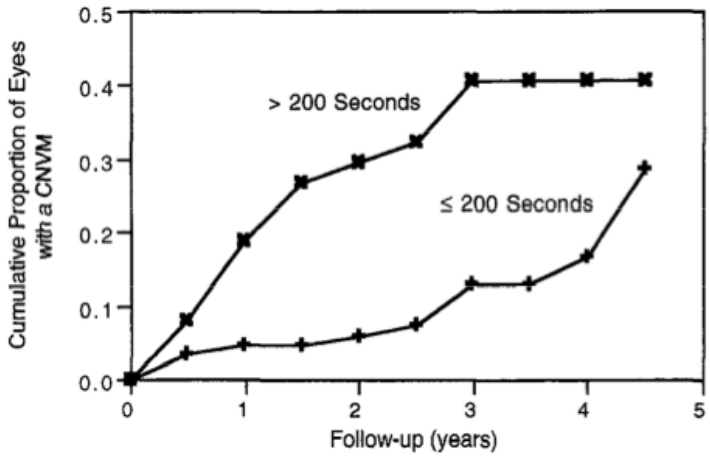

Figure 25. Cumulative proportion of at-risk patients who developed nAMD in their study eye statified by baseline PSRT. The number of patients at baseline were 88 in the group with a PSRT 200 seconds or less and 39 in the group with PSRT more than 200 seconds (Sandberg et al. 1998).

In conclusion, patients with early AMD clearly demonstrate a delay in PSRT compared with healthy controls. Whilst PSRT effectively reflects the kinetics of photopigment regeneration, as does the assessment of cone dark adaptation, the advantage of the

former is that it may be assessed rapidly in the clinic using basic equipment such as an ophthalmoscope and visual acuity chart. In addition, the recovery time may have the potential to predict those eyes at high risk of developing nAMD. However, a repeatable, standardised technique still needs to be developed in order for photostress recovery to be implemented in a clinical setting.

1.6.4 Colour Vision

Colour vision is another aspect of visual function that can be altered in AMD. The term colour vision describes the ability to distinguish objects on the basis of the wavelengths of light they emit. An individual will perceive a colour as a result of the photoreceptor reactions to the wavelength distribution and spatial variables (Neelam et al. 2009). There are three classes of cone photopigment: long-wavelength sensitive (L-cones), middle-wavelength sensitive (M-cones) and short-wavelength sensitive (S- cones). Figure 26 shows how these three have different spectral sensitivities; yet they overlap in some parts of the spectrum. L&M cones predominate in the fovea, whereas S cones, which make up 8-10% of total cone density, are relatively sparse at the fovea, peaking in concentration at the foveal slope (Williams et al. 1981; Neelam et al. 2009)

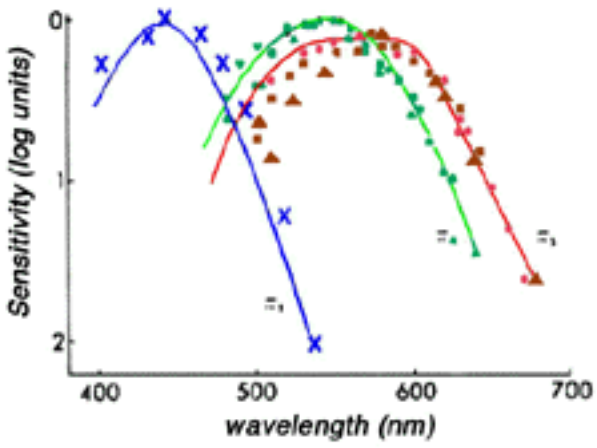

Figure 26. The absorption spectra of S-, M- and L-cones (Kalloniatis and Luu, 2011b).

A colour vision defect may be either congenital or acquired. The latter can be caused by a defect in any part of the chromatic pathway from the photoreceptors to the visual cortex. Changes to the optical media are also known to impair colour vision. One of the earliest changes to the visual system in degenerative retinal conditions, such as AMD, is a disruption of normal colour vision (Pokorny and Birch 1979). Certainly, a person

with macular disease can present with chromatic defects even when their visual acuity is normal (Bowman 1980; Applegate et al. 1987; Collins 1986). Table 4 (Appendix 1) summarises the main studies investigating colour vision defects in AMD. In 1912, Köllner postulated that blue-yellow defects are most prevalent in macular disease. This rule has since been corroborated by numerous studies (Collins 1986; Applegate et al. 1987; Cheng and Vingrys 1993; Holz et al. 1995; Arden and Wolf 2004). Red-green discrimination is thought to be more affected in the later stages of the disease (O'Neill-Biba et al. 2010). A number of techniques have been developed to assess these impairments in chromatic sensitivity, for example, surface colour methods (colour arrangement tests), colour matching and colour contrast sensitivity.

1.6.4.1 Colour Arrangement Tests

Surface colour tests have been the most commonly used techniques in both research and clinical environments to assess acquired chromatic loss. The Farnsworth-Munsell (FM) 100 hue test is often preferred for research purposes as it provides quantitative information regarding colour discrimination. However, in clinical practice, the Panel D-15 test is more often used because it takes less time and is simpler to perform. Note that it is necessary for these tests to be carried out under standard illumination levels (Commission Internationale de l'Eclairage, Standard Illuminant C) to provide accurate results (Neelam et al. 2009).

The FM-100 hue test was used in early studies to determine the relationship between colour vision and AMD. These studies showed an increase in tritan-like thresholds in the early stages of the disease (Bowman 1980; Applegate et al. 1987). Furthermore, colour vision was found to deteriorate with decreasing luminance to a greater extent in patients with AMD than in elderly controls (Bowman 1978; Bowman 1980). Applegate et al. (1987) tested the colour vision of 3 people with early AMD every 3-4 months for 2 years using the FM-100 hue and D-15 tests. Despite the modest sample size, it was found that tritan-like defects increased over time, particularly in one patient who developed a small, exudative PED. An increase in red-green sensitivity loss was also found in this patient at this stage. In contrast to the previous reports, Midena et al. (1997) failed to detect impairments in the chromatic sensitivity of 47 patients with early

AMD using the FM-100 hue test. They postulated that this was because the colour vision impairments in early AMD are too subtle to be detected by commercially available tests, such as the FM-100 hue. Atchison and Lovie-Kitchin (1990) also failed to observe a difference in chromatic discrimination between 15 early AMD subjects and 15 age-matched controls using the desaturated D-15. However, this was probably due to the fact that the early AMD cohort only had hard drusen and early pigmentary changes, which is a description of normal ageing changes rather than AMD.

Using the desaturated D-15 test, Collins (1986) found significant blue-yellow sensitivity losses in patients with normal visual acuity (6/6 or better) and pigmentary disturbances at the macula, compared with 11 age-matched controls. This implies that the desaturated D-15 test is more sensitive in detecting early functional defects than visual acuity. Unfortunately it is limited by a low specificity and has proved difficult for elderly patients to perform, hence producing many false positives (Cheng and Vingrys 1993). Additionally, a prospective 1-year study of 13 patients with early AMD found no significant change in the desaturated D-15 score over time (Feigl et al. 2004). This suggests that either chromatic sensitivity did not significantly deteriorate during this period, or that the test was simply unable to detect the deterioration. However, the study was limited by its small sample size, thus may not have been powered to detect significant changes in one year. Further longitudinal analysis using different tests is needed to determine the validity of using colour vision surface tests as a predictive biomarker for AMD.

1.6.4.2 Colour Matching

The trichromacy of normal human colour vision enables all colours to be matched by a mixture of three colours. This is the principle behind the anomaloscope, the gold standard method of distinguishing protan from deutan deficiencies. The observer is required to colour-match one half of a circular field illuminated with yellow with a mixture of red and green in the other half. Eisner and colleagues examined the predictive value of this technique and the D-15 test in their prospective study of 47 participants with unilateral nAMD who were followed for at least 18 months (Eisner et al. 1992). The D-15 test at baseline was moderately sensitive at predicting those subjects who would progress to nAMD, with 8 out of 11 failing the D-15 at baseline. However, as described above, it was neither specific nor independent of age. The

colour-match area, i.e. the difference in the amount of red and green required to match a smaller and larger subfield and thought to be an indicator of the quantum catching ability of foveal cones (Smith et al. 1988), was in the best predictor of disease progression when combined with dark adaptation time constant. The effectiveness of this combination was equal to the most effective funduscopic risk indicators. This may be due to the reduced quantal absorption capacity in some eyes with a neovascular outcome, resulting in a spuriously normal DA result, but an abnormal colour-match area.

1.6.4.3 Colour Contrast Sensitivity

The chromatic sensitivity of a normal trichromat can be displayed using a sequence of ellipses on the 1931 CIE chromaticity diagram. Isochromatic zones represent the corresponding results for dichromats (Birch et al. 1992). Provided that no luminance difference can be detected, colours within ellipses or isochromatic zones appear the same. It is essential for colour matching tests to achieve isoluminance by removing luminance contrast. Colour contrast sensitivity (CS) tests employ isoluminant stimuli which allow separation of a chromatic defect along the colour confusion lines (protan, deutan and tritan) from luminance contrast differences (Holz et al. 1995).

Holz et al. (1995) used a computer graphics technique developed by Arden et al. (1988) to evaluate colour contrast sensitivity in 84 patients with early AMD compared with age-matched controls over a 2 year follow-up period. At baseline, the mean foveal tritan threshold was elevated to 26% whereas the parafoveal tritan threshold was within normal limits. However, the parafoveal tritan threshold did not change significantly over time, whereas the foveal tritan threshold did. The colour contrast sensitivity for green and red did not show any significant change at either location. This implies that YB colour contrast sensitivity may serve as a measure of assessing progression of AMD over time, prior to visual acuity loss. In addition, the eight patients who developed nAMD or GA during the study had significantly higher tritan thresholds at baseline than those who did not progress to advanced AMD, which suggests that an increased tritan threshold may allow the identification of patients at higher risk of progression. This theory was substantiated by Frennesson et al. (1995) in their study of 27 patients with soft drusen, in which a correlation was found between tritan threshold and

fluorescein angiography. In 2004, Arden and Wolf measured colour contrast thresholds along tritan and protan confusion axes for two sizes of optotypes (6.5^{o} and 1.5^{o}). Every one of the 24 patients with AMD had tritan test results for the 1.5^{o} optotype greater than 2 standard deviations above the normal mean, and tritan abnormalities were even identified in the unaffected eyes of people with unilateral AMD (Arden and Wolf 2004).

A new computer-based technology has recently been developed for the assessment of colour vision by the Civil Aviation Authority. The Colour Assessment and Diagnosis (CAD) test employs the statistical limits of colour discrimination in normal trichromats and is thought to be able to detect, classify and monitor both small and large colour deficiencies (Barbur and Rodriguez-Carmona 2006). The CAD test is able to isolate red-green (RG) and yellow-blue (YB) thresholds by using dynamic luminance contrast noise to mask any luminance contrast cues that may be present in the test stimulus (Birch et al. 1992). A four-alternative, forced-choice technique is used to measure the patient's chromatic thresholds along 16 different directions in colour space, ensuring that the patient is relying entirely on the use of colour signals to discriminate the direction of motion of the colour-defined stimulus (Barbur et al. 2009a). The thresholds of 238 normal trichromats and 250 colour deficient observers have been measured to provide the statistical limits for the standard normal (SN) observer on the CAD test (Barbur and Rodriguez-Carmona 2006). Figure 27 shows the CAD test template for the SN observer.

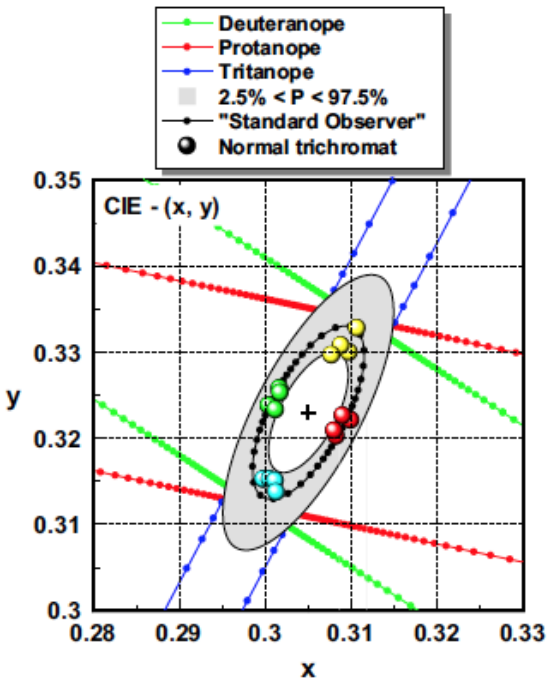

Figure 27. Data showing the 97.5 and 2.5% statistical limits that define the "standard" normal CAD test observer (in grey). The dotted, black ellipse is based on the median RG and YB thresholds measured in 250 observers. The deuteranopic, protanopic and tritanopic confusion bands are displayed in gree, red and blue, respectively. The background chromaticity (x,y) is indicated by the black cross (0.305, 0.323). The coloured symbols show data measured for a typical normal trichromat. (Barbur and Rodriguez-Carmona 2006).

In 2010, O'Neill-Biba et al. examined the loss of chromatic sensitivity in both eyes of 18 patients with varying severity of AMD severity using the CAD test (O'Neill-Biba et al. 2010). All subjects with AMD displayed abnormal YB and RG thresholds. The greatest loss was recorded in YB thresholds, and was seen to increase linearly with disease severity. This once again suggests that YB loss is a good indicator of disease progression. Interestingly, the fellow normal eye of one patient with unilateral nAMD showed the greatest YB loss in the clinically normal eye. It would therefore be of value to see if this finding extends to other patients with unilateral nAMD, and to determine whether YB CAD thresholds can be used to determine the eyes at risk of progression. The authors postulated that the greater YB than RG loss found may be due to the relative fragility and scarcity of S-cones, which would therefore have a larger effect on YB sensitivity (Nork 2000). The loss may also be due to receptoral or post-receptoral damage (O'Neill-Biba et al. 2010), or a selective susceptibility of the S-cone pathway to hypoxic damage (Hood et al. 1984). Evidently, the structural cause behind this

functional abnormality remains to be seen. However, it is clear that the YB chromatic deficiencies found in early AMD have the potential to be used as biomarkers for disease progression, and further longitudinal studies are necessary to substantiate this possibility.

1.6.5 Temporal Sensitivity

Temporal sensitivity describes the ability of the eye to respond to a flickering light. It has been suggested that temporally modulated stimuli may be used to detect functional deficiencies of the retina earlier than static stimuli due to the increased metabolic demand elicited by the task (Phipps et al. 2004; Kiryu et al. 1995). The human eye is able to resolve flickering stimuli up to 60-80 Hertz (Hz) (Brown and Kitchin 1987b). However, above 10-20 Hz, visual sensitivity is reduced due to the numerous neural filtering stages, distributed across retinal and cortical loci, that are involved in the processing of high temporal frequencies (Shady et al. 2004). The magnocellular and parvocellular visual pathways are thought to be sensitive to higher and lower temporal frequencies, respectively (Seiple et al. 2001).

The two types of stimuli used in assessment of temporal sensitivity are mean-modulated flicker (Figure 28, top panel) and luminance-pedestal flicker (Figure 28, bottom panel). The former modulates luminance about a mean background level and so does not alter the time-averaged luminance (Mayer et al. 1992b). The latter modulates a luminance increment, which results in a flickering component and increases the time-averaged luminance above the background level (Phipps et al. 2004). Flicker can also be modulated according to different temporal luminance profiles, for example, square-wave, sinusoidal and saw tooth. The opponent (chromatic) and non-opponent (luminance) systems mediate flicker detection for low and high alteration rates, respectively (Mayer et al. 1994).

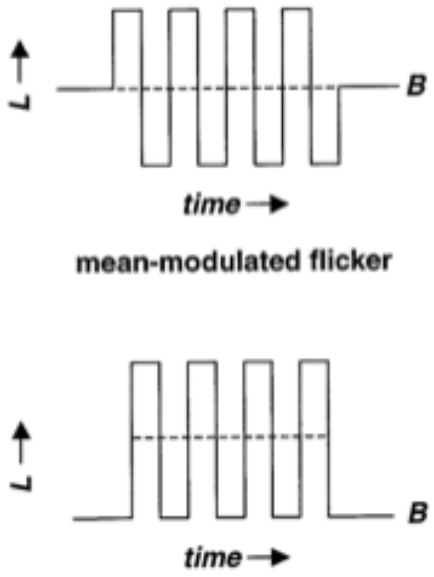

Figure 28. Diagram illustrating the differences between mean-modulated flicker and luminance-pedestal flicker. L: luminance; B: background luminance (Anderson and Vingrys 2000).

A number of studies (Table 5, Appendix I) have established a loss of temporal sensitivity in patients with AMD (Mayer et al. 1992a; Mayer et al. 1992b; Mayer et al. 1994; Phipps et al. 2004; Dimitrov et al. 2011; Luu et al. 2013), which is greater than the generalised loss of flicker sensitivity that occurs in normal ageing (Kim and Mayer 1994).

1.6.5.1 Critical Flicker Frequency

The critical flicker frequency (CFF) is the highest rate of flicker that can be detected at a given modulation depth, and is the temporal analogue of spatial visual acuity resolution. Since it only measures one part of the temporal contrast sensitivity function, it provides less information regarding the eye's temporal sensitivity (Alexander and Fishman 1984). Brown and Lovie-Kitchin demonstrated a significant reduction in CFF in patients with early AMD compared with age-matched controls (Brown and Lovie-Kitchin 1987b). Furthermore, unlike in healthy contral eyes, they found no variation in CFF with increasing retinal eccentricity in patients with AMD, indicating that temporal function does not vary across the retina. These authors later found that temporal summation was unaffected in AMD, and concluded that the mechanisms that mediate

temporal summation are more resistant than temporal discrimination to the structural damage which occurs in AMD (Brown and Lovie-Kitchin 1989).

1.6.5.2 Temporal Contrast Sensitivity

The temporal contrast sensitivity (TCS) function, as depicted in Figure 29, is a measure of how temporal contrast sensitivity varies with the temporal frequency of a sinusoidal flickering stimulus (Neelam et al. 2009). The eye is most sensitive to flicker of 15 to 20Hz at high luminances, i.e. photopic vision. Temporal sensitivity decreases gradually, and peak sensitivity and the high frequency cut-off shift towards lower temporal frequencies, as luminance is reduced.

Brown and Lovie-Kitchin investigated TCS in people with early AMD compared with age-matched controls across a wide range of temporal frequencies, and found that AMD causes the greatest reduction in sensitivity at low and medium temporal frequencies (Brown and Lovie-Kitchin 1987b). It is debatable as to whether temporal sensitivity loss in AMD is caused by photoreceptoral or post-receptoral damage (Hogg and Chakravarthy 2006). An investigation of two-colour increment thresholds and flicker contrast thresholds in patients with AMD and healthy controls revealed that the ability to detect 25Hz flicker was significantly reduced in AMD, despite having normal L-cone increment thresholds (Haegerstrom-Portnoy and Brown 1989). This was substantiated by Applegate et al, who detected a 0.5 log unit reduction in flicker sensitivity in patients with early AMD with normal L-M cone sensitivities (Applegate et al. 1987). If temporal sensitivity loss occurred at the level of the photoreceptors, there would have been a greater L-M cone deficiency. This led both groups to propose that a post-receptoral channel involved in flicker detection may be affected in AMD.

Visual stimulation by a flickering stimulus increases the metabolic demand of the inner retina (Falsini et al. 2002), leading to increased optic nerve blood flow (Garhöfer et al. 2004) and chorioretinal vascular oxygen tension (Shakoor et al. 2006) in addition to a compensatory retinal vasodilation (Formaz et al. 1997). In patients with AMD, these structural mechanisms may be impeded so that further compensation cannot occur, allowing clinical detection of the resulting functional impairments (Feigl et al. 2007a).

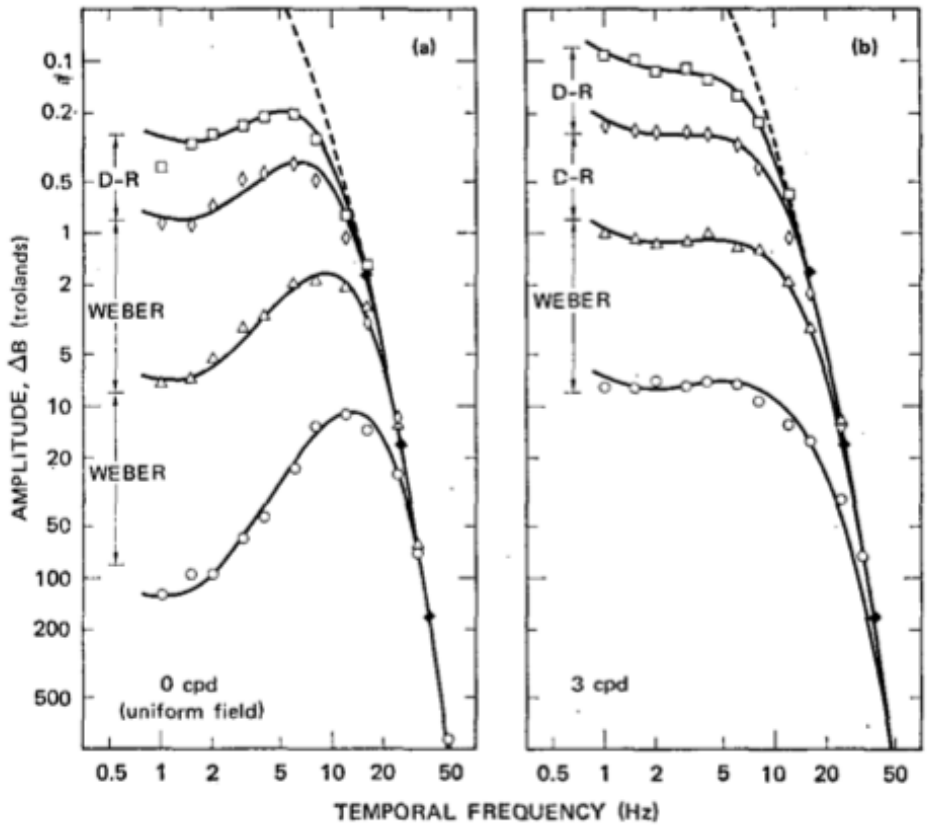

Figure 29. Temporal Contrast Sensitivity Function for spatial frequencies of 0 (a) and 3 (b) cycles/deg, and different adaptation levels of 1.67 (squares), 16.7 (diamonds), 167 (triangles) and 1670 td (circles) (Kelly 1972).

Mayer and colleagues investigated temporal contrast sensitivity in the fellow eyes of patients with unilateral nAMD. They, too, found the greatest reduction in foveal flicker sensitivity at mid-temporal frequencies in patients with AMD (Mayer et al. 1992b). Using step-wise discriminant analysis, they also found that healthy eyes could be distinguished from those at risk of developing nAMD with a 78% accuracy using 10 or 14Hz flickering stimuli (Mayer et al. 1992a). In a longitudinal follow-up study, they found that flicker modulation sensitivity (5 and 10Hz) at baseline was able to discriminate a pre-exudative eye from a healthy eye with 100% accuracy (Mayer et al. 1994). However, since this was a post-hoc analysis, it should be interpreted with caution.

Similarly, Dimitrov et al. (2011) found that 4 and 14Hz flicker thresholds had a moderate ability to detect abnormal cases of AMD, and were able to diagnose AMD with a ROC analysis AUC of 0.82 (±0.023) and 0.84 (±0.021) respectively. Flicker is

an ideal test to monitor functional changes in early AMD, as it is fast, reproducible, user-friendly and highly diagnostic. For this reason, Dimitrov and colleagues rated 14 Hz flicker highest amongst a battery of other functional tests as the most potentially useful clinical tool in the diagnosis and monitoring of AMD (Dimitrov et al. 2011). In a further study of 357 participants (64 controls and 293 AMD patients classified into 12 subgroups according to disease severity), the same group found that 14Hz flicker declined gradually along the entire hierarchy of retinal changes (Dimitrov et al. 2012). This supports the claim that flicker may be an effective tool for following AMD progression and assessing the efficacy of therapeutic interventions. However, more prospective studies need to be carried out in order to substantiate these findings.

1.6.6 Spatial Contrast Sensitivity

Spatial contrast threshold describes the smallest detectable difference in luminance between two components of a scene, as a proportion of the mean or background light level. The clinically measured contrast sensitivity (CS) is the reciprocal of this threshold. Figure 30 depicts the contrast sensitivity function (CSF) for different age groups, which is determined by measuring the spatial contrast threshold for the detection of sinusoidal gratings over a range of spatial frequencies. The curve follows a band-pass function, peaking at mid-spatial frequencies (2-6 cycles/degree) with a gradual roll-off at lower and a steeper cut-off at higher spatial frequencies (Campbell and Green 1965). Visual acuity represents the maximum spatial frequency that can be detected at 100% contrast. The main factors limiting the CSF include optical changes such as diffraction and aberrations, and neural changes such as spatial summation (Owsley et al. 1983; Owsley 2003).

Since CS is mediated by lateral inhibitory mechanisms from retinal horizontal and amacrine cells, it may be more sensitive to local retinal pathology than other functional techniques (Hogg and Chakravarthy 2006). Furthermore, the assessment of contrast sensitivity may be a better indicator of an individual's visual abilities in daily life compared with the traditional high-contrast visual acuity measurement. Indeed, a two-fold decline in CS is associated with a three- to fivefold increased chance of reporting difficulty with daily tasks (Rubin et al. 2001).

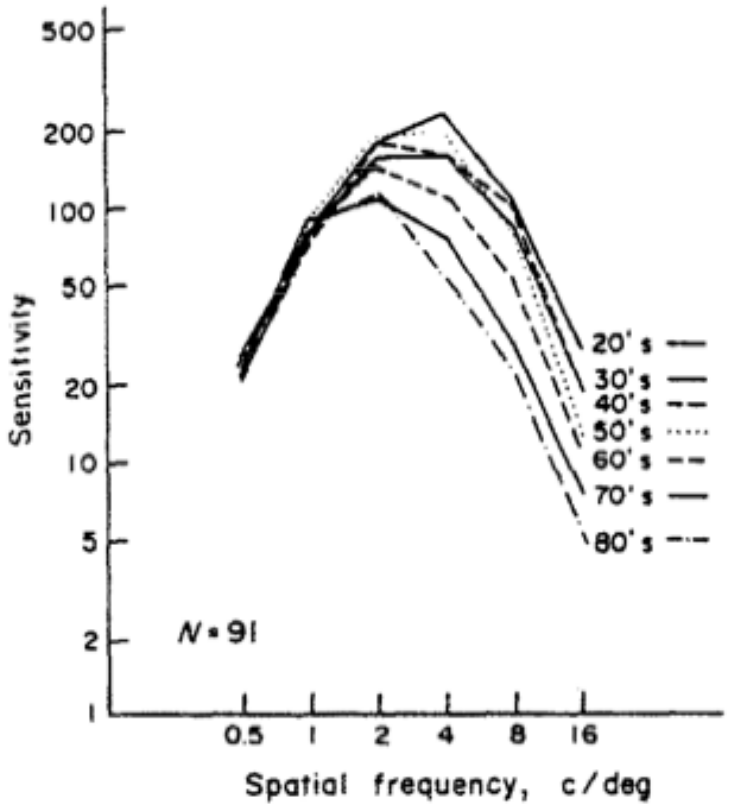

Figure 30.

Photopic contrast sensitivity function for different age groups (Owsley et al. 1983).

The most common method used to measure CS in clinical research is to use sinusoidal gratings of varying contrast, presented on a computer monitor. However, despite their ability to measure CS over a wide range of spatial frequencies, the task is time-consuming and therefore unsuitable for use in clinical practice. A viable alternative is to use letter-optotype charts, for example, the Pelli-Robson chart. The advantages of this chart are that patients are more familiar with the task, it is inexpensive, abnormal results can be compared with normative data (Elliott et al. 1990) and it is a reliable indicator of reading performance (Whittaker and Lovie-Kitchin 1993). However, threshold is assessed for one letter size only, so limited spatial frequency data are obtained.

It is well known that most older adults exhibit a reduction in photopic spatial contrast sensitivity in the absence of ocular or neurological disease, as seen in Figure 30 (Owsley et al. 1983; Burton et al. 1993; Elliott et al. 1990). However, sensitivity to lower spatial frequencies is relatively spared in photopic conditions (Owsley 2011). Using the Pelli-Robson chart, Elliott and colleagues found that the average CS among

older adults was 1.65 log units, compared with 1.80 log units in the younger population. Furthermore, older adults in their 70s require three times more contrast to detect a stimulus than adults in their 20s. The reduction in CS with increasing age should therefore be taken into consideration when examining visual function in AMD.

1.6.6.1 Contrast Sensitivity and AMD

The earliest study examining the effect of AMD on contrast sensitivity was conducted by Sjostrand and Frisen in 1977. In their cohort of 3 subjects with AMD and 10 healthy controls, it was found that patients with relatively good visual acuity showed a marked deficit in contrast sensitivity for medium and high spatial frequencies. In more advanced AMD, the impairment also extended to lower spatial frequencies (Sjostrand and Frisén 1977). A later study postulated that this might be because advanced AMD affects a wider retinal area (Sjostrand 1979). However, since the control subjects were not age-matched, this finding could simply be due to normal ageing changes. A larger study involving 100 patients with AMD found a reduction in peak contrast sensitivity in 80% of the AMD cohort compared with elderly controls (Alexander et al. 1988). Peak contrast sensitivity and visual acuity had a correlation coefficient of 0.62 in this study; however, Hyvarinen et al. showed that AMD can cause a considerable dissociation between these two functional tests. They proposed the concept of "hidden vision" in which advanced AMD patients may have greatly reduced visual acuity with nearly normal CS at medium and low spatial frequencies, or vice versa (Hyvärinen et al. 1983).

People with AMD often have difficulties in adapting to changes in luminance level. These symptoms led Brown and colleagues to examine the effect of luminance on the CSF of 6 people with AMD and 5 age-matched controls (Brown and Kitchin 1983). The contrast sensitivity of the individuals with AMD was depressed at photopic and mesopic luminances and relatively spared at scotopic luminances, with the peak of their CSF shifting to low SFs at all luminance levels. These findings suggest that the adaptation mechanisms responsible for achieving optimal contrast sensitivity in medium and high light levels are disrupted in AMD.

Several cross-sectional studies have been conducted to determine whether there is any correlation between CS and disease progression. Midena et al. (1997) examined the

contrast sensitivity of 47 subjects with early AMD, using sinusoidal gratings of five different SFs. Although contrast sensitivity was significantly impaired in the participants with early AMD compared with age-matched controls, there was no significant difference between subjects with bilateral early AMD and unilateral neovascular AMD. This substantiates the previous findings of Stangos and colleagues, who concluded that contrast sensitivity was not a good predictor of conversion to neovascular AMD (Stangos et al. 1995). However, in the same study Midena did find a progressive impairment of contrast sensitivity at higher spatial frequencies, which was associated with the severity of fundus appearance in terms of drusen confluence, presence of geographic atrophy and focal RPE hyperpigmentation (Midena et al. 1997). Similarly, Kleiner et al. found a reduction in peak CS with increasing drusen severity (Kleiner et al. 1988). This suggests that CS loss may reflect disease progression in terms of retinal appearance, and may be due to a selective impairment of different retinal cells and neural channels in AMD.

One of the main limitations of CS is that it is not selectively affected in AMD. Despite this, it is still a useful functional test. Indeed, various clinical trials of therapeutic interventions for AMD have used contrast sensitivity as an outcome measure (Bellmann et al. 2003; Bressler 2001). Bellmann et al. (2003) looked at VA and CS changes over 2 years and found that, although VA and CS only show a moderate correlation, they both provide important information regarding functional ability. There is a strong association between CS loss and difficulty in daily living tasks such as facial recognition, seeing kerbs and other low-contrast structures (Marron and Bailey 1982). For this reason, contrast sensitivity is able to examine the functional effect of potential new therapies on a patient's visual disability and hence, their quality of life.

1.6.7 Discussion

Studies investigating colour-matching ranges (Smith et al. 1988; Eisner et al. 1992), cone-adaptational kinetics (Phipps et al. 2003; Dimitrov et al. 2008; Gaffney et al. 2011; Dimitrov et al. 2011; Dimitrov et al. 2012), colour contrast sensitivity (Holz et al. 1995; Arden and Wolf 2004; O'Neill-Biba et al. 2010), temporal vision (Brown and Kitchin 1987b; Mayer et al. 1992b; Mayer et al. 1994; Phipps et al. 2004; Dimitrov et al. 2011; Dimitrov et al. 2012; Luu et al. 2013), and contrast sensitivity (Sjostrand and Frisén

1977; Sjostrand 1979; Brown and Garner 1983; Brown and Kitchin 1987a; Kleiner et al. 1988; Midena et al. 1997) all report that there is a high degree of cone dysfunction in early AMD. Abnormal rod function is evidenced by the elevation of scotopic thresholds (Brown and Kitchin 1983; Steinmetz et al. 1993; Owsley et al. 2000; Owsley et al. 2001) and delayed rates of rod adaptation (Owsley et al. 2001; Haimovici et al. 2002; Owsley et al. 2007; Jackson and Edwards 2008; Dimitrov et al. 2008; Dimitrov et al. 2011; Dimitrov et al. 2012; Jackson et al. 2014).

Histopathological studies on donor retinas show that there is a preferential loss of rods over cones in early AMD with maximum loss occuring in the parafovea i.e. 3.5-10 degrees from fixation. Furthermore, the vast majority of photoreceptors remaining in eyes with late AMD are cones (Curcio et al. 1996; Medeiros and Curcio 2001). Whilst this may support the evidence of rod dysfunction in AMD, it does not explain the mounting psychophysical evidence that shows cone dysfunction to be a reliable predictor of early AMD. This discrepancy led Shelley and colleagues to study the morphological differences between the macular photoreceptors in eyes with AMD compared with normals (Shelley et al. 2009). They found that although rod death did indeed precede cone death, numerous cone nuclei were displaced or prolapased, which would cause them to lose their synaptic contact and thus affect their functionality (Gartner and Henkind 1981). Furthermore, they found an abnormal distribution of opsin and distal cone axon anomalies in the normal aged macula which may suggest a predilection to AMD. Sullivan, Woldemussie and Pow (2007) reported similar findings of aberrant cone axon projections into the OPL in AMD . This new evidence provides a possible explanation as to why cone function has been repeatedly found to be affected in psychophysical AMD studies.

As outlined in Section 1.3.7, a complex interaction of oxidative stress, genetics, inflammation and environmental influences have been linked to the pathogenesis of AMD (Lange and Bainbridge 2012). It has also been suggested that outer retinal ischaemia and hypoxia are involved in AMD progression (Feigl 2009; Stefánsson et al. 2011). It is still not certain whether the functional deficits found in early AMD, such as abnormal dark adaptation kinetics, are originally caused by photoreceptoral or post-receptoral abnormalities (Feigl et al. 2007a), or by morphological changes to structures such as the RPE/Bruch's membrane complex (Guymer et al. 1999; Pauleikhoff et al.

1990) and the choroid (Chen et al. 1992; Ciulla et al. 2002; Metelitsina et al. 2008). If the primary location of damage is known, it will improve the efficiency of future therapies in early AMD.

1.7 Overview and Aims

Age-related macular degeneration is the leading cause of visual impairment in the developed world. Despite recent developments in treatment options for wet AMD with the introduction of anti-VEGF therapies such as Ranibizumab, there remains as yet no treatment for dry AMD. With the predicted ageing of the population in future years, the prevalence of this blinding eye condition will continue to escalate, causing not only personal suffering for those affected but also significant financial burdens on national healthcare institutions. For this reason, there is a pressing need to evaluate new treatments for early AMD to prevent the progression of the disease. Furthermore, with the development of these novel therapies, there is also a need for functional biomarkers with a high sensitivity and specificity in order to identify patients at risk of the development and progression of AMD and to evaluate the efficacy of new treatment options.

There is a body of evidence to suggest that outer retinal hypoxia may play a role in the pathogenesis of AMD. The oxygen demand of the retina is at its greatest in the dark, when the metabolic activity of the photoreceptors is upregulated to support the dark current. It has been hypothesized that, by illuminating the retina with a low level of light through the night, the progression of diseases with a hypoxic mechanism may be slowed. In order to conduct a clinical trial of such an intervention, it is first necessary to use the current evidence base to optimize the study design.

Therefore, the aims of this study were to:

1) Develop functional biomarkers for early AMD, and to determine their repeatability so that they may be implemented in future clinical trials exploring novel interventions for age-related macular degeneration.

2) Investigate the topography of dark adaptation deficits in AMD in order to determine the most appropriate stimulus for assessing dark adaptation in future clinical trials of treatments for AMD.

3) Develop a protocol for a clinical trial investigating the effect of low-level night-time light therapy in age-related macular degeneration.

Chapter 2. The Topography, Repeatability and Diagnostic Validity of Dark Adaptation

2.1 Introduction

Dark adaptation kinetics have been examined since 1935 in order to evaluate outer retinal function (Hecht et al. 1935; Hecht et al. 1937; Haig 1941; Henson and North 1979; Lamb and Pugh 2004; Jackson and Edwards 2008) and have played a significant role in the diagnosis of conditions such as retinitis pigmentosa (Sandberg et al. 1999), vitamin A deficiency (Kemp et al. 1988; Cideciyan et al. 1997) Oguchi disease (Lamb and Pugh 2004), fundus albipunctatus (Cideciyan et al. 2000), diabetic retinopathy (Phipps et al. 2006) and AMD (Owsley et al. 2001; Phipps et al. 2003; Binns and Margrain 2007; Owsley et al. 2007; Dimitrov et al. 2008; Dimitrov et al. 2011; Gaffney et al. 2011).

Only a small number of studies have examined the effect of retinal location on the dynamics of dark adaptation (Hecht et al. 1935; Dimitrov et al. 2008; Gaffney et al. 2011). These are in agreement that with increasing retinal eccentricity, the RCB takes place sooner, the rod branch of the curve is more prominent and a lower final threshold is obtained. A possible reason for this variability in dark adaptation with different retinal locations is the relative photoreceptor density and receptive field size. The maximum density of cone photoreceptors is found at the fovea (200,000cells/mm^2), decreasing rapidly with increasing eccentricity. This is reflected in the shape of the dark adaptation curve using a foveal stimulus, in which a prominent cone branch is produced. Ganglion cell density peaks 1.5-7^o from the fovea and declines with increasing eccentricity so that the dendritic and thus receptive field size has to increase accordingly (Dacey and Petersen 1992). Rod photoreceptors first appear in the parafovea, increasing with eccentricity to a maximum density at approximately 12-18^o from the fovea (150,000cells/mm^2) (Curcio et al. 1990). Consequently, the rod branch of the dark adaptation curve becomes increasingly more prominent and the absolute threshold decreases.

There is a growing amount of evidence to suggest that dark adaptation is a sensitive biomarker in AMD (Brown and Kitchin 1983; Eisner et al. 1991; Owsley et al. 2001;

Phipps et al. 2003; Binns and Margrain 2007; Owsley et al. 2007; Dimitrov et al. 2008; Dimitrov et al. 2011; Gaffney et al. 2011; Dimitrov et al. 2012). Indeed, abnormalities in dark adaptation appear to be the most sensitive indicators of the condition when compared with other aspects of visual function (Eisner et al. 1991; Owsley et al. 2001; Phipps et al. 2003; Dimitrov et al. 2011). For example, Dimitrov et al. found the rate of rod recovery in dark adaptation to have the best diagnostic capacity compared with flicker sensitivity, photostress recovery and colour vision (Dimitrov et al. 2011). However, the lengthy recording period and test difficulty led the researchers to conclude that it had limited clinical applicability. For this reason, the measurement of cone dark adaptation has been of interest due to its ability to detect people with AMD with a shorter test duration (Phipps et al. 2003; Dimitrov et al. 2008; Gaffney et al. 2011)

Gaffney et al. (2011) investigated the diagnostic ability of cone dark adaptation using a foveal spot of 0.5^{o} radius and achromatic annuli of 2^{o}, 7^{o} and 12^{o} radii. They found that the time constant of cone recovery had the greatest diagnostic potential when measured using a 12^{o} annular stimulus, providing an area under the ROC curve of 0.99 ± 0.02. Given that this parameter may be quantified in as little as 10 minutes, this has great clinical potential. However, due to the relatively small sample size (n=10), the results of the study may have been influenced by outliers. In addition, since the stimuli investigated were not area-matched, there remains some uncertainty as to whether the 12^{o} stimulus truly has a greater diagnostic potential than the 0.5 ^{o}, 2^{o} or 7^{o} stimuli, or whether it just had less variability due to the larger area of retina stimulated. Furthermore, for dark adaptation to be implemented as a functional biomarker in a clinical trial, it is necessary to determine its inter-session repeatability.

2.2 Aims

Given the heterogeneity of the retinal mosaic, one would assume that dark adaptation would vary with retinal location. The first aim of this study was to re-assess the dynamics of dark adaptation as a function of retinal eccentricity in a group of healthy participants using area-matched stimuli. Since the ultimate goal is to implement the dark adaptation procedure in a clinical environment, the second aim was to assess the inter-session repeatability of dark adaptation at each retinal location. The final aim was to assess the diagnostic ability of dark adaptation in the assessment of AMD, to

determine which retinal location provided the best discrimination between people with early AMD and healthy controls.

2.3 Methods

Participants

The first part of this study addressing aims 1 and 2 involved the recruitment of 10 healthy older adults and 11 healthy young adults. To address aim 3, an additional 11 participants with AMD were recruited. All participants had a corrected visual acuity of 6/7.5 or better in the test eye, clear ocular media, Van Herick anterior chamber angle grade 2 or higher, normal retinal appearance and no history of ocular or systemic pathology or medication known to alter retinal function. Written informed consent was received from all participants prior to commencing the study, and all procedures were carried out in accordance with the tenets of the Declaration of Helsinki.

Apparatus

All stimuli were displayed on a calibrated, high-resolution CRT monitor (Iiyama LS 902UT) driven by an 8-bit graphics board (nVIDIA Geforce 9) under software control (MATLAB, R2009a, The MathWorks Inc). The luminance output of the monitor was γ-corrected (Metha et al. 1993) and its background luminance (-0.85 log cd/m2) was attenuated throughout all recordings by a 1.2 neutral density (ND) filter. As the subject approached the lower end of the luminance range, additional filters were mounted on the screen to determine the full extent of retinal threshold recovery. The three stimuli generated were a spot of 2 ^{o} radius, 2^{o} width (area 12.56) and annuli of 7^{o} radius, 0.3^{o} width (area 12.91) and 12^{o} radius 0.2^{o} width (area 14.95), as depicted in Figure 31.

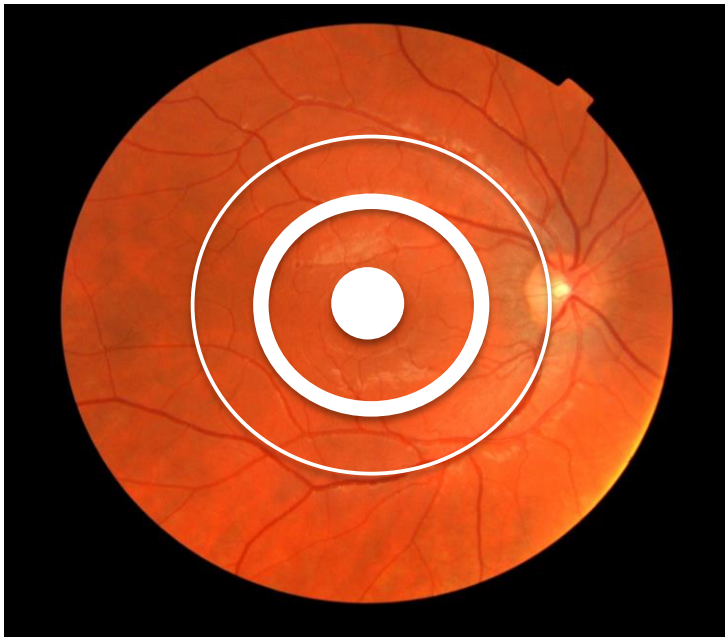

Figure 31. Diagrammatic representation of the three stimuli (2^{o} radius spot, 7^{o} radius annulus and 12^{o} radius annulus) centred on the fovea of a healthy participant.

Dark adaptation was monitored using a computerized 3-down 1-up modified staircase psychophysical procedure (Jackson et al. 1999). The protocol was similar to previous work carried out and published in our laboratory (Gaffney et al 2011). Each stimulus was presented for 200ms followed by a 600ms response window with a random interstimulus delay of 0.9 to 2.4 seconds. If the subject failed to respond to the stimulus in 600ms, the intensity of the stimulus was increased by 0.1 log units. If, however, the participant responded correctly to the stimulus within 600ms, the luminance of the stimulus was reduced by 0.3 log units on the following presentation. Dark adaptation recovery was sampled for 25 minutes in all participants. The code for this MATLAB programme can be found in Appendix II ('The topography of dark adaptation').

Experimental procedure

At the participant's first visit, baseline examinations of patient history, logMAR visual acuity (ETDRS), fundus photography (Canon CR-DGi Camera) and media opacity grading (Chylack et al. 1993) were conducted. Participants were then dilated with one drop of 1.0% tropicamide in the test eye before dark adaptation was carried out. The eye with better visual acuity was chosen as the test eye. If acuities were equal, the right eye was tested. Refractive correction was worn as necessary and the fellow eye was occluded with an eye patch. All participants were given instruction on how to perform

the dark adaptation test, after which they undertook a 5-minute practice session. This was repeated until the participant's performance was deemed to be proficient by the investigator.

A Maxwellian view optical system (Figure 32) incorporating an amber filter (LEE filters HT 015 'deep straw') was used to bleach 84% of cone photopigment and 74% of rod photopigment (5.20 log phot Td.s^{-1}) (Hollins and Alpern 1973) in the central 43.6^{o} of the test eye for 120 seconds. After the bleach, all lights were extinguished and participants were instructed to place their chin on the rest facing the computer screen and the dark adaptation programme simultaneously commenced. Participants focused their test eye on the fixation cross in the centre of the screen (or the gap in the middle of the cross for the 2^{o} spot stimulus) and indicated when they perceived the flashing stimulus using the computer keyboard. Threshold recovery was continuously monitored for 25 minutes for each stimulus.

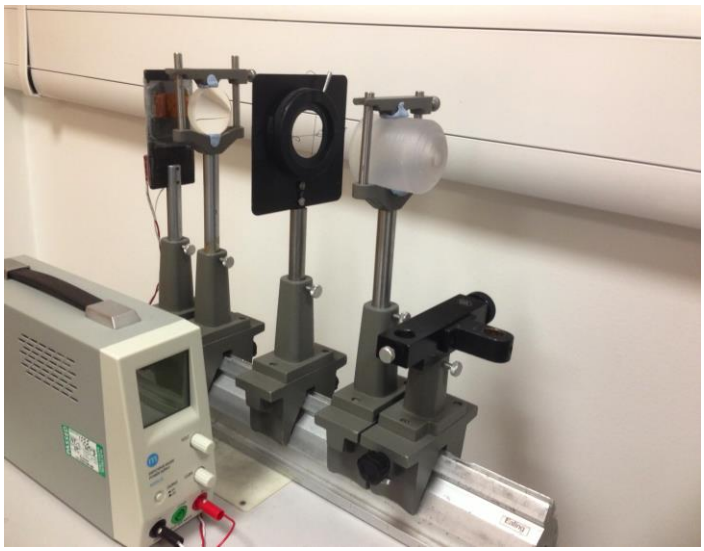

Figure 32. The Maxwellian view optical system. The participant positioned their chin on the rest at the front of the device and fixated the central cross for 120 seconds.

Three different dark adaptation functions were recorded in a randomised order, using the 2^{o}, 7^{o} and 12^{o} radius stimuli, centred on the fovea. A one-hour washout period separated successive bleaches. In the healthy control participants, the entire procedure was repeated on a separate day within a one-month period so that each participant completed a total of six dark adaptation functions. Some participants with AMD

required a second visit if fatigue prevented the collection of all data on a single occasion.

Statistical analysis

All threshold recovery data were fitted using an exponential-linear model of dark adaptation (McGwin et al. 1999) on a least squares basis using the solver function in Microsoft Excel (2003) (Equation 2). Cone threshold recovery was modelled by the exponential component of the curve, and rod recovery by the linear components. The two parameters of interest were the time constant of cone recovery (cone τ) and time to rod-cone-break (RCB). The recording protocol was not long enough to reliably obtain the rod recovery parameters from all participants, but the inclusion of the linear portion of the model facilitated the localisation of the RCB.

Equation 2. $T(t) = [a + (b.\exp^{(-t/\tau)})] + [c.(\max(t - rcb,0))]$

where T is the threshold (log cd/m^2) at time t after termination of the bleach, a is the final cone threshold, b is the change in cone threshold from t = 0, τ is the time constant of cone recovery, c is the slope of the second component of rod recovery, *max* is a logic statement and *rcb* describes the time to the RCB from cessation of the bleach (McGwin et al. 1999).

The repeatability of cone τ and time to RCB were assessed using established statistical techniques such as the coefficient of repeatability (CoR) (Bland and Altman 1986). The CoR was calculated by multiplying the standard deviation of the differences between the two visits by 1.96. Confidence intervals for the CoR were calculated by determining the appropriate point of the t-distribution with n-1 degrees of freedom. The confidence intervals were from the observed value minus t standard errors to the observed value plus t standard errors (Bland and Altman 1986). Repeatability was graphically analysed using the method advocated by Bland and Altman (1986) whereby the differences between visits for each individual are plotted against the mean value. Paired t-tests were carried out to determine any significant differences in parameters between visit one and visit two, which may be suggestive of a learning effect. Receiver operating characteristic (ROC) curves were constructed using statistical software (SPSS, Version 20.0) to assess the diagnostic potential of dark adaptation parameters that showed a statistically significant difference between the AMD and control groups.

2.4 Results

Dark adaptation data were obtained from 28 healthy control participants, 2 of whom withdrew from the study after their first visit and 4 were excluded either due to an inability to understand the test or to follow the instructions given. One additional person was excluded due to an uncertain AMD status. Therefore, dark adaptation curves for each of the 3 stimuli on 2 occasions were analysed from 11 healthy younger participants (mean age 23.3 ± 4.7 years) and 10 healthy older participants (mean age 72.7 ± 6.0 years). Typical recovery data for the three retinal locations at both visits from one older and one younger participant are displayed in Figure 33 and Figure 34 respectively. In all observers, as the retinal eccentricity of the stimulus increased, the time constant of cone recovery was shorter, the RCB took place earlier and the rod branch of the dark adaptation function became more prominent with a lower final threshold. Tables 6 and 7 display the cone tau and RCB data from all participants at all 3 locations.

Figure 33. Dark adaptation curves recorded for a typical older participant (CR, 62 years) in

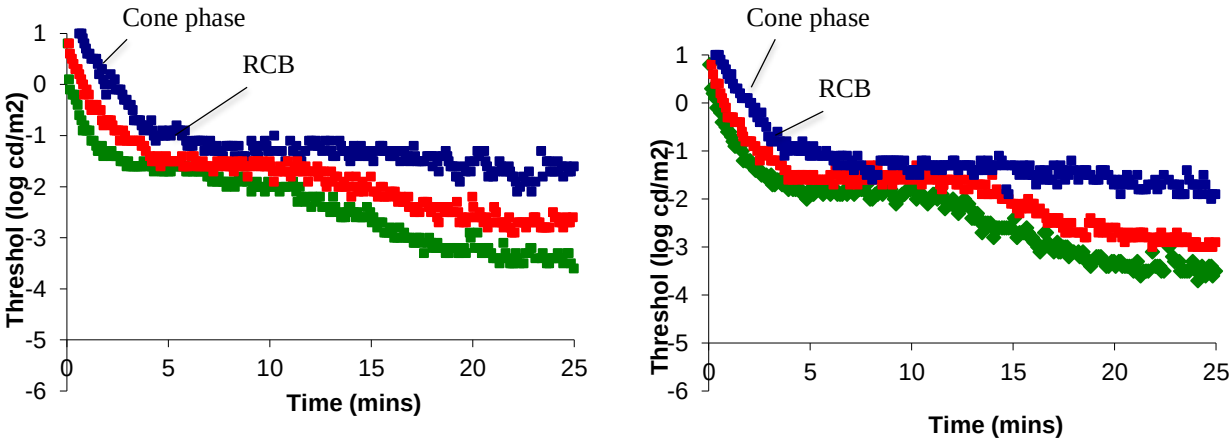

response to all three stimulus sizes: 2 degree (blue), 7 degree (red) and 12 degree (green) on visit 1 (left panel) and visit 2 (right panel). The 12 degree curve is correctly placed with respect to the vertical axis. The other two curves have been displaced upwards by an additional 0.5 log units to aid visualisation. The cone phase and rod-cone break (RCB) are indicated on the curves.

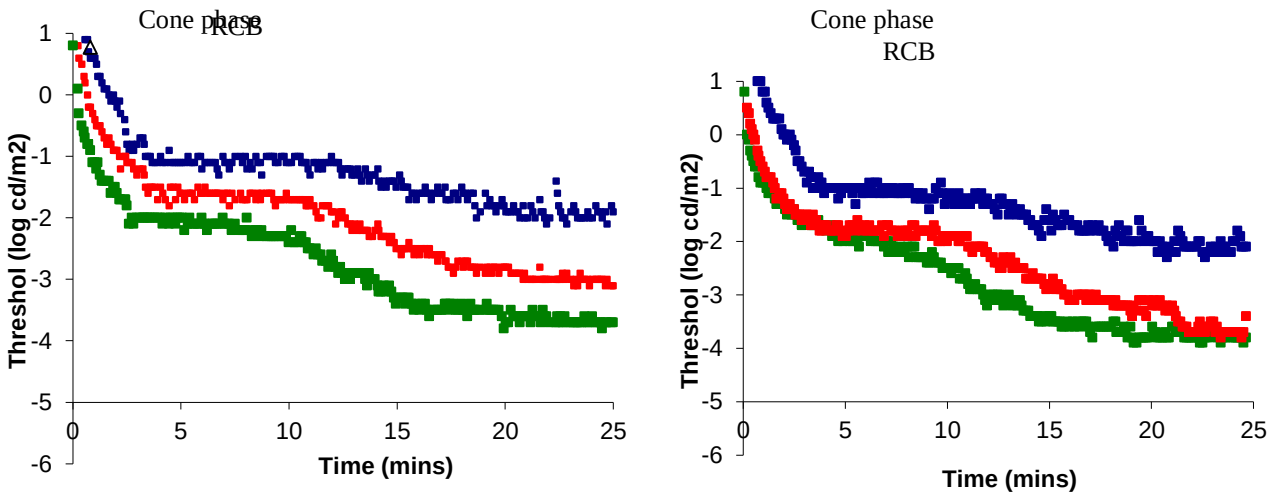

Figure 34. Dark adaptation curves recorded for a typical younger participant (CM, 23 years) in response to all three stimulus sizes: 2 degree (blue), 7 degree (red) and 12 degree (green) on visit 1 (left panel) and visit 2 (right panel). The 12 degree curve is correctly placed with respect to the vertical axis. The other two curves have been displaced upwards by an additional 0.5 log units to aid visualisation. The cone phase and rod-cone break (RCB) are indicated on the curves.

Participant	2 º Cone τ (mins)		7 º Cone τ (mins)		12 º Cone τ (mins)	
	Visit 1	**Visit 2**	**Visit 1**	**Visit 2**	**Visit 1**	**Visit 2**
AB	2.57	2.73	1.29	1.29	1.52	1.29
CM	1.59	1.44	1.10	1.34	1.41	1.07
AA	1.70	1.75	1.38	1.35	1.16	1.23
JB	1.63	1.96	1.29	1.31	1.31	1.39
NM	2.15	1.95	1.39	1.66	1.43	1.48
RN	1.78	0.90	1.25	1.24	1.34	1.57
NS	1.94	1.52	*	1.09	*	*
SP	1.80	2.08	1.48	1.37	1.11	1.59
AA	1.48	1.59	0.39	1.05	0.62	0.85
JB	1.30	1.29	0.85	0.54	0.60	0.82
RB	1.78	1.72	0.90	1.37	0.90	1.08
CR	2.40	2.28	1.90	1.53	0.99	1.42
AB	2.76	2.66	1.06	1.15	1.24	1.00
MH	2.56	2.42	1.79	1.23	1.31	0.97
CS	2.20	2.50	1.44	1.58	0.73	1.35
DT	2.93	3.74	2.21	2.18	1.24	1.39
DG	3.33	3.35	2.91	2.27	1.82	1.01
EBM	2.91	3.52	2.89	2.68	2.05	1.61
PF	3.61	4.25	3.67	2.55	2.62	2.59
RG	2.89	2.25	1.43	1.11	1.40	1.31
RE	1.38	1.95	1.39	1.40	0.74	1.13
MEAN	2.22	2.28	1.64	1.49	1.28	1.31
SD	0.67	0.86	0.77	0.52	0.49	0.39

Table 6. Cone τ for all participants using 2 º, 7 º and 12º stimuli. * Indicates results that were excluded from analysis due to variability of results as caused by fatigue.

Participant	2 º RCB (mins)		7º RCB (mins)		12 º RCB (mins)	
	Visit 1	**Visit 2**	**Visit 1**	**Visit 2**	**Visit 1**	**Visit 2**
AB	7.87	8.75	7.97	7.97	8.05	7.97
CM	10.84	11.52	9.62	9.48	6.69	8.17
AA	10.22	10.81	10.33	9.77	6.73	8.70
JB	9.79	8.69	10.38	6.61	8.47	9.15
NM	11.76	11.86	9.06	10.34	7.28	7.01
RN	12.36	11.65	9.04	10.05	9.86	6.71
NS	8.51	8.76	*	9.34	*	*
SP	10.81	11.19	7.89	9.47	7.87	8.51
AA	11.20	7.91	3.66	9.89	5.44	5.46
JB	12.17	10.93	7.34	4.36	7.15	5.86
RB	12.00	10.15	8.88	8.79	5.54	6.56
CR	15.55	13.43	11.30	13.13	7.09	10.43
AB	5.74	14.25	6.34	10.80	9.73	7.56
MH	11.80	13.21	8.12	7.80	8.92	5.73
CS	14.40	14.35	11.25	10.84	6.63	8.28
DT	19.23	11.85	11.88	11.45	8.12	12.07
DG	22.75	17.69	11.50	8.28	9.47	10.42
EBM	25	25	10.28	10.53	7.16	7.87
PF	25	25	16.69	18.75	11.90	10.22
RG	15.47	15.32	12.25	10.64	9.19	9.89
RE	12.82	12.92	10.35	9.63	7.48	7.47
MEAN	13.59	13.11	9.70	9.90	7.94	8.20
SD	5.31	4.62	2.65	2.72	1.58	1.77

Table 7. Time to rod-cone-break (RCB) for all participants using 2 º, 7 º and 12º stimuli. * Indicates results that were excluded from analysis due to variability of results as caused by fatigue.

Bland-Altman plots of the difference in cone τ and time to RCB recorded at the first and second visit against the mean cone τ and time to RCB for each stimulus size are displayed in Figure 35 and Figure 36. Figure 35 shows that all 3 stimuli had an equally small range between the limits of agreement for the cone τ. Figure 36 shows that with the time to RCB, there is a progressively smaller range between the two limits of agreement with increasing stimulus eccentricity. The Bland Altman plots all showed a mean difference between visits that was around zero, indicating a lack of bias in the data, i.e. there was no significant learning effect between visits.

a.

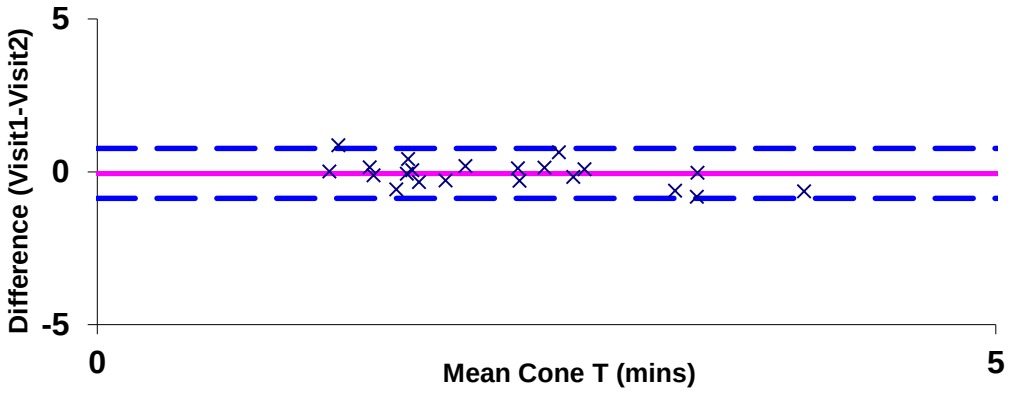

b.

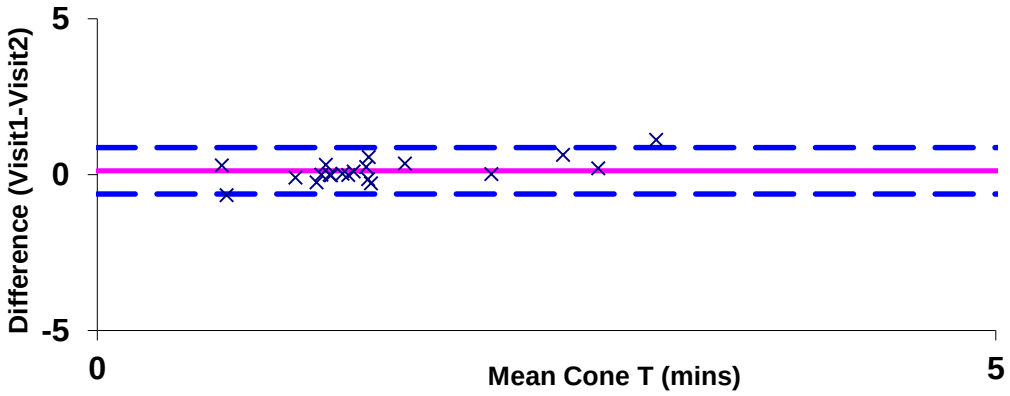

c.

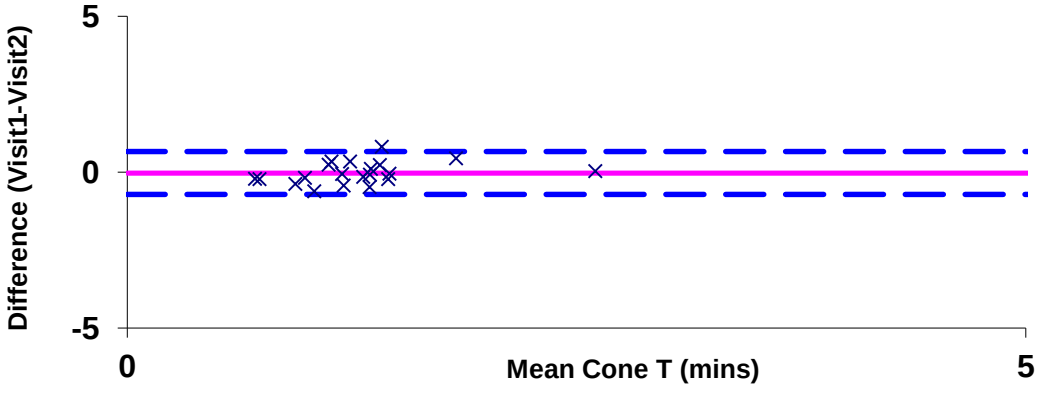

Figure 35. Bland-Altman plots for 2º (a), 7º (b) and 12º (c) radius stimuli cone τ. The difference between the value recorded at visit 1 and visit 2 is plotted as a function of the mean value for all participants with the bias (solid pink line) and 95% limits of agreement (dashed blue lines).

a.

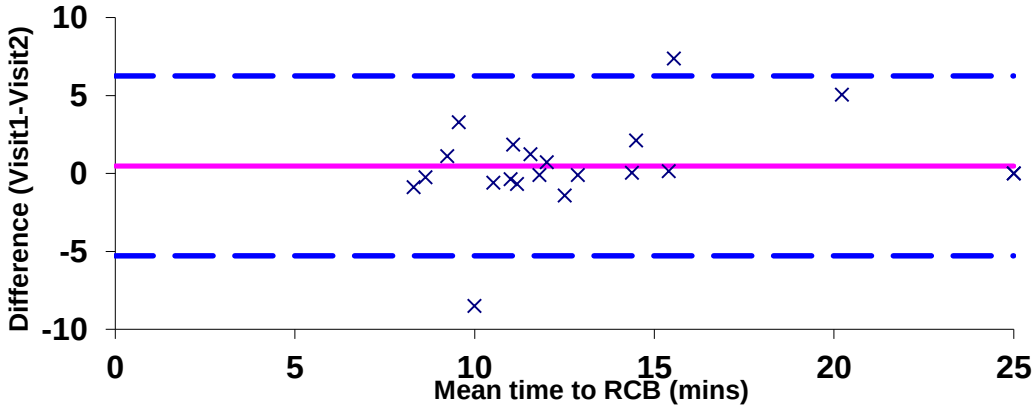

b.

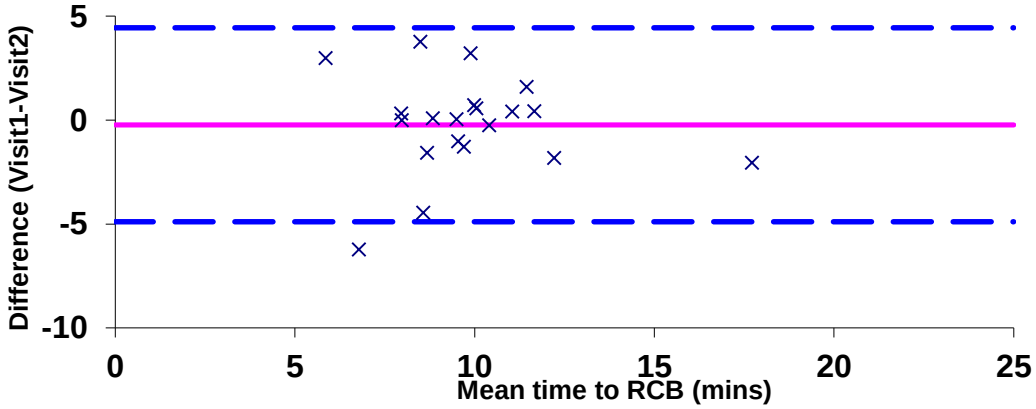

c.

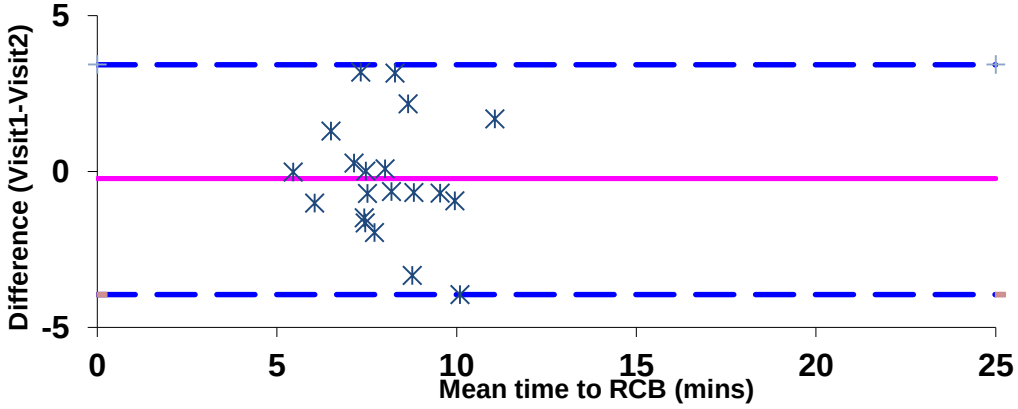

Figure 36. Bland-Altman plot for 2º (a), 7º (b) and 12º (c) radius stimuli time to RCB. The difference between the value recorded at visit 1 and visit 2 is plotted as a function of the mean value for all participants with the bias (solid pink line) and 95% limits of agreement (dashed blue lines).

The COR for each parameter was determined, as shown in Table 8. The COR was also expressed as a percentage of the group mean for each parameter to facilitate comparison. The percentage COR ranged from 36.4% to 53.3%. The lowest percentage COR was obtained using the 2° radius stimulus. Figure 37 displays this graphically, with the associated 95% confidence intervals. For both parameters, it is seen that the confidence intervals are overlapping for the different stimuli, suggesting that there is no significant difference in repeatability between the retinal locations.

Psychophysical Method	Coefficient of Repeatability (mins)	Coefficient of Repeatability (%)
2° τ	0.82	36.4
7° τ	0.74	47.1
12 ° τ	0.69	53.3
2 ° RCB	5.77	43.2
7 ° RCB	4.67	47.5
12° RCB	3.69	45.9

Table 8. Coefficient of Repeatability for the 6 psychophysical parameters investigated, also expressed as a percentage of the group mean value.

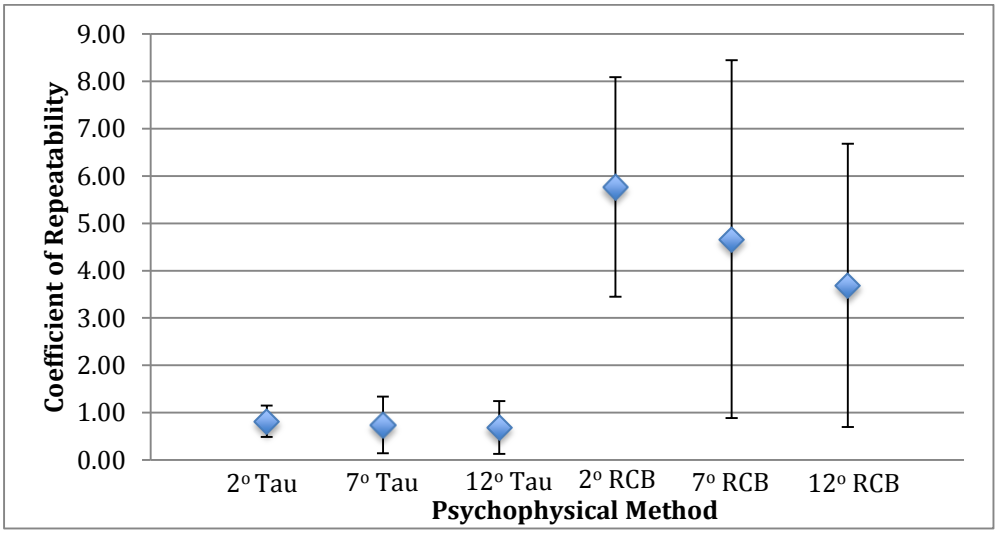

Figure 37. Coefficient of Repeatability for each psychophysical parameter (i.e. cone tau and time to RCB for stimuli of radius 2°, 7°, 12° with 95% confidence limits.

The means (± standard deviation) of cone τ and time to RCB for visits one and two for all 21 participants are shown in Table 9. There was no statistically significant difference in any of these parameters between the two visits (paired two-tailed t-test, $p > 0.05$), which signifies that there was no significant bias, for example, no learning effect upon

the second visit.

	Mean (± standard deviation)		p-value (paired t-test)
	Visit 1	Visit 2	
2° Cone τ (mins)	2.22 (± 0.67)	2.28 (± 0.86)	0.556
7° Cone τ (mins)	1.64 (± 0.77)	1.49 (± 0.52)	0.149
12° Cone τ (mins)	1.28 (± 0.49)	1.31 (± 0.39)	0.716
2° RCB (mins)	13.59 (± 5.31)	13.11 (± 4.62)	0.464
7° RCB (mins)	9.70 (± 2.65)	9.90 (± 2.72)	0.675
12° RCB (mins)	7.94 (± 1.58)	8.20 (± 1.77)	0.537

Table 9. Mean (± standard deviation) of dark adaptation parameters assessed at visits one and two. P-values relate to a paired t-test comparing data from visits one and two.

The clinical characteristics of the AMD cohort are shown in Table 10. One participant with AMD was unable to perform the test due to physical restrictions, and so was excluded from the study. In total, the dark adaptation data from 10 participants with AMD were analysed. There was no significant difference in mean age between the AMD (mean age 72.9 ± 7.23 years) and control (mean age 72.7 ± 6.0 years) groups (independent samples two-tailed t-test, p=0.95).

			Test Eye			Fellow Eye	
Participant	Age	Gender	Eye	VA	AMD status	VA	AMD status
RS	78	M	R	0.04	Early	0.24	Intermediate
RJ	68	M	L	0.0	Early	1.2	Advanced
AP	82	F	R	0.0	Early	0.0	Early
WG	76	M	R	-0.1	Normal	-0.1	Early
UH	77	F	R	-0.06	Early	0.02	Advanced
DP	62	M	R	-0.08	Early	0.0	Early
DN	83	M	R	0.06	Early	0.24	Early
AD	70	M	L	-0.08	Early	-0.04	Advanced
LG	67	F	R	-0.1	Early	-0.1	Early
ED	66	F	R	-0.06	Early	0.32	Early

Table 10. Clinical characteristics of the AMD cohort. AMD status was determined according to the Age-Related Eye Disease Study severity scale (Davis et al. 2005) in which step 1 represents normal retinal ageing changes, steps 2-6 indicate early AMD, steps 7-9 denote intermediate AMD and steps 10-11 represent advanced AMD. VA was measured in logMAR.

Table 11 shows the cone τ and time to RCB at three retinal eccentricities for each older control and for each participant with AMD determined by the best fitting exponential-linear model. An example of typical dark adaptation curves for a participant with AMD

is shown in Figure 38, which can be compared with the typical dark adaptation data of an older control as shown previously in Figure 33.

Participant	2 º stimulus		7º stimulus		12 º stimulus	
	Cone τ (mins)	RCB (mins)	Cone τ (mins)	RCB (mins)	Cone τ (mins)	RCB (mins)
Controls						
CR	2.40	15.55	1.90	11.30	0.99	7.09
AB	2.76	5.74	1.06	6.34	1.24	9.73
MH	2.56	11.80	1.79	8.12	1.31	8.92
CS	2.20	14.40	1.44	11.25	0.73	6.63
DT	2.93	19.23	2.21	11.88	1.24	8.12
DG	3.33	22.75	2.91	11.50	1.82	9.47
EBM	2.91	25	2.89	10.28	2.05	7.16
PF	3.61	25	3.67	16.69	2.62	11.90
RG	2.89	15.47	1.43	12.25	1.40	9.19
RE	1.38	12.82	1.39	10.35	0.74	7.48
AMD						
RS	4.03	25	3.31	17.62	2.45	16.48
RJ	5.61	25	3.69	25	2.38	16.20
AP	10.09	25	5.47	25	3.06	18.46
WG	4.78	25	2.58	12.79	1.70	10.63
UH	9.41	25	4.77	25	3.30	25
DP	1.80	13.36	1.47	11.38	1.31	6.83
DN	7.34	25	3.77	25	4.73	25
AD	3.65	25	2.22	15.69	1.46	10.25
LG	3.98	25	2.75	18.58	2.50	14.14
ED	6.15	25	3.17	25	2.10	10.94

Table 11. Cone τ and time to RCB, determined by the best fitting exponential-linear model for all older controls and participants with AMD at each retinal location. Where there was no RCB within the trial period, it was assigned a value of 25 minutes.

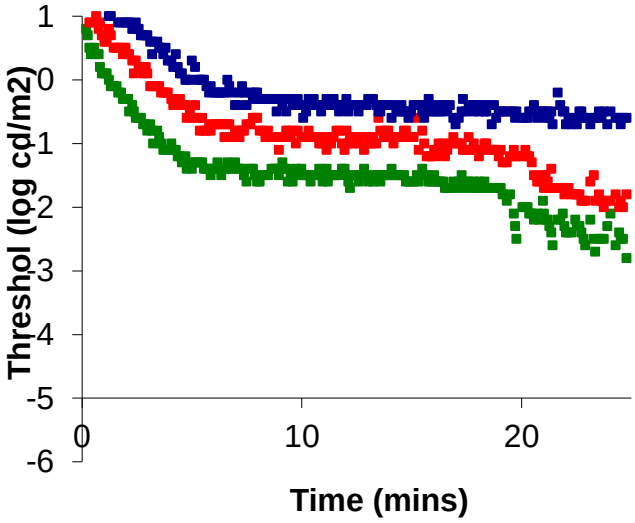

Figure 38. Dark adaptation curves recorded for a typical participant with AMD (RS) in response to all three stimuli: 2° (blue), 7° (red) and 12° (green). The 12° curve is correctly placed with respect to the vertical axis. The other two curves have been displaced upwards by an additional 0.5 log units to aid visualisation.

The mean dark adaptation parameters for the two groups are given in Table 12. In cases where the RCB did not occur within the recording period, it was assigned a value of 25 minutes. Therefore, the full extent of the delay in rod dark adaptation with AMD is not demonstrated in the figures below. The mean times to RCB and cone τ at all 3 retinal locations for control and AMD groups are also displayed graphically in Figure 39, with 95% confidence intervals.

	Stimulus radius	**Control**	**AMD**	**Univariate comparison**
Cone τ (mins)	2°	2.70 (0.62)	5.84 (2.89)	p= 0.009
	7°	2.07 (0.84)	3.41 (1.32)	p= 0.040
	12°	1.41 (0.60)	2.69 (1.30)	p= 0.017
Time to RCB (mins)	2°	16.78 (6.22)	23.84 (4.11)	p= 0.024
	7°	11.0 (2.71)	19.68 (5.97)	p= 0.004
	12°	8.57 (1.60)	16.10 (6.70)	p= 0.012

Table 12. Mean (± standard deviation) dark adaptation parameters in older control and AMD groups. P-values relate to independent samples t-tests comparing parameters between groups

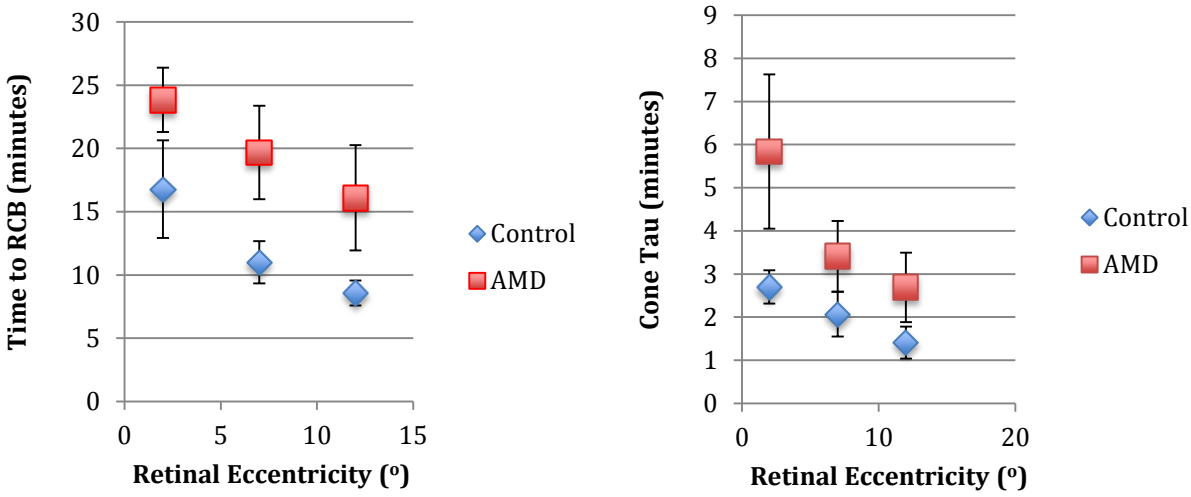

Figure 39. Summary of mean time to RCB (left panel) and cone τ (right panel) at each retinal eccentricity, shown with 95% confidence intervals.

Significant differences between groups were evident for all stimuli for both parameters (two-tailed t-test, $p < 0.05$). The greatest absolute difference in cone recovery time between participants with AMD compared with controls was found using the 2° radius stimulus and this difference was highly significant ($p=0.009$). However, with respect to time to RCB, the difference between groups was most significant for the 7° radius stimulus ($P=0.004$), possibly due to the high level of variability in the control data for time to RCB of the 2° radius stimulus.

Receiver operating characteristic (ROC) curves for all parameters are shown in Figure 40. The area under the curve (AUC) provides a global assessment of the diagnostic performance of each parameter. This area indicates the probability that a test has a higher diagnostic value than random chance. For example, an AUC of 1 indicates 100% sensitivity and specificity, whilst an AUC of 0.5 indicates that the test is no better than chance alone at distinguishing between groups (Altman and Bland 1994). Both the time to RCB and cone τ were highly diagnostic for AMD, with AUCs ranging from 0.83 to 0.94. If a cone tau greater than 3.63 minutes is considered to be abnormal, the test is able to distinguish between controls and people with AMD with a sensitivity of 90% and a specificity of 100%. There were no statistically significant differences in the AUC obtained for the 3 stimuli for either parameter ($z < 1.96$) (Hanley and McNeil 1982).

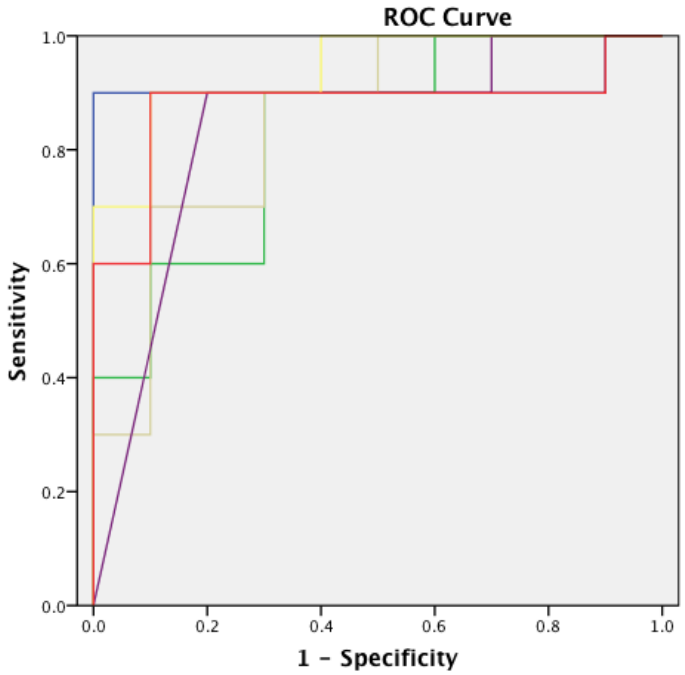

Test Parameter	AUC
2° cone τ (blue line)	.910
7° cone τ (green line)	.830
12° cone τ (brown line)	.850
2° RCB (purple line)	.840
7° RCB (yellow line)	.940
12° RCB (red line)	.880

Figure 40. ROC curves (plots of sensitivity against 1-specificity) for all parameters for 10 older controls and 10 participants with AMD, and areas under the ROC curves.

2.5 Discussion

These data demonstrate that cone adaptation, measured at different macular locations is highly diagnostic for AMD. This study has also shown that this technique has good inter-session repeatability in normal subjects. In agreement with previous studies (Hecht et al. 1935; Dimitrov et al. 2008), the results showed that as the eccentricity of the stimulus increased, dark adaptation recovery (cone τ and time to RCB) was faster, revealing a more prominent rod curve and a lower final threshold.

Consistent with Dimitrov et al. (2008), cone dark adaptation took longer at the fovea, the location of peak cone photoreceptor density (Curcio et al. 1990). The increased photoreceptor density increases competition for the limited supply of 11-cis retinal available, which may account for the slower cone recovery at the fovea. The time to RCB, a measure of rod function, was faster with increasing retinal eccentricity. This is possibly due to the increased rod photoreceptor density, receptive field size and spatial summation that occurs as retinal eccentricity increases from a foveal to a more peripheral location (Dacey and Petersen 1992).

When assessing a technique's clinical applicability, it is necessary to calculate the coefficient of repeatability (CoR), a measure of the inherent variability in a test, which

can determine the smallest change over time that can be deemed to be clinically significant (Bland and Altman 1986). This is particularly important if a technique is to be used in a longitudinal study, such as a clinical trial. A clinically significant change in dark adaptation recovery between visits must be greater than or equal to the CoR value. Therefore, the lower the CoR, the greater the test's potential to pick up small functional losses associated with disease progression. The CoR obtained for cone τ and time to RCB using the 3 different stimuli ranged from 36.4% to 53.3% of the group mean value for these parameters. There were no significant differences in the repeatability of cone τ and time to RCB parameters between the 3 retinal locations. Therefore, any of these stimuli may be used in the longitudinal assessment of dark adaptation. If the 2^o cone tau, which produced the lowest CoR, was chosen as a parameter in a longitudinal study of dark adaptation, any difference between two measurements greater than 0.82 minutes may be considered to be clinically significant. The mean difference in 2^o cone tau between healthy controls and participants with AMD was 3.14 minutes, which is considerably greater than the repeatability limit of 0.82 minutes, therefore has sufficient repeatability to detect disease effects.

The investigation of dark adaptation parameters in participants with AMD and older controls revealed that cone τ and time to RCB are both highly diagnostic for all stimuli, with areas under ROC curves between 0.83 and 0.94. For example, if a cone τ greater than 3.63 minutes is considered to be abnormal, the 2^o stimulus is able to distinguish those subjects with AMD from healthy older controls with 90% sensitivity and 100% specificity. There was no significant difference in the AUC for cone τ or time to RCB for any stimulus. Consequently, both parameters, regardless of stimulus size, can be used to identify patients with AMD with similar sensitivity and specificity. The greatest difference in mean cone τ between groups was at the fovea, which is consistent with previous studies (Dimitrov et al. 2008; Gaffney et al. 2011). Since cone density is maximal at the fovea (200,000 cells/mm^2) (Curcio et al. 1990), there will be more competition for 11-*cis*-retinal, which may explain the greater functional deficit seen at this location. Contrary to the findings of Gaffney et al. (2011), the foveal stimulus did not show elevated variability compared to other locations and thus the separation between groups at this location was good, as depicted in Figure 39. Gaffney, however, used a smaller stimulus than that used in this study (1^o vs. 4^o diameter). Due to the heterogenous nature of AMD lesions, the results obtained with smaller stimuli will be

more influenced by the chance of the stimulus targeting a healthy or unhealthy part of the retina. Using a larger spot size will ensure that the thresholds obtained will be determined by the part of the retina that is most healthy, thus providing less variable results, as found in this study.

A limitation of the 2^o stimulus is that it produced the least separation between groups in the time to RCB. This is because the vast majority of participants with AMD did not reach their RCB within the 25-minute trial period, and so the time to RCB was assigned a nominal value of 25 minutes, which would underestimate their actual measurement. Also, this stimulus gave the most variable results for the control group with respect to time to RCB. Therefore, if a measure of rod function is required as a diagnostic tool, the 7^o annular stimulus would be more suitable. However, given that the 2^o cone τ produced the greatest separation between subjects with AMD and healthy controls and can be measured within a few minutes (Gaffney et al 2011), it would be an appropriate parameter to use as a functional biomarker in AMD.

The results from this study confirm the previous findings of delayed cone dark adaptation in the peripheral macular region (Gaffney et al 2011), which was contradictory to the work of Owsley et al. (2007) who failed to find a significant effect of AMD on cone dark adaptation at 12^o retinal eccentricity. A possible explanation for these discrepancies lies in the different techniques used to bleach the photopigment. Owsley and colleagues used a photo-flash method, in which small errors in exposure time will have a relatively large effect on the amount of photopigment bleached (Margrain and Thomson 2002). Following the longer duration bleach used in this study, that produces an equilibrium bleach, the time constant of cone recovery is not dependent on the percentage of photopigment bleached, and the effects of blinking and eye movements during flash delivery are minimised (Hollins and Alpern 1973). Furthermore, recovery is faster following a photoflash even if the same percentage of pigment is bleached, therefore less time would be available to collect recovery data.

There is a further, physiological explanation for the greater deficit in cone adaptation recorded following an equilibrium bleach. The regeneration of visual pigment following a bleach is dependent upon the local availability of 11-*cis*-retinal (Lamb and Pugh 2004). Cones have an additional Müller cell pathway that allows them to regenerate visual pigment more rapidly than rods, which are solely dependent on the

RPE. It is possible that the prolonged metabolic activity that occurs during a longer duration bleach could be detrimental to the Müller cell retinoid pathway, causing cone photoreceptors to be more dependent on the RPE-derived 11-*cis*-retinal. Since the RPE is one of the primary sites of damage in AMD, any impairment to cone-mediated dark adaptation would be more apparent under these conditions than with a photo-flash bleaching technique (Gaffney et al. 2011).

A limitation of the time to RCB as a measure of rod function is that it also depends on cone final threshold. However, Gaffney et al. (2011) found no difference between cone final threshold in subjects with early AMD compared with healthy controls. Hence, any delay in the time to RCB may be assumed to be due to an abnormality in the individual's rod adaptation. Although this study had a modest sample size, our intention was to determine whether dark adaptation was both reproducible and able to distinguish persons with early AMD from age-matched controls and to determine the retinal location that provided the best repeatability and diagnostic capacity. Despite the small sample, there was a statistically significant difference between the two groups in both cone recovery and time to RCB.

In conclusion, this study has demonstrated that the inter-session repeatability of dark adaptation was not significantly different between the three retinal locations investigated. Nevertheless, the repeatability values reported in the results of this study may be used in future clinical trials to determine the smallest change that can be considered to be clinically significant. Furthermore, it was found that all three retinal locations were able to discriminate between people with early AMD and healthy controls. Although the 2^{o} radius stimulus produced the greatest separation between these two groups with respect to cone tau, and the 7^{o} radius stimulus was most diagnostic in terms of time to RCB, these differences between stimuli were not statistically significant. However, since the 2^{o} stimulus may be used to measure the time constant of cone recovery in as little as 10 minutes, it would be a suitable parameter to use in future clinical trials using dark adaptation as a functional biomarker.

Chapter 3. The Repeatability of Functional Biomarkers for AMD

3.1 Introduction

With the imminent development of new therapies for AMD, a potential obstruction to their clinical evaluation is the lack of an outcome measure that can evaluate a reduction in disease progression over a relatively short timeframe. Early AMD develops very slowly over time (Davis et al. 2005) and, therefore, it is not practicable to use end stage disease as an outcome measure in early stage trials. For this reason, there is a pressing need to develop biomarkers that are able to reliably and repeatably detect small changes in visual function, acting as surrogate markers of disease progression.

Given that AMD is a disease primarily affecting the outer retina, tests that specifically target the photoreceptors, RPE and Bruch's membrane should be most sensitive to disease progression. However, the standard method of assessing retinal function, visual acuity (VA), involves a considerable amount of higher order cortical processing (Thibos and Bradley 1993). Furthermore, the inherent between session variability of this test (8 letters, logMAR 0.15) (Siderov and Tiu 1999) will often mask the small changes in VA that occur in early AMD (2 letter loss, logMAR 0.04) (Klein et al. 1995). Alternative functional tests examining the outer retina more directly would, therefore, be likely to be better able to monitor disease progression.

Although histopathological studies have reported that cones are relatively spared in early AMD (Curcio et al. 1996), this does mean that they are not affected by the disease. Shelley and colleagues found that numerous cone nuclei were displaced and prolapsed in AMD, which would cause them to lose their synaptic contact and thus affect their functionality (Shelley et al. 2009). Furthermore, there is mounting psychophysical evidence to show cone function to be a reliable indicator of AMD. Indeed, (Eisner et al. 1992) found that the colour-match area, in combination with dark adaptation, was the best predictor of disease progression in AMD. Tritan colour contrast thresholds are abnormal in patients with AMD and minimal lens opacities (Arden and Wolf 2004), and they also change significantly more over time in patients with early AMD compared with age-matched controls (Holz et al. 1995). However, for chromatic

sensitivity to be employed as a functional biomarker of AMD, a means of accurately quantifying chromatic thresholds is required, which falls beyond the remit of standard clinical colour vision tests. A computer-based technology has recently been developed for the assessment of colour contrast sensitivity by the Civil Aviation Authority (CAA), which is now being used as their gold standard colour vision test. The Colour Assessment and Diagnosis (CAD) test is postulated to be able to detect, classify and monitor both large and small colour vision deficiencies. The statistical limits for the standard normal (SN) observer were established using the thresholds of 238 normal trichromats and 250 patients with colour deficiencies (Barbur and Rodriguez-Carmona 2006). By implementing dynamic luminance contrast noise, it is able to isolate red-green (RG) and yellow-blue (YB) thresholds (Birch et al. 1992). This allows a rapid quantification of thresholds along 16 different directions in the x,y co-ordinates of CIE colour space (Barbur et al 2009b). Using the CAD test, YB thresholds in patients with AMD have been shown to increase linearly with disease severity, which again indicates that YB loss is a good indicator of disease progression (O'Neill-Biba et al. 2010). O'Neill-Biba et al. (2010) reported evidence of an elevation in threshold, even when the retina appeared normal, in individuals whose fellow eye demonstrated signs of advanced AMD, indicating that impaired colour vision may be an early functional indicator of retinal dysfunction in AMD. Barbur and Konstantakopoulou (2012) evaluated an approach to maximizing the diagnostic sensitivity of the test through the calculation of an index representing chromatic threshold as a function of light level in the low photopic, high mesopic range (Barbur and Konstantakopoulou 2012). This resulted in a reduction in the substantial between subject variability in chromatic thresholds conferred by individual differences in factors such as media opacity, pupil diameter and macular pigment optical density, and removed the effect of age on colour vision in healthy individuals. However, to date, the only data that have been published regarding the between session variability of the CAD test is on a computer-based web version under different experimental conditions (Seshadri et al. 2005).

Numerous studies have found that temporal sensitivity is also adversely affected in patients with AMD (Mayer et al 1992b; Mayer et al. 1994; Phipps et al. 2003; Phipps et al. 2004; Dimitrov et al. 2011; Dimitrov et al. 2012; Luu et al. 2013), to a greater extent than the generalised loss which occurs due to normal ageing (Kim and Mayer 1994). This is thought to be due to the compromised outer retinal oxygen supply in

AMD being unable to meet the increased metabolic demand elicited by flickering stimuli (Kiryu et al. 1995; Riva et al. 2001). Flicker frequencies of above 10Hz have been shown to increase the difference in oxygen tension between retinal arterial and venous blood substantially more than lower frequencies (Shakoor et al. 2006). This indicates that the metabolic activity of the retinal tissue is upregulated in response to this high temporal frequency stimulation. Given the recent evidence to suggest that early functional changes in AMD are initiated by chronic retinal ischemia (Feigl et al. 2007a), a functional test which causes a greater demand on the retinal oxygen metabolism is more likely to detect the ischemic deficits in early AMD.

Flicker detection is a desirable test to use when monitoring functional changes in AMD as it can be performed quickly, is reproducible and diagnostically sensitive (Phipps et al. 2004; Dimitrov et al. 2011). For this reason, Dimitrov et al. rated 14 Hz flicker threshold measurement as having the highest potential clinical value out of a battery of functional tests in the diagnosis and monitoring of AMD (Dimitrov et al. 2011). Furthermore, flicker threshold has also been shown to increase gradually with disease progression (Dimitrov et al. 2012), thus supporting the claim that temporal sensitivity may also be an effective tool for monitoring AMD progression and assessing the efficacy of therapeutic interventions. The flickering stimulus can be generated by either modulating luminance about a mean background level (mean-modulated flicker) (Mayer et al 1992b) or by modulating a luminance increment (luminance-pedestal flicker) (Anderson and Vingrys 2000). The latter is thought to be superior in detecting early AMD, due to its invocation of local adaptation effects (Anderson and Vingrys 2000) and rod-cone interactions from neighbouring areas (Coletta and Adams 1984).

Clinical tests must fulfill two key requirements to be useful as biomarkers for use as outcome measures in clinical trials: they must be sensitive to disease progression, and they must show a good level of between session repeatability. It is clear that both the 14-Hz flicker threshold and CAD chromatic sensitivity tests may be useful functional biomarkers, fulfilling the first requirement of showing a sensitivity to increased severity of funduscopic changes associated with AMD (O'Neill-Biba et al. 2010; Dimitrov et al. 2011; Dimitrov et al. 2012). Repeatability data have recently been published for the assessment of cone dark adaptation (Gaffney et al. 2014), another potentially important biomarker for early AMD (Brown and Kitchin 1983; Eisner et al. 1991; Owsley et al.

2001; Owsley et al. 2007; Binns and Margrain 2007; Gaffney et al. 2011; Dimitrov et al. 2011; Dimitrov et al. 2012). However, there is currently little published data regarding the inter-session repeatability of the flicker and chromatic threshold assessment techniques. This is crucial in determining the minimum change in each parameter which may be considered to be clinically significant – an important issue when powering trials and interpreting outcomes, as well as in the clinical management of patients with early AMD. The data presented in this section has been accepted for publication in a peer-reviewed journal (see Appendix IV).

3.2 Aims

The aim of this study was to assess the inter-session repeatability of the colour assessment and diagnosis (CAD) test and the 14-Hz flicker test in a population of healthy participants.

3.3 Methods

Participants

Thirty healthy adults with limited experience in psychophysical experiments were recruited to the study from the staff and students at the School of Optometry and Vision Sciences, Cardiff University. This study was powered to detect within subject standard deviation to within 25% of the true population value (Bland 2010). All participants had corrected visual acuity of 6/6 or better (logMAR 0.0) in their test eye, age-normal lens clarity, a normal retinal appearance with no history of any ocular or systemic disease known to affect visual function. As a random sample of the population was desired, subjects were not excluded on the basis of having a colour vision defect. The School's Research Ethics Committee approved the study and all procedures were carried out in accordance with the tenets of the Declaration of Helsinki. All participants provided written consent to taking part in the study, having received an information sheet prior to their appointment and having had the opportunity to ask any questions.

Experimental procedure

All participants attended the laboratory on two separate days within a period of two weeks. Baseline data were obtained at the beginning of the first session. This included patient history, logMAR visual acuity (ETDRS) OCT and fundus photography (Topcon 3D OCT 1000). Lens clarity was assessed using a slit lamp biomicroscope, and graded

according to the LOCS III system for nuclear opalescence (NO), nuclear colour (NC), cortical opacity (C) and posterior subcapsular opacity (P) (Chylack et al. 1993).

Stimuli for both psychophysical tests were presented on a calibrated, high-resolution 24" widescreen LCD monitor (NEC MultiSync PA241W) with a frame rate of 60Hz, as depicted in Figure 41. The luminance of the monitor was ϒ-corrected (Appendix III) (Metha et al. 1993). In a dimly illuminated room, participants were positioned 1.4m away from the monitor, and any required refractive correction, appropriate for the viewing distance, was provided. The test eye was the eye with better visual acuity or, in the case of equal acuity, the right eye was selected. The fellow eye was occluded. The test order was randomised between subjects, but kept the same on both visits for each subject.

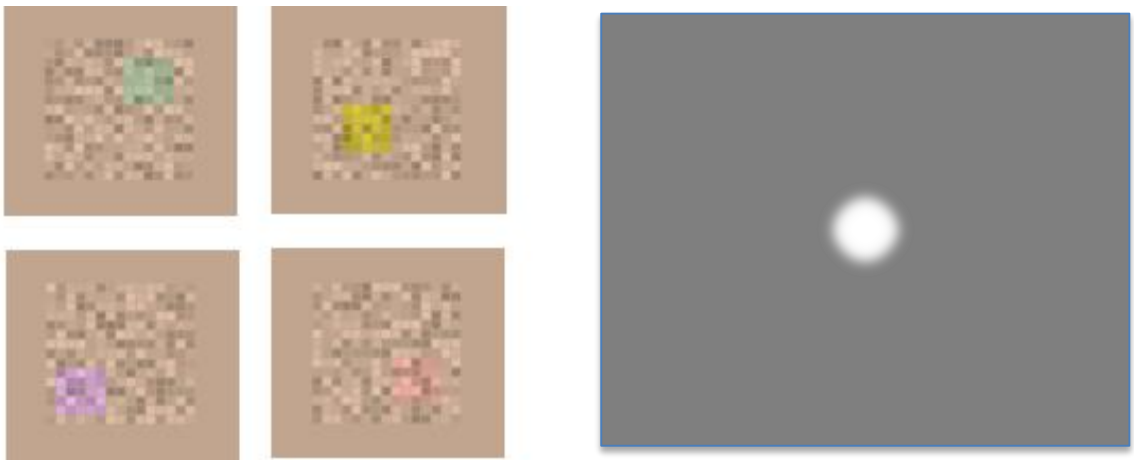

Figure 41. Images showing the appearance of the moving coloured stimulus (Barbur et al. 2006) (left panel) and flickering stimulus (right panel) used during the test.

14-Hz Flicker Sensitivity

Flicker thresholds were determined using the well-established Bayesian adaptive psychometric method known as QUEST (Watson and Pelli 1983; King-Smith et al. 1994). In this method, the strength of each successive stimulus presentation is set to match the current most probable estimate of threshold. In practice, QUEST was implemented in Matlab (The Math Works Inc.) using routines available within Psychophysics Toolbox to drive a go / no-go adaptive staircase (Brainard 1997). The results from a practice run that included 10 trials were used as the starting point for a

final threshold estimate that converged after 40 trials. False positive responses were deemed to be responses that occurred more than 1s after stimulus offset.

Subjects were asked to fixate the centre of the screen where the test stimulus, a 4^{o} diameter foveated Gaussian blob at a temporal frequency of 14Hz, was presented for a duration of 2 seconds. The flickering stimulus was generated by modulating a luminance increment following a sinusoidal temporal profile. The mean luminance of the monitor was 51 cd/m^2 and the x,y chromaticity co-ordinates of CIE colour space were 0.305, 0.323. To ensure that participants could not anticipate the next presentation, the inter stimulus interval was varied randomly between 4 and 10 seconds. The participants received verbal instructions on how to perform the test before undertaking the familiarisation trial. Their task was to press a button on a keypad as soon as they perceived a flickering stimulus in the centre of the monitor. If more than one false positive response was made, the practice trial was repeated until they were able to complete the familiarisation trial with a maximum of 1 false positive response.

Colour Contrast Sensitivity

Colour contrast sensitivity was assessed using the CAD test (v2.2.4, City Occupational Ltd). RG and YB colour detection thresholds were measured by employing coloured stimuli moving against an achromatic background. The background (CIE x,y chromaticity co-ordinates 0.305, 0.323; mean luminance 26 cd/m^2) comprised a checkerboard of 15x15 squares (total 3.3 degrees diameter), which fluctuated randomly in luminance above and below the average background level in order to generate dynamic luminance contrast noise. The check luminance was distributed with equal probability within +/- 55% of background luminance. This noise masked the detection of residual luminance contrast cues in the isoluminant coloured stimulus. The colour-defined stimulus comprised a checkerboard of 5 × 5 squares (total 1.1° diameter) moving diagonally across the checkerboard, in one of four directions. The stimulus duration was 600ms. A four-alternative forced choice procedure was used. Displacement thresholds were measured in 16 directions in colour space (6 red, 6 green, 2 blue, 2 yellow), with colour directions selected to correspond to the red / green colour confusion lines (140 to 175 degrees) and the S-cone isolating axes (58 to 68 degrees). Threshold was determined using a two-down, one-up staircase in which colour intensity was reduced by an initial step size of 0.006 CAD units until the coloured stimulus could

not be distinguished from the background by the observer. This staircase procedure was repeated for nine reversals, at each of which the step size was reduced by 0.001 CAD units until a final step size of 0.002 CAD units was attained. Thresholds were obtained by averaging the chromatic distance in the CIE colour space during the last four staircase reversals.

The participant's task was to press one of four buttons on a keypad to indicate the observed direction of motion of the coloured stimulus. Each stimulus presentation was followed by an audible 'bleep' to indicate when to respond. A response was required, even if the participant was uncertain of the direction of movement. Any trial could be presented for a second time at the participant's request. A suprathreshold familiarisation trial lasting 1 minute was performed prior to the main trial. A 100% correct response rate was required to ensure that the subject understood the requirements of the test. The 'definitive' CAD program was then implemented and RG and YB thresholds were measured over 12 to 15 minute period.

Figure 42 below shows the CAD test template for the standard normal (SN) observer, in which the shaded area represents the normal colour vision spectrum. The two ellipses denote the 2.5% and 97.5% confidence limits for a normal population and the black dotted line represents the median value for the standard normal CAD observer, i.e. 1 standard normal unit (SNU) (Barbur and Rodriguez-Carmona 2006). The CAD test background had a luminance of 26 cd/m^2.

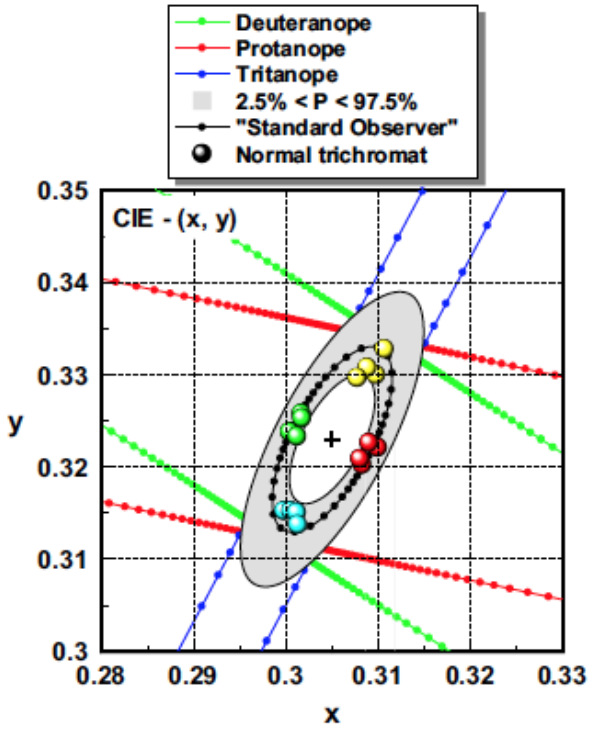

Figure 42. The dotted, black ellipse is based on the median RG and YB thresholds from 250 observers, with the grey shaded area representing the 95% limits of variability of these observers. The deuteranopic, protanopic and tritanopic confusion bands are displayed in green, red and blue, respectively. The background chromaticity (x,y) is indicated by the black cross (0.305, 0.323). The coloured symbols show data measured for a typical normal trichromat (Barbur and Rodriguez-Carmona 2006).

Statistical Analysis

Flicker thresholds were transformed into Weber contrast values by dividing pedestal luminance ($I - I_b$) by the average luminance (I_b). The repeatability of the colour and flicker thresholds was assessed using established statistical techniques (Bland and Altman 1986). The coefficient of repeatability (CoR) was calculated by multiplying the standard deviation of the differences between the two visits by 1.96. Confidence intervals for the CoR were calculated according to the method described by Bland and Altman (Bland and Altman 1986).

3.4 Results

The thirty participants (13 female) were aged between 22-72 years (mean 36.3 ± 14.1 years). All participants had a LOCS score of 0 for all parameters, apart from RE, who had NO2 and NC2 (LOCS III) (Chylack et al. 1993). One participant TM had a previously diagnosed protanopic colour vision defect.

Chromatic sensitivity and flicker thresholds were successfully obtained from all 30 participants on two separate days. Data from the 2 visits were generally collected on successive days but always within two weeks. None of the participants required additional practice sessions for either test, which minimized potential inter-individual differences in any learning effect. An example of the flicker data obtained on both visits from a typical participant (AB) is shown in Figure 43. In each plot, the solid horizontal line represents the final threshold and the dashed horizontal lines denote the 95% confidence intervals. Sample CAD results from the same observer are shown in Figure 44.

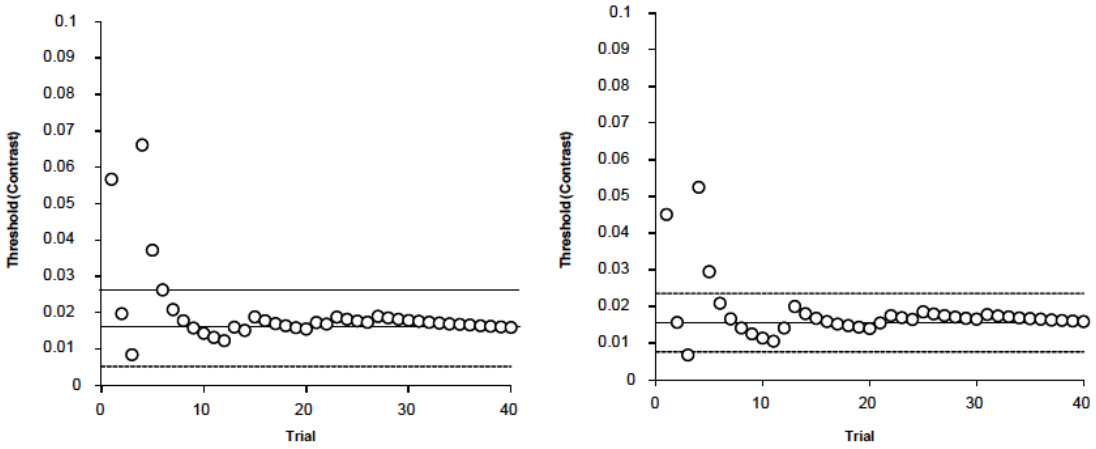

Figure 43. 14Hz Flicker data for participant AB at visit 1 (a) and visit 2 (b), shown with the threshold in decibels. The dashed lines represent the 95% confidence intervals, with the solid line depicting the final threshold.

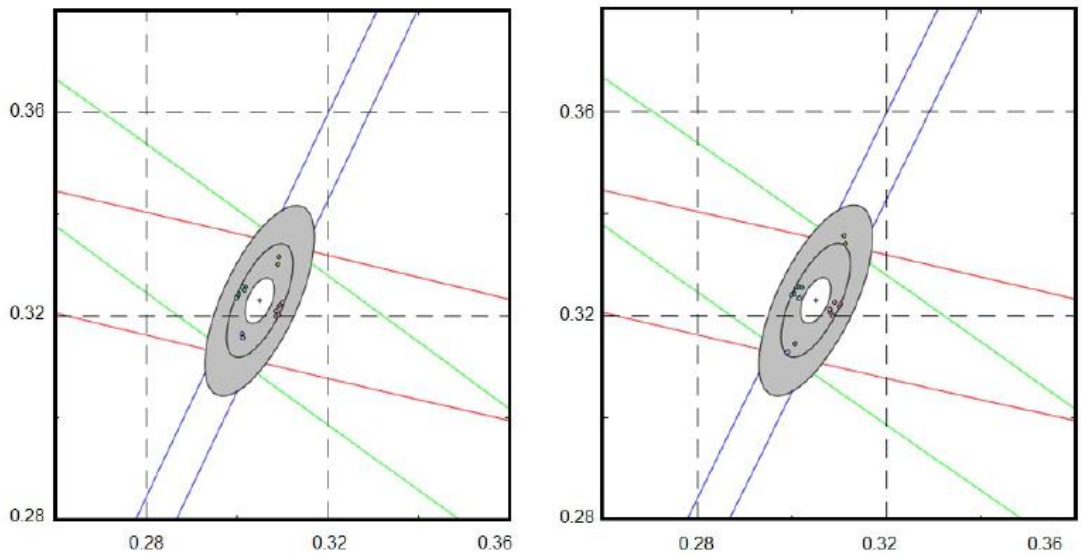

Figure 44. CAD data for participant AB at visit 1 (left panel) and visit 2 (right panel). The dotted black ellipse is based on the median RG and YB thresholds, with the grey shaded area representing the 95% limits of variability. The green, red and blue bands display the deuteranopic, protanopic and tritanopic confusion lines, respectively. The coloured symbols show the data measured for participant AB.

Table 13 shows the CAD and flicker thresholds obtained for all 30 participants. Only 1 subject (TM) with a congenital protanopic deficiency had a RG CAD threshold outside of the statistically determined normal limits (Barbur and Rodriguez-Carmona 2006). Similarly, only 1 subject (RE) had YB thresholds outside of the normal range. The lens opacities of this 72-year old participant had been graded as NO2 and NC2 (LOCS III) (Chylack et al. 1993), so this abnormal YB defect is most likely due to the early stages of nuclear cataract. Both of these participants, whilst falling outside of the published limits of normality (Barbur and Rodriguez-Carmona 2006), showed repeatable results.

The difference in RG thresholds recorded at the first and second visit is plotted as a function of the mean RG threshold for all 30 participants in the Bland and Altman plots shown in Figure 45a, whereas Figure 45b shows the Bland Altman plot for RG thresholds with the protanopic individual's data point removed to aid visualisation of the spread of the other data. Similar plots for all 30 individuals are shown for YB and 14Hz flicker thresholds in Figure 45c and d.

Participant	RG Threshold (CAD units)		YB Threshold (CAD units)		14Hz Flicker Threshold (Decibels)	
	Visit 1	Visit 2	Visit 1	Visit 2	Visit 1	Visit 2
RH	1.26	1.08	1.06	1.05	0.025	0.034
CM	1.31	1.32	0.87	1.07	0.021	0.018
RN	1.47	1.26	1.91	2.05	0.027	0.024
JS	1.53	1.66	1.33	1.5	0.025	0.025
FVN	1.55	1.48	1.27	1.17	0.045	0.038
BF	1.33	1.5	1.14	1.12	0.039	0.030
EM	1.55	1.39	1.93	1.84	0.032	0.033
CJ	1.26	1.12	1.2	1.31	0.014	0.008
SH	1.94	1.78	1.84	1.39	0.020	0.013
GM	1.54	1.37	1.18	1.21	0.044	0.033
AW	1.48	1.37	1.46	1.19	0.032	0.024
MD	1.49	2.01	1.16	1.11	0.039	0.019
AB	1.1	1.12	1.08	0.75	0.016	0.016
RW	1.32	1.3	1.28	0.82	0.032	0.031
PB	1.19	1.09	0.82	0.94	0.039	0.032
JT	1.12	1.01	0.99	0.76	0.039	0.018
LT	2.08	2.03	1.71	1.7	0.027	0.027
JC	1.84	1.4	1.14	1.5	0.051	0.036
TH	1.49	1.25	1.06	0.75	0.030	0.024
TR	0.91	0.99	0.88	0.67	0.024	0.018
RD	1.61	1.39	2.35	2.04	0.037	0.031
AN	1.35	1.02	1.66	1.65	0.025	0.023
NW	2.21	2.31	1.73	1.96	0.033	0.029
TK	1.41	1.03	1.06	1.03	0.022	0.024
JF	1.24	0.98	1.14	0.76	0.016	0.017
EM	1.47	1.19	1.32	1.26	0.022	0.016
KA	1.27	1.26	1.59	1.19	0.031	0.047
JA	1.24	1.2	1.34	1.36	0.019	0.018
TM	26.48	26.39	1.42	1.17	0.015	0.015
RE	2.77	2.32	3.69	3.43	0.059	0.046

Table 13. RG, YB and 14Hz flicker thresholds for all 30 participants.

a.

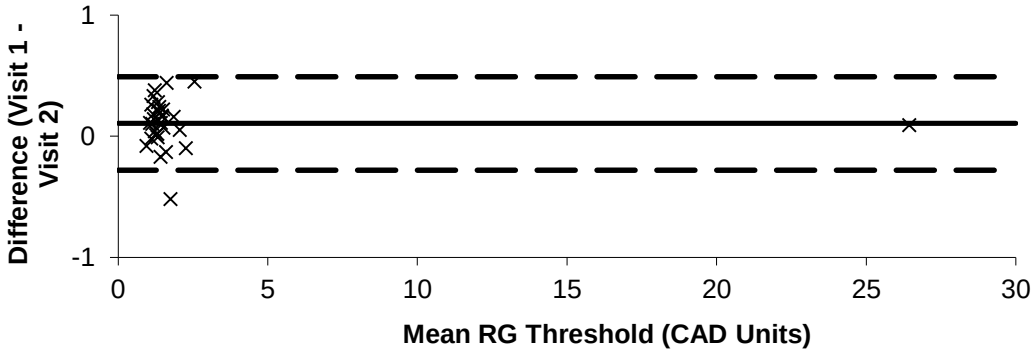
Difference (Visit 1 - Visit 2)
1
0
-1
0
5
10
15
20
25
30
Mean RG Threshold (CAD Units)

b.

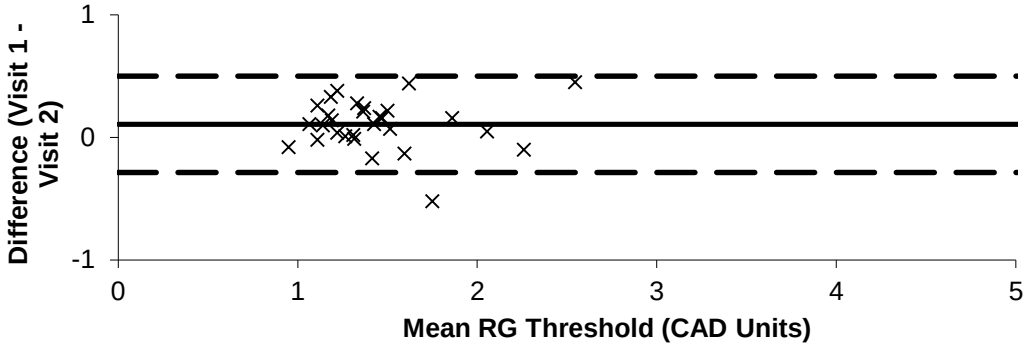
Difference (Visit 1 - Visit 2)
1
0
-1
0
1
2
3
4
5
Mean RG Threshold (CAD Units)

c.

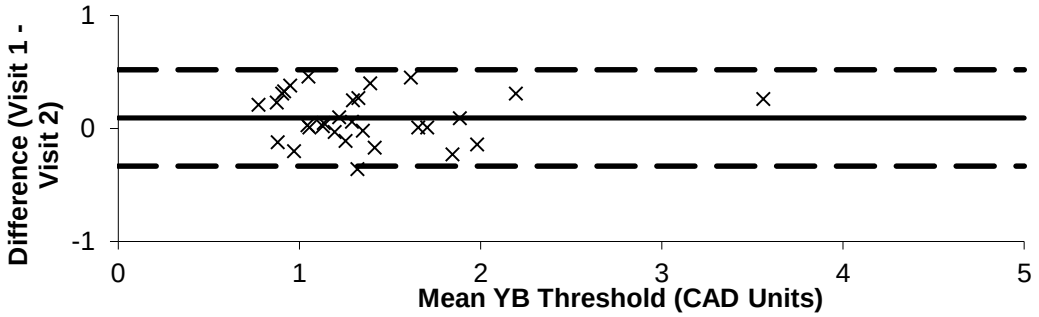
Difference (Visit 1 - Visit 2)
1
0
-1
0
1
2
3
4
5
Mean YB Threshold (CAD Units)

d.

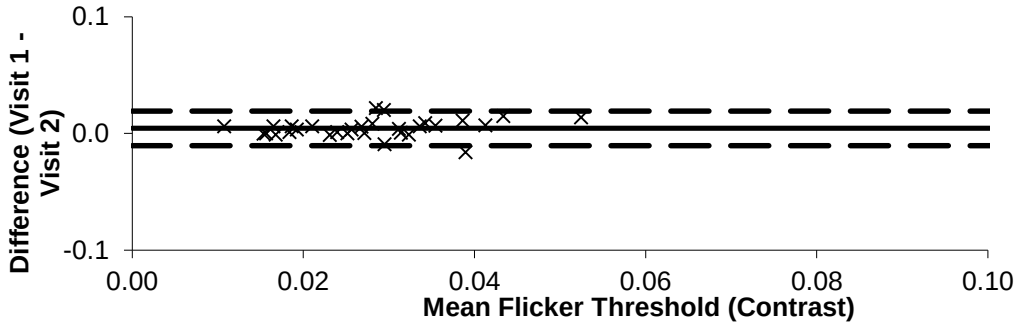

Figure 45. Bland Altman plots for RG chromatic thresholds (a), RG chromatic thresholds excluding participant TM (b), YB chromatic thresholds (c) and 14Hz flicker thresholds (d). The difference between the measurements from visits 1 and 2 is plotted as a function of the mean of visits 1 and 2 for all 30 participants, and is shown with the bias (solid line) and 95% limits of agreement (dashed lines).

In each graph in Figure 45, the solid horizontal line depicts the bias, i.e. the mean difference between the two visits, and the dashed horizontal lines represent the 95% limits of agreement, i.e. the mean difference ± the coefficient of repeatability (CoR). These plots describe the between session repeatability for all 3 measures. There was no evidence of a systematic change in repeatability with increasing thresholds (i.e. no heteroscadicity). The bias line crosses the y-axis slightly above 0 in all cases. Relative to visit 1, thresholds improved by 4.72%, 6.33% and 13.3% for RG, YB and 14-Hz flicker respectively, indicating the presence of a possible small learning effect.

The mean RG, YB chromatic thresholds and 14-Hz flicker thresholds for visits one and two are shown in Table 14, along with the CoR for each test. The expression of the CoR as a percentage of the group averaged test result (at visits 1 and 2) allows a direct comparison of the repeatability of parameters with different units. Although the RG thresholds were more repeatable than the YB thresholds, the difference in the CoR was not significant (95% confidence intervals did not overlap). There was also no significant difference in repeatability between the YB CAD thresholds and 14-Hz flicker. However, the CoR for the RG CAD thresholds was significantly better than that of the 14-Hz flicker (see Table 14). Scatter plots showing the effect of age on the between visit variability are shown in Figure 46. There was no evidence of any systematic effect of age on variability for any parameter.

	Mean (± standard deviation)		CoR (95% CI)	CoR as % of mean threshold (95% CI)
	Visit 1	Visit 2		
RG Threshold	2.33 (± 4.58)	2.22 (± 4.58)	0.39 (± 0.13)	17.1 (± 5.6%)
YB Threshold	1.42 (± 0.56)	1.33 (± 0.56)	0.43 (± 0.14)	31.1 (± 10.2%)
14-Hz Flicker Threshold	0.030 (± 0.01)	0.026 (± 0.009)	0.015 (± 0.005)	53.4 (± 17.6%)

Table 14. Mean (± standard deviation) of all three parameters assessed at visit one and visit two. Coefficient of repeatability is given for each parameter, and as a percentage of the mean value.

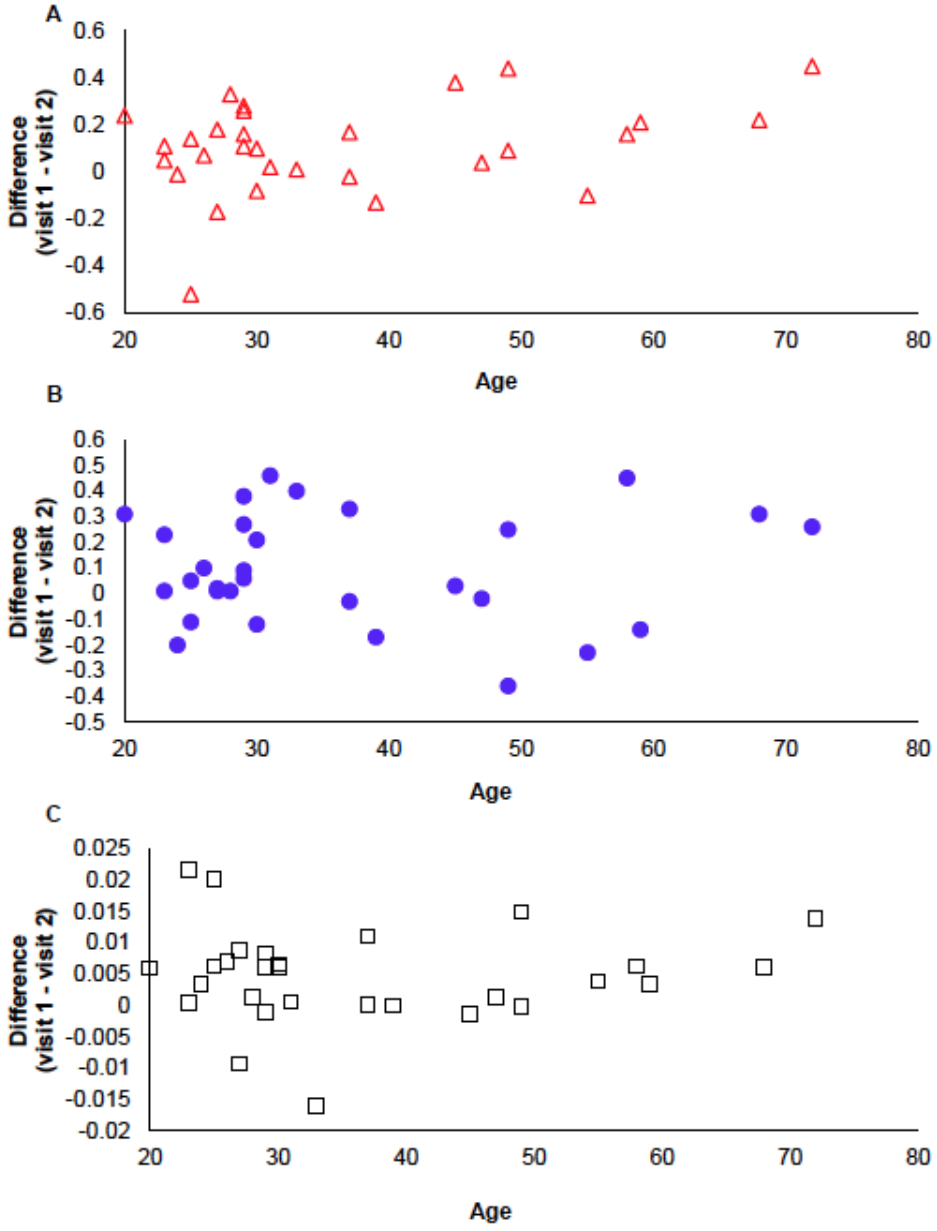

Figure 46. Scatter plots demonstrating the relationship between age and between visit threshold

variation for RG chromatic thresholds (A), YB chromatic thresholds (B) and 14-Hz flicker thresholds (C). Note the lack of a systematic relationship with age for any parameter.

3.5 Discussion

In order to monitor the progression of AMD and determine the efficacy of novel therapies, functional tests must be used that are reliable, repeatable and clinically applicable. This will allow candidate treatments to be assessed with maximum efficiency by minimising the sample size and follow-up duration required to achieve a useful end point. The development of functional tests sensitive to subtle changes in AMD status is also important in the clinical diagnosis and management of the condition in clinical settings. Visual acuity, despite the common acknowledgement that it is a poor assay of early AMD, is still the standard functional vision test amongst both clinicians and researchers. It is therefore necessary that new visual function tests are introduced that are as quick to perform and have the same ease of use as VA, but with improved sensitivity to disease progression and better inter-session repeatability. Two such tests that have shown to sensitive to disease severity in AMD are the 14Hz flicker and CAD chromatic sensitivity test (O'Neill-Biba et al. 2010; Dimitrov et al. 2011; Dimitrov et al. 2012). The flicker test employs a stimulus which is bigger (4 degrees diameter) than the stimulus presented in the CAD test (1.1 degree diameter). However, the CAD stimulus moves out from a central fixation position to a location extending to 2.3 degrees into the parafovea. Hence both stimuli are assessing a region of the macula extending to around 2 degrees from fixation. This targets the parafoveal region in which functional deficits have been identified early in the AMD disease process (Owsley et al. 2001).

The coefficient of repeatability (CoR) is an important statistical technique due to its potential to describe the smallest change that can be deemed clinically significant (Bland and Altman 1986). This is helpful in identifying those individuals who have shown a "clinically significant decline" in performance, and can therefore be used to determine the optimal sample size for a trial, i.e. it can be powered to detect a certain percentage of participants who show this level of functional decline. The most repeatable test was found to be the RG CAD threshold test. This performed significantly better than the 14-Hz flicker test which produced the least repeatable results.

The Bland Altman plots all showed a mean difference between visits that was slightly above zero, suggesting a small learning effect for both the 14-Hz flicker test and the CAD parameters. This was confirmed by a post hoc paired samples *t*-test ($p < 0.05$) for all tests. This learning effect may have been minimised by the familiarisation trials which were carried out for the two techniques before both visits. If more than 1 false positive occurred on the 14-Hz flicker practice trial lasting 1 minute or if the subject did not score 100% in the CAD practice trial which also took 1 minute to complete, they were made to repeat it until they achieved the required standard and were deemed competent in task performance. However, the familiarisation trials were clearly not sufficient to saturate learning.

A limitation of the study is that different repeatability values will need to be established if the tests are applied under different experimental conditions. A change in stimulus size, eccentricity, temporal frequency, retinal illuminance, or a change in the psychophysical procedure used, are all likely to affect the measured variability of the techniques. The repeatability index may also be different if the patient has disease or colour vision loss. For example, in their recent evaluation of the effect of retinal illuminance on chromatic thresholds, Barbur et al. hypothesized that the assessment of colour vision at mesopic levels may increase the diagnostic sensitivity of the test, through the exacerbation of the effect of disease-related hypoxia (Barbur and Konstantakopoulou 2012). Their 'healthy retina index' (HR_{index}) is a measure of the effect of retinal illuminance on chromatic thresholds. Additional repeatability data will be required to evaluate the clinical interpretation of mesopic chromatic thresholds and the HR_{index}. Inter-session repeatability is also likely to be influenced by the characteristics of the patient population. Hence, a further potential limitation of the repeatability data reported in this study is that the participant cohort was recruited from a University environment, and may not be generalizable to the population of patients with age-related macular degeneration. However, the age-range of participants extended to 72 years, and only 3 of the participants had previously taken part in psychophysical experiments hence, the group may be considered to be broadly representative of naïve participants in a clinical environment. Furthermore, we found no evidence of an effect of age on the between session variability, suggesting that the findings of this study will be broadly applicable across age groups.

One limitation of the go / no-go adaptive staircase procedure used in the flicker sensitivity test is that results are dependent on stimulus strength and an individual's response criterion i.e. their willingness to guess. Response criterion can vary between and within individuals. We attempted to minimize within subject changes in response criteria by providing identical instructions at each visit. However, we cannot rule out the possibility that the systematic difference between visits (i.e. the bias) was due to a change in response criterion. Many things, including instructions, can induce the observer to raise or lower his or her criterion, causing threshold to shift up or down. This unknown internal criterion of the observer typically differs among observers and may vary across populations and over time. The four alternative forced choice paradigm employed by the CAD test negates the effect of inter-individual differences in the response criterion.

The published limits of normality for the CAD test are based on data collected from 250 colour normal participants (Barbur and Rodriguez-Carmona 2006). The majority of participants in this study produced thresholds which fell within these limits, apart from one protanope (TM), and one older participant with significant nuclear lens opacities (RE). Excluding these 2 participants, the mean (SD) RG thresholds for visit 1 were 1.45 (0.29) and for YB 1.34 (0.37). The RG threshold is very similar to that reported by O'Neill-Biba et al. (2010) but the YB value is somewhat lower than that reported previously 1.6 (0.15). Control participants in the O'Neill-Biba study were on average 20 years older than those studied here and increasing lens opacification may therefore, explain the difference. Barbur et al reported that chromatic thresholds, uncorrected for differences in media absorption and pupil diameter, increase significantly with increasing age in the healthy population (Barbur and Konstantakopoulou 2012).

In summary, this study has described the inter session repeatability of two tests that may be used in the diagnosis and monitoring of AMD. Both colour vision and flicker sensitivity tests have been shown to have excellent diagnostic capacity (Bowman 1978; Collins 1986; Brown and Kitchin 1987b; Applegate et al. 1987; Eisner et al. 1991; Holz et al. 1995; Frennesson et al. 1995; Phipps et al. 2003; Phipps et al. 2004; Arden and Wolf 2004; O'Neill-Biba et al. 2010; Dimitrov et al. 2011; Dimitrov et al. 2012; Luu

et al. 2013). The results of this study will help clinicians to determine if changes observed over time are due to measurement imprecision or disease progression, provided that the experimental conditions and psychophysical procedures are kept constant. The observation that a small but significant learning effect exists highlights the need for control groups in clinical trials of new AMD therapies. These and other candidate biomarkers must now be validated in longitudinal studies to confirm their prognostic and predictive capabilities.

Chapter 4. Clinical Trial Development

As discussed in section 1.4, there is an growing amount of evidence implicating hypoxia as a major factor in the pathogenesis of AMD (Feigl 2007; Feigl 2009; Stefánsson et al. 2011). The maintenance of the dark current requires a vast oxygen supply. When this oxygen supply is further depleted in AMD, the resultant hypoxia may initiate increased VEGF production and apoptosis (Witmer et al. 2003). The metabolic demands of the outer retina could be significantly reduced by increasing environmental light levels during the night, thus reducing the oxygen demand and delaying hypoxia-induced disease progression (Arden 2001). Recent clinical trials in diabetes showed low-level night-time light therapy to be safe, well tolerated by patients and caused a reduction in diabetic macular oedema (Arden et al. 2010; Arden et al. 2011). The same therapy could have substantial therapeutic benefits for people with AMD.

This chapter will discuss the design of a pilot randomised controlled trial to investigate the effectiveness of low-level night-time light therapy for the treatment of AMD. The study design considerations include determining the optimal retinal illuminance for the therapy and the optimal mode of light presentation, as well as the specification of outcome measures, eligibility criteria, and sample size. The manuscript of this clinical trial protocol has been accepted for publication in a peer-reviewed journal (see Appendix IV).

4.1 Calculating Retinal Illuminance

Scotopic trolands are a measure of the retinal illuminance. If we designate corneal luminance as C (cd/m^2), pupil area as P (πr^2) then the resulting retinal illuminance, I, in trolands (Td) is described by Equation 3 (Thomas and Lamb 1999).

Equation 3. $$I = CP$$

For a flash stimulus of duration t (s), the integrated retinal illuminance (L) is defined by Equation 4 (Thomas and Lamb 1999).

Equation 4. $$L = I\,t$$

Scotopic trolands may then be converted to the number of photoisomerisations per rod, Φ, using a conversion factor *K*, described in Equation 5 (Thomas and Lamb 1999).

Equation 5. $$\Phi = LK$$

Where $K = 8.6$ photoisomerisations s^{-1} per rod per scotopic troland. Note that this only applies if the bleach is not overly bright and the retina has recovered from any prior bleach (Thomas and Lamb 1999).

As seen above, the measurement of scotopic trolands relies upon knowledge of the pupil diameter. Winn et al. (1994) measured the pupil diameters of 91 subjects (aged 17 to 83 years) using an objective infrared-based continuous recording technique (Winn et al. 1994), at a luminance level of $9cdm^{-2}$. Figure 47 shows that the average pupil diameter in low-level lighting is between 4-6mm for people in the age range affected by AMD i.e. over 55 years of age.

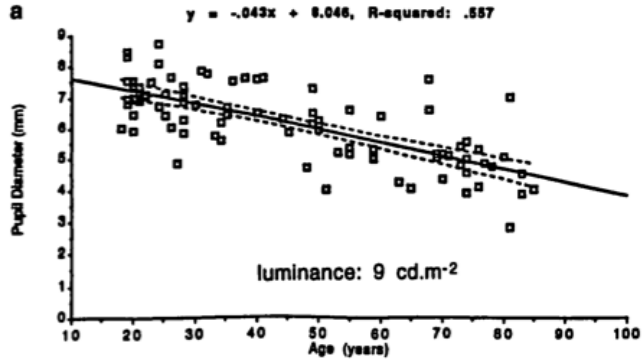

Figure 47. Pupil diameter as a function of age for a luminance of $9cdm^{-2}$. Data are fitted by linear regression with the 95% confidence limits indicated by the dotted line (Winn et al. 1994).

4.2 Determining the optimal retinal illuminance for low level night-time light therapy

The light level employed must be sufficient to adequately suppress the rod circulating current, and at the same time be dim enough so as to not disrupt melatonin secretion and, consequently, circadian rhythms. The exact amount by which the rod circulating current needs to be reduced to produce a disease modifying effect on the level of retinal hypoxia is not known at present. Arden et al. used a retinal illuminance of 2 scotopic trolands in their recent clinical trial, citing Hamer et al. (2005) as the scientific justification for this value (Arden et al. 2011).

Hamer et al. aimed to produce a unified model of vertebrate rod phototransduction (Hamer et al. 2005). Part of their work involved an investigation into the effects of light adaptation on circulating current in toads and salamander rods (using previous data from Koutalos et al. (1995)). Increasing the intensity of the background adapting light was found to cause the circulating current to progressively decrease until, at the highest intensity background, circulating current was completely eradicated (Figure 48).

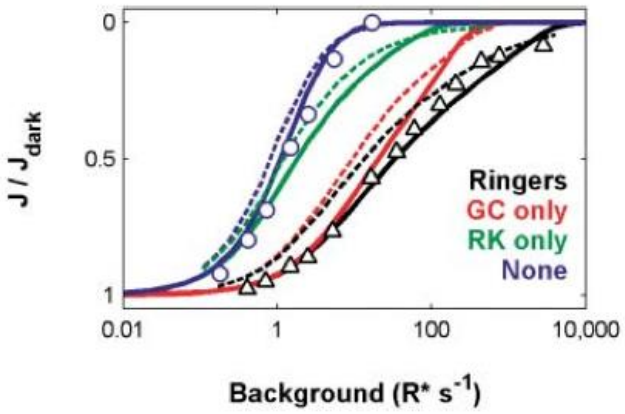

Figure 48. The unified model is a reproduction of Koutalos et al.'s steady-state measurements of circulating current as a function of background light adaptation in salamander rods (Koutalos et al. 1995). J/J_{dark} is the ratio of circulating current to dark adapted circulated current. R^*s^{-1} is the number of isomerized rhodopsin molecules per second. *Data points:* Koutalos et al.'s measures of rod steady-state current in Ringers (black triangles) or under a calcium clamp (blue circles). *Dashed curves:* Koutalos et al.'s model with a dark calcium value of 500nM. Data and model were shifted along the horizontal axis to compensate for differences in sensitivity between the salamander rods and Hamer et al.'s toad model. *Solid curves:* Corresponding predictions from Hamer et al.'s unified model. (Hamer et al. 2005).

Arden et al. (2011) determined that the 505nm light used in their trial increased rod threshold by approximately 3 log units, which equated to a retinal illuminance of 2 scotopic trolands (Td). It was stated that this would considerably reduce rod dark current and hence diminish oxygen demand, citing the work of Hamer et al. (2005) to substantiate this claim. However, this conflicts with previous reports from Thomas and Lamb (1999), who examined steady state light adaptation in eight human adults. The maximum size of the a-wave of the electroretinogram, a_{max}, which provides a measure of the total rod photoreceptor circulating current (Hood et al. 1993), was recorded

during light and dark adaptation. This was determined by analysing the rising phase of the rod-isolated flash responses over a wide range of light intensities. Prior to the start of any recordings, the participant was dark adapted for 15 minutes. Bleaching was accomplished by presenting at least 1 'white' flash for a duration of 1 millisecond in a Ganzfeld bowl. The larger bleaches were achieved by presenting multiple flashes at 5 second intervals.

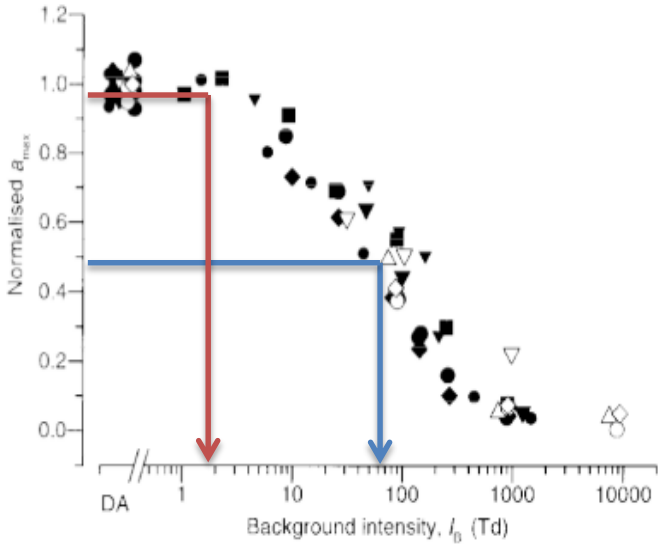

Figure 49. Dependence of maximal response a_{max} on background intensity collected from eight human subjects. The blue arrow indicates that a background intensity of 70 scotopic Td is needed to achieve a 50% reduction in a_{max}. The red arrow indicates that 2 scotopic Td does not significantly reduce a_{max} (Thomas and Lamb 1999).

As shown in Figure 49, Thomas and Lamb found that the rod's circulating current declined to half at a steady-state background intensity of 70 scotopic Td, which corresponds to approximately 600 photoisomerisations s^{-1} per rod. This suggests that the light intensity used by Arden et al. did not significantly reduce the circulating current (see red arrow in Figure 49). The data from Thomas and Lamb (1999) is substantiated by Nikonov et al. (2000), who found that about 400 photoisomerisations s^{-1} reduced the circulating current by 50% in salamander rods (see Figure 50). It is also comparable to the value of 100 Td that can be extracted for one human subject from 97B of Pepperberg et al. (1997) and is close to the 58 scotopic Td (500 photoisomerisations sec^{-1}) required to reduce circulating current by 50% in a human subject from Kraft et al. (1993), shown in Figure 51 below. It also compares with findings from further animal studies, such as the 250 photoisomerisations s^{-1} per rod

required to diminish the rod circulating current by 50% in a mouse, shown in Figure 52 (Lyubarsky et al. 1999).

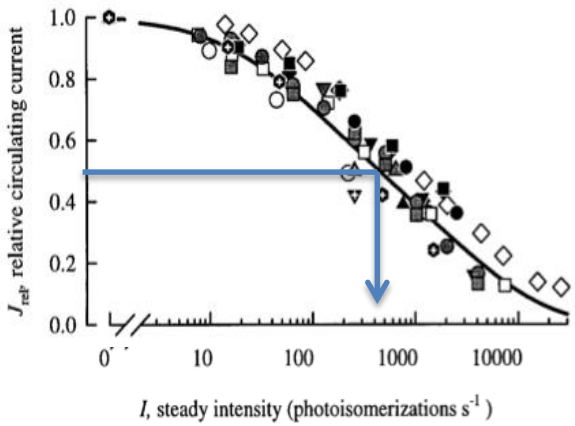

Figure 50. Dependence of steady circulating current of salamander rods on background intensity. Filled symbols indicated results from Nikonov et al.'s investigation, symbols from three previous studies are: ○, Hodgkin and Nunn, 1988; □, Matthews et al. 1988, average of seven cells; ⬨, Koutalos et al. 1995b, average of six cells (Nikonov et al. 2000).

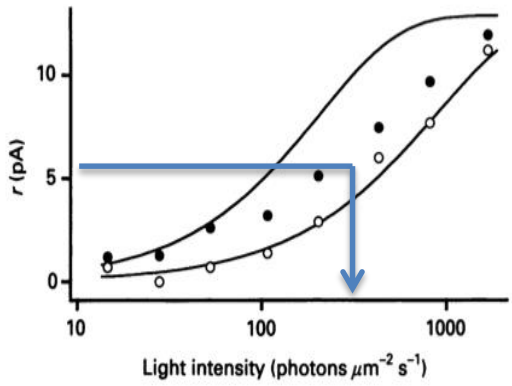

Figure 51. Responses to steps of light from rod photoreceptors. Filled circles plot steady-state response amplitude averaged over t = 4-6s as a function of light intensity. Open circles plot the amplitudes at 200ms. The curves plot the expected response amplitudes based on the instantaneous saturation function measured with brief flashes (Kraft et al. 1993)

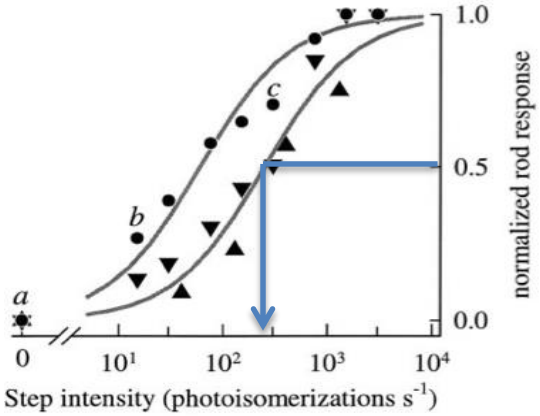

Figure 52. Inferred steady "photocurrent" response amplitudes of rods to the background light steps, derived from a separate a-wave ERG (circles) and from data of two other mice (triangles) (Lyubarsky et al. 1999).

Given this substantial evidence, including human data, it seems that 2 scotopic trolands is not a sufficient retinal illuminance to be confident of adequately reducing the rod circulating current. Whilst it is not known how much of a reduction would be 'adequate' to slow disease progression, a reduction of 50% will certainly reduce the oxygen demand in the outer retina in the dark. Using the data from Thomas and Lamb (1999), which is corroborated by Nikonov et al. (2000), Pepperberg et al. (1997) and Kraft et al. (1993), this suggests that 70 scotopic trolands may be a desirable light intensity for low-level light therapy.

4.3 Potential problems associated with melatonin disruption

4.3.1 Disruption of Circadian Rhythms

A concern regarding the use of low-level light at night is the potential disruption of circadian rhythms due to a reduction in melatonin secretion (Brainard et al. 2001a). It is important in designing a night time light therapy to consider the light intensity at which melatonin secretion is likely to be affected.

Circadian rhythms describe biological processes with an endogenously generated, 24-hour cycle. They are generated by the central circadian pacemaker located in the suprachiasmatic nucleus (SCN) of the hypothalamus and are primarily entrained to the 24-hour day by the light-dark cycle (Skene and Arendt 2006). Examples of human circadian rhythms include core body temperature and secretion of hormones such as cortisol and melatonin. As seen in Figure 53, these rhythms have a phase relationship

i.e. a set time interval between the different rhythms, however the timing of these rhythms is also entrained by the cycle of exogenous lightness and darkness. Indeed, because blind individuals lack a light-dark cycle, their circadian rhythms can become desynchronised from the 24-hour day (Lockley et al. 1997).

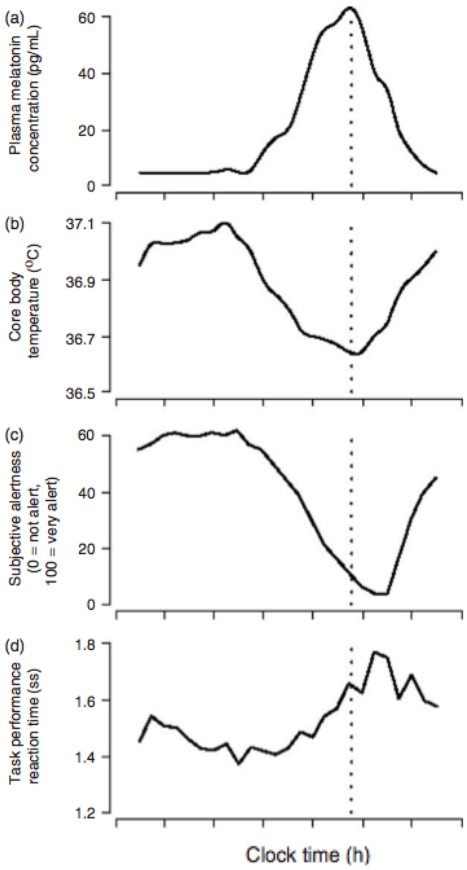

Figure 53. Diagrammatic representation of the circadian rhythms of plasma melatonin, core body temperature, subjective alertness and task performance. The peak in the melatonin rhythm is indicated by the dotted line (Skene and Arendt 2006).

Both animal (Lyubarsky et al. 1999; Lucas et al. 1999) and human (Brainard et al. 2001a; Thapan et al. 2001) studies have discovered a novel photoreceptor system which is responsible for mediating non-image forming functions such as synchronisation of the circadian clock, inhibition of pineal melatonin, core body temperature elevation, alertness and performance. The discovery of the photopigment melanopsin (Provencio et al. 1998) and a network of melanopsin-containing intrinsically photosensitive retinal ganglion cells (ipRGCs) (Berson et al. 2002) provides a framework for understanding how light signals are transmitted to the SCN and consequently to the pineal gland. In primates, ipRGCs are larger, but display similar morphologies to mice (Dacey et al.

2005). These ipRGCs are now known to be critical in modulating numerous behaviors including circadian photoentrainment, the pupillary light reflex and sleep/arousal (Berson et al. 2002; Göz et al. 2008; Güler et al. 2008; Altimus et al. 2010; Ecker et al. 2010).

The pineal hormone melatonin is a primary circadian pacemaker, synchronising the endogenous hormonal environment to the exogenous light-dark cycle. Plasma melatonin is a most reliable indicator for the timing of the circadian rhythm and it is thought to be a valid biomarker of circadian disruption in humans (Kerenyi et al. 1990; Klerman et al. 2002; Mirick and Davis 2008). Melatonin in saliva, plasma or urine is preferable to other biomarkers such as core body temperature due to its comparative robustness in the presence of external influences such as stress and physical activity (Stevens and Davis 1996; Pandi-Perumal et al. 2007). During clinical investigations of circadian dysfunction, the melatonin "onset" i.e. the beginning of the evening rise in melatonin levels has been often used as a phase marker of the body clock, since it is simple and fast to measure. The disadvantage to this is that nothing is known of the duration, total production or peak level of melatonin secretion (Arendt 2005).

The synthesis and secretion of melatonin from the pineal gland is most active during the night. Indeed, exposure to light can greatly suppress melatonin secretion (Lewy et al. 1980; Boyce and Kennaway 1987). The level of suppression is determined not only by the intensity of light, but also by its wavelength. Brainard and colleagues (2001) showed that in healthy humans, monochromatic light at 505 nm is circa four times stronger than 555 nm in suppressing melatonin (Brainard et al. 2001b). Lewy and colleagues (1980) were the first to discover that light intensity had an effect on the plasma melatonin levels in humans, shown in Figure 54 below. They found that 2500 lux was able to suppress melatonin to daytime levels in 6 normal humans; 1500 lux produced an intermediate amount of inhibition and 500 lux was insufficient to cause suppression.

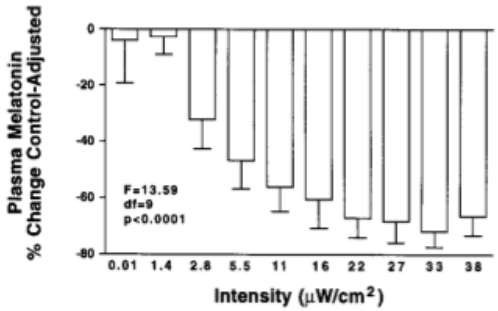

Figure 54. The mean + SEM % control-adjusted melatonin change values (N=8) at 505nm monochromatic light exposure. Note that progressively higher light irradiance exposure produces increasing melatonin suppression (Lewy et al. 1980).

Boyce and Kennaway (1987) found rather different results to those of Lewy et al. in that 2500 lux in their study did not suppress melatonin to daytime levels, as depicted in Figure 55. They postulated that the reason for this discrepancy was that their study was conducted at midnight, whereas Lewy's study was carried out between 2 and 4am. If such a circadian variation exists, it suggests that more light is required to suppress melatonin in the middle of the dark phase than early morning.

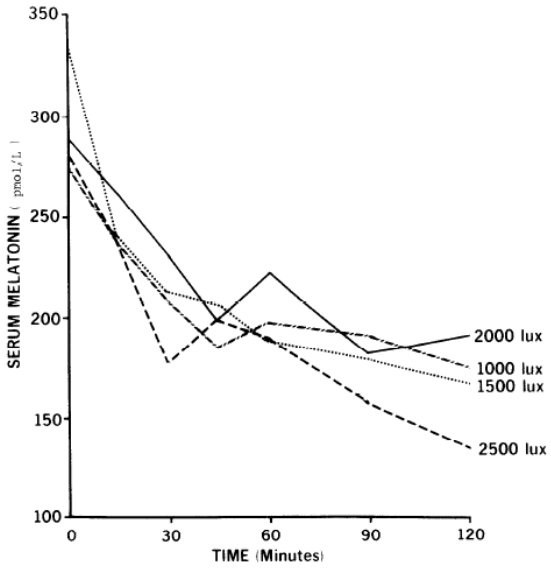

Figure 55. Serum melatonin with 4 different light intensities (Boyce and Kennaway 1987)

In 1989, McIntyre et al. examined the effect of five intensities of light on melatonin concentrations following one hour of light at midnight (McIntyre et al. 1989). Maximum suppression of melatonin was 71%, 67%, 44%, 38%, and 16% with intensities of 3,000, 1,000, 500, 350, and 200 lux, respectively. Unlike Boyce and

Kennaway, they found that 1000lux was sufficient to suppress melatonin to near daytime levels.

Brainard and colleagues (1988) exposed 6 healthy adult males to 0.01, 0.3, 1.6,5, or 13 $\mu W/cm^2$ of 509 nm monochromatic light for 1 h during the night on separate occasions (Brainard et al. 1988). Light irradiance was found to reduce melatonin in a dose-response pattern, the results of which are shown in Table 15. This shows that approximately 5 $\mu W/cm^2$ (86 Scotopic lux) is sufficient to suppress the melatonin secretion by 50%. Arden et al. (2011) stated that the retinal illumination (480 nm) required to reduce melatonin secretion by 50% is 25 $\mu W/cm^2$ (Arden et al. 2011), using data from the rod and cone outer segments of rhesus monkeys (Young 1971) and Sprague-Dawley rats (Schremser and Williams 1995) to justify this. Given the substantial published data regarding the effect of light on melatonin suppression in humans, it seems more appropriate to use this evidence as the basis for determining the threshold light level that reduces melatonin secretion by 50%, i.e. the more conservative estimate of 5 $\mu W/cm^2$. Therefore, the irradiance employed by the sleep mask must be less than 5 $\mu W/cm^2$ so as to not significantly disrupt the circadian cycle.

$\mu W/cm^2$	*Photons/cm^2*	*Photopic lux*	*Scotopic lux*	*Mean percent melatonin suppresion*
0.01	9.19×10^{13}	0.03	0.17	−9.67
0.3	2.76×10^{15}	1.03	5.25	1.83
1.6	1.47×10^{16}	5.50	27.98	37.33
5.0	4.59×10^{16}	17.18	85.90	51.67
13.0	1.19×10^{17}	44.66	227.37	60.67

Table 15. The effect of 509nm irradiances on suppression of plasma melatonin (Brainard et al. 1988).

4.3.2 Increased cancer risk

One of the main concerns regarding exposure to artificial light at night is the hypothesis that the decreased melatonin production increases the risk of developing cancer (Kerenyi et al. 1990). Indeed, Stevens and Davis (1996) postulated that the light-induced reduction in melatonin secretion led to an increased risk of breast cancer due to the increase in reproductive hormones such as oestrogens, which induced hormone-sensitive tumours in breast tissue. Experimental studies support this hypothesis, showing that physiological and pharmacological doses of melatonin reduce the growth

of malignant cells in the breast (Hill and Blask 1988; Cos et al. 1996) and other tumour locations (Petranka et al. 1999). Furthermore, clinical trials have demonstrated the therapeutic potential of melatonin in the treatment of cancer (Lissoni et al. 1995).

Numerous studies have been carried out to assess the risk of shift work on the development of breast cancer. In hospitals and office environments, where the majority of these studies have been conducted, the photopic illuminance is approximately between 100 and 300 photopic lux compared with 0.1 and 5 lux when asleep during the night and day, and 10,000 lux outdoors during daylight (Figueiro et al. 2006). A suggested threshold level for melatonin suppression is 30 lux of white light (Figueiro et al. 2006). On this basis, it is a reasonable assumption that night-shift women experience light levels that are bright enough and long enough to suppress nocturnal melatonin. A meta-analysis of 13 observational studies in 2005 suggested that shift work increased the risk of breast cancer by 48% (Megdal et al. 2005). However, there was evidence suggestive of confounding due to incomplete adjustment for risk factors such as reproductive history. Swerdlow (2003) mirrored this statement in his critical review of the epidemiological evidence. He concluded that although there is notable evidence for an association between shift work and breast cancer, it remains unclear whether this is simply as a consequence of confounding factors (Swerdlow 2003). A further systematic review also examined the role of nightshift work in other tumour locations, such as prostate and colon cancer. Three of the eight studies on breast cancer in women showed that long-term shift work (greater than 20-30 years) significantly increased the risk of breast cancer. However, since risk estimates were only moderately raised, there were few studies conducted and the studies all involved the same occupational group (nurses on nightshift), the results may be subject to bias, chance and confounding. The author found insufficient evidence of a causal association for any other cancers investigated (Kolstad 2008).

O'Leary et al. (2006) found that women who frequently turned lights on at home during the night (≥ twice/week and ≥ twice/night) had increased risks of developing breast cancer. However, this may simply reflect response biases, especially since the overnight shift workers interviewed yielded reduced risk estimates. Similarly, Davis et al. (2001) asked 813 breast cancer patients and 793 control subjects about their bedroom ambient light levels, by selecting one of three categories (see hand in front of face; see the end

of the bed; read comfortably). The brightest bedrooms had an increased risk of breast cancer among subjects, however the result was not statistically significant (Odds ratio (OR) = 1.4, Confidence interval (CI)= 0.8 to 2.6).

The limitation of these two studies is that they both relied upon self-report outcome measures. Hence, information bias may have played a significant role in these findings. At present, it is uncertain as to whether low-level lighting would have a significant effect on nocturnal melatonin production. Therefore, it is necessary for further experimental studies on the effect of chronic low-level light on melatonin expression to be conducted.

4.4 Light Attenuation by the Human Eyelid

In order to determine the retinal illuminance provided during sleep by an external light source, it is necessary to know how much light is transmitted through the eyelid. This has been investigated by several different researchers, the findings of which are summarised below.

Moseley et al. (1988) transilluminated closed eyelids of 3 subjects (1 Asian, 1 Caucasian, 1 Oriental) with an embedded optic fibre in an opaque contact lens. Light transmission at 500nm was found to be approximately 1%, with no significant difference between races. Later, Robinson et al. (1991) measured light transmission in vivo in 5 adults and 9 neonatals using a monochromatic grating presented though a fibre-optic mounted onto a contact lens underneath the lid and the signal was detected using a photodiode on the skin. At 505nm, about 2% light was transmitted through the eyelid, as depicted in Figure 56.

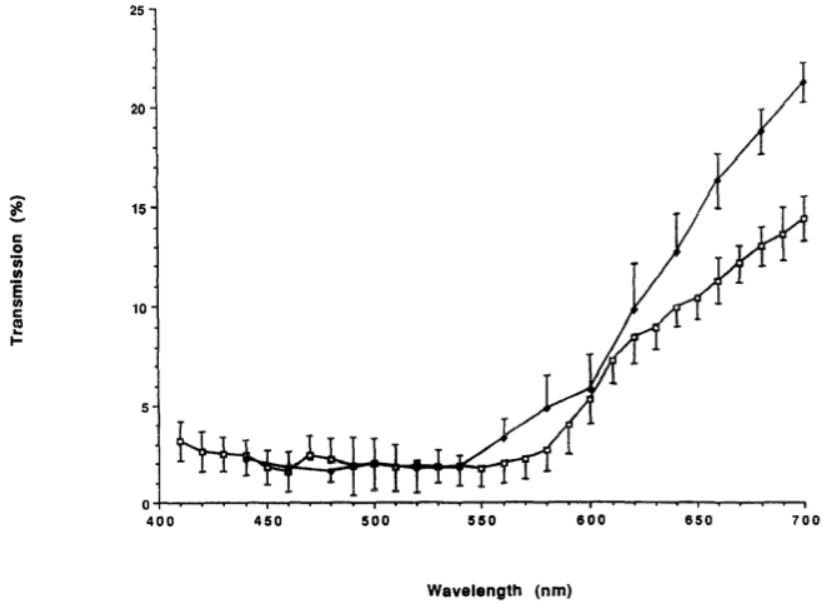

Figure 56.

Transmission of light through the adult and neonatal human eyelid. Each point represents the mean of the data obtained from 5 adult subjects or 9 neonatals. The bars indicated the SEM (Robinson et al. 1991).

More recently, Ando and Kripke (1996) used an optical diffuser, illuminated by a LED and placed 2cm from the eye, to measure light transmission. 11 subjects (6 men, 5 women, 8 Caucasian, 3 Asian) were examined, and visual thresholds were determined for large fields and short exposure. Estimated light transmission for blue light was 0.3% (±0.2), with no significant different difference in the age or race of subjects. Females were found to transmit a slightly higher percentage of light.

The difference in values for transmission found by the 3 studies is likely to be mainly due to the differences in measurement techniques. Moseley et al. (1988) required precise alignment of the source and detector to obtain maximum signal strength, whereas Robinson et al. had 200x larger sample and reference signals, enabling a better signal-noise ratio. Both of these studies used a contact lens, which caused measurement of scattered light to be variable. Ando and Kripke used a method that examined light from a wide visual field. In conclusion, the light transmission through the human eyelid at 505nm is approximately 1%.

4.5 Delivery of Light

As discussed in Section 4.2, it would be desirable to reduce rod dark current and thus oxygen consumption of rods by approximately 50%. The illumination required to

preferentially stimulate rod photoreceptors would have a peak output of approximately 500nm, with less output at longer and shorter wavelengths. The latter is particularly important to avoid the 'blue light hazard' that occurs below 480nm (Taylor et al. 1992; Bradnam et al. 1995), in which the short-wavelength photons can cause damage at lower fluxes. Furthermore, the 500nm wavelength is close to the peak rod sensitivity, and so will be efficient at suppressing the rod dark current.

One simple, cost-effective means of delivering light to patients during sleep is the use of a simple bedside lamp. The advantage of this is that it could be easily implemented in homes without creating substantial financial burdens on either the individual or the NHS. In order to ensure that both eyes were receiving the same level of illumination using an angle poise lamp, the sleep position of the participant would need to be supine. However, adults are much more likely to adopt a lateral sleeping position (De Koninck et al. 1983). Therefore, it would be impossible to ensure that all participants were receiving a standardised amount of light during the night. Although this would be acceptable for a pragmatic phase III clinical trial, it would not be appropriate for an exploratory phase I/II trial with a small number of subjects.

An alternative method of light delivery is for participants to wear an eye mask that emits a small amount of illumination during the night. In the pilot study of the effect of light therapy on diabetic retinopathy, Arden et al. (2010) made a mask that involved chemical luminescent 'glow patches' designed by Omniglow Corporation. These were safety certified, soft capsules with the appearance of a standard eye patch. When compressed, the two chemicals inside the capsules mixed together producing light with a dominant wavelength through the lids of 550nm. Headbands were needed to keep the glow patch in place, which were made of a light plastic that was inert and medically approved for comfort and safety. The 12 patients in the study who wore the glow patch over one eye for periods of up to 1 year had no ocular or systemic adverse effects, and did not suffer from any sleep disruption whilst wearing the glow patches. Since there were no dropouts during the study, it suggests that the non-invasive sleep mask was acceptable to the participants. However, the illumination of these disposable devices was not consistent and reduced significantly with time. For this reason, in their second trial, light emitting diodes (LEDs) were preferred as the new light source (Arden et al. 2011). The replacement frequency was modified from daily replacement to a 2-yearly

disposable eye mask, which permitted a more reliable and efficient light source. The four LEDs, each drawing 200uA current producing a peak wavelength of 505nm, were contained in a transparent silicone rubber shell and the printed circuit board was enclosed in a thick cotton cover, held against the eyes by an elastic headband. The device was driven by a battery that was recharged every morning. After 6 months, none of the participants reported any difficulty in wearing the masks, or any sleeping problems or mood alterations during the trial period. A limitation of the masks is that they had no means of assessing whether the LEDs were always positioned in front of the pupil during the night. This risk could be reduced by ensuring that the masks are properly fitted on the patient, with the headbands securely fastened.

A 12-weekly disposable light mask (Polyphotonix Medical, UK) has been developed recently, which is able to deliver precise illumination levels. The replacement frequency is higher than that of the previous light mask used by Arden et al. (2011), which ensures that the illumination remains constant over time. It presents organic LED illumination with a peak output of 502nm and a luminance of 75 photopic cd/m^2. This equates to 186 scotopic cd/m^2 when adjusted for the spectral sensitivity of rod photoreceptors (Wyszechki and Stiles 1982). Under this illumination, pupil diameter for people aged 60-85 years is approximately 4mm (Winn et al. 1994). This will produce a retinal illuminance of 23 scotopic trolands, assuming an eyelid transmission of 1%. This will reduce the rod circulating current by approximately 25%, according to the human data presented in Figure 49.

In order to standardise the period of mask usage by all individuals, the masks can be pre-programmed to function during a specific time period e.g. 8pm to 8am. If worn outside of these hours, the masks will not function. The mask illuminates when a sensor on the device is lightly pressed for 3 seconds. The mask will deactivate if not worn continuously for the first 15 minutes, after which it will remain on for 8 hours. The mask also contains a chip with a sensor that records when the mask is in contact with the face, providing precise information regarding the number of hours the mask is worn each night. This enables study investigators to objectively evaluate treatment fidelity. Each mask is also encrypted with a unique patient identification code, so that compliance data will be non-identifiable except via a password-protected database. In

order to assess treatment acceptability, a monthly interview would be recommended with each participant, during which a diary of mask usage should be discussed.

4.6 Summary of Study Design

A prospective Phase I/IIa proof of concept randomised controlled trial (RCT), consisting of two parallel groups with a 12-month follow-up period is proposed. Trial recruitment and data collection will take place in a medical retina clinic at a local eye hospital. Ophthalmologists will identify potential trial participants who are attending for their first appointment at the wet AMD clinic. Eligible participants will have neovascular AMD in one eye, and early AMD only in the fellow eye. The early AMD eye will be the study eye. Sixty participants will be recruited to the trial. In addition, 40 control participants and participants with grade 1 AMD (AREDS simplified scale) for a baseline cross-sectional analysis will be recruited by local optometrists in Bristol and Cardiff, from a database of elderly volunteers, from the Bristol Eye Hospital, from the list of research volunteers at the Cardiff University Eye Clinic and from staff and students of Cardiff University. The 60 participants taking part in the clinical trial will be stratified according to risk of AMD progression using the AREDS simplified scale (Ferris et al 2005) and randomly allocated to receive either light mask or no intervention in a 1:1 ratio using computer generated random permuted blocks (both groups will continue to receive Ranibizumab injections as required for the fellow eye). It is not appropriate in this study to use a sham treatment since a non-illuminated mask may have a physiological effect on the retina and patients would be aware that they weren't perceiving light and so would be unmasked to their intervention group. The intervention will be the Polyphotonix eye mask (see Section 4.5) that emits a dim green light through organic LEDs, illuminating the retina through closed eyelids at night. This is designed to reduce the metabolic activity of the retina, thereby reducing the potential risk of hypoxia. Participants will wear the mask every night for 12 months. A study flow diagram is shown in Figure 57 below.

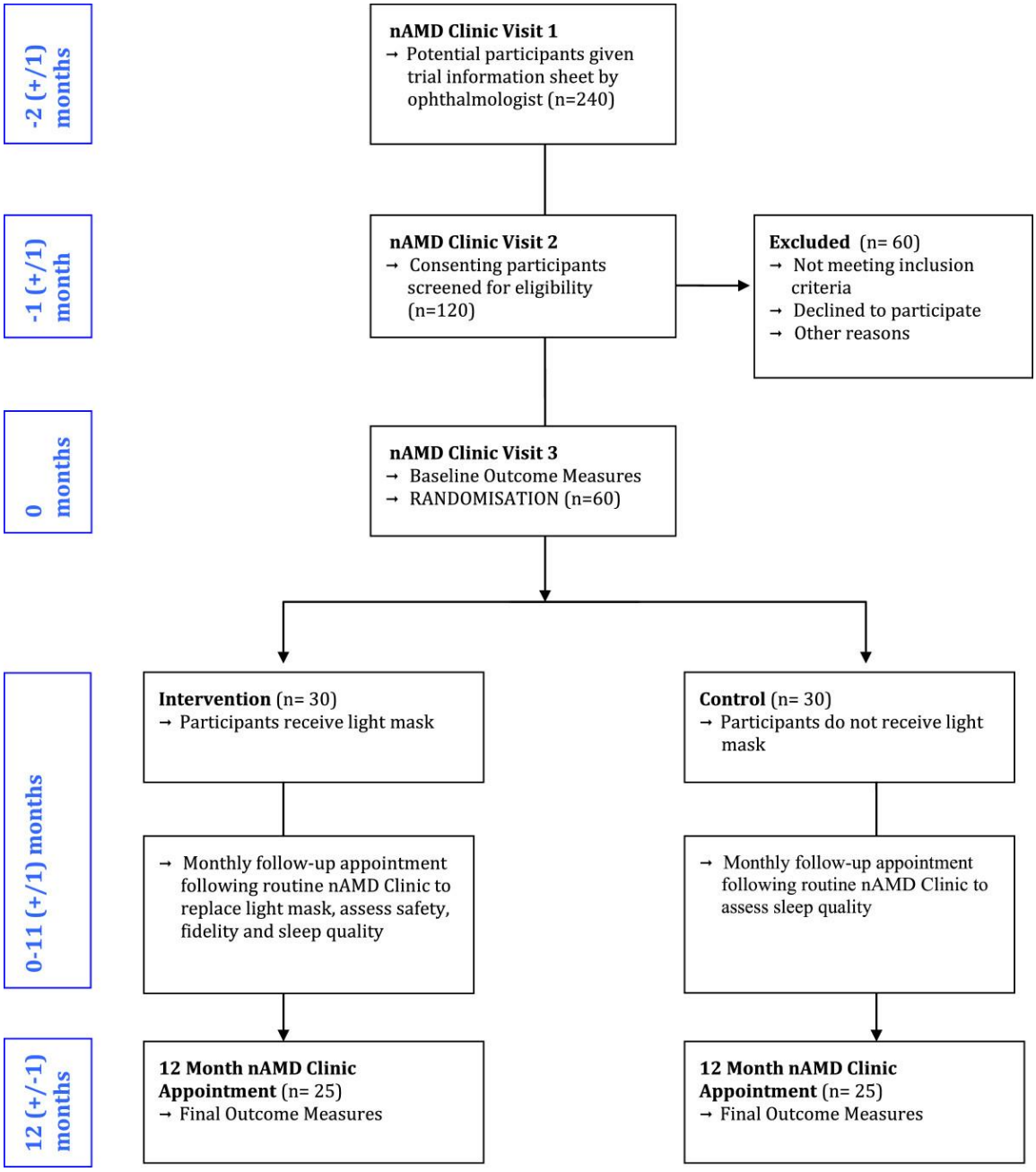

Figure 57. Study flow diagram showing participant timeline

4.7 Trial Objectives

The primary aim of this trial is to collect preliminary data from people with early AMD in one eye and neovascular AMD in the fellow eye, in order to assess the effect of low-level light therapy at night, compared with no intervention, on the progression of early AMD. Secondly, the safety of the intervention will be assessed since this is the first trial investigating light therapy in patients with AMD.

The secondary aims of the study are to:

1) Establish the effect of low-level night-time light therapy, compared with no treatment control, on secondary outcome measures, including: change in drusen volume from baseline in the eye with early AMD; Ranibizumab retreatment rates in the fellow eye with nAMD; progression of early AMD on the basis of change in functional outcome measures; change in health related QoL (assessed using the EuroQol EQ-5D instrument); change in self reported visual function assessed using the 48-item Veterans Affairs Low Vision Visual Functioning Questionnaire (VA LV VFQ-48).

2) Establish the acceptability of low-level night-time light therapy in people with AMD by monthly qualitative interviews.

3) Determine the effect of low-level night-time light therapy on sleep patterns by conducting the Pittsburgh Sleep Quality Index (PSQI) questionnaire every month with both intervention arms by interview with the study investigator.

4) Establish the relationship between baseline functional biomarker outcomes and the severity of AMD (assessed using simplified AREDS grading scale and initial drusen volume).

5) Evaluate the ability of all clinical tests to act as prognostic biomarkers for AMD progression.

6) Evaluate the ability of all clinical tests to act as predictive biomarkers for low-level night-time light therapy in people with AMD.

7) Compare the sensitivity of all clinical tests to disease progression over 12 months.

4.8 Eligibility criteria

Inclusion criteria

- Between the ages of 55-88 years
- ETDRS visual acuity 40 letters or better in the test eye
- Early AMD in the study eye
- nAMD in the fellow eye, within a month of 3rd Ranibizumab injection (trial only)
- Willing to adhere to allocated treatment for duration of trial

Exclusion criteria

- Ocular pathology other than macular disease

- Significant systemic disease or medication known to affect visual function
- Systemic disease that would compromise participation in a 1 year study (trial only)
- Insufficient English language comprehension
- Cognitive impairment as determined using an abridged Mini Mental State Examination (MMSE)
- Oxygen mask worn at night

Suspension criteria for the Trial

- Participant wishes to discontinue the study
- Serious adverse events (e.g. conversion of nAMD in the test eye) or unexpected changes in clinical status

4.9 Intervention

Participants will be randomly allocated to either the treatment arm, or a no treatment control group. Those allocated to the treatment group will be given a 12 weekly disposable light mask (Polyphotonix Medical, UK) that presents organic LED illumination (peak output 502 nm) to both eyes, overnight, for 12 weeks. Light masks will be replaced every 12 weeks at the participant's routine appointment at the nAMD clinic so that the total duration of mask usage is 12 months.

The current management of patients with early AMD involves advising on modifying their lifestyle, for instance, cessation of smoking and improving diet. The only other intervention which is based on evidence from a robust RCT is the provision of a nutritional supplement consisting of high dose antioxidants plus zinc. This AREDS formula (vitamin C, 500 mg; vitamin E, 400 IU; beta carotene, 15 mg and zinc, 80 mg) has been shown to reduce risk of progression from early to advanced AMD by around 20% over 5 years in people with specific features of AMD (AREDS 2001a). However, a recent systematic review by the Cochrane Collaboration indicated that there may be an increased risk of mortality in individuals taking vitamin E and beta carotene supplementation (Evans and Lawrenson 2012). As this was recently published, it is not reflected in the current guidelines for the management of AMD. For this reason, the low level light therapy will be compared to a no-treatment control, rather than to the AREDS formula as the best current intervention.

Participants in both groups will receive routine ophthalmological care for the eye with nAMD (i.e. Ranibizumab injections). If the eye with early AMD converts to nAMD, they will proceed to Ranibizumab treatment for this eye also, and will be withdrawn from the study.

4.10 Sample Size

The aim of this Phase I/IIa proof of concept study is to assess the acceptability of night-time light therapy, and to provide baseline data to enable a larger Phase III randomised controlled trial to be carried out. Therefore, it will not be powered to detect small changes. The aim is to recruit 60 people, which, allowing for a 15% dropout throughout the 12-month period, will leave a final cohort of 51. This will be enough to detect a 50% reduction in participants showing disease progression at a probability level of 0.2 with a power of 80%, and a change in the time constant of cone adaptation of 1 minute to be detected at a probability level of 0.05 with a power of 80%.

4.11 Statistical Analysis

Statistical analysis will be carried out on an intention-to-treat basis. There will be no interim analysis, but conversions to nAMD in the eye with early AMD at baseline, and ranibizumab retreatments for the fellow eye, will be recorded at each participant visit to the nAMD clinic for safety monitoring purposes. This trial will primarily be concerned with providing information about the safety of the device in the treatment of AMD, and the magnitude of any treatment effect. On this basis, descriptive statistics will be carried out to summarise the demographic characteristics of the two groups, as well as the proportion of individuals showing disease progression in each group, the magnitude of changes in secondary outcome measures, including drusen volume, measures of visual function, and the self-report tests, and the fellow eye retreatment rates.

The primary outcome measure will be the proportion of patients demonstrating disease progression at 12 months. Comparisons will be performed using stratified Mantel-Haenszel tests and presented as forest plots. Formal statistical analysis will also include linear regression analysis to investigate changes in drusen volume controlling for intervention arm, baseline drusen volume and patient characteristics. Analysis of covariance (ANCOVA) will be carried out to compare the change in secondary outcome measures and the ranibizumab retreatment rates over 12 months between the

two intervention arms. Note that all analysis except for the ranibizumab retreatment rate pertains to the eye with early AMD. To establish the relationship between baseline functional biomarker outcomes and the severity of AMD, a one-way analysis of variance (ANOVA) will be conducted to compare the mean results at baseline between participants with grades of AMD in each group on the AREDS simplified scale. This analysis will take place when the baseline data collection is complete. To assess the ability of the clinical tests to act as prognostic and predictive biomarkers, receiver operating characteristics curves will be constructed to plot the sensitivity and specificity of the baseline measures in predicting outcomes within the control and intervention arms, respectively. When the trial is completed, linear regression analysis will be used to determine how well the change in the functional measures relate to the change in our primary outcome measure (drusen volume), which is a validated biomarker for disease progression.

4.12 Outcome Measures

This study will include two co-primary outcome measures, one examining structural changes and one measuring functional changes. The former will be the proportion of people demonstrating disease progression in the eye with early AMD during the 12-month trial period. This will be based on an increase in drusen volume beyond the test-retest confidence intervals (Yehoshua et al. 2011a) or the development of advanced AMD. The drusen analysis software available for the Cirrus OCT, described in Section 1.3.5, allows drusen volume to be objectively assessed. No matter what the initial drusen volume, approximately 50% of people with AMD will have a significant increase in drusen volume over 12 months (Yehoshua et al. 2011a). A recent trial shows that about 10% of people will develop advanced AMD within 12 months (Neelam et al. 2008). Therefore, it is expected that 60% of participants would have an increase in drusen volume or a progression to advanced AMD. The development of the latter would be diagnosed by an ophthalmologist at the patient's monthly Ranibizumab clinic appointment. The primary functional outcome measure will be the change in the rate of retinal adaptation i.e. the time taken for photoreceptors to regain sensitivity following exposure to a bright flash of light.

Secondary outcome measures include the change in drusen volume over the 12-month trial period; the number of Ranibizumab retreatments required during the trial period in the fellow eye with wet AMD; changes in chromatic thresholds using the CAD test,

changes in visual acuity, psychophysical 14Hz flicker thresholds, self-report outcome measures including health related quality-of-life (EQ-5D) and visual function (VFQ-48), a sleep quality questionnaire (Pittsburgh Sleep Quality Index, PSQI) and a semi-structured interview (via monthly phone calls) to determine intervention acceptability.

The primary outcome measures and the first secondary outcome measure (the change in drusen volume) will be assessed at baseline and then at monthly intervals using OCT images obtained at the regular Ranibizumab follow-up appointments, in order to gain a better understanding about the time-course of structural changes as a result of the intervention.

4.13 Safety

Since low-level light-therapy is non-invasive, the risk of safety issues associated with the device is low. It is unlikely that any chemical, electrical or mechanical damage from the light-mask would occur, since the components of the light source and battery are sealed in a plastic casing. Allergic reaction to the foam that contacts the patient is also unlikely, since the plastic is inert. There is a potential for the device to disturb sleep. However, two previous trials using light-masks have not reported any adverse effects due to sleep disruption (Arden et al. 2010; Arden et al. 2011). The potential impact of device failure is that no light will be emitted and the device will be replaced. Therefore, no serious ethical considerations are apparent.

However, as this is the first clinical trial investigating the effect of low-level light therapy on AMD, it is important to monitor safety closely. All adverse events (AE) and serious adverse events (SAE) will be recorded. The chief investigator of the trial will be updated on AEs every month, and SAEs within two working days. Since the trial does not involve medicinal product or life-threatening procedure, the risk of a SAE is low. However, potential SAEs include an increased rate of developing wet AMD in the eye with early AMD and an increased rate of neovascular AMD recurring in the fellow eye, resulting in increased Ranibizumab retreatment rates. These SAEs would be diagnosed by ophthalmologists at the monthly Ranibizumab clinic and recorded by the study investigator by monthly assessment of medical records. In a recent meta-analysis of 5 studies investigating the development of wet AMD in the fellow eye, it was reported that the cumulative incidence of wet AMD in the 426 patients was 12.2% (CI 1.7% - 30.6%) (Wong et al. 2008). Therefore, a reasonable upper limit for the number

of people likely to convert to wet AMD each month would be n x (30.6% / 12 months), where n is the number of people wearing the light mask in the trial.

It is up to the chief investigator to evaluate the nature of the AEs and SAEs for seriousness, causality and expectedness. If an SAE occurs that is both related and unexpected, the chief investigator will notify the National Research Ethics Service, the Trial Steering Committee, and the Device Manufacturer who will in turn notify the MHRA within 15 days of being informed of the SAE.

4.14 Summary

Age-related macular degeneration (AMD) is the leading cause of blindness among older adults in the developed world. The only treatments currently available, such as Ranibizumab injections, are for neovascular AMD, which accounts for only 10-15% of people with the condition. Hypoxia has been implicated as one of the primary causes of AMD, and is most acute at night when the retina is most metabolically active. By increasing light levels at night, the metabolic requirements of the retina and hence the hypoxia will be significantly reduced. In this chapter, the development of a clinical trial protocol has been described which seeks to determine whether low-level night-time light therapy in patients with early AMD can prevent the progression of early AMD. This will be the first randomised controlled trial of its kind in AMD.

The intervention is an eye mask which emits a dim green light which illuminates the retina through closed eyelids at night. This is designed to reduce the metabolic activity of the retina, thereby reducing the potential risk of hypoxia. The retinal illuminance required to reduce oxygen demand by 50% in the dark is approximately 70 scotopic trolands. There is a concern that this light during the night will disrupt circadian rhythms due to a reduction in melatonin secretion. Therefore, the retinal illuminance employed by the sleep mask must be less than the threshold that reduces melatonin secretion by 50% so as to not significantly disrupt the circadian cycle. A luminance of 75 photopic cd/m^2 (equivalent to a retinal illuminance of 23 scotopic trolands) is sufficient to substantially reduce oxygen demand whilst not disrupting circadian rhythms, and hence sleep quality.

Chapter 5. Discussion and Future Work

This thesis has presented the development and evaluation of three functional biomarkers for the assessment of progression of AMD. It has confirmed that delayed dark adaptation is highly diagnostic for early AMD. Three stimuli, evaluating different macular locations, were compared, and it was determined that the assessment of foveal cone adaptation was optimal when using a 2^o radius stimulus (although the diagnostic capacity did not differ significantly from that provided by the other stimuli). Cone tau using the 2^o radius stimulus was able to distinguish patients with early AMD from healthy controls with a sensitivity of 90% and a specificity of 100%, and with an inter-session repeatability of 36.4%. The inter-session repeatability of two further functional tests known to be sensitive to early AMD, 14-Hz flicker thresholds and CAD chromatic sensitivity, was also established. The most repeatable test was found to be the RG CAD test, which performed significantly better than the 14-Hz flicker test. Finally, these outcome measures were used in the development of a protocol for a clinical trial examining the impact of low-level light therapy, a novel therapeutic intervention, on the progression of AMD.

5.1 Discussion

Age-related macular degeneration (AMD) is responsible for more than 50% of visual impairment registrations in the UK (Bunce et al. 2010) and is the leading cause of blindness in the developed world (Resnikoff et al. 2004). For the majority of people with AMD, there is no treatment. The remaining 10-15% of people with the advanced, neovascular form of the disease are mainly treated with intra-ocular injections of Ranibizumab. Follow up for these patients is long term and places a significant burden on the NHS. Indeed, advanced AMD currently costs the British economy £1.2B to £3.7B p.a (Access Economics 2009; Cruess et al. 2008). Furthermore, the disease is associated with depression, falls and social isolation (Dargent-Molina et al. 1996; Margrain et al. 2012). Given that the average age of the UK population is predicted to increase during the next two decades (Office for National Statistics 2009), this significant socioeconomic problem will simply continue to worsen as the incidence of AMD increases. Therefore, there is a great need to evaluate potential therapeutic interventions that endeavor to treat the disease at an early stage, to prevent sight loss from occurring.

Early AMD develops slowly over time, and therefore end stage disease is not a suitable outcome measure to use in Phase II clinical trials of novel interventions. Therefore, biomarkers must be implemented as surrogate outcome measures, which are both sensitive to changes in visual function over time and have a high level of intersession repeatability. Visual acuity is the most commonly used psychophysical test of visual function in clinical trials. However, VA is relatively unaffected during the early stages of AMD, making it insensitive to early changes in disease progression. Furthermore, the inherent variability of the test (1.5 logMAR lines) (Siderov and Tiu 1999) will often mask the minute changes in VA that occur in early AMD (2 letter loss) (Klein et al 1995). Therefore, recent cross-sectional studies have evaluated a number of alternative functional biomarkers for AMD, including dark adaptation (Gaffney et al. 2011; Dimitrov et al. 2011; Dimitrov et al. 2012), temporal sensitivity (Dimitrov et al. 2011; Dimitrov et al. 2012) and colour vision (O'Neill-Biba et al. 2010).

Dark Adaptation

Dark adaptation describes the recovery of visual sensitivity following exposure to a bright light which bleaches a substantial proportion of photopigment (Lamb and Pugh 2004). There is a growing body of evidence to suggest that dark adaptation is a sensitive biomarker in AMD, as discussed in Chapter 1 (Brown and Kitchin 1983; Brown et al. 1986a; Owsley et al. 2001; Owsley et al. 2007; Dimitrov et al. 2008; Dimitrov et al. 2011). Indeed, Dimitrov et al. (2011) rated rod recovery during dark adaptation to have the greatest diagnostic capacity compared to a battery of other tests including flicker sensitivity, photostress recovery and colour vision. However, due to its lengthy recording period and relative test difficulty it was deemed to have limited clinical applicability. Cone dark adaptation, on the other hand, is able to detect early AMD with a shorter test duration (Phipps et al. 2003; Dimitrov et al. 2008; Gaffney et al. 2011).

Gaffney et al. (2011) found that the time constant of cone recovery (cone τ) and the time to rod-cone break (RCB) were most diagnostic for early AMD when measured at 12^o from the fovea compared to 0.5^o, 2^o and 7^o retinal eccentricities. However, since the stimuli were not area-matched, it was not clear whether the 12^o stimulus truly had the greatest diagnostic potential or whether it simply had less variability due to the larger retinal area stimulated. Therefore, in Chapter 2, the dynamics of dark adaptation

were assessed using 3 area-matched stimuli (2^o radius spot and 7^o and 12^o radii annuli) in 10 participants with early AMD and 10 age-matched controls. The cone τ and time to RCB were highly diagnostic for AMD using all 3 stimuli, yielding areas under the ROC curves between 0.830 and 0.940. No statistically significant differences were found in the diagnostic performance between any parameter. This is contradictory to the previous findings of Gaffney et al. (2011), and suggests that the annular stimulus at 12^o was found to be most diagnostic in their study because the larger retinal area reduced variability. Therefore, all three stimuli would be suitable to use in the diagnosis of AMD.

However, for dark adaptation to be implemented as a biomarker in clinical trials, it is necessary to calculate its inter-session repeatability. This will enable clinicians to determine whether changes observed over time are due to measurement imprecision or disease progression. For this reason, the repeatability of cone τ and time to RCB was assessed using the same three stimuli in a cohort of 11 healthy young adults and 10 healthy older adults. The time constant of cone recovery using the 2^o stimulus produced the lowest coefficient of repeatability, although this was not significantly different from the other stimuli. There was no statistically significant difference in repeatability between the 6 parameters investigated (cone τ and time to RCB for 2^o spot, 7^o and 12^o radii annuli), with CoRs ranging between 36.4% and 53.3%. Therefore, any of the 3 stimuli may be used to monitor the progression of AMD and determine the efficacy of novel therapeutic interventions.

<u>14-Hz Flicker Test and Colour Assessment and Diagnosis (CAD) Test</u>

A number of studies have found temporal sensitivity to be reduced in patients with AMD (Mayer et al. 1992b; Mayer et al. 1994; Phipps et al. 2003; Phipps et al. 2004; Dimitrov et al. 2011; Luu et al. 2013). This is thought to be due to a compromised outer retinal oxygen supply in AMD being unable to meet increased metabolic demand elicited by flickering stimuli (Kiryu et al. 1995; Riva et al. 2001). The threshold for flicker detection has been rated as having the highest potential clinical value in the diagnosis and monitoring of AMD as it can be performed quickly, is reproducible and diagnostically sensitive (Phipps et al. 2004; Dimitrov et al. 2011). Furthermore, flicker threshold has also been shown to increase gradually with disease progression (Dimitrov et al. 2012).

An increase in chromatic thresholds, especially in the YB domain, has long been reported to occur in early AMD. Tritan colour contrast thresholds are abnormal in patients with AMD and minimal lens opacities (Arden and Wolf 2004), and they also change significantly over time in patients with early AMD compared with age-matched controls (Holz et al. 1995). A new computer-based technology, the CAD test, has recently been developed which enables the rapid quantification of chromatic thresholds (Barbur and Rodriguez-Carmona 2006). Using this test, YB thresholds have been found to increase linearly with disease severity (O'Neill-Biba et al. 2010).

In Chapter 3, the coefficient of repeatability of these two candidate functional biomarkers was evaluated in 30 healthy adult participants. The most repeatable test was found to be the RG CAD threshold test, which performed significant better than the 14-Hz flicker test. A small learning effect was found for both the 14-Hz flicker and the CAD parameters, indicating that the familiarisation trials were not sufficient to saturate learning. This observation indicates that a control group is required if these biomarkers are to be implemented in clinical trials of new interventions for AMD. The results of this study will help clinicians determine if changes over time are due to measurement imprecision or disease progression, provided that the experimental conditions and psychophysical procedures are kept constant. These, and other candidate biomarkers such as cone dark adaptation, must now be assessed in longitudinal studies to validate their prognostic and predictive capabilities.

Clinical Trial Development

Age-Related Macular Degeneration is characterised by the dysfunction and death of photoreceptors in the central retina. There is an increasing amount of evidence to implicate hypoxia in its pathogenesis (Feigl 2009; Stefánsson et al. 2011). By increasing the light level during the night, the metabolic demands of the outer retina could be significantly reduced, thus reducing the oxygen requirements, and potentially providing an intervention which would reduce the progression of conditions with a hypoxic aetiology, such as AMD and diabetic retinopathy (Arden 2001). Indeed, a recent clinical trial in patients with diabetic macular oedema who wore a low-level light mask during the night for 6 months found a reduction in oedema and an improvement in functional measures in the treated eye only, which was ascribed to the obviation of

hypoxia (Arden et al. 2011). Chapter 4 described the development of a clinical trial protocol that seeks to determine whether the same intervention (low level light therapy) could prevent the development of AMD.

A literature review of the effects of background luminance on the rod circulating current determined that 50 scotopic Td would provide a 50% reduction in the dark current. However, to minimise the effect of the intervention on the night-ime melatonin production, a retinal illuminance of 23 scotopic Td (causing a 25% reduction in circulating current) was selected for the trial. This chapter also reviewed literature on the best way of presenting this retinal illuminance, and determined that a light mask strapped to the participant's head at night would eliminate the problems represented by differences in the sleep position of different individuals when attempting to standardise the dose of light presented.

In summary, the main conclusions of this thesis are:

- Cone dark adaptation is a sensitive functional biomarker for early AMD.
- Area-matched stimuli of 2^o, 7^o and 12^o radii have equal diagnostic validity and inter-session repeatability for the assessment of cone dark adaptation in early AMD .
- The red-green CAD threshold test was significantly more repeatable than the 14-Hz flicker test.
- A small, but significant, learning effect exists for both the 14-Hz flicker test and the CAD parameters.
- A low level night time light therapy may be trialled using an eye mask which is able to substantially reduce the rod circulating current, but care should be taken to ensure that the irradiance does not exceed $5\mu W/cm^2$ in order to minimise the potential negative effects of melatonin production suppression.

5.2 Further Work

A primary aim of this thesis was the optimisation of cone dark adaptation protocols for the diagnosis of early AMD, and the measurement of the inter-session repeatability of three candidate functional biomarkers for AMD: cone dark adaptation; 14-Hz flicker and the CAD test. However, there is a lack of studies investigating the predictive value

of these tests in identifying persons at risk of disease progression. There is some evidence from small cohorts that cone dark adaptation and abnormal flicker sensitivity may predict the onset of nAMD (Mayer et al. 1992a; Mayer et al. 1994; Sandberg et al. 1998). However, further longitudinal studies are required to test this hypothesis. A predictive test is valuable as it enables the clinician to build an enhanced risk profile for each patient, allowing a suitable monitoring plan to be developed.

Further longitudinal data is also required to determine the ability of the tests to monitor disease progression. Dimitrov et al. (2012) investigated the relationship between visual function and fundus appearance by classifying almost 300 participants with AMD into 12 subgroups based on the International Classification and Grading System. They found that both 14-Hz flicker and colour vision declined linearly across the hierarchy of fundus changes, whereas dark adaptation appeared to become abnormal early, reached a point of poor function and then remained at this low level. This suggests that steady-state tests of visual function, namely 14-Hz flicker and colour vision, would have a potential value in monitoring disease progression. However, only a prospective study that monitors individuals with early AMD over time using these tests can truly validate this postulation.

For this reason, the clinical trial protocol that has been described in Chapter 4 has a secondary aim of evaluating the ability of these clinical tests to act as predictive biomarkers for low-level light therapy in people with AMD, and to compare the sensitivity of these tests to disease progression over the 12-month follow-up period.

In Chapter 3, it was found that the 14-Hz flicker test was significantly less repeatable than the RG CAD test parameter. It is possible that the repeatability of the test could be improved by extending the test duration in order to achieve a more reliable final threshold. Therefore, the inter-session repeatability should be re-assessed using an extended number of trials in the QUEST adaptive procedure to confirm this theory.

In Chapter 4, the development of a clinical trial protocol was described, which commenced in May 2014. Its primary aim is to collect preliminary Phase I/IIa proof of concept trial data from a cohort of participants with early AMD in one eye and advanced, wet AMD in the fellow eye, in order to assess the effect of low-level night-time light therapy, compared with no intervention, on disease progression in early AMD. Furthermore, the safety of the intervention will be assessed.

References

Ablonczy, Z., Higbee, D., Anderson, D.M., Dahrouj, M., Grey, A.C., Gutierrez, D., Koutalos, Y., et al. 2013. Lack of correlation between the spatial distribution of A2E and lipofuscin fluorescence in the human retinal pigment epithelium. *Investigative Ophthalmology & Visual Science* 54(8), pp. 5535–5542.

Access Economics 2009. *Future sight loss UK (1): The economic impact of partial sight and blindness in the UK adult population.* London: RNIB.

Age-Related Eye Disease Study Research Group 2001a. A randomized, placebo-controlled, clinical trial of high-dose supplementation with vitamins C and E and beta carotene for age-related cataract and vision loss: AREDS report no. 9. *Archives of Ophthalmology* 119(10), pp. 1439–1452.

Age-Related Eye Disease Study Research Group 2001b. The Age-Related Eye Disease Study system for classifying age-related macular degeneration from stereoscopic colour fundus photographs: the Age-Related Eye Disease Study Report Number 6. *American Journal of Ophthalmology* 132(5), pp. 668–681.

Age-Related Eye Disease Study 2 Research Group 2013. Lutein + zeaxanthin and omega-3 fatty acids for age-related macular degeneration: the Age-Related Eye Disease Study 2 (AREDS2) randomized clinical trial. *The Journal of the American Medical Association* 309(19), pp. 2005–2015.

Ahmed, S.S., Lott, M.N. and Marcus, D.M. 2005. The macular xanthophylls. *Survey of Ophthalmology* 50(2), pp. 183–193.

Aiello, L.P., Northrup, J.M., Keyt, B.A., Takagi, H. and Iwamoto, M.A. 1995. Hypoxic Regulation of Vascular Endothelial Growth Factor in Retinal Cells. *Archives of Ophthalmology* 113(12), pp. 1538–1544.

Alder, V.A., Su, E.N., Yu, D.Y., Cringle, S.J. and Yu, P.K. 1997. Diabetic retinopathy: early functional changes. *Clinical and Experimental Pharmacology and Physiology* 24(9- 10), pp. 785–788.

Alexander, K.R. and Fishman, G.A. 1984. Rod-cone interaction in flicker perimetry. *British Journal of Ophthalmology* 68(5), pp. 303–309.

Alexander, M.F., Maguire, M.G., Lietman, T.M., Snyder, J.R., Elman, M.J. and Fine, S.L. 1988. Assessment of visual function in patients with age-related macular degeneration and low visual acuity. *Archives Ophthalmology* 106(11), pp. 1543–1547.

Alm, A. and Bill, A. 1970. Blood flow and oxygen extraction in the cat uvea at normal and high intraocular pressures. *Acta physiologica Scandinavica* 80(1), pp. 19–28.

Alm, A. and Bill, A. 1972. The oxygen supply to the retina. II. Effects of high intraocular pressure and of increased arterial carbon dioxide tension on uveal and retinal blood flow in cats. A study with radioactively labelled microspheres including flow determinations in brain and some other tissues. *Acta Physiologica Scandinavica* 84(3), pp. 306–319.

Alm, A. and Bill, A. 1973. Ocular and optic nerve blood flow at normal and increased intraocular pressures in monkeys (Macaca irus): a study with radioactively labelled microspheres including flow determinations in brain and some other tissues. *Experimental eye research* 15(1), pp. 15–29.

Altimus, C.M., Güler, A.D., Alam, N.M., Arman, A.C., Prusky, G.T., Sampath, A.P. and Hattar, S. 2010. Rod photoreceptors drive circadian photoentrainment across a wide range of light intensities. *Nature Neuroscience* 13(9), pp. 1107–1112.

Altman, D.G.D. and Bland, J.M.J. 1994. Diagnostic tests 3: receiver operating characteristic plots. *British Medical Journal (Abstracts)* 309(6948), p. 188.

Ambati, J., Ambati, B.K., Yoo, S.H., Ianchulev, S. and Adamis, A.P. 2003. Age-Related Macular Degeneration: Etiology, Pathogenesis, and Therapeutic Strategies. *Survey of Ophthalmology* 48(3), pp. 257–293.

Ambati, J. and Fowler, B.J. 2012. Mechanisms of Age-Related Macular Degeneration. *Neuron* 75(1), pp. 26–39.

Ambati, J., Atkinson, J.P. and Gelfand, B.D. 2013. Immunology of age-related macular degeneration. *Nature Reviews: Immunology* 13(6), pp. 438–451.

Anderson, A.J. and Vingrys, A.J. 2000. Interactions between flicker thresholds and luminance pedestals. *Vision Research* 40(19), pp. 2579–2588.

Anderson, D.H. and Fisher, S.K. 1976. The photoreceptors of diurnal squirrels: outer segment structure, disc shedding, and protein renewal. *Journal of Ultrastructure Research* 55(1), pp. 119–141.

Anderson, D.H.D., Mullins, R.F.R., Hageman, G.S.G. and Johnson, L.V.L. 2002. A role for local inflammation in the formation of drusen in the aging eye. *American Journal of Ophthalmology* 134(3), pp. 411–431.

Ando, K. and Kripke, D.F. 1996. Light attenuation by the human eyelid. *Biological Psychiatry* 39(1), pp. 22–25.

Applegate, R.A., Adams, A.J., Cavender, J.C. and Zisman, F. 1987. Early colour vision changes in age-related maculopathy. *Applied Optics* 26(8), pp. 1458–1462.

Arden, G., Gündüz, K. and Perry, S. 1988. Colour vision testing with a computer graphics system: preliminary results. *Documenta Ophthalmologica* 69(2), pp. 167–174.

Arden, G.B. 2001. The absence of diabetic retinopathy in patients with retinitis pigmentosa: implications for pathophysiology and possible treatment. *The British Journal of Ophthalmology* 85(3), pp. 366–370.

Arden, G.B. and Wolf, J.E. 2004. Colour vision testing as an aid to diagnosis and management of age related maculopathy. *British Journal of Ophthalmology* 88(9), pp. 1180–1185.

Arden, G.B., Sidman, R.L., Arap, W. and Schlingemann, R.O. 2005. Spare the rod

and spoil the eye. *British Journal of Ophthalmology* 89(6), pp. 764–769.

Arden, G.B., Gündüz, M.K., Kurtenbach, A., Völker, M., Zrenner, E., Gündüz, S.B., Kamis, U., et al. 2010. A preliminary trial to determine whether prevention of dark adaptation affects the course of early diabetic retinopathy. *Eye* 24(7), pp. 1149–1155.

Arden, G.B., Jyothi, S., Hogg, C.H., Lee, Y.F. and Sivaprasad, S. 2011. Regression of early diabetic macular oedema is associated with prevention of dark adaptation. *Eye* 25(12), pp. 1546–1554.

AREDS2-HOME Study Research Group, Chew, E.Y., Clemons, T.E., Bressler, S.B., Elman, M.J., Danis, R.P., Domalpally, A., et al. 2014. Randomized trial of a home monitoring system for early detection of choroidal neovascularization home monitoring of the Eye (HOME) study. *Ophthalmology* 121(2), pp. 535–544.

Arendt, J. 2005. Melatonin: characteristics, concerns, and prospects. *Journal of Biological Rhythms* 20(4), pp. 291–303.

Atchison, D.A. and Lovie-Kitchin, J.E. 1990. Investigation of central visual fields in patients with age-related macular changes. *Optometry & Vision Science* 67(3), pp. 179-183.

Axer-Siegel, R.R., Ehrlich, R.R., Yassur, Y.Y., Rosenblatt, I.I., Kramer, M.M., Priel, E.E., Benjamini, Y.Y., et al. 2004. Photodynamic therapy for age-related macular degeneration in a clinical setting: visual results and angiographic patterns. *American Journal of Ophthalmology* 137(2), pp. 7.

Azab, M., Boyer, D.S., Bressler, N.M., Bressler, S.B., Cihelkova, I., Hao, Y., Immonen, I., et al. 2005. Verteporfin therapy of subfoveal minimally classic choroidal neovascularization in age-related macular degeneration: 2-year results of a randomized clinical trial. *Archives of Ophthalmology* 123(4), pp. 448–457.

Baffi, J., Byrnes, G., Chan, C.C. and Csaky, K.G. 2000. Choroidal neovascularization in the rat induced by adenovirus mediated expression of vascular endothelial growth factor. *Investigative Ophthalmology & Visual Science* 41(11), pp. 3582–3589.

Bailey, T.A., Kanuga, N., Romero, I.A., Greenwood, J., Luthert, P.J. and Cheetham, M.E. 2004. Oxidative stress affects the junctional integrity of retinal pigment epithelial cells. *Investigative Ophthalmology & Visual Science* 45(2), pp. 675–684.

Barbur, J.L. and Rodriguez-Carmona, M. 2006. Establishing the statistical limits of 'normal' chromatic sensitivity. *Proceedings of the ISCC/CIE Expert Symposium 2006 "75 Years of the CIE Standard Colourimetric Observer",* Ottawa, Ontario, Canada.

Barbur, J., Rodriguez-Carmona, M., Evans, S. and Milburn, N. 2009. Minimum colour vision requirements for professional flight wrew, part III: recommendations for new colour vision standards. Available at http://www.faa.gov/library/reports/medical/oamtechreports/2000s/media/200911.pdf. Accessed 6th June 2014.

Barbur, J.L. and Konstantakopoulou, E. 2012. Changes in colour vision with decreasing light level: separating the effects of normal aging from disease. *Journal of*

the Optical Society of America A 29, pp. A27-A35.

Bartlett, H., Davies, L.N. and Eperjesi, F. 2004. Reliability, normative data, and the effect of age-related macular disease on the Eger Macular Stressometer photostress recovery time. *Ophthalmic & Physiological Optics* 24(6), pp. 594–599.

Beatty, S., Boulton, M., Henson, D., Koh, H. and Murray, I.J. 1999. Macular pigment and age related macular degeneration. *British Journal of Ophthalmology* 83(7), pp. 867–877.

Beatty, S., Koh, H., Phil, M., Henson, D. and Boulton, M. 2000. The role of oxidative stress in the pathogenesis of age-related macular degeneration. *Survey of Ophthalmology* 45(2), pp. 115–134.

Bellmann, C., Unnebrink, K., Rubin, G.S., Miller, D. and Holz, F.G. 2003. Visual acuity and contrast sensitivity in patients with neovascular age-related macular degeneration. Results from the Radiation Therapy for Age-Related Macular Degeneration (RAD-) Study. *Graefe's Archive for Clinical and Experimental Ophthalmology* 241(12), pp. 968–974.

Bergeron-Sawitzke, J., Gold, B. and Olsh, A. 2009. Multilocus analysis of age-related macular degeneration. *European Journal of Human Genetics* 17(9), pp. 1190-1199.

Berson, D.M., Dunn, F.A. and Takao, M. 2002. Phototransduction by retinal ganglion cells that set the circadian clock. *Science* 295(5557), pp. 1070–1073.

Binns, A.M. and Margrain, T.H. 2007. Evaluating retinal function in age-related maculopathy with the ERG photostress test. *Investigative Ophthalmology & Visual Science* 48(6), pp. 2806–2813.

Birch, J., Barbur, J.L. and Harlow, A.J. 1992. New method based on random luminance masking for measuring isochromatic zones using high resolution colour displays. *Ophthalmic & Physiological Optics* 12(2), pp. 133–136.

Bird, A.C. 1992. Bruch's membrane change with age. *British Journal of Ophthalmology* 76(3), pp. 166–168.

Bird, A.C., Bressler, N.M., Bressler, S.B., Chisholm, I.H., Coscas, G., Davis, M.D., de Jong, P.T., et al. 1995. An international classification and grading system for age-related maculopathy and age-related macular degeneration. The International ARM Epidemiological Study Group. *Survey of Ophthalmology* 39(5), pp. 367–374.

Blaauwgeers, H.G.H., Holtkamp, G.M.G., Rutten, H.H., Witmer, A.N.A., Koolwijk, P.P., Partanen, T.A.T., Alitalo, K.K., et al. 1999. Polarized Vascular Endothelial Growth Factor Secretion by Human Retinal Pigment Epithelium and Localization of Vascular Endothelial Growth Factor Receptors on the Inner Choriocapillaris. *The American Journal of Pathology* 155(2), pp. 421-428.

Bland, J.M. and Altman, D.G. 1986. Statistical methods for assessing agreement between two methods of clinical measurement. *Lancet* 1, pp. 307–310.

Bok, D. 1993. The retinal pigment epithelium: a versatile partner in vision. *Journal of*

Cell Science. Supplement 17, pp. 189–195.

Booij, J.C., Baas, D.C., Beisekeeva, J., Gorgels, T.G.M.F. and Bergen, A.A.B. 2010. The dynamic nature of Bruch's membrane. *Progress in Retinal and Eye Research* 29(1), pp. 1–18.

Borodoker, N., Spaide, R.F., Maranan, L., Murray, J., Freund, K.B., Slakter, J.S., Sorenson, J.A., et al. 2002. Verteporfin infusion-associated pain. *American Journal of Ophthalmology* 133(2), pp. 211–214.

Bosch, M.M., Merz, T.M., Barthelmes, D., Petrig, B.L., Truffer, F., Bloch, K.E., Turk, A., et al. 2009. New insights into ocular blood flow at very high altitudes. *Journal of Applied Physiology* 106(2), pp. 454–460.

Boulton, M. 1998. The role of melanin in the RPE. In: Marmor, M., Wolfensberger, T., [eds.] *The retinal pigment epithelium.* Oxford: Oxford University Press, pp. 68-85.

Bowman, K.J. 1978. The effect of illuminance on colour discrimination in senile macular degeneration. *Modern Problems in Ophthalmology* 19, pp. 71–76.

Bowman, K.J. 1980. The clinical assessment of colour discrimination in senile macular degeneration. *Acta Ophthalmologica* 58(3), pp. 337–346.

Bowman, K.J., Collins, M.J. and Henry, C.J. 1984. The effect of age on performance on the Panel D-15 and Desaturated D-15: A quantitative evaluation. *Documenta Ophthalmologica Proceedings Series* 39, pp. 227–231.

Boyce, P. and Kennaway, D.J. 1987. Effects of light on melatonin production. *Biological Psychiatry* 22(4), pp. 473–478.

Bradnam, M.S., Montgomery, D.M., Moseley, H. and Dutton, G.N. 1995. Quantitative assessment of the blue-light hazard during indirect ophthalmoscopy and the increase in the ‘safe’ operating period achieved using a yellow lens. *Ophthalmology* 102(5), pp. 799–804.

Brainard, D.H. 1997. The Psychophysics Toolbox. *Spatial Vision* 10(4), pp. 433–436.

Brainard, G.C., Lewy, A.J., Menaker, M., Fredrickson, R.H., Miller, L.S., Weleber, R.G., Cassone, V., et al. 1988. Dose-response relationship between light irradiance and the suppression of plasma melatonin in human volunteers. *Brain Research* 454(1-2), pp. 212–218.

Brainard, G.C., Hanifin, J.P., Greeson, J.M., Byrne, B., Glickman, G., Gerner, E. and Rollag, M.D. 2001a. Action spectrum for melatonin regulation in humans: evidence for a novel circadian photoreceptor. *The Journal of Neuroscience: The Official Journal of the Society for Neuroscience* 21(16), pp. 6405–6412.

Brainard, G.C., Hanifin, J.P., Rollag, M.D., Greeson, J., Byrne, B., Glickman, G., Gerner, E., et al. 2001b. Human melatonin regulation is not mediated by the three cone photopic visual system. *The Journal of Clinical Endocrinology and Metabolism* 86(1), pp. 433–436.

Braun, R.D., Linsenmeier, R.A. and Goldstick, T.K. 1995. Oxygen consumption in the inner and outer retina of the cat. *Investigative Ophthalmology & Visual Science* 36(3), pp. 542–554.

Bressler, N.M. 2001. Photodynamic therapy of subfoveal choroidal neovascularization in age-related macular degeneration with verteporfin: two-year results of 2 randomized clinical trials-tap report 2. *Archives of Ophthalmology* 119(2), pp. 198–207.

Bressler, N.M., Silva, J.C., Bressler, S.B., Fine, S.L. and Green, W.R. 1994. Clinicopathologic correlation of drusen and retinal pigment epithelial abnormalities in age-related macular degeneration. *Retina* 14(2), pp. 130–142.

Brown, B.B. and Garner, L.F. 1983. Effects of luminance on contrast sensitivity in senile macular degeneration. *American Journal of Optometry and Physiological Optics* 60(9), pp. 788–793.

Brown, B.B. and Kitchin, J.L.J. 1983. Dark adaptation and the acuity/luminance response in senile macular degeneration (SMD). *American Journal of Optometry and Physiological Optics* 60(8), pp. 645–650.

Brown, B., Adams, A.J., Coletta, N.J. and Haegerstrom Portnoy, G. 1986a. Dark adaptation in age-related maculopathy. *Ophthalmic and Physiological Optics* 6(1), pp. 81–84.

Brown, B., Tobin, C., Roche, N. and Wolanowski, A. 1986b. Cone adaptation in age-related maculopathy. *American Journal of Optometry and Physiological Optics* 63(6), pp. 450–454.

Brown, B. and Kitchin, J.L. 1987a. Contrast sensitivity in central and paracentral retina in age related maculopathy. *Clinical and Experimental Optometry* 70, pp. 112-116.

Brown, B. and Kitchin, J.L. 1987b. Temporal function in age related maculopathy. *Clinical and Experimental Optometry*.

Brown, B. and Lovie-Kitchin, J. 1989. Temporal Summation in Age-Related Maculopathy. *Optometry and vision science : official publication of the American Academy of Optometry* 66(7), pp. 426–429.

Brown, D.M., Kaiser, P.K., Michels, M., Soubrane, G., Heier, J.S., Kim, R.Y., Sy, J.P., et al. 2006. Ranibizumab versus verteporfin for neovascular age-related macular degeneration. *New England Journal of Medicine* 355(14), pp. 1432–1444.

Brown, D.M., Michels, M., Kaiser, P.K., Heier, J.S., Sy, J.P. and Ianchulev, T. 2009. Ranibizumab versus Verteporfin Photodynamic Therapy for Neovascular Age-Related Macular Degeneration: Two-Year Results of the ANCHOR Study. *Ophthalmology* 116(1), pp. 57-65.e5.

Bullimore, M.A.M., Bailey, I.L.I. and Wacker, R.T.R. 1991. Face recognition in age-related maculopathy. *Investigative Ophthalmology & Visual Science* 32(7), pp. 2020–2029.

Bunce, C., Xing, W. and Wormald, R. 2010. Causes of blind and partial sight certifications in England and Wales: April 2007-March 2008. *Eye* 24(11), pp. 1692–1699.

Bunt-Milam, A.H. and Saari, J.C. 1983. Immunocytochemical localization of two retinoid-binding proteins in vertebrate retina. *The Journal of Cell Biology* 97(3), pp. 703–712.

Burns, M.E. and Baylor, D.A. 2001. Activation, deactivation, and adaptation in vertebrate photoreceptor cells. *Annual Review of Neuroscience* 24(1), pp. 779–805.

Burton, K.B., Owsley, C. and Sloane, M.E. 1993. Aging and neural spatial contrast sensitivity: photopic vision. *Vision Research* 33(7), pp. 939–946.

Campbell, F.W. and Green, D.G. 1965. Optical and retinal factors affecting visual resolution. *The Journal of physiology* 181(3), pp. 576–593.

Cao, J., McLeod, D.S., Merges, C.A. and Lutty, G.A. 1998. Choriocapillaris Degeneration and Related Pathologic Changes in Human Diabetic Eyes. *Archives of ophthalmology* 116(5), pp. 589–597.

Carr, R.E. 1974. Congenital stationary nightblindness. *Transactions of the American Ophthalmological Society* 72, pp. 448–487.

Chakravarthy, U., Soubrane, G., Bandello, F., Chong, V., Creuzot-Garcher, C., Dimitrakos, S.A., Korobelnik, J.F., et al. 2006. Evolving European guidance on the medical management of neovascular age related macular degeneration. *British Journal of Ophthalmology* 90(9), pp. 1188–1196.

Chakravarthy, U., Wong, T.Y., Fletcher, A., Piault, E., Evans, C., Zlateva, G., Buggage, R., et al. 2010. Clinical risk factors for age-related macular degeneration: a systematic review and meta-analysis. *BMC Ophthalmology* 10, p. 31.

Chakravarthy, U., Harding, S.P., Rogers, C.A., Downes, S.M., Lotery, A.J., Culliford, L.A. and Reeves, B.C. 2013. Alternative treatments to inhibit VEGF in age-related choroidal neovascularisation: 2-year findings of the IVAN randomised controlled trial. *The Lancet* 382(9900), pp. 1258-1267.

Chen, J.C., Fitzke, F.W., Pauleikhoff, D. and Bird, A.C. 1992. Functional loss in age-related Bruch's membrane change with choroidal perfusion defect. *Investigative ophthalmology & Visual Science* 33(2), pp. 334-340.

Cheng, A.S. and Vingrys, A.J. 1993. Visual Losses in Early Age Related Maculopathy. *Optometry and Vision Science* 70(2), pp. 89–96.

Cheung, C.M.G. and Wong, T.Y. 2013. Treatment of age-related macular degeneration. *Lancet* 382(9900), pp. 1230–1232.

Chew, E.Y.E., Lindblad, A.S.A. and Clemons, T.T. 2009. Summary results and recommendations from the age-related eye disease study. *Archives of Ophthalmology* 127(12), pp. 1678–1679.

Chilaris, G. 1962. Recovery time after macular illumination as a diagnostic and prognostic test. *American Journal of Ophthalmology* 53, pp. 311–314.

Cho, E., Hankinson, S.E., Willett, W.C., Stampfer, M.J., Spiegelman, D., Speizer, F.E., Rimm, E.B., et al. 2000. Prospective study of alcohol consumption and the risk of age-related macular degeneration. *Archives of Ophthalmology* 118(5), pp. 681–688.

Chylack, L.T., Wolfe, J.K., Friend, J., Khu, P.M., Singer, D.M., McCarthy, D., del Carmen, J., et al. 1993. Quantitating cataract and nuclear brunescence, the Harvard and LOCS systems. *Optometry and Vision Science* 70(11), pp. 886–895.

Cideciyan, A.V., Haeseleer, F., Fariss, R.N., Aleman, T.S., Jang, G.F., Verlinde, C.L., Marmor, M.F., et al. 2000. Rod and cone visual cycle consequences of a null mutation in the 11-cis-retinol dehydrogenase gene in man. *Visual neuroscience* 17(5), pp. 667–678.

Cideciyan, A.V., Pugh, E.N., Lamb, T.D., Huang, Y. and Jacobson, S.G. 1997. Rod plateaux during dark adaptation in Sorsby's fundus dystrophy and vitamin A deficiency. *Investigative Ophthalmology & Visual Science* 38(9), pp. 1786–1794.

Ciulla, T.A., Harris, A., Chung, H.S., Danis, R.P., Kagemann, L., McNulty, L., Pratt, L.M., et al. 1999. Colour Doppler imaging discloses reduced ocular blood flow velocities in nonexudative age-related macular degeneration. *American Journal of Ophthalmology* 128(1), pp. 75–80.

Ciulla, T.A., Harris, A. and Martin, B.J. 2001. Ocular perfusion and age-related macular degeneration. *Acta ophthalmologica Scandinavica* 79(2), pp. 108–115.

Ciulla, T.A., Harris, A., Kagemann, L., Danis, R.P., Pratt, L.M., Chung, H.S., Weinberger, D., et al. 2002. Choroidal perfusion perturbations in non-neovascular age related macular degeneration. *British Journal of Ophthalmology* 86(2), pp. 209–213.

Clark, M.E., McGwin, G., Neely, D., Feist, R., Mason, J.O., Thomley, M., White, M.F., et al. 2011. Association between retinal thickness measured by spectral-domain optical coherence tomography (OCT) and rod-mediated dark adaptation in non-exudative age-related maculopathy. *The British Journal of Ophthalmology* 95(10), pp. 1427–1432.

Coile, D.C. and Baker, H.D. 1992. Foveal dark adaptation, photopigment regeneration, and aging. *Visual Neuroscience* 8(1), pp. 27–39.

Coletta, N.J. and Adams, A.J. 1984. Rod-cone interaction in flicker detection. *Vision Research* 24(10), pp. 1333–1340.

Collins, M.J. 1986. Pre- age related maculopathy and the desaturated D- 15 colour vision test. *Clinical and Experimental Optometry* 69(6), pp. 223-227.

Collins, M.J. and Brown, B. 1989. Glare Recovery and Age-Related Maculopathy. *Clinical Vision Sciences* 4(2), pp. 145–153.

Complications of Age-Related Macular Degeneration Prevention Trial Research Group 2006. Laser treatment in patients with bilateral large drusen: the complications

of age-related macular degeneration prevention trial. *Ophthalmology* 113(11), pp. 1974–1986.

Cong, R., Zhou, B., Sun, Q., Gu, H., Tang, N. and Bin Wang 2008. Smoking and the Risk of Age-related Macular Degeneration: A Meta-Analysis. *Annals of Epidemiology* 18(8), p. 10.

Congdon, N., O'Colmain, B., Klaver, C.C.W., Klein, R., Muñoz, B., Friedman, D.S., Kempen, J., et al. 2004. Causes and prevalence of visual impairment among adults in the United States. *Archives of Ophthalmology* 122(4), pp. 477–485.

Connolly, D.M. 2011. Oxygenation State and Twilight Vision at 2438 m. *Aviation* 82(1), pp. 2–8.

Connolly, D.M. and Hosking, S.L. 2006. Aviation-related respiratory gas disturbances affect dark adaptation: a reappraisal. *Vision Research* 46(11), pp. 1784–1793.

Connolly, D.M. and Hosking, S.L. 2008. Oxygenation and gender effects on photopic frequency-doubled contrast sensitivity. *Vision Research* 48(2), pp. 281–288.

Connolly, D.M. and Serle, W.P. 2014. Assisted Night Vision and Oxygenation State: 'Steady Adapted Gaze'. *Aviation* 85(2), pp. 120–129.

Connolly, D.M., Barbur, J.L., Hosking, S.L. and Moorhead, I.R. 2008. Mild hypoxia impairs chromatic sensitivity in the mesopic range. *Investigative Ophthalmology & Visual Science* 49(2), pp. 820–827.

Cornwall, M.C. and Fain, G.L. 1994. Bleached pigment activates transduction in isolated rods of the salamander retina. *The Journal of Physiology* 480, pp. 261–279.

Corson, D.W., Cornwall, M.C., Macnichol, E.F., Jin, J., Johnson, R., Derguini, F., Croucht, R.K., et al. 1990. Sensitization of bleached rod photoreceptors by 11-cis-locked analogues of retinal. *Proceedings of the National Academy of Sciences of the United States of America* 87, pp. 6823–6827.

Cos, S., Fernández, F. and Sánchez-Barceló, E.J. 1996. Melatonin inhibits dna synthesis in mcf-7 human breast cancer cellsin vitro. *Life Sciences* 58(26), pp. 2447–2453.

Crossland, M. and Rubin, G. 2007. The Amsler chart: absence of evidence is not evidence of absence. *British Journal of Ophthalmology* 91(3), pp. 391–393.

Cruess, A.F., Zlateva, G., Xu, X., Soubrane, G., Pauleikhoff, D., Lotery, A., Mones, J., et al. 2008. Economic burden of bilateral neovascular age-related macular degeneration: multi-country observational study. *Pharmacoeconomics* 26(1), pp. 57–73.

Cruess, A.F., Zlateva, G., Pleil, A.M. and Wirostko, B. 2009. Photodynamic therapy with verteporfin in age-related macular degeneration: a systematic review of efficacy, safety, treatment modifications and pharmacoeconomic properties. *Acta Ophthalmologica* 87(2), pp. 118–132.

Curcio, C.A., Sloan, K.R., Kalina, R.E. and Hendrickson, A.E. 1990. Human photoreceptor topography. *Journal of Comparative Neurology* 292(4), pp. 497–523.

Curcio, C.A., Millican, C.L., Allen, K.A. and Kalina, R.E. 1993. Aging of the human photoreceptor mosaic: evidence for selective vulnerability of rods in central retina. *Investigative Ophthalmology & Visual Science* 34(12), pp. 3278–3296.

Curcio, C.A., Medeiros, N.E. and Millican, C.L. 1996. Photoreceptor loss in age-related macular degeneration. *Investigative Ophthalmology & Visual Science* 37(7), pp. 1236–1249.

Curtis, L.H., Hammill, B.G., Qualls, L.G., DiMartino, L.D., Wang, F., Schulman, K.A. and Cousins, S.W. 2012. Treatment patterns for neovascular age-related macular degeneration: analysis of 284 380 medicare beneficiaries. *American Journal of Ophthalmology* 153(6), pp. 1116–24.e1.

Dacey, D.M. and Petersen, M.R. 1992. Dendritic field size and morphology of midget and parasol ganglion cells of the human retina. *Proceedings of the National Academy of Sciences of the United States of America* 89(20), pp. 9666-9670.

Dacey, D.M., Liao, H.W., Peterson, B.B., Robinson, F.R., Smith, V.C., Pokorny, J., Yau, K.W., et al. 2005. Melanopsin-expressing ganglion cells in primate retina signal colour and irradiance and project to the LGN. *Nature* 433(7027), pp. 749–754.

Dargent-Molina, P., Favier, F., Grandjean, H., Baudoin, C., Schott, A.M., Hausherr, E., Meunier, P.J., Breart, G. 1996. Fall-related factors and risk of hip fracture: the EPIDOS prospective study. *Lancet* 348(9021), pp. 145–149.

Das, S.R., Bhardwaj, N., Kjeldbye, H. and Gouras, P. 1992. Muller cells of chicken retina synthesize 11-cis-retinol. *Biochemical Journal* 285, pp. 907–913.

Davis, S., Mirick, D.K., Stevens, R.G. 2001. Night shift work, light at night, and risk of breast cancer. *Journal of the National Cancer Institute* 93(20), pp. 1557-1562

Davis, M.D., Gangnon, R.E., Lee, L.Y., Hubbard, L.D., Klein, B.E.K., Klein, R., Ferris, F.L., et al. 2005. The Age-Related Eye Disease Study severity scale for age-related macular degeneration: AREDS Report No. 17. *Archives of Ophthalmology* 123(11), pp. 1484–1498.

De Koninck, J., Gagnon, P. and Lallier, S. 1983. Sleep positions in the young adult and their relationship with the subjective quality of sleep. *Sleep* 6(1), pp. 52–59.

Dean, F.M., Arden, G.B. and Dornhorst, A. 1997. Partial reversal of protan and tritan colour defects with inhaled oxygen in insulin dependent diabetic subjects. *British Journal of Ophthalmology* 81, pp. 27-30.

Delori, F.C., Dorey, C.K., Staurenghi, G., Arend, O., Goger, D.G. and Weiter, J.J. 1995. In vivo fluorescence of the ocular fundus exhibits retinal pigment epithelium lipofuscin characteristics. *Investigative Ophthalmology & Visual Science* 36(3), pp. 718–729.

Delori, F.C., Goger, D.G., Keilhauer, C., Salvetti, P. and Staurenghi, G. 2006.

Bimodal spatial distribution of macular pigment: evidence of a gender relationship. *Journal of the Optical Society of America. A* 23(3), pp. 521–538.

Despriet, D.D.G., van Duijn, C.M., Oostra, B.A., Uitterlinden, A.G., Hofman, A., Wright, A.F., Brink, ten, J.B., et al. 2009. Complement Component C3 and Risk of Age-Related Macular Degeneration. *Ophthalmology* 116(3), pp. 474–480.e2.

DeWan, A., Liu, M., Hartman, S., Zhang, S.S.-M., Liu, D.T.L., Zhao, C., Tam, P.O.S., et al. 2006. HTRA1 Promoter Polymorphism in Wet Age-Related Macular Degeneration. *Science* 314(5801), pp. 989–992.

Dhalla, M.S. and Fantin, A. 2005. Macular photostress testing: sensitivity and recovery with an automated perimeter. *Retina* 25(2), pp. 189–192.

Dhalla, M.S., Fantin, A., Blinder, K.J. and Bakal, J.A. 2007. The macular automated photostress test. *American Journal of Ophthalmology* 143(4), pp. 596–600.

Dimitrov, P.N., Guymer, R.H., Zele, A.J., Anderson, A.J. and Vingrys, A.J. 2008. Measuring rod and cone dynamics in age-related maculopathy. *Investigative Ophthalmology & Visual Science* 49(1), pp. 55–65.

Dimitrov, P.N., Robman, L.D., Varsamidis, M., Aung, K.Z., Makeyeva, G.A., Guymer, R.H. and Vingrys, A.J. 2011. Visual function tests as potential biomarkers in age-related macular degeneration. *Investigative Ophthalmology & Visual Science* 52(13), pp. 9457–9469.

Dimitrov, P.N., Robman, L.D., Varsamidis, M., Aung, K.Z., Makeyeva, G., Busija, L., Vingrys, A.J., et al. 2012. Relationship between clinical macular changes and retinal function in age-related macular degeneration. *Investigative Ophthalmology \& Visual Science* 53(9), pp. 5213–5220.

Dowling, J.E. 1960. Chemistry of Visual Adaptation in the Rat. *Nature* 188, pp. 114–118.

Drasdo, N., Chiti, Z., Owens, D.R. and North, R.V. 2002. Effect of darkness on inner retinal hypoxia in diabetes. *The Lancet* 359(9325), pp. 2251–2253.

Drexler, W. 2004. Ultrahigh-resolution optical coherence tomography. *Journal of Biomedical Optics* 9(1), pp. 47–74.

Drexler, W. and Fujimoto, J.G. 2008. *Optical Coherence Tomography: Technology and Applications*. Berlin: Springer.

Drexler, W.W., Sattmann, H.H., Hermann, B.B., Ko, T.H.T., Stur, M.M., Unterhuber, A.A., Scholda, C.C., et al. 2003. Enhanced visualization of macular pathology with the use of ultrahigh-resolution optical coherence tomography. *Archives of Ophthalmology* 121(5), pp. 695–706.

Du, H., Lim, S.L., Grob, S. and Zhang, K. 2011. Induced pluripotent stem cell therapies for geographic atrophy of age-related macular degeneration. *Seminars in Ophthalmology* 26(3), pp. 216–224.

Ecker, J.L., Dumitrescu, O.N., Wong, K.Y., Alam, N.M., Chen, S.-K., LeGates, T., Renna, J.M., et al. 2010. Melanopsin-expressing retinal ganglion-cell photoreceptors: cellular diversity and role in pattern vision. *Neuron* 67(1), pp. 49–60.

Edwards, A.O., Ritter, R., Abel, K.J., Manning, A., Panhuysen, C. and Farrer, L.A. 2005. Complement factor H polymorphism and age-related macular degeneration. *Science* 308(5720), pp. 421–424.

Eisner, A., Fleming, S.A., Klein, M.L. and Mauldin, W.M. 1987. Sensitivities in older eyes with good acuity: eyes whose fellow eye has exudative AMD. *Investigative Ophthalmology & Visual Science* 28(11), pp. 1832–1837.

Eisner, A., Stoumbos, V.D., Klein, M.L. and Fleming, S.A. 1991. Relations between fundus appearance and function. Eyes whose fellow eye has exudative age-related macular degeneration. *Investigative Ophthalmology & Visual Science* 32(1), pp. 8–20.

Eisner, A., Klein, M.L., Zilis, J.D. and Watkins, M.D. 1992. Visual function and the subsequent development of exudative age-related macular degeneration. *Investigative Ophthalmology & Visual Science* 33(11), pp. 3091–3102.

Elliott, D.B., Sanderson, K. and Conkey, A. 1990. The reliability of the Pelli-Robson contrast sensitivity chart. *Ophthalmic & Physiological Optics* 10(1), pp. 21–24.

Espinosa-Heidmann, D.G., Suner, I.J. and Catanuto, P. 2006. Cigarette smoke–related oxidants and the development of sub-RPE deposits in an experimental animal model of dry AMD. *Investigative Ophthalmology & Visual Science* 47(2), pp. 729-737.

Evans, J. 2008. Antioxidant supplements to prevent or slow down the progression of AMD: a systematic review and meta-analysis. *Eye* 22(6), pp. 751–760.

Evans, J.R. 2001. Risk Factors for Age-related Macular Degeneration. *Progress in Retinal and Eye Research* 20(2), pp. 227–253.

Evans, J.R. and Lawrenson, J.G. 2012. Antioxidant vitamin and mineral supplements for slowing the progression of age-related macular degeneration. *Cochrane Database of Systematic Reviews* 11, pp. CD000254–CD000254.

Eye Disease Case-Control Study Group 1992. Risk factors for neovascular age-related macular degeneration. *Archives of Ophthalmology* 110(12), pp. 1701–1708.

Falsini, B., Riva, C.E. and Logean, E. 2002. Flicker-evoked changes in human optic nerve blood flow: relationship with retinal neural activity. *Investigative Ophthalmology & Visual Science* 43(7), pp. 2309–2316.

Farwick, A., Dasch, B., Weber, B., Pauleikhoff, D. and Stoll, M. 2009. Variations in five genes and the severity of age-related macular degeneration: results from the Muenster aging and retina study. *Eye* 23(12), pp. 2238-2244.

Feigl, B. 2009. Age-related maculopathy - linking aetiology and pathophysiological changes to the ischaemia hypothesis. *Progress in Retinal and Eye Research* 28(1), pp. 63–86.

Feigl, B. 2007. Age-related maculopathy in the light of ischaemia. *Clinical & Experimental Optometry* 90(4), pp. 263–271.

Feigl, B., Brown, B., Lovie-Kitchin, J. and Swann, P. 2004. Monitoring retinal function in early age-related maculopathy: visual performance after 1 year. *Eye* 19(11), pp. 1169–1177.

Feigl, B., Brown, B., Lovie-Kitchin, J. and Swann, P. 2007a. Functional loss in early age-related maculopathy: the ischaemia postreceptoral hypothesis. *Eye* 21(6), pp. 689–696.

Feigl, B., Stewart, I. and Brown, B. 2007b. Experimental hypoxia in human eyes: implications for ischaemic disease. *Clinical Neurophysiologyy* 118(4), pp. 887–895.

Feigl, B., Stewart, I.B., Brown, B. and Zele, A.J. 2008. Local neuroretinal function during acute hypoxia in healthy older people. *Investigative Ophthalmology & Visual Science* 49(2), pp. 807–813.

Feigl, B., Zele, A.J. and Stewart, I.B. 2011. Mild systemic hypoxia and photopic visual field sensitivity. *Acta Ophthalmologica* 89(2), pp. e199–e204.

Ferris, F.L., Davis, M.D., Clemons, T.E., Lee, L.Y., Chew, E.Y., Lindblad, A.S., Milton, R.C., et al. 2005. A simplified severity scale for age-related macular degeneration: AREDS Report No. 18. *Archives of Ophthalmology* 123(11), pp. 1570–1574.

Figueiro, M.G., Rea, M.S. and Bullough, J.D. 2006. Does architectural lighting contribute to breast cancer? *Journal of Carcinogenesis* 5, p. 20.

Fine, A.M., Elman, M.J., Ebert, J.E., Prestia, P.A., Starr, J.S. and Fine, S.L. 1986. Earliest symptoms caused by neovascular membranes in the macula. *Archives of Ophthalmology* 104(4), pp. 513–514.

Formaz, F., Riva, C.E. and Geiser, M. 1997. Diffuse luminance flicker increases retinal vessel diameter in humans. *Current Eye Research* 16(12), pp. 1252–1257.

Forsius, H., Eriksson, A.W. and Krause, U. 1964. The dazzling test in diseases of the retina. *Acta Ophthalmologica* 42(1), pp. 55–63.

Frank, R.N., Amin, R.H., Eliott, D., Puklin, J.E. and Abrams, G.W. 1996. Basic fibroblast growth factor and vascular endothelial growth factor are present in epiretinal and choroidal neovascular membranes. *American Journal of Ophthalmology* 122(3), pp. 393–403.

Freeman, W.R., El-Bradey, M. and Plummer, D.J. 2004. Scanning laser entoptic perimetry for the detection of age-related macular degeneration. *Archives of Ophthalmology* 122(11), pp. 1647–1651.

Frennesson, C., Nilsson, U.L. and Nilsson, S. 1995. Colour contrast sensitivity in patients with soft drusen, an early stage of ARM. *Documenta Ophthalmologica* 90(4), pp. 377-386.

Friedman, E., Krupsky, S., Lane, A.M., Oak, S.S., Friedman, E.S., Egan, K. and Gragoudas, E.S. 1995. Ocular blood flow velocity in age-related macular degeneration. *Ophthalmology* 102(4), pp. 640–646.

Fulk, G.W., West, R.W. and Nakagawara, V.B. 1991. Effect of Simulated Altitude on the Visual Fields of Glaucoma Patients and the Elderly. *Optometry and Vision Science* 68(5), pp. 344-350.

Gaffney, A.J., Binns, A.M. and Margrain, T.H. 2011. Topography of cone dark adaptation deficits in age-related maculopathy. *Optometry and Vision Science* 88(9), pp. 1080–1087.

Gaffney, A.J., Binns, A.M. and Margrain, T.H. 2012. Aging and cone dark adaptation. *Optometry and vision science : official publication of the American Academy of Optometry* 89(8), pp. 1219–1224.

Gaffney, A.J., Binns, A.M. and Margrain, T.H. 2013. The effect of pre-adapting light intensity on dark adaptation in early age-related macular degeneration. *Documenta Ophthalmologica* 127(3), pp. 191–199.

Gaffney, A.J., Binns, A.M. and Margrain, T.H. 2014. Measurement of cone dark adaptation: a comparison of four psychophysical methods. *Documenta Ophthalmologica* 128(1), pp. 33–41.

Garhöfer, G., Zawinka, C., Resch, H., Huemer, K.H., Dorner, G.T. and Schmetterer, L. 2004. Diffuse luminance flicker increases blood flow in major retinal arteries and veins. *Vision Research* 44(8), pp. 833–838.

Gartner, S. and Henkind, P. 1981. Aging and degeneration of the human macula. 1. Outer nuclear layer and photoreceptors. *The British Journal of Ophthalmology* 65(1), pp. 23–28.

Gass, J.D.J. 1973. Drusen and disciform macular detachment and degeneration. *Archives of ophthalmology* 90(3), pp. 206–217.

Geirsdottir, A., Palsson, O., Hardarson, S.H., Olafsdottir, O.B., Kristjansdottir, J.V. and Stefansson, E. 2012. Retinal Vessel Oxygen Saturation in Healthy Individuals. *Investigative Ophthalmology & Visual Science* 53(9), pp. 5433–5442.

Geirsdóttir, A., Hardarson, S.H., Olafsdottir, O.B. and Stefánsson, E. 2014. Retinal oxygen metabolism in exudative age-related macular degeneration. *Acta Ophthalmologica* 92(1), pp. 27–33.

Glaser, J.S., Savino, P.J., Sumers, K.D., McDonald, S.A. and Knighton, R.W. 1977. The photostress recovery test in the clinical assessment of visual function. *American Journal of Ophthalmology* 83(2), pp. 255–260.

Gold, B., Merriam, J.E., Zernant, J., Hancox, L.S., Taiber, A.J., Gehrs, K., Cramer, K., et al. 2006. Variation in factor B (BF) and complement component 2 (C2) genes is associated with age-related macular degeneration. *Nature Genetics* 38(4), pp. 458–462.

Goldberg, M.F., Dhaliwal, R.S. and Olk, R.J. 1998. Indocyanine green angiography patterns of zones of relative decreased choroidal blood flow in patients with exudative age-related macular degeneration. *Ophthalmic Surgery and Lasers* 29(5), pp. 385–390.

Göz, D., Studholme, K., Lappi, D.A., Rollag, M.D., Provencio, I. and Morin, L.P. 2008. Targeted destruction of photosensitive retinal ganglion cells with a saporin conjugate alters the effects of light on mouse circadian rhythms. *PLoS One* 3(9), p. e3153.

Gragoudas, E.S., Adamis, A.P., Cunningham, E.T., Feinsod, M. and Guyer, D.R. 2004. Pegaptanib for neovascular age-related macular degeneration. *New England Journal of Medicine* 351(27), pp. 2805–2816.

Granit, R., Holmberg, T. and Zewi, M. 1938. On the mode of action of visual purple on the rod cell. *The Journal of Physiology* 94, pp. 430–440.

Greenstein, V.C., Thomas, S.R., Blaustein, H., Koenig, K. and Carr, R.E. 1993. Effects of early diabetic retinopathy on rod system sensitivity. *Optometry and Vision Science* 70(1), pp. 18–23.

Gregori, G., Wang, F., Rosenfeld, P.J., Yehoshua, Z., Gregori, N.Z., Lujan, B.J., Puliafito, C.A., et al. 2011. Spectral Domain Optical Coherence Tomography Imaging of Drusen in Nonexudative Age-Related Macular Degeneration. *Ophthalmology* 118(7), pp. 1373–1379.

Grey, A.C., Crouch, R.K., Koutalos, Y., Schey, K.L. and Ablonczy, Z. 2011. Spatial localization of A2E in the retinal pigment epithelium. *Investigative Ophthalmology & Visual Science* 52(7), pp. 3926–3933.

Grossniklaus, H.E., Martinez, J.A., Brown, V.B., Lambert, H.M., Sternberg, P., Capone, A., Aaberg, T.M., et al. 1992. Immunohistochemical and histochemical properties of surgically excised subretinal neovascular membranes in age-related macular degeneration. *American Journal of Ophthalmology* 114(4), pp. 464–472.

Guymer, R., Luthert, P. and Bird, A. 1999. Changes in Bruch's membrane and related structures with age. *Progress in Retinal and Eye Research* 18(1), pp. 59–90.

Güler, A.D., Ecker, J.L., Lall, G.S., Haq, S., Altimus, C.M., Liao, H.-W., Barnard, A.R., et al. 2008. Melanopsin cells are the principal conduits for rod-cone input to non-image-forming vision. *Nature* 453(7191), pp. 102–105.

Haegerstrom-Portnoy, G. and Brown, B. 1989. Two-colour increment thresholds in early age related maculopathy. *Clinical Vision Sciences* 4(2), pp. 165–172.

Hageman, G. 2001. An Integrated Hypothesis That Considers Drusen as Biomarkers of Immune-Mediated Processes at the RPE-Bruch's Membrane Interface in Aging and Age-Related Macular Degeneration. *Progress in Retinal and Eye Research* 20(6), pp. 705–732.

Hageman, G.S., Marmor, M.F., Yao, X.Y. and Johnson, L.V. 1995. The interphotoreceptor matrix mediates primate retinal adhesion. *Archives of*

Ophthalmology 113(5), pp. 655–660.

Haig, C. 1941. The course of rod dark adaptation as influenced by the intensity and duration of pre-adaptation to light. *The Journal of General Physiology* 1938, pp. 735–751.

Haimovici, R., Owens, S.L., Fitzke, F.W. and Bird, A.C. 2002. Dark adaptation in age-related macular degeneration: relationship to the fellow eye. *Graefe's Archive for Clinical and Experimental Ophthalmology* 240(2), pp. 90-95.

Haines, J.L., Hauser, M.A., Schmidt, S., Scott, W.K., Olson, L.M., Gallins, P., Spencer, K.L., et al. 2005. Complement factor H variant increases the risk of age-related macular degeneration. *Science* 308(5720), pp. 419–421.

Hamann, S. 2002. Molecular mechanisms of water transport in the eye. *International Review of Cytology* 215, pp. 395–431.

Hamer, R.D., Nicholas, S.C., Tranchina, D., Lamb, T.D. and Jarvinen, J.L.P. 2005. Toward a unified model of vertebrate rod phototransduction. *Visual Neuroscience* 22(4), pp. 417–436.

Hammond, C.J., Webster, A.R., Snieder, H. and Bird, A.C. 2002. Genetic influence on early age-related maculopathy: a twin study. *Ophthalmology* 109(4), pp. 730-736

Hanley, J.A.J. and McNeil, B.J.B. 1982. The meaning and use of the area under a receiver operating characteristic (ROC) curve. *Radiology* 143(1), pp. 29–36.

Harris, A., Arend, O., Danis, R.P., Evans, D., Wolf, S. and Martin, B.J. 1996. Hyperoxia improves contrast sensitivity in early diabetic retinopathy. *British Journal of Ophthalmology* 80(3), pp. 209–213.

Hassan, S.E.S., Lovie-Kitchin, J.E.J. and Woods, R.L.R. 2002. Vision and mobility performance of subjects with age-related macular degeneration. *Optometry and Vision Science* 79(11), pp. 697–707.

Havelius, U., Bergqvist, D., Falke, P., Hindfelt, B. and Krakau, T. 1997a. I. Impaired dark adaptation in symptomatic carotid artery disease. *Neurology* 49(5), pp. 1353-1359.

Havelius, U., Bergqvist, D., Hindfelt, B. and Krakau, T. 1997b. II. Improved dark adaptation after carotid endarterectomy Evidence of a long-term ischemic penumbra? *Neurology* 49(5), pp. 1360-1369.

Hecht, S., Haig, C. and Wald, G. 1935. The dark adaptation of retinal fields of different size and location. *Journal of General Physiology* 19(2), pp. 321–337.

Hecht, S., Haig, C. and Chase, A.M. 1937. The influence of light adaptation on subsequent dark adaptation of the eye. *Journal of General Physiology* 20(6), pp. 831–850.

Heiba, I.M.I., Elston, R.C.R., Klein, B.E.B. and Klein, R.R. 1994. Sibling correlations and segregation analysis of age-related maculopathy: the Beaver Dam Eye Study.

Genetic Epidemiology 11(1), pp. 51–67.

Hendrickson, A. 2005. Organization of the Adult Primate Fovea. In: *Macular Degeneration*. Berlin/Heidelberg: Springer-Verlag, pp. 1–23.

Henschel, A., Spital, G., Lommatzsch, A. and Pauleikhoff, D. 2009. Optical coherence tomography in neovascular age related macular degeneration compared to fluorescein angiography and visual acuity. *European Journal of Ophthalmology* 19(5), pp. 831–835.

Henson, D.B. and North, R.V. 1979. Dark adaptation in diabetes mellitus. *British Journal of Ophthalmology* 63(8), pp. 539-541.

Hibbs, S.P., Smith, A., Chow, L.P. and Downes, S.M. 2011. Colour photographs for screening in neovascular age-related macular degeneration: are they necessary? *Eye* 25(7), pp. 918–921.

Hill, S.M. and Blask, D.E. 1988. Effects of the pineal hormone melatonin on the proliferation and morphological characteristics of human breast cancer cells (MCF-7) in culture. *Cancer Research* 48(21), pp. 6121–6126.

Ho, L., van Leeuwen, R., Witteman, J.C.M., van Duijn, C.M., Uitterlinden, A.G., Hofman, A., de Jong, P.T.V.M., et al. 2011. Reducing the genetic risk of age-related macular degeneration with dietary antioxidants, zinc, and ω-3 fatty acids: the Rotterdam study. *Archives of Ophthalmology* 129(6), pp. 758–766.

Hogan, M. 1961. Ultrastructure of the choroid. Its role in the pathogenesis of chorioretinal disease. *Transactions of the Pacific Coast Ophthalmological Society Annual Meeting* 42, pp. 61–87.

Hogg, R.E. and Chakravarthy, U. 2006. Visual function and dysfunction in early and late age-related maculopathy. *Progress in Retinal and Eye Research* 25(3), pp. 249–276.

Holekamp, N.M., Bouck, N. and Volpert, O. 2002. Pigment epithelium-derived factor is deficient in the vitreous of patients with choroidal neovascularization due to age-related macular degeneration. *American Journal of Ophthalmology* 134(2), pp. 220–227.

Hollins, M. and Alpern, M. 1973. Dark adaptation and visual pigment regeneration in human cones. *Journal of General Physiology* 62(4), pp. 430–447.

Holz, F.G., Sheraidah, G., Pauleikhoff, D. and Bird, A.C. 1994. Analysis of lipid deposits extracted from human macular and peripheral Bruch's membrane. *Archives of Ophthalmology* 112(3), pp. 402–406.

Holz, F.G., Gross-Jendroska, M. and Eckstein, A. 1995. Colour contrast sensitivity in patients with age-related Bruch's membrane changes. *German Journal of Ophthalmology* 4(6), pp. 336-341.

Holz, F.G., Bellman, C., Staudt, S., Schütt, F. and Völcker, H.E. 2001. Fundus autofluorescence and development of geographic atrophy in age-related macular

degeneration. *Investigative Ophthalmology & Visual Science* 42(5), pp. 1051–1056.

Holz, F.G., Bindewald-Wittich, A., Fleckenstein, M., Dreyhaupt, J., Scholl, H.P. and Schmitz-Valckenberg, S. 2007. Progression of geographic atrophy and impact of fundus autofluorescence patterns in age-related macular degeneration. *American Journal of Ophthalmology* 143(3), pp. 463-472.

Hood, D.C., Benimoff, N.I. and Greenstein, V.C. 1984. The response range of the blue-cone pathways: a source of vulnerability to disease. *Investigative Ophthalmology & Visual Science* 25(7), pp. 864–867.

Hood, D.C., Shady, S. and Birch, D.G. 1993. Heterogeneity in retinal disease and the computational model of the human-rod response. *Journal of the Optical Society of America A* 10(7), pp. 1624–1630.

Hood, D.C.D., Frishman, L.J.L., Saszik, S.S. and Viswanathan, S.S. 2002. Retinal origins of the primate multifocal ERG: implications for the human response. *Investigative Ophthalmology & Visual Science* 43(5), pp. 1673–1685.

Hughes, B.A. and Gallemore, R.P. 1998. *Transport mechanisms in the retinal pigment epithelium*. New York: Oxford University Press.

Hwang, J.C., Chan, J.W.K., Chang, S. and Smith, R.T. 2006. Predictive value of fundus autofluorescence for development of geographic atrophy in age-related macular degeneration. *Investigative Ophthalmology & Visual Science* 47(6), pp. 2655–2661.

Hyvärinen, L., Laurinen, P. and Rovamo, J. 1983. Contrast sensitivity in evaluation of visual impairment due to macular degeneration and optic nerve lesions. *Acta Ophthalmologica* 61(2), pp. 161–170.

Inoue, Y., Yanagi, Y., Matsuura, K., Takahashi, H., Tamaki, Y. and Araie, M. 2007. Expression of hypoxia-inducible factor 1α and 2α in choroidal neovascular membranes associated with age-related macular degeneration. *The British Journal of Ophthalmology* 91(12), pp. 1720–1721.

Iwama, D., Hangai, M., Ooto, S., Sakamoto, A., Nakanishi, H., Fujimura, T., Domalpally, A., et al. 2012. Automated assessment of drusen using three-dimensional spectral-domain optical coherence tomography. *Investigative Ophthalmology & Visual Science* 53(3), pp. 1576–1583.

Jackson, G.R. and Edwards, J.G. 2008. A short-duration dark adaptation protocol for assessment of age-related maculopathy. *Journal of Ocular Biology, Diseases, and Informatics* 1(1), pp. 7–11.

Jackson, G.R., Felix, T. and Owsley, C. 2006. The Scotopic Sensitivity Tester-1 and the detection of early age-related macular degeneration. *Ophthalmic & Physiological Optics* 26(4), pp. 431–437.

Jackson, G.R., Jackson, G.R., Owsley, C., Owsley, C., Cordle, E.P., Price Cordle, E., Finley, C.D., et al. 1998. Aging and scotopic sensitivity. *Vision Research* 38(22), pp. 3655–3662.

Jackson, G.R., Owsley, C. and McGwin, G. 1999. Aging and dark adaptation. *Vision Research* 39(23), pp. 3975–3982.

Jackson, G.R., Scott, I.U., Kim, I.K., Quillen, D.A., Iannaccone, A. and Edwards, J.G. 2014. Diagnostic sensitivity and specificity of dark adaptometry for detection of age-related macular degeneration. *Investigative Ophthalmology & Visual Science* 55(3), pp. 1427–1431.

Jacobson, S.G., Cideciyan, A.V., Regunath, G., Rodriguez, F.J., Vandenburgh, K., Sheffield, V.C. and Stone, E.M. 1995. Night blindness in Sorsby's fundus dystrophy reversed by vitamin A. *Nature Genetics* 11(1), pp. 27–32.

Jain, N., Farsiu, S., Khanifar, A.A., Bearelly, S., Smith, R.T., Izatt, J.A. and Toth, C.A. 2010. Quantitative Comparison of Drusen Segmented on SD-OCT versus Drusen Delineated on Colour Fundus Photographs. *Investigative Ophthalmology & Visual Science* 51(10), pp. 4875–4883.

Jain, S., Hamada, S., Membrey, W.L. and Chong, V. 2006. Screening for age-related macular degeneration using nonstereo digital fundus photographs. *Eye* 20(4), pp. 471–475.

Jampol, L.M. and Tielsch, J. 1992. Race, macular degeneration, and the Macular Photocoagulation Study. *Archives of Ophthalmology* 110(12), pp. 1699–1700.

Jiang, S., Moriarty-Craige, S.E., Orr, M., Cai, J., Sternberg, P. and Jones, D.P. 2005. Oxidant-induced apoptosis in human retinal pigment epithelial cells: dependence on extracellular redox state. *Investigative Ophthalmology & Visual Science* 46(3), pp. 1054–1061.

Johnson, L.V.L., Ozaki, S.S., Staples, M.K.M., Erickson, P.A.P. and Anderson, D.H.D. 2000. A Potential Role for Immune Complex Pathogenesis in Drusen Formation. *Experimental Eye Research* 70(4), p. 9.

Kalloniatis, M. and Luu, C. 2011a. *Psychophysics of Vision.* http://webvision.med.utah.edu/book/part-viii-gabacreceptors/light -and-dark-adaptation/. Accessed 6th June 2014.

Kalloniatis, M. and Luu, C. 2011b. *Psychophysics of Vision.* http://webvision.med.utah.edu/book/part-viii-gabac-receptors/colour-perception/. Accessed 6th June 2014.

Kanda, A., Abecasis, G. and Swaroop, A. 2008. Inflammation in the pathogenesis of age-related macular degeneration. *British Journal of Ophthalmology* 92(4), pp. 448–450.

Karakucuk, S., Oner, A.O., Goktas, S., Siki, E. and Kose, O. 2004. Colour vision changes in young subjects acutely exposed to 3,000 m altitude. *Aviation Space and Environmental Medicine* 75(4), pp. 364–366.

Kelly, D.H. 1972. Adaptation effects on spatio-temporal sine-wave thresholds. *Vision Research* 12, pp 89-101.

Kelly, S.P., Thornton, J., Lyratzopoulos, G., Edwards, R. and Mitchell, P. 2004. Smoking and blindness. *British Medical Journal (Abstracts)* 328(7439), pp. 537–538.

Kemp, C.M., Jacobson, S.G., Faulkner, D.J. and Walt, R.W. 1988. Visual function and rhodopsin levels in humans with vitamin A deficiency. *Experimental Eye Research* 46(2), pp. 185–197.

Kerenyi, N.A., Pandula, E. and Feuer, G.M. 1990. Oncostatic effects of the pineal gland. *Drug Metabolism and Drug Interactions* 8(3-4), pp. 313–319.

Kern, T.S. and Engerman, R.L. 1996. Capillary lesions develop in retina rather than cerebral cortex in diabetes and experimental galactosemia. *Archives of Ophthalmology* 114(3), pp. 306–310.

Khan, J.C., Thurlby, D.A., Shahid, H., Clayton, D.G., Yates, J.R.W., Bradley, M., Moore, A.T., et al. 2006. Smoking and age related macular degeneration: the number of pack years of cigarette smoking is a major determinant of risk for both geographic atrophy and choroidal neovascularisation. *British Journal of Ophthalmology* 90(1), pp. 75–80.

Khandhadia, S. and Lotery, A. 2010. Oxidation and age-related macular degeneration: insights from molecular biology. *Expert Reviews in Molecular Medicine* 12, pp. e34–e34.

Khanifar, A.A.A., Koreishi, A.F.A., Izatt, J.A.J. and Toth, C.A.C. 2008. Drusen ultrastructure imaging with spectral domain optical coherence tomography in age-related macular degeneration. *Ophthalmology* 115(11), pp. 1883–1890.

Kim, C.B. and Mayer, M.J. 1994. Foveal flicker sensitivity in healthy aging eyes. II. Cross-sectional aging trends from 18 through 77 years of age. *Journal of the Optical Society of America* 11(7), pp. 1958–1969.

Kim, Y.H., He, S., Kase, S., Kitamura, M., Ryan, S.J. and Hinton, D.R. 2009. Regulated secretion of complement factor H by RPE and its role in RPE migration. *Graefe's Archive for Clinical and Experimental Ophthalmology* 247(5), pp. 651–659.

King-Smith, P.E., Grigsby, S.S., Vingrys, A.J., Benes, S.C. and Supowit, A. 1994. Efficient and unbiased modifications of the QUEST threshold method: theory, simulations, experimental evaluation and practical implementation. *Vision Research* 34(7), pp. 885–912.

Kiryu, J., Asrani, S., Shahidi, M., Mori, M. and Zeimer, R. 1995. Local response of the primate retinal microcirculation to increased metabolic demand induced by flicker. *Investigative Ophthalmology & Visual Science* 36(7), pp. 1240–1246.

Kita, M. and Marmor, M.F. 1992. Effects on retinal adhesive force in vivo of metabolically active agents in the subretinal space. *Investigative Ophthalmology & Visual Science* 33(6), pp. 1883–1887.

Klais, C.M.C., Ober, M.D.M., Freund, K.B.K., Ginsburg, L.H.L., Luckie, A.A., Mauget-Faÿsse, M.M., Coscas, G.G., et al. 2005. Choroidal infarction following photodynamic therapy with verteporfin. *Archives of Ophthalmology* 123(8), pp.

1149–1153.

Klaver, C.C.W., Assink, J.J.M., van Leeuwen, R., Wolfs, R.C.W., Vingerling, J.R., Stijnen, T., Hofman, A., et al. 2001. Incidence and Progression Rates of Age-Related Maculopathy: The Rotterdam Study. *Investigative Ophthalmology & Visual Science* 42(10), pp. 2237-2241.

Klein, R., Davis, M.D.M., Magli, Y.L.Y., Segal, P.P., Klein, B.E.B. and Hubbard, L.L. 1991. The Wisconsin age-related maculopathy grading system. *Ophthalmology* 98(7), pp. 1128–1134.

Klein, R., Wang, Q., Klein, B.E., Moss, S.E. and Meuer, S.M. 1995. The relationship of age-related maculopathy, cataract, and glaucoma to visual acuity. *Investigative Ophthalmology & Visual Science* 36(1), pp. 182–191.

Klein, R., Klein, B.E.K., Tomany, S.C., Meuer, S.M. and Huang, G.H. 2002. Ten-year incidence and progression of age-related maculopathy: The Beaver Dam eye study. *Ophthalmology* 109(10), pp. 1767–1779.

Klein, R., Klein, B.E.K., Marino, E.K.E., Kuller, L.H.L., Furberg, C.C., Burke, G.L.G. and Hubbard, L.D.L. 2003. Early age-related maculopathy in the cardiovascular health study. *Ophthalmology* 110(1), pp. 25–33.

Klein, R., Klein, B.E.K., Knudtson, M.D., Wong, T.Y., Cotch, M.F., Liu, K., Burke, G., et al. 2006. Prevalence of Age-Related Macular Degeneration in 4 Racial/Ethnic Groups in the Multi-ethnic Study of Atherosclerosis. *Ophthalmology* 113(3), p. 8.

Klein, R., Klein, B.E.K., Knudtson, M.D., Meuer, S.M., Swift, M. and Gangnon, R.E. 2007. Fifteen-year cumulative incidence of age-related macular degeneration: the Beaver Dam Eye Study. *Ophthalmology* 114(2), pp. 253–262.

Klein, R., Knudtson, M.D., Klein, B.E., Wong, T.Y., Cotch, M.F., Liu, K., Cheng, C.Y., et al. 2008a. Inflammation, Complement Factor H, and Age-Related Macular Degeneration: The Multi-Ethnic Study of Atherosclerosis. *Ophthalmology* 115(10), pp. 1742–1749.

Klein, R., Knudtson, M.D.M., Cruickshanks, K.J.K. and Klein, B.E.K. 2008b. Further observations on the association between smoking and the long-term incidence and progression of age-related macular degeneration: the Beaver Dam Eye Study. *Archives of Ophthalmology* 126(1), pp. 115–121.

Klein, R. 2011. Race/ethnicity and age-related macular degeneration. *American Journal of Ophthalmology* 152(2), pp. 153–154.

Klein, R., Chou, C.F., Klein, B.E.K., Zhang, X., Meuer, S.M. and Saaddine, J.B. 2011. Prevalence of age-related macular degeneration in the US population. *Archives of Ophthalmology* 129(1), pp. 75–80.

Kleiner, R.C., Enger, C., Alexander, M.F. and Fine, S.L. 1988. Contrast sensitivity in age-related macular degeneration. *Archives of Ophthalmology* 106(1), pp. 55–57.

Klerman, E.B., Gershengorn, H.B., Duffy, J.F. and Kronauer, R.E. 2002.

Comparisons of the variability of three markers of the human circadian pacemaker. *Journal of Biological Rhythms* 17(2), pp. 181–193.

Klettner, A., Kauppinen, A., Blasiak, J., Roider, J., Salminen, A. and Kaarniranta, K. 2013. Cellular and molecular mechanisms of age-related macular degeneration: from impaired autophagy to neovascularization. *The International Journal of Biochemistry & Cell Biology* 45(7), pp. 1457–1467.

Ko, A., Cao, S., Pakzad-Vaezi, K., Brasher, P.M., Merkur, A.B., Albiani, D.A., Kirker, A.W., et al. 2013. Optical coherence tomography-based correlation between choroidal thickness and drusen load in dry age-related macular degeneration. *Retina* 33(5), pp. 1005-1010.

Kokkinaki, M.M., Sahibzada, N.N. and Golestaneh, N.N. 2011. Human induced pluripotent stem-derived retinal pigment epithelium (RPE) cells exhibit ion transport, membrane potential, polarized vascular endothelial growth factor secretion, and gene expression pattern similar to native RPE. *Stem Cells* 29(5), pp. 825–835.

Kolb, H. 2003. Simple anatomy of the retina. In: Kolb, H., Fernandez, E. and Nelson, R. [eds.] Webvision, *http://webvision.med.utah.edu/.* Accessed 6th June 2014.

Kolstad, H.A. 2008. Nightshift work and risk of breast cancer and other cancers--a critical review of the epidemiologic evidence. *Scandinavian Journal of Work, Environment & Health* 34(1), pp. 5–22.

Kong, X., Wang, K., Sun, X. and Witt, R.E. 2010. Comparative study of the retinal vessel anatomy of rhesus monkeys and humans. *Clinical and Experimental Ophthalmology* 38(6), pp. 629–634.

Koutalos, Y., Nakatani, K. and Yau, K.W. 1995. The cGMP-phosphodiesterase and its contribution to sensitivity regulation in retinal rods. *The Journal of General Physiology* 106(5), pp. 891–921.

Kraft, T.W., Schneeweis, D.M. and Schnapf, J.L. 1993. Visual transduction in human rod photoreceptors. *The Journal of Physiology* 464, pp. 747–765.

Krishnadev, N., Meleth, A.D. and Chew, E.Y. 2010. Nutritional supplements for age-related macular degeneration. *Current Opinion in Ophthalmology* 21(3), pp. 184–189.

Kvanta, A., Algvere, P.V., Berglin, L. and Seregard, S. 1996. Subfoveal fibrovascular membranes in age-related macular degeneration express vascular endothelial growth factor. *Investigative Ophthalmology & Visual Science* 37(9), pp. 1929–1934.

Lakowski, J., Baron, M., Bainbridge, J., Barber, A.C., Pearson, R.A., Ali, R.R. and Sowden, J.C. 2010. Cone and rod photoreceptor transplantation in models of the childhood retinopathy Leber congenital amaurosis using flow-sorted Crx-positive donor cells. *Human Molecular Genetics* 19(23), pp. 4545–4559.

Lamb, L.E. and Simon, J.D. 2004. A2E: a component of ocular lipofuscin. *Photochemistry and Photobiology* 79(2), pp. 127–136.

Lamb, T.D. 1981. The involvement of rod photoreceptors in dark adaptation. *Vision*

Research 21(12), pp. 1773–1782.

Lamb, T.D., Cideciyan, A.V., Jacobson, S.G. and Pugh, E.N. 1998. Towards a molecular description of human dark adaptation. *The Journal of Physiology* 506, p. 88P.

Lamb, T.D. and Pugh, E.N. 2004. Dark adaptation and the retinoid cycle of vision. *Progress in Retinal and Eye Research* 23(3), pp. 307–380.

Lamb, T.D. and Pugh, E.N. 2006. Phototransduction, dark adaptation, and rhodopsin regeneration the proctor lecture. *Investigative Ophthalmology and Visual Science* 47(12), pp. 5138-5152

Lange, C.A.K. and Bainbridge, J.W.B. 2012. Oxygen sensing in retinal health and disease. *Ophthalmologica* 227(3), pp. 115–131.

Langmann, T. 2007. Microglia activation in retinal degeneration. *Journal of Leukocyte Biology* 81(6), pp. 1345–1351.

Leveziel, N., Tilleul, J., Puche, N., Zerbib, J., Laloum, F., Querques, G. and Souied, E.H. 2011. Genetic factors associated with age-related macular degeneration. *Ophthalmologica* 226(3), pp. 87–102.

Lewy, A.J., Wehr, T.A., Goodwin, F.K., Newsome, D.A. and Markey, S.P. 1980. Light suppresses melatonin secretion in humans. *Science* 210(4475), pp. 1267–1269.

Li, Y., Tsai, Y.-T., Hsu, C.-W., Erol, D., Yang, J., Wu, W.-H., Davis, R.J., et al. 2012. Long-term safety and efficacy of human-induced pluripotent stem cell (iPS) grafts in a preclinical model of retinitis pigmentosa. *Molecular Medicine* 18, pp. 1312–1319.

Liem, A.T.A., Keunen, J.E.E., Norren, D.V. and Kraars, J.V.D. 1991. Rod densitometry in the aging human eye. *Investigative Ophthalmology & Visual Science* 32(10), pp. 2676–2682.

Lim, L.S., Mitchell, P., Seddon, J.M., Holz, F.G. and Wong, T.Y. 2012. Age-related macular degeneration. *The Lancet* 379(9827), pp. 1728–1738.

Linsenmeier, R.A., Braun, R.D. and McRipley, M.A. 1998. Retinal hypoxia in long-term diabetic cats. *Investigative Ophthalmology & Visual Science* 39(9), pp. 1647-1657.

Lissoni, P., Barni, S., Meregalli, S., Fossati, V., Cazzaniga, M., Esposti, D. and Tancini, G. 1995. Modulation of cancer endocrine therapy by melatonin: a phase II study of tamoxifen plus melatonin in metastatic breast cancer patients progressing under tamoxifen alone. *British Journal of Cancer* 71(4), pp. 854–856.

Lockley, S.W., Skene, D.J., Arendt, J., Tabandeh, H., Bird, A.C. and Defrance, R. 1997. Relationship between melatonin rhythms and visual loss in the blind. *The Journal of Clinical Endocrinology and Metabolism* 82(11), pp. 3763–3770.

Loewenstein, A., Malach, R., Goldstein, M., Leibovitch, I., Barak, A., Baruch, E., Alster, Y., et al. 2003. Replacing the Amsler grid: a new method for monitoring

patients with age-related macular degeneration. *Ophthalmology* 110(5), pp. 966–970.

Lovie-Kitchin, J.E. and Brown, B. 2000. Repeatability and intercorrelations of standard vision tests as a function of age. *Optometry and Vision Science* 77(8), pp. 412–420.

Lucas, R.J., Freedman, M.S., Muñoz, M., Garcia-Fernández, J.M. and Foster, R.G. 1999. Regulation of the mammalian pineal by non-rod, non-cone, ocular photoreceptors. *Science* 284(5413), pp. 505–507.

Luu, C.D., Dimitrov, P.N., Wu, Z., Ayton, L.N., Makeyeva, G., Aung, K.Z., Varsamidis, M., et al. 2013. Static and flicker perimetry in age-related macular degeneration. *Investigative Ophthalmology & Visual Science* 54(5), pp. 3560–3568.

Lütjen-Drecoll, E. 2006. Choroidal innervation in primate eyes. *Experimental Eye Research* 82(3), pp. 357–361.

Lyubarsky, A.L., Falsini, B., Pennesi, M.E., Valentini, P. and Pugh, E.N. 1999. UV- and midwave-sensitive cone-driven retinal responses of the mouse: a possible phenotype for coexpression of cone photopigments. *The Journal of Neuroscience* 19(1), pp. 442–455.

Ma, W., Coon, S., Zhao, L., Fariss, R.N. and Wong, W.T. 2013. A2E accumulation influences retinal microglial activation and complement regulation. *Neurobiology of Aging* 34(3), pp. 943–960.

Ma, W., Zhao, L., Fontainhas, A.M., Fariss, R.N. and Wong, W.T. 2009. Microglia in the Mouse Retina Alter the Structure and Function of Retinal Pigmented Epithelial Cells: A Potential Cellular Interaction Relevant to AMD. *PLoS One* 4(11), p. e7945.

Macular Photocoagulation Study Group 1991. Argon laser photocoagulation for neovascular maculopathy. Five-year results from randomized clinical trials. *Archives of Ophthalmology* 109(8), pp. 1109–1114.

Macular Photocoagulation Study Group 1994. Persistent and recurrent neovascularization after laser photocoagulation for subfoveal choroidal neovascularization of age-related macular degeneration. *Archives of Ophthalmology* 112(4), pp. 489–499.

Maller, J.B., Fagerness, J.A., Reynolds, R.C., Neale, B.M., Daly, M.J. and Seddon, J.M. 2007. Variation in complement factor 3 is associated with risk of age-related macular degeneration. *Nature Genetics* 39(10), pp. 1200–1201.

Mares-Perlman, J.A., Brady, W.E., Klein, R., VandenLangenberg, G.M., Klein, B.E.K. and Palta, M. 1995. Dietary Fat and Age-Related Maculopathy. *Archives of Ophthalmology* 113(6), pp. 743–748.

Margrain, T.H. and Thomson, D. 2002. Sources of variability in the clinical photostress test. *Ophthalmic & Physiological Optics* 22(1), pp. 61–67.

Margrain, T.H., Nollett, C., Shearn, J., Stanford, M., Edwards, R., Ryan, B., Bunce, C., et al. 2012. The Depression in Visual Impairment Trial (DEPVIT): trial design and

protocol. *BMC psychiatry* 12(1), p. 57.

Marmor, M.F. 2000. A brief history of macular grids: from Thomas Reid to Edvard Munch and Marc Amsler. *Survery of Ophthalmology* 44(4), pp. 343-353.

Marron, J.A. and Bailey, I.L. 1982. Visual factors and orientation-mobility performance. *American Journal of Optometry and Physiological Optics* 59(5), pp. 413–426.

Martin, D.F., Maguire, M.G., Ying, G.-S., Grunwald, J.E., Fine, S.L.S. and Jaffe, G.J. 2011. Ranibizumab and bevacizumab for neovascular age-related macular degeneration. *New England Journal of Medicine* 364(20), pp. 1897–1908.

Mata, N.L., Radu, R.A., Clemmons, R.S. and Travis, G.H. 2002. Isomerization and oxidation of vitamin A in cone-dominant retinas: a novel pathway for visual pigment regeneration in daylight. *Neuron* 36(1), pp. 69–80.

Mayer, M.J., Spiegler, S.J., Ward, B., Glucs, A. and Kim, C.B. 1992a. Foveal flicker sensitivity discriminates ARM-risk from healthy eyes. *Investigative Ophthalmology \& Visual Science* 33(11), pp. 3143–3149.

Mayer, M.J., Spiegler, S.J., Ward, B., Glucs, A. and Kim, C.B. 1992b. Mid-frequency loss of foveal flicker sensitivity in early stages of age-related maculopathy. *Investigative Ophthalmology & Visual Science* 33(11), pp. 3136–3142.

Mayer, M.J., Ward, B., Klein, R., Talcott, J.B., Dougherty, R.F. and Glucs, A. 1994. Flicker sensitivity and fundus appearance in pre-exudative age-related maculopathy. *Investigative Ophthalmology & Visual Science* 35(3), pp. 1138–1149.

McFarland, R.A. and Evans, J.N. 1939. Alterations in dark adaptation under reduced oxygen tensions. *American Journal of Physiology* 127, pp. 37-50.

McGregor, L.N. and Chaparro, A. 2005. Visual difficulties reported by low-vision and nonimpaired older adult drivers. *Human Factors* 47(3), pp. 469–478.

McGwin, G., Jackson, G.R. and Owsley, C. 1999. Using nonlinear regression to estimate parameters of dark adaptation. *Behavior Research Methods, Instruments & Computers* 31(4), pp. 712–717.

McIntyre, I.M., Norman, T.R., Burrows, G.D. and Armstrong, S.M. 1989. Human melatonin suppression by light is intensity dependent. *Journal of Pineal Research* 6(2), pp. 149–156.

Medeiros, N.E. and Curcio, C.A. 2001. Preservation of Ganglion Cell Layer Neurons in Age-Related Macular Degeneration. *Investigative Ophthalmology & Visual Science* 42(3), pp. 795–803.

Megdal, S.P., Kroenke, C.H., Laden, F., Pukkala, E. and Schernhammer, E.S. 2005. Night work and breast cancer risk: A systematic review and meta-analysis. *European Journal of Cancer* 41(13), pp. 2023–2032.

Mendrinos, E. and Pournaras, C.J. 2009. Topographic variation of the choroidal

watershed zone and its relationship to neovascularization in patients with age-related macular degeneration. *Acta Ophthalmologica* 87(3), pp. 290–296.

Metelitsina, T.I., Grunwald, J.E., DuPont, J.C., Ying, G.-S., Brucker, A.J. and Dunaief, J.L. 2008. Foveolar choroidal circulation and choroidal neovascularization in age-related macular degeneration. *Investigative Ophthalmology & Visual Science* 49(1), pp. 358–363.

Metha, A.B., Vingrys, A.J. and Badcock, D.R. 1993. Calibration of a colour monitor for visual psychophysics. *Behavior Research Methods, Instruments & Computers* 25(3), pp. 371–383.

Midena, E., Angeli, C.D., Blarzino, M.C., Valenti, M. and Segato, T. 1997. Macular function impairment in eyes with early age-related macular degeneration. *Investigative Ophthalmology & Visual Science* 38(2), pp. 469–477.

Midena, E.E., Vujosevic, S.S., Convento, E.E., Manfre, A.A., Cavarzeran, F.F. and Pilotto, E.E. 2007. Microperimetry and fundus autofluorescence in patients with early age-related macular degeneration. *British Journal of Ophthalmology* 91(11), pp. 1499–1503.

Miller, S.S. and Steinberg, R.H. 1977. Active transport of ions across frog retinal pigment epithelium. *Experimental Eye Research* 25(3), pp. 235–248.

Milton, R.C. 1979. The Framingham eye study. *American Journal of Ophthalmology* 88(2), pp. 269–269.

Mirick, D.K. and Davis, S. 2008. Melatonin as a Biomarker of Circadian Dysregulation. *Cancer Epidemiology Biomarkers & Prevention* 17(12), pp. 3306–3313.

Mitchell, P., Korobelnik, J.F., Lanzetta, P., Holz, F.G., Prünte, C., Schmidt-Erfurth, U., Tano, Y., et al. 2010. Ranibizumab (Lucentis) in neovascular age-related macular degeneration: evidence from clinical trials. *British Journal of Ophthalmology* 94(1), pp. 2–13.

Mole, D.R., Maxwell, P.H., Pugh, C.W. and Ratcliffe, P.J. 2001. Regulation of HIF by the von Hippel-Lindau tumour suppressor: Implications for cellular oxygen sensing. *IUBMB Life* 52(1-2), pp. 43–47.

Moore, D.J. and Clover, G.M. 2001. The effect of age on the macromolecular permeability of human Bruch's membrane. *Investigative Ophthalmology & Visual Science* 42(12), pp. 2970–2975.

Moseley, M.J., Bayliss, S.C. and Fielder, A.R. 1988. Light transmission through the human eyelid: in vivo measurement. *Ophthalmic & Physiological Optics* 8(2), pp. 229–230.

Mote, F.A. and Riopelle, A.J. 1951. The effect of varying the intensity and the duration of pre-exposure upon subsequent dark adaptation in the human eye. *The Journal of General Physiology* 34(5), pp. 657–674.

Murphy, R.P., Yeo, J.H. and Green, W.R. 1985. Dehiscences of the pigment epithelium. *Transactions of the American Ophthalmological Society* 83, pp. 63-81.

Mutlukan, E. 2006. Red dots visual field test with blue on yellow & blue on red macula test grid. *Eye* 20(4), pp. 506–8; author reply 508–9.

Neelam, K., Hogg, R.E., Stevenson, M.R., Johnston.E., Anderson,R.A., Beatty,S., Chakravarthy,U. 2008. Carotenoids and co-antioxidants in age-related maculopathy: design and methods. *Ophthalmic Epidemiology* 15(6), pp. 389-401.

Neelam, K., Nolan, J., Chakravarthy, U. and Beatty, S. 2009. Psychophysical function in age-related maculopathy. *Survey of Ophthalmology* 54(2), pp. 167–210.

Newsome, D.A., Huh, W. and Green, W.R. 1987. Bruch's membrane age-related changes vary by region. *Current Eye Research* 6(10), pp. 1211–1221.

Nikonov, S., Lamb, T.D. and Pugh, E.N. 2000. The role of steady phosphodiesterase activity in the kinetics and sensitivity of the light-adapted salamander rod photoresponse. *The Journal of General Physiology* 116(6), pp. 795–824.

Nork, T.M. 2000. Acquired colour vision loss and a possible mechanism of ganglion cell death in glaucoma. *Transactions of the American Ophthalmological Society* 98, pp. 331–363.

Nowak, J.Z. 2006. Age-related macular degeneration (AMD): pathogenesis and therapy. *Pharmacological Reports* 58(3), pp. 353–363.

Okawa, H., Sampath, A.P., Laughlin, S.B. and Fain, G.L. 2008. ATP Consumption by Mammalian Rod Photoreceptors in Darkness and in Light. *Current Biology* 18(24), pp. 1917–1921.

Osakada, F., Ikeda, H., Sasai, Y. and Takahashi, M. 2009. Stepwise differentiation of pluripotent stem cells into retinal cells. *Nature Protocols* 4(6), pp. 811–824.

O'Leary, E.S., Schoenfeld, E.R., Stevens, R.G., Kabat, G.C., Henderson, K., Grimson, M.D., et al. 2006. Shift work, light at night, and breast cancer on Long Island, New York. *American Journal of Epidemiology* 164(4), pp. 358-366.

Osterberg, G. 1935. Topography of the layer of rods and cones in the human retina. *Acta Ophthalmologica Supplement* 6, pp. 1-103.

Owen, C.G., Jarrar, Z., Wormald, R., Cook, D.G., Fletcher, A.E. and Rudnicka, A.R. 2012. The estimated prevalence and incidence of late stage age related macular degeneration in the UK. *British Journal of Ophthalmology* 96(5), pp. 752–756.

Owsley, C. 2011. Aging and vision. *Vision research* 51(13), pp. 1610–1622.

Owsley, C. 2003. Contrast sensitivity. *Ophthalmology Clinics of North America* 16(2), pp. 171–177.

Owsley, C., Sekuler, R. and Siemsen, D. 1983. Contrast sensitivity throughout adulthood. *Vision Research* 23(7), pp. 689–699.

Owsley, C., Jackson, G.R., Cideciyan, A.V., Huang, Y., Fine, S.L., Ho, A.C., Maguire, M.G., et al. 2000. Psychophysical evidence for rod vulnerability in age-related macular degeneration. *Investigative Ophthalmology & Visual Science* 41(1), pp. 267–273.

Owsley, C., Jackson, G.R., White, M., Feist, R. and Edwards, D. 2001. Delays in rod-mediated dark adaptation in early age-related maculopathy. *Ophthalmology*. 108(7), pp. 1196-1202.

Owsley, C., McGwin, G., Jackson, G.R., Heimburger, D.C., Piyathilake, C.J., Klein, R., White, M.F., et al. 2006. Effect of short-term, high-dose retinol on dark adaptation in aging and early age-related maculopathy. *Investigative Ophthalmology & Visual Science* 47(4), pp. 1310–1318.

Owsley, C., McGwin, G., Jackson, G.R., Kallies, K. and Clark, M. 2007. Cone- and rod-mediated dark adaptation impairment in age-related maculopathy. *Ophthalmology* 114(9), pp. 1728–1735.

Ozaki, E., Campbell, M., Kiang, A.-S., Humphries, M., Doyle, S.L. and Humphries, P. 2014. Inflammation in age-related macular degeneration. *Advances in Experimental Medicine and Biology* 801(Chapter 30), pp. 229–235.

O'Neill-Biba, M., Sivaprasad, S., Rodriguez-Carmona, M., Wolf, J.E. and Barbur, J.L. 2010. Loss of chromatic sensitivity in AMD and diabetes: a comparative study. *Ophthalmic & Physiological Optics* 30(5), pp. 705–716.

Palsson, O., Geirsdóttir, A., Hardarson, S.H., Olafsdottir, O.B., Kristjansdottir, J.V. and Stefánsson, E. 2012. Retinal oximetry images must be standardized: a methodological analysis. *Investigative Ophthalmology & Visual Science* 53(4), pp. 1729–1733.

Pandi-Perumal, S.R., Smits, M., Spence, W., Srinivasan, V., Cardinali, D.P., Lowe, A.D. and Kayumov, L. 2007. Dim light melatonin onset (DLMO): a tool for the analysis of circadian phase in human sleep and chronobiological disorders. *Progress in Neuro-Psychopharmacology & Biological Psychiatry* 31(1), pp. 1–11.

Pauleikhoff, D., Harper, C.A., Marshall, J. and Bird, A.C. 1990. Aging changes in Bruch's membrane. A histochemical and morphologic study. *Ophthalmology* 97(2), pp. 171–178.

Pauleikhoff, D., Spital, G., Radermacher, M., Brumm, G.A., Lommatzsch, A. and Bird, A.C. 1999. A fluorescein and indocyanine green angiographic study of choriocapillaris in age-related macular disease. *Archives of Ophthalmology* 117(10), pp. 1353–1358.

Pauleikhoff, D., Löffert, D., Spital, G., Radermacher, M., Dohrmann, J., Lommatzsch, A. and Bird, A.C. 2002. Pigment epithelial detachment in the elderly. Clinical differentiation, natural course and pathogenetic implications. *Graefe's Archive for Clinical and Experimental Ophthalmology* 240(7), pp. 533–538.

Pavlidis, M., Stupp, T., Georgalas, I., Georgiadou, E., Moschos, M. and Thanos, S. 2005. Multifocal electroretinography changes in the macula at high altitude: a report

of three cases. *Ophthalmologica* 219(6), pp. 404-412.

Penfold, P.L., Madigan, M.C., Gillies, M.C. and Provis, J.M. 2001. Immunological and aetiological aspects of macular degeneration. *Progress in Retinal and Eye Research* 20(3), pp. 385–414.

Pepperberg, D.R., Brown, P.K., Lurie, M. and Dowling, J.E. 1978. Visual Pigment and Photoreceptor Sensitivity in the Isolated Skate Retina. *The Journal of General Physiology* 71, pp. 369–396.

Petranka, J., Baldwin, W., Biermann, J., Jayadev, S., Barrett, J.C. and Murphy, E. 1999. The oncostatic action of melatonin in an ovarian carcinoma cell line. *Journal of Pineal Research* 26(3), pp. 129–136.

Phipps, J.A., Dang, T.M., Vingrys, A.J. and Guymer, R.H. 2004. Flicker perimetry losses in age-related macular degeneration. *Investigative Ophthalmology & Visual Science* 45(9), pp. 3355–3360.

Phipps, J.A., Guymer, R.H. and Vingrys, A.J. 2003. Loss of cone function in age-related maculopathy. *Investigative Ophthalmology & Visual Science* 44(5), pp. 2277–2283.

Phipps, J.A., Yee, P., Fletcher, E.L. and Vingrys, A.J. 2006. Rod photoreceptor dysfunction in diabetes: activation, deactivation, and dark adaptation. *Investigative Ophthalmology & Visual Science* 47(7), pp. 3187–3194.

Plantner, J.J., Barbour, H.L. and Kean, E.L. 1988. The rhodopsin content of the human eye. *Current Eye Research* 7(11), pp. 1125–1129.

Plummer, D.J., Azen, S.P. and Freeman, W.R. 2000. Scanning laser entoptic perimetry for the screening of macular and peripheral retinal disease. *Archives of Ophthalmology* 118(9), pp. 1205–1210.

Pokorny, J. and Birch, J. 1979. *Congenital and acquired colour vision defects.* New York: Grune & Stratton.

Polak, K., Schmetterer, L. and Riva, C.E. 2002. Influence of flicker frequency on flicker-induced changes of retinal vessel diameter. *Investigative Ophthalmology & Visual Science* 43(8), pp. 2721–2726.

Polyak, S.L. 1941. *The Retina*. Chicago: University of Chicago Press.

Pournaras, C.J., Rungger-Brändle, E., Riva, C.E., Hardarson, S.H. and Stefánsson, E. 2008. Regulation of retinal blood flow in health and disease. *Progress in Retinal and Eye Research* 27(3), pp. 284–330.

Provencio, I., Jiang, G., De Grip, W.J., Hayes, W.P. and Rollag, M.D. 1998. Melanopsin: An opsin in melanophores, brain, and eye. *Proceedings of the National Academy of Sciences of the United States of America* 95(1), pp. 340–345.

Provis, J.M., Penfold, P.L., Cornish, E.E., Sandercoe, T.M. and Madigan, M.C. 2005. Anatomy and development of the macula: specialisation and the vulnerability to

macular degeneration. *Clinical and Experimental Optometry* 88(5), pp. 269–281.

Pugh Jr, E.N. and Lamb, T.D. 2000. *Phototransduction in Vertebrate Rods and Cones: Molecular Mechanisms of Amplification, Recovery and Light Adaptation.* In: Handbook of Biological Physics. Vol. 3, Molecular Mechanisms of Visual Transduction. Amsterdam: Elsevier.

Raoul, W., Auvynet, C. and Camelo, S. 2010. CCL2/CCR2 and CX3CL1/CX3CR1 chemokine axes and their possible involvement in age-related macular degeneration. *Journal of Neuroinflammation* 7, p. 87.

Remulla, J.F., Gaudio, A.R., Miller, S. and Sandberg, M.A. 1995. Foveal electroretinograms and choroidal perfusion characteristics in fellow eyes of patients with unilateral neovascular age-related macular degeneration. *British Journal of Ophthalmology* 79(6), pp. 558–561.

Resnikoff, S., Pascolini, D., Etya'ale, D., Kocur, I., Pararajasegaram, R., Pokharel, G.P. and Mariotti, S.P. 2004. Global data on visual impairment in the year 2002. *Bulletin of the World Health Organization* 82(11), pp. 844–851.

Richer, S.C. and Ford, W. 2001. A critical investigation of NADPH oxidase activity in human spermatozoa. *Molecular Human Reproduction* 7(3), pp. 237-244.

Ritter, L.L., Klein, R., Klein, B., Mares-Perlman, J.A. and Jensen, S.C. 1995. Alcohol-Use and Age-Related Maculopathy in the Beaver Dam Eye Study. *American Journal of Ophthalmology* 120(2), pp. 190–196.

Riva, C.E., Falsini, B. and Logean, E. 2001. Flicker-evoked responses of human optic nerve head blood flow: luminance versus chromatic modulation. *Investigative Ophthalmology & Visual Science* 42(3), pp. 756–762.

Riva, C.E., Logean, E. and Falsini, B. 2005. Visually evoked hemodynamical response and assessment of neurovascular coupling in the optic nerve and retina. *Progress in Retinal and Eye Research* 24(2), pp. 183–215.

Robinson, J., Bayliss, S.C. and Fielder, A.R. 1991. Transmission of light across the adult and neonatal eyelid in vivo. *Vision Research* 31(10), pp. 1837–1840.

Rochtchina, E., Wang, J.J., Flood, V.M. and Mitchell, P. 2007. Elevated serum homocysteine, low serum vitamin B12, folate, and age-related macular degeneration: the Blue Mountains Eye Study. *American Journal of Ophthalmology* 143(2), pp. 344–346.

Rosenfeld, P.J., Brown, D.M., Heier, J.S., Boyer, D.S., Kaiser, P.K., Chung, C.Y., Kim, R.Y., et al. 2006. Ranibizumab for neovascular age-related macular degeneration. *New England Journal of Medicine* 355(14), pp. 1419–1431.

Roth, F., Bindewald, A. and Holz, F.G. 2004. Keypathophysiologic pathways in age-related macular disease. *Graefe's Archive for Clinical and Experimental Ophthalmology* 242(8), pp. 710–716.

Office for National Statistics. 2009. *National Population Projections, 2009: UK*

population projected to grow by 4 million over the next decade. http://www.statistics.gov.uk/statbase/Product.asp?vlnk=8519 Accessed: 6th June 2014.

Rubin, G.S., Roche, K.B. and Huang, G.H. 2001. The association of multiple visual impairments with self-reported visual disability: SEE project. *Investigative Ophthalmology & Visual Science* 42(1), pp.64-72.

Rückmann, von, A., Fitzke, F.W. and Bird, A.C. 1997. Fundus autofluorescence in age-related macular disease imaged with a laser scanning ophthalmoscope. *Investigative Ophthalmology & Visual Science* 38(2), pp. 478–486.

Saari, J.C. and Bredberg, D.L. 1987. Photochemistry and stereoselectivity of cellular retinaldehyde-binding protein from bovine retina. *The Journal of biological chemistry* 262(16), pp. 7618–7622.

Sakamoto, T., Sakamoto, H., Murphy, T.L., Spee, C., Soriano, D., Ishibashi, T., Hinton, D.R., et al. 1995. Vessel formation by choroidal endothelial cells in vitro is modulated by retinal pigment epithelial cells. *Archives of Ophthalmology* 113(4), pp. 512–520.

Sandberg, M.A. and Gaudio, A.R. 1995. Slow photostress recovery and disease severity in age-related macular degeneration. *Retina* 15(5), pp. 407–412.

Sandberg, M.A., Weiner, A., Miller, S. and Gaudio, A.R. 1998. High-risk characteristics of fellow eyes of patients with unilateral neovascular age-related macular degeneration. *Ophthalmology* 104(3), pp. 441-447.

Sandberg, M.A., Pawlyk, B.S. and Berson, E.L. 1999. Acuity recovery and cone pigment regeneration after a bleach in patients with retinitis pigmentosa and rhodopsin mutations. *Investigative Ophthalmology & Visual Science* 40(10), pp. 2457–2461.

SanGiovanni, J.P. and Chew, E.Y. 2005. The role of omega-3 long-chain polyunsaturated fatty acids in health and disease of the retina. *Progress in Retinal and Eye Research* 24(1), pp. 87–138.

SanGiovanni, J.P., Agrón, E., Meleth, A.D., Reed, G.F., Sperduto, R.D., Clemons, T.E. and Chew, E.Y. 2009. Omega-3 long-chain polyunsaturated fatty acid intake and 12-y incidence of neovascular age-related macular degeneration and central geographic atrophy: AREDS report 30, a prospective cohort study from the Age-Related Eye Disease Study. *The American Journal of Clinical Nutrition* 90(6), pp. 1601–1607.

Sarks, J.P., Sarks, S.H. and Killingsworth, M.C. 1988. Evolution of geographic atrophy of the retinal pigment epithelium. *Eye* 2(5), pp. 552–577.

Sarks, S.H. 1976. Ageing and degeneration in the macular region: a clinico-pathological study. *British Journal of Ophthalmology* 60(5), pp. 324–341.

Schatz, A., Breithaupt, M., Hudemann, J., Niess, A., Messias, A., Zrenner, E., Bartz-Schmidt, K.U., et al. 2014. Electroretinographic assessment of retinal function during acute exposure to normobaric hypoxia. *Graefe's Archive for Clinical and*

Experimental Ophthalmology 252(1), pp. 43–50.

Schlanitz, F.G., Baumann, B., Spalek, T., Schütze, C., Ahlers, C., Pircher, M., Götzinger, E., et al. 2011. Performance of automated drusen detection by polarization-sensitive optical coherence tomography. *Investigative Ophthalmology & Visual Science* 52(7), pp. 4571–4579.

Schmidt-Erfurth, U., Miller, J.W., Sickenberg, M., Laqua, H., Barbazetto, I., Gragoudas, E.S., Zografos, L., et al. 1999. Photodynamic therapy with verteporfin for choroidal neovascularization caused by age-related macular degeneration: results of retreatments in a phase 1 and 2 study. *Archives of Ophthalmology* 117(9), pp. 1177–1187.

Schmitt, N.J., Grover, D.A. and Feldon, S.E. 2003. The Eger macular stressometer: pilot study. *American Journal of Ophthalmology* 136(2), pp. 314–317.

Schmitz-Valckenberg, S., Bindewald-Wittich, A., Dolar-Szczasny, J., Dreyhaupt, J., Wolf, S., Scholl, H.P.N. and Holz, F.G. 2006. Correlation between the area of increased autofluorescence surrounding geographic atrophy and disease progression in patients with AMD. *Investigative Ophthalmology & Visual Science* 47(6), pp. 2648–2654.

Schmitz-Valckenberg, S., Fleckenstein, M., Scholl, H.P.N. and Holz, F.G. 2009. Fundus autofluorescence and progression of age-related macular degeneration. *Survey of Ophthalmology* 54(1), pp. 96–117.

Scholl, H., Bellmann, C., Dandekar, S.S. and Bird, A.C. 2004. Photopic and scotopic fine matrix mapping of retinal areas of increased fundus autofluorescence in patients with age-related maculopathy. *Investigative Ophthalmology & Visual Science* 45(2): 574-583

Schremser, J.L. and Williams, T.P. 1995. Rod outer segment (ROS) renewal as a mechanism for adaptation to a new intensity environment. I. Rhodopsin levels and ROS length. *Experimental Eye Research* 61, pp. 17-23

Schuchard, R.A.R. 1993. Validity and interpretation of Amsler grid reports. *Archives of Ophthalmology* 111(6), pp. 776–780.

Schwartz, S. 2009. *Visual Perception: A Clinical Orientation, Fourth Edition*. New York: McGraw Hill

Schwartz, S.D., Hubschman, J.P. and Heilwell, G. 2012. Embryonic stem cell trials for macular degeneration: a preliminary report. *The Lancet* 379, pp. 713-720.

Schweitzer, D., Hammer, M., Kraft, J., Thamm, E., Konigsdorffer, E. and Strobel, J. 1999. In vivo measurement of the oxygen saturation of retinal vessels in healthy volunteers. *Biomedical Engineering, IEEE Transactions* 46(12), pp. 1454–1465.

Schwesinger, C., Yee, C., Rohan, R.M. and Joussen, A.M. 2001. Intrachoroidal neovascularization in transgenic mice overexpressing vascular endothelial growth factor in the retinal pigment epithelium. *The American Journal of Pathology* 158(3), pp. 1161-1172.

Seddon, J.M. 2013. Genetic and Environmental Underpinnings to Age-Related Ocular Diseases. *Investigative Ophthalmology & Visual Science* 54(14), pp. 28–30.

Seddon, J.M., Cote, J. and Page, W.F. 2005. The US twin study of age-related macular degeneration: relative roles of genetic and environmental influences. *Archives of Ophthalmology* 123(3), pp. 321-327.

Seddon, J.M., Francis, P.J., George, S., Schultz, D.W., Rosner, B. and Klein, M.L. 2007. Association of CFH Y402H and LOC387715 A69S With Progression of Age-Related Macular Degeneration. *The Journal of the American Medical Association* 297(16), pp. 1793–1800.

Seddon, J.M., Reynolds, R., Maller, J., Fagerness, J.A., Daly, M.J. and Rosner, B. 2009. Prediction Model for Prevalence and Incidence of Advanced Age-Related Macular Degeneration Based on Genetic, Demographic, and Environmental Variables. *Investigative Ophthalmology & Visual Science* 50(5), pp. 2044–2053.

Seiple, W., Holopigian, K., Shnayder, Y. and Szlyk, J.P. 2001. Duration thresholds for target detection and identification in the peripheral visual field. *Optometry and vision science : official publication of the American Academy of Optometry* 78(3), pp. 169–176.

Seshadri, J., Christensen, J., Lakshminarayanan, V. and Bassi, C.J. 2005. Evaluation of the new web-based "Color Assessment and Diagnosis" test. *Optometry and Vision Science* 82(10), pp. 882-885.

Severin, S., Harper, C. and Culver, J. 1963. Photostress test for the evaluation of macular function. *Archives of ophthalmology* 70, pp. 593–597.

Shady, S., MACLEOD, D. and Fisher, H.S. 2004. Adaptation from invisible flicker. *Proceedings of the National Academy of Sciences of the United States of America* 101(14), pp. 5170–5173.

Shakoor, A., Blair, N.P., Mori, M. and Shahidi, M. 2006. Chorioretinal vascular oxygen tension changes in response to light flicker. *Investigative Ophthalmology & Visual Science* 47(11), pp. 4962–4965.

Shelley, E.J., Madigan, M.C., Natoli, R., Penfold, P.L. and Provis, J.M. 2009. Cone degeneration in aging and age-related macular degeneration. *Archives of ophthalmology* 127(4), pp. 483–492.

Sheraidah, G., Steinmetz, R., Maguire, J., Pauleikhoff, D., Marshall, J. and Bird, A.C. 1993. Correlation between lipids extracted from Bruch's membrane and age. *Ophthalmology* 100(1), pp. 47–51.

Sheridan, C.M., Pate, S., Hiscott, P., Wong, D., Pattwell, D.M. and Kent, D. 2009. Expression of hypoxia-inducible factor−1α and −2α in human choroidal neovascular membranes. *Graefe's Archive for Clinical and Experimental Ophthalmology* 247(10), pp. 1361–1367.

Siderov, J. and Tiu, A.L. 1999. Variability of measurements of visual acuity in a large eye clinic. *Acta Ophthalmologica Scandinavica* 77(6), pp. 673–676.

Silvestri, G.G., Johnston, P.B.P. and Hughes, A.E.A. 1994. Is genetic predisposition an important risk factor in age-related macular degeneration? *Eye* 8 (Pt 5), pp. 564–568.

Singh, A., Falk, M.K., Hviid, T.V.F. and Sørensen, T.L. 2013. Increased Expression of CD200 on Circulating CD11b+ Monocytes in Patients with Neovascular Age-related Macular Degeneration. *Ophthalmology* 120(5), pp. 1029–1037.

Sjostrand, J. 1979. Contrast sensitivity in macular disease using a small-field and a large-field TV system. *Acta Ophthalmologica*. 57(5), pp 832-846.

Sjostrand, J. and Frisén, L. 1977. Contrast sensitivity in macular disease. A preliminary report. *Acta Ophthalmologica* 55(3), pp. 507–514.

Skene, D.J. and Arendt, J. 2006. Human circadian rhythms: physiological and therapeutic relevance of light and melatonin. *Annals of Clinical Biochemistry* 43(Pt 5), pp. 344–353.

Smiddy, W.E. and Fine, S.L. 1984. Prognosis of patients with bilateral macular drusen. *Ophthalmology* 91(3), pp. 271–277.

Smith, R.T., Bernstein, P.S. and Curcio, C.A. 2013. Rethinking A2E. *Investigative Ophthalmology & Visual Science* 54(8), pp. 5543–5543.

Smith, R.T., Chan, J.K., Nagasaki, T., Sparrow, J.R. and Barbazetto, I. 2005. A method of drusen measurement based on reconstruction of fundus background reflectance. *British Journal of Ophthalmology* 89(1), pp. 87–91.

Smith, V.C., Ernest, J.T. and Pokorny, J. 1976. Effect of hypoxia on FM 100-Hue test performance. *Modern Problems in Ophthalmology* 17, pp. 248-256.

Smith, V.C., Pokorny, J. and Diddie, K.R. 1988. Colour matching and the Stiles-Crawford effect in observers with early age-related macular changes. *Journal of the Optical Society of America* 5(12), pp. 2113–2121.

Smith, W., Mitchell, P. and Leeder, S.R. 1996. Smoking and age-related maculopathy. The Blue Mountains Eye Study. *Archives of Ophthalmology* 114(12), pp. 1518–1523.

Smith, W., Mitchell, P., Leeder, S.R. and Wang, J.J. 1998. Plasma fibrinogen levels, other cardiovascular risk factors, and age-related maculopathy: the Blue Mountains Eye Study. *Archives of Ophthalmology* 116(5), pp. 583–587.

Snodderly, D.M. 1995. Evidence for protection against age-related macular degeneration by carotenoids and antioxidant vitamins. *The American Journal of Clinical Nutrition* 62(6 Suppl), pp. 1448S–1461S.

Solbach, U.U., Keilhauer, C.C., Knabben, H.H. and Wolf, S.S. 1997. Imaging of retinal autofluorescence in patients with age-related macular degeneration. *Retina* 17(5), pp. 385–389.

Spaide, R.F.R. 2003. Fundus autofluorescence and age-related macular degeneration.

Ophthalmology 110(2), pp. 392–399.

Sparrow, J.R. and Boulton, M. 2005. RPE lipofuscin and its role in retinal pathobiology. *Experimental Eye Research* 80(5), pp. 595–606.

Sparrow, J.R., Dowling, J.E. and Bok, D. 2013. Understanding RPE Lipofuscin. *Investigative Ophthalmology & Visual Science* 54(13), pp. 8325–8326.

Spencer, K.L., Hauser, M.A., Olson, L.M., Schmidt, S., Scott, W.K., Gallins, P., Agarwal, A., et al. 2008. Deletion of CFHR3 and CFHR1 genes in age-related macular degeneration. *Human Molecular Genetics* 17(7), pp. 971–977.

Spilsbury, K.K., Garrett, K.L.K., Shen, W.Y.W., Constable, I.J.I. and Rakoczy, P.E.P. 2000. Overexpression of vascular endothelial growth factor (VEGF) in the retinal pigment epithelium leads to the development of choroidal neovascularization. *The American Journal of Pathology* 157(1), pp. 135–144.

Bearelly. S., 2011. Use of Fundus Autofluorescence Images to Predict Geographic Atrophy Progression. *Retina* 31(1), pp. 81–86.

Srinivasan, V.J.V., Wojtkowski, M.M., Witkin, A.J.A., Duker, J.S.J., Ko, T.H.T., Carvalho, M.M., Schuman, J.S.J., et al. 2006. High-Definition and 3-dimensional Imaging of Macular Pathologies with High-speed Ultrahigh-Resolution Optical Coherence Tomography. *Ophthalmology* 113(11), pp. 2054.e1-14.

Stangos, N., Voutas, S., Topouzis, F. and Karampatakis, V. 1995. Contrast sensitivity evaluation in eyes predisposed to age-related macular degeneration and presenting normal visual acuity. *Ophthalmologica* 209(4), pp. 194–198.

Stefánsson, E., Geirsdóttir, A. and Sigurdsson, H. 2011. Metabolic physiology in age related macular degeneration. *Progress in Retinal and Eye Research* 30(1), pp. 9–9.

Steinberg, R.H. 1985. Interactions between the retinal pigment epithelium and the neural retina. *Documenta Ophthalmologica* 60(4), pp. 327–346.

Steinmetz, R.L., Haimovici, R. and Jubb, C. 1993. Symptomatic abnormalities of dark adaptation in patients with age-related Bruch's membrane change. *British Journal of Ophthalmology* 77(9), pp. 549–554.

Stevens, R.G. and Davis, S. 1996. The melatonin hypothesis: electric power and breast cancer. *Environmental Health Perspectives* 104 Supplement, pp. 135–140.

Stiles, W.S. and Crawford, B.H. 1932. Equivalent adaptational levels in localized retinal areas. In: *Report of a Joint Discussion on Vision. Physical Society of London*. Cambridge: Cambridge University Press.

Strauss, O. 2005. The Retinal Pigment Epithelium in Visual Function. *Physiological Reviews* 85(3), pp. 845-881

Sturr, J.F., Zhang, L., Taub, H.A., Hannon, D.J. and Jackowski, M.M. 1997. Psychophysical evidence for losses in rod sensitivity in the aging visual system. *Vision Research* 37(4), pp. 475–481.

Sullivan, R.K., Woldemussie, E., Pow, D.V. 2007. Dendritic and synaptic plasticity of neurons in the human age-related macular degeneration retina. *Investigative Ophthalmology and Visual Science* 48(6), pp. 2782-2791

Sunness, J.S., Johnson, M.A., Massof, R.W. and Marcus, S. 1988. Retinal Sensitivity Over Drusen and Nondrusen Areas: A Study Using Fundus Perimetry. *Archives of Ophthalmology* 106(8), pp. 1081–1084.

Sunness, J.S., Massof, R.W., Johnson, M.A., Bressler, N.M., Bressler, S.B. and Fine, S.L. 1989. Diminished foveal sensitivity may predict the development of advanced age-related macular degeneration. *Ophthalmology* 96(3), pp. 375–381.

Sunness, J.S., Rubin, G.S., Zuckerbrod, A. and Applegate, C.A. 2008. Foveal-Sparing Scotomas in Advanced Dry Age-Related Macular Degeneration. *Journal of Visual Impairment & Blindness* 102(10), pp. 600–610.

Suter, M.M., Remé, C.C., Grimm, C.C., Wenzel, A.A., Jäättela, M.M., Esser, P.P., Kociok, N.N., et al. 2000. Age-related macular degeneration. The lipofusion component N-retinyl-N-retinylidene ethanolamine detaches proapoptotic proteins from mitochondria and induces apoptosis in mammalian retinal pigment epithelial cells. *The Journal of Biological Chemistry* 275(50), pp. 39625–39630.

Swerdlow, A. 2003. *Shift work and breast cancer: a critical review of the epidemiological evidence, Research Report 132.* Surrey: Institute of Cancer Research

Szkulmowski, M.M., Wojtkowski, M.M., Sikorski, B.B., Bajraszewski, T.T., Srinivasan, V.J.V., Szkulmowska, A.A., Kałuzny, J.J.J., et al. 2007. Analysis of posterior retinal layers in spectral optical coherence tomography images of the normal retina and retinal pathologies. *Journal of Biomedical Optics* 12(4), p. 041207.

Tan, J.S.L., Mitchell, P., Smith, W. and Wang, J.J. 2007. Cardiovascular Risk Factors and the Long-term Incidence of Age-Related Macular Degeneration. *Ophthalmology* 114(6), pp. 1143–1150.

Tan, J.S.L., Wang, J.J., Flood, V., Rochtchina, E., Smith, W. and Mitchell, P. 2008. Dietary antioxidants and the long-term incidence of age-related macular degeneration: the Blue Mountains Eye Study. *Ophthalmology* 115(2), pp. 334–341.

Tan, J.S.L., Wang, J.J., Flood, V. and Mitchell, P. 2009. Dietary Fatty Acids and the 10-Year Incidence of Age-Related Macular Degeneration: The Blue Mountains Eye Study. *Archives of Ophthalmology* 127(5), pp. 656–665.

Taylor, H.R., West, S., Muñoz, B., Rosenthal, F.S., Bressler, S.B. and Bressler, N.M. 1992. The long-term effects of visible light on the eye. *Archives of Ophthalmology* 110(1), pp. 99–104.

Terman, A. and Brunk, U.T. 2006. Oxidative stress, accumulation of biological'garbage', and aging. *Antioxidants & Redox Signaling* 6(1), pp. 15-26.

Tezel, T.H., Bora, N.S. and Kaplan, H.J. 2004. Pathogenesis of age-related macular degeneration. *Trends in Molecular Medicine* 10(9), pp. 417–420.

Thapan, K., Arendt, J. and Skene, D.J. 2001. An action spectrum for melatonin suppression: evidence for a novel non-rod, non-cone photoreceptor system in humans. *The Journal of Physiology* 535(Pt 1), pp. 261–267.

Thibos, L. and Bradley, A. 1993. New Methods for Discriminating Neural and Optical Losses of Vision. *Optometry and Vision Science* 70(4), pp. 279-287.

Thomas, M.M. and Lamb, T.D. 1999. Light adaptation and dark adaptation of human rod photoreceptors measured from the a-wave of the electroretinogram. *The Journal of Physiology* 518, pp. 479–496.

Thornton, J., Edwards, R., Mitchell, P., Harrison, R.A., Buchan, I. and Kelly, S.P. 2005. Smoking and age-related macular degeneration: a review of association. *Eye* 19(9), pp. 935–944.

Tinjust, D., Kergoat, H.E.L.E.N. and Lovasik, J.V. 2002. Neuroretinal function during mild systemic hypoxia. *Aviation Space and Environmental Medicine* 73(12), pp. 1189–1194.

Uğurlu, N., Aşık, M.D., Yülek, F., Neselioglu, S. and Cagil, N. 2013. Oxidative stress and anti-oxidative defence in patients with age-related macular degeneration. *Current Eye Research* 38(4), pp. 497–502.

van de Ven, J., Nilsson, S.C., Tan, P.L. and Buitendijk, G. 2013. A functional variant in the CFI gene confers a high risk of age-related macular degeneration. *Nature Genetics* 45, pp. 813-817.

van Leeuwen, R., Ikram, M.K., Vingerling, J.R., Witteman, J.C.M., Hofman, A. and de Jong, P.T.V. 2003. Blood pressure, atherosclerosis, and the incidence of age-related maculopathy: the Rotterdam Study. *Investigative Ophthalmology & Visual Science* 44(9), pp. 3771–3777.

Vingrys, A.J. and Garner, L.F. 1987. The effect of a moderate level of hypoxia on human colour vision. *Documenta Ophthalmologica* 66(2), pp. 171–185.

Wald, G. 1968. The Molecular Basis of Visual Excitation. *Nature* 219, pp. 800–807.

Wald, G. and Clark, A.B. 1937. Visual adaptation and chemistry of the rods. *The Journal of General Physiology* 21(1), p. 93.

Wall, M. and Sadun, A.A. 1986. Threshold Amsler grid testing. Cross-polarizing lenses enhance yield. *Archives of Ophthalmology* 104(4), pp. 520–523.

Wang, J.S. and Kefalov, V.J. 2009. An alternative pathway mediates the mouse and human cone visual cycle. *Current Biology* 19(19), pp. 1665–1669.

Wang, J.S. and Kefalov, V.J. 2011. The cone-specific visual cycle. *Progress in Retinal and Eye Research* 30(2), pp. 115–128.

Wang, J.J., Foran, S., Smith, W. and Mitchell, P. 2003. Risk of Age-Related Macular Degeneration in Eyes With Macular Drusen or HyperpigmentationThe Blue Mountains Eye Study Cohort. *Archives of Ophthalmology* 121(5), pp. 658–663.

Wangsa-Wirawan, N.D. and Linsenmeier, R.A. 2003. Retinal oxygen: fundamental and clinical aspects. *Archives of Ophthalmology* 121(4), pp. 547–557.

Watson, A.B. and Pelli, D.G. 1983. Quest: A Bayesian adaptive psychometric method. *Perception & psychophysics* 33(2), pp. 113–120.

Wells, J.A., Murthy, R., Chibber, R., Nunn, A., Molinatti, P.A., Kohner, E.M. and Gregor, Z.J. 1996. Levels of vascular endothelial growth factor are elevated in the vitreous of patients with subretinal neovascularisation. *British Journal of Ophthalmology* 80(4), pp. 363–366.

Whittaker, S.G. and Lovie-Kitchin, J. 1993. Visual Requirements for Reading. *Optometry and vision science* 70(1), pp. 54-65.

Williams, D., MacLeod, D.I. and Hayhoe, M. 1981. Punctate sensitivity of the blue-sensitive mechanism. *Vision Research* 21(9), pp. 1357–1375.

Williamson, T.H.T. and Keating, D.D. 1998. Telemedicine and computers in diabetic retinopathy screening. *British Journal of Ophthalmology* 82(1), pp. 5–6.

Wing, G.L., Blanchard, G.C. and Weiter, J.J. 1978. The topography and age relationship of lipofuscin concentration in the retinal pigment epithelium. *Investigative Ophthalmology & Visual Science* 17(7), pp. 601–607.

Winn, B., Whitaker, D., Elliott, D.B. and Phillips, N.J. 1994. Factors affecting light-adapted pupil size in normal human subjects. *Investigative Ophthalmology & Visual Science* 35(3), pp. 1132–1137.

Winsor, C.P. and Clark, A.B. 1936. Dark Adaptation after Varying of Light Adaptation. *Proceedings of the National Academy of Sciences of the United States of America* 22(6), p. 400.

Wise, G.N., Dollery, C.T. and Henkind, P. 1971. *The retinal circulation.* New York: Harper & Row

Witmer, A.N., Vrensen, G.F.J.M., Van Noorden, C.J.F. and Schlingemann, R.O. 2003. Vascular endothelial growth factors and angiogenesis in eye disease. *Progress in retinal and eye research* 22(1), pp. 1–29.

Wolffsohn, J.S., Anderson, S.J., Mitchell, J., Woodcock, A., Rubinstein, M., Ffytche, T., Browning, A., et al. 2006. Effect of age related macular degeneration on the Eger macular stressometer photostress recovery time. *British Journal of Ophthalmology* 90(4), pp. 432–434.

Wong, T.Y., Liew, G. and Mitchell, P. 2007. Clinical update: new treatments for age-related macular degeneration. *Lancet* 370(9583), pp. 204–206.

Wong, T.Y., Wong, T., Chakravarthy, U., Klein, R., Mitchell, P., Zlateva, G., Buggage, R., et al. 2008. The natural history and prognosis of neovascular age-related macular degeneration: a systematic review of the literature and meta-analysis. *Ophthalmology* 115(1), pp. 116–126.

Wood, A., Margrain, T. and Binns, A. 2011. The effect of bleach duration and age on the ERG photostress test. *Graefe's Archive for Clinical and Experimental Ophthalmology* 249(9), pp. 1359–1365.

Wu, G., Weiter, J.J., Santos, S., Ginsburg, L. and Villalobos, R. 1990. The macular photostress test in diabetic retinopathy and age-related macular degeneration. *Archives of Ophthalmology* 108(11), pp. 1556–1558.

Wu, Y., Yanase, E., Feng, X., Siegel, M.M. and Sparrow, J.R. 2010. Structural characterization of bisretinoid A2E photocleavage products and implications for age-related macular degeneration. *Proceedings of the National Academy of Sciences* 107(16), pp. 7275–7280.

Wyszechki, G. and Stiles, W.S. 1982. *Colour Science: Concepts and Methods, Quantitative Data and Formulae.* New York: John Wiley & Sons.

Xu, W., Grunwald, J.E., Metelitsina, T.I., DuPont, J.C., Ying, G.S., Martin, E.R., Dunaief, J.L., et al. 2010. Association of risk factors for choroidal neovascularization in age-related macular degeneration with decreased foveolar choroidal circulation. *American Journal of Ophthalmology* 150(1), pp. 40–47.e2.

Yannuzzi, L.A. 2011. Indocyanine Green Angiography: A Perspective on Use in the Clinical Setting. *American Journal of Ophthalmology* 151(5), pp. 745–751.e1.

Yap, M., Garner, L.F., Legg, S. and Faris, J. 1995. Effects of exposure to simulated altitudes on visual fields, contrast sensitivity, and dazzle recovery. *Aviation, Space and Environmental Medicine* 66(3), pp. 243-246

Yehoshua, Z., Gregori, G., Sadda, S.R., Penha, F.M., Goldhardt, R., Nittala, M.G., Konduru, R.K., et al. 2013. Comparison of drusen area detected by spectral domain optical coherence tomography and colour fundus imaging. *Investigative Ophthalmology & Visual Science* 54(4), pp. 2429–2434.

Yehoshua, Z., Wang, F., Rosenfeld, P.J., Penha, F.M., Feuer, W.J. and Gregori, G. 2011a. Natural History of Drusen Morphology in Age-Related Macular Degeneration Using Spectral Domain Optical Coherence Tomography. *Ophthalmology* 118(12), pp. 2434–2441.

Yehoshua, Z.Z., Rosenfeld, P.J.P. and Albini, T.A.T. 2011b. Current Clinical Trials in Dry AMD and the Definition of Appropriate Clinical Outcome Measures. *Seminars in Ophthalmology* 26(3), pp. 167–180.

Yi, K., Mujat, M., Park, B.H., Sun, W., Miller, J.W., Seddon, J.M., Young, L.H., et al. 2009. Spectral domain optical coherence tomography for quantitative evaluation of drusen and associated structural changes in non-neovascular age-related macular degeneration. *British Journal of Ophthalmology* 93(2), pp. 176–181.

Young, R.W. 1971. The renewal of rod and cone outer segments in the rhesus monkey. *The Journal of Cell Biology* 49(2), pp. 303–318.

Yu, Y., Bhangale, T.R., Fagerness, J., Ripke, S., Thorleifsson, G., Tan, P.L., Souied, E.H., et al. 2011. Common variants near FRK/COL10A1 and VEGFA are associated

with advanced age-related macular degeneration. *Human Molecular Genetics* 20(18), pp. 3699–3709.

Zarbin, M.A.M. 2004. Current concepts in the pathogenesis of age-related macular degeneration. *Archives of Ophthalmology* 122(4), pp. 598–614.

Zayit-Soudry, S., Moroz, I. and Loewenstein, A. 2007. Retinal pigment epithelial detachment. *Survey of Ophthalmology* 52(3), pp. 227–243.

Zhang, P., Wang, Y., Hui, Y., Hu, D., Wang, H., Zhou, J. and Du, H. 2007. Inhibition of VEGF expression by targeting HIF-1 alpha with small interference RNA in human RPE cells. *Ophthalmologica* 221(6), pp. 411–417.

Appendix I. Journal Tables

Study	Study Design	Participants	Visual Acuity	AMD Classification	Methods	Visual Function	Results
(Brown and Kitchin 1983)	Case-control	8 AMD *(66-83yrs)* 6 Control *(63-74 yrs)*	20/60 to 20/400 20/20	*	Four LEDs flashed 15° from fovea.	Scotopic sensitivity	AMD group had significant reduction in scotopic sensitivity for rods and cones 50% had increased time constant of recovery for rod function compared with controls.
(Brown et al. 1986a)	Case-control	4 AMD *(67-74 yrs)* 5 Control (*58-74 yrs)*	20/25 to 20/40 20/20	Drusen ± pig. change (2pts), CNV (1pt), GA (1pt)	Green and red LEDs flashed at 5, 10, 15 and 25° eccentric to fovea after 6 min 1160cd/m^2 pre-adaptation.	Scotopic and photopic sensitivity	Rod and cone thresholds elevated in AMD, (0.5-1.5 log units), so AMD may not be confined to macula. Greatest sensitivity loss in macular area.
(Brown et al. 1986b)	Case-control	6 AMD *(69-78 yrs)* 6 Control *(63-82 yrs)*	6/7.5 to 6/95$^-$ ≥6/6	Drusen ± pig. change	Four LEDs flashed 5, 10, 20 and 40° eccentricity after 3 min, 130cd/m^2 bleach.	Cone-mediated DA	Thresholds significantly elevated in AMD, consistent at all eccentricities. No consistent difference between time constants of recovery for AMD vs controls.
(Sunness et al. 1988)	Cross sectional	8 AMD *(55-86 yrs)*	20/16 to 20/40	Drusen only ± pig. change (5pts), CNV only in fellow eye(2pts), CNV in fellow eye + PED in test eye (1pt)	Fundus camera stimulator compared sensitivity between drusen and drusen-free areas.	Scotopic sensitivity	No significant difference in retinal sensitivity between drusen and non-drusen areas in AMD, but marked sensitivity losses were found in areas of advanced AMD such as PED.
(Sunness et al. 1989)	Prospective (median 45 months)	18 AMD *(57-81 yrs)*	20/16 to 20/50	Study eye: drusen Gd0 (no drusen>125µm) to Gd6 (large, confluent drusen) Fellow eye: drusen (7pts), CNV (7pts), PED (3pts), GA (1pt)	Tubinger perimeter measured absolute sensitivity after 1 hour in dark using 1.8° red foveal stimulus	Absolute scotopic foveal sensitivity	Absolute foveal sensitivity predicted the development of advanced AMD with 100% sensitivity and 92% specificity, and was a better predictor than status of fellow eye, initial VA and high-risk drusen characteristics.
(Eisner et al. 1991)	Cross sectional	41 AMD *(≥ 60 yrs)*	≥ 20/25	Fellow eyes of unilateral nAMD: 32 high risk, 9 low risk	3° 660nm stimuli after 3 min 20,000 Td bleach.	Cone-mediated DA	High risk eyes generally had slower rates of DA ($P<0.001$). 30/32 high-risk eyes had slow DA and abnormal colour matching.

(Eisner et al. 1992)	Prospective (18 months)	47 AMD *(55-86 yrs)*	≥ 20/25	Fellow eyes of unilateral nAMD (hyperpig ± drusen ± atrophy)	3º, 160ms, 660nm test after 3min 20,000 Td, 580nm bleach. Time constant to recovery measured.	Cone-mediated DA	A combination of colour matching and DA was most effective at distinguishing the eyes which developed nAMD at 18 months.
(Steinmetz et al. 1993)	Case-control	12 AMD *(54-86 yrs)* * Control	≥ 6/12 *	Study eye: drusen (50% delayed choroidal filling & 75% hypofluorescent on FFA.) Fellow eye: 42% drusen only, 8% PED, 50% CNV	Modified HFA measured scotopic conditions and DA. In DA, 2 min bleach of >95% rhodopsin preceded testing on HFA.	Scotopic sensitivity	Scotopic thresholds were reduced in 50% AMD pts who had poor night vision or central scotoma in the dark. DA was delayed, but no correlation was found between the quantity of drusen and severity of functional defect.
(Owsley et al. 2000)	Case-control	80 AMD *(59-91 yrs)* 12 Control *(62-80 yrs)*	≥ 20/60 ≥ 20/30	Early: 5 or more drusen >63µm ± hyperpig (71pts) Late: CNV (3pts) or GA >175µm (6pts)	Dark and light-adapted static threshold were measured at 52 loci in the central 38° of retina using modified HFA.	Scotopic and photopic sensitivity	Mean dark-adapted sensitivity was significantly lower in AMD than in controls. The greatest severity was 2° to 4° from the fovea, and decreased with increasing eccentricity.
(Owsley et al. 2001)	Case-control	20 AMD *(66-88 yrs)* 16 Control *(62-79 yrs)*	≥ 20/25 *	Early AMD: one or more drusen >63µm ± focal hyperpig	Scotopic sensitivity and rate of rod-mediated DA measured at 12° eccentricity using modified HFA after 0.25ms, 7.65 log scot Td s^{-1} (98%) bleach.	Scotopic sensitivity and rod-mediated DA	Early AMD exhibited deficits in almost all rod-mediated parameters of DA compared with controls. AMD more likely to fall outside normal range for variables representing DA kinetics (85%)than for steady-state functions like scotopic sensitivity (25%).
(Haimovici et al. 2002)	Case-control	31 AMD *(mean 71yrs)* 11 Control *(mean 71yrs)*	≥ 6/9 ≥ 6/9	Study eye: macular drusen only Fellow eye: Gp I: PED and RPE tears (11pts); Gp II: CNV (10pts); Gp III: drusen only (10pts)	Modified HFA measured time constant to recovery in DA & scotopic sensitivity	Scotopic sensitivity, rod- and cone-mediated DA	Scotopic sensitivities were largely normal in all groups. Both rod- and cone- DA abnormal, but rods were more severely affected. Dysfunction was most marked near the fovea and in pts with PED/RPE tear in fellow eye.
(Phipps et al. 2003)	Case-control	16 AMD *(62-78yrs)* 14 Control *(64-80yrs)*	>6/12 >6/12	Study eye: five or more soft drusen > 63µm ± hyperpig. Fellow eye: drusen only (11pts), CNV (3pts), PED (2pts)	0.5º foveal stimuli flickering at 5Hz presented on gamma-corrected colour TV monitor after 40s (>95%) bleach	Cone-mediated DA	Cone pigment regeneration delayed in most AMD eyes and most affected visual function compared with steady-state parameters.

(Scholl et al. 2004)	Cross sectional	7 AMD *(68-80 yrs)*	20/20 to 20/40	Study eye: drusen only (3pts); nAMD (2pts); GA (2pts). All 7 had increased fundus autofluorescence, FAF.	Photopic and scotopic fine matrix mapping performed using modified HFA.	Photopic and scotopic sensitivity	Areas of increased FAF had moderate to severe scotopic but not photopic sensitivity loss, implying that increased FAF in EARLY AMD has a functional correlate and predilection to rod loss.
(Jackson et al. 2006)	Case-control	19 AMD *(mean 74 yrs)* 17 Old Control *(mean 69 yrs)* 12 Young Control *(mean 23 yrs)*	0.22 *(SD 0.20)* 0.09 *(SD 0.35)* -0.05 *(SD 0.05)*	Early AMD: soft drusen > 63µm ± hyperpig. ± hypopig.	Scotopic Sensitivity Tester-1 (SST-1) with 0.5s, full-field stimulus after 1min, 1000cdm^{-2} bleach.	Rod- mediated DA	Significant delay in rod-mediated DA in old vs. young controls, but no significant delay in AMD vs. old controls.
(Owsley et al. 2007)	Case-control	45 early AMD *(72.5 yrs, SD 9.0)* 21 inter AMD *(75.9 yrs, SD 9.4)* 17 late AMD *(68.8yrs, SD 7.1)* 43 Control *(68.7yrs, SD 7.0)*	0.16 *(SD 0.14)* 0.19 *(SD 0.15)* 0.30 *(SD 0.22)* 0.10 *(SD 0.12)*	AREDS Study step 2-6 AREDS Study step 7-9 AREDS Study step 10-11 AREDS Study step 1	A modified HFA tested DA at 12° eccentricity after 11ms, 7.65 log scot Td s^{-1} (98%) bleach.	Cone- and rod-mediated DA	AMD pts had significant impairments in rod-mediated but not cone-mediated DA in the parafovea at 12° eccentricity, which were increasingly abnormal as disease severity increased.
(Jackson and Edwards 2008)	Case-control	17 AMD *(mean 75.1 yrs)* 8 Young Control *(mean 32.6 yrs)* 9 Old Control *(mean 73.1 yrs)*	0.14 *(SD 0.40)* 0.05 *(SD 0.1)* 0.14 *(SD 0.21)*	AREDS Fundus Grading System where 1 is old control and 10 is advanced AMD	DA measured at 5^{o} eccentricity with AdaptDx. after 0.25ms, 6.38log scot Td s^{-1} bleach.	Rod-mediated DA	AMD had significantly slower DA than old controls. No difference between young and old controls. DA impairment increased with AMD severity.
(Dimitrov et al. 2008)	Case-control	27 AMD *(67.5 ±5.0 yrs)* 22 Control *(66.8 , ± 5.9 yrs)*	0.026 *(SD .078)* -0.017 *(SD .083)*	Study eye: at least one large drusen >125µm within inner macula (3000µm centred on fovea) ± hyperpig. ± hypopig.	A CRT dark adaptometer measured DA with a 4° foveated, spot after 11ms, 6.48 log scot Td s^{-1} (30% rhodopsin) bleach	Rod- and cone-mediated DA	Slowed cone and rod recovery and a delayed RCB were evident in the eyes with AMD.

(Gaffney et al. 2011)	Case-control	10 AMD *(mean 68.3 yrs)* 10 Control *(mean 70 yrs)*	0.09 *(SD 0.11)* -0.002 *(SD 0.10)*	*AREDS Severity Scale:* Test eye: early AMD (8pts) inter AMD (2pts) Fellow eye: early AMD (5pts), adv. AMD (5pts)	A CRT dark adaptometer measured DA using 4 foveal annuli (0.5, 2, 7, 12º radius) after 80% cone bleach (2min 5.1log phot. Td).	Cone- mediated DA	Cone-mediated DA significantly impaired in early AMD. High diagnostic potential of time constant of cone recovery using annular stimuli at 12º.
(Dimitrov et al. 2011)	Case-control	221 EARLY AMD *(72.86 ±9.94 yrs)* 109 Control *(73.07±10.32 yrs)*	≥20/60 ≥20/20	Study eye: soft (>125µm) or reticular drusen ± hyperpig. ± hypopig. Fellow eye: drusen± pig. changes (129pts), CNV (8pts), GA ± CNV (84pts)	A CRT dark adaptometer measured DA with a 4° spot at fovea, 3.5 and 10º eccentricity after 11ms, 6.48 log scot Td s^{-1} (30% rhodopsin) bleach.	Rod- and cone-mediated DA	Cone recovery rate in DA (62%) and PSR (63%) both equally effective. Rod recovery rate in DA had greatest diagnostic capacity (87%), although a combination of 14Hz flicker and PSR (71%) was favoured due to test reproducibility and clinical applicability.
(Clark et al. 2011)	Cross sectional	74 Pts *(53-95 yrs)*	20/16 to 20/632	G1: <10 small drusen <63 µm (17pts); G2: ≥10 small drusen or <15 inter drusen 63-125 µm ± hyperpig (18pts).; G3: ≥15 inter drusen or any large drusen≥ 125µm (20pts); G4: GA (19pts);	DA measured over 20min for 500nm target at 5º eccentricity using AdaptDx after 0.25ms photoflash 6.38log scot Td sec^{-1} (82% rhodopsin) bleach.	Rod-mediated DA	In AMD, thinning of retina measured using SDOCT is associated with reduced rod-mediated light sensitivity.
(Dimitrov et al. 2012)	Case -control	293 AMD *(72.64 ± 10.04yrs)* 64 Control *(69.16 ± 11.35yrs)*	20/10 to 20/60 ≥20/20	*AMD classified into 12 subgroups using ICGS.* Hard drusen only (59pts), inter drusen (12pts), soft drusen >125µm (121pts), noncentral GA study eye (14pts), late AMD fellow eye (87pts)	2 steady-state (14 Hz flicker and isoluminant blue colour and 2 adaptation tests (PSR and rod DA recovery rate). A CRT dark adaptometer measured DA with a 2° spot at 3.5º eccentricity after 11ms, 6.48 log scot Td s^{-1} (30% rhodopsin) bleach.	Rod-mediated DA	Rod-mediated DA significantly abnormal with hard and/or intermediate drusen, worse with more advanced fundus changes, but limited ability to discriminate between these cases. Steady state tests and clinical signs showed significant concordance with increasing AMD severity.

(Gaffney et al. 2013)	Case-control	10 AMD *(73.0 ± 7.01yrs)* 10 Control *(73.3 ± 4.11yrs)*	0.08 ± 0.12 logMAR 0.03 ± 0.11 logMAR	*AREDS Severity Scale:* Test eye: early AMD (10pts) Fellow eye: early AMD (2pts), adv. AMD (8pts)	A CRT dark adaptometer measured DA using a 12º radius annulus after exposure to 3 pre-adapting light intensities (4.90, 5.20 and 5.50 log phot.Td).	Cone- mediated DA	Dark adaptation was highly diagnostic for early AMD at all pre-adapting bleaching intensities. Lower bleaching intensities may be used to expedite DA whilst maintaining the integrity of the data.
(Jackson et al. 2014)	Case-control	127 AMD *(mean 73 years)* 21 Control *(mean 65 years)*	Mean 78 letters Mean 77 leters	*AREDS Severity Scale:* 41 Early AMD 72 Intermediate AMD 14 Advanced AMD	DA measured at 5º eccentricity for up to 6.5 minutes with AdaptDx. after 0.8ms, $1.8x10^4$ scot cd/m^2 bleach.	Rod- and cone-mediated DA	The rapid DA test (≤ 6.5 minutes) had a diagnostic sensitivity of 90.6% and a specificity of 90.5%, suggesting that it is useful for the detection of AMD. The rapid test duration limited its ability to differentiate disease severity.

* Data unavailable. AMD: Age-related macular degeneration. CNV: choroidal neovascularization. nAMD: neovascular AMD. GA: Geographic atrophy. HFA: Humphrey Field Analyzer. PED: Pigment epithelial Detachment. RPE: Retinal Pigment Epithelium. VA: Visual Acuity. ICGS: International Classification and Grading System

Table 2. Studies Investigating Dark Adaptation Function and Age-Related Macular Degeneration.

Study	Study Design	Participants	Visual Acuity	AMD Classification	Light Source	Outcome Measure	Results
(Chilaris 1962)	Case report	1 AMD *(62 years)* 10/10	6/10 10/10	Early AMD (pigmentary changes) Fellow eye normal	Direct ophthalmoscope for 30s	VA	PSRT was delayed in eye with early AMD compared with fellow, normal eye.
(Severin et al. 1963)	Case-control	1 AMD *(57 years)* 57 Controls *(23-41 years)*	RE: 20/70 LE: 20/20 *	AMD- * Fellow eye normal	Zeiss light coagulator (242,600 lux) for 150ms	VA and contrast discrimination	PSRT delayed in eye with AMD and moderately prolonged in fellow, normal eye compared with controls.
(Forsius et al. 1964)	Case-control	* AMD 402 Controls *(*)*	*	Dry AMD * nAMD (at least 4 pts)	Keeler ophthalmoscope (2145 lux) for 15s at 30cm	VA	PRST not delayed in dry AMD, irrespective of VA. 3 nAMD pts had normal PRST. 1 nAMD pt had delayed PRST (follow-up 4 years).
(Glaser et al. 1977)	Case-control	29 AMD 179 Control *(55 pts ≤30yrs, 72 pts 31-60yrs, 52 pts ≥ 61yrs)*	6/6 to 6/12	Submacular drusen (18pts) AMD (11pts)	Penlight (2340 lumens/m^2) for 10s at 2-3cm	VA	Prolonged PSRT in all AMD pts and 7/18 patients with drusen.
(Smiddy and Fine 1984)	Prospective (4.3 years)	71 AMD	20/15 to 20/100	Bilateral drusen ± pigmentation	Penlight for 20s at 2 inches	VA	No correlation between PSRT and VA, age or severity of drusen.
(Wu et al. 1990)	Case-control	17 AMD *(59-79, 72yrs)* 18 Controls *(18-77, 47yrs)*	20/25 to 20/70 20/15 to 20/40	Soft/hard drusen only	Indirect ophthalmoscope (6V), for 10s at 10cm	VA	PSRT significantly longer in AMD compared with controls (mean 122.9s and 23.2s respectively). PSRT did not significantly increase with age or worsening VA.

(Collins and Brown 1989)	Case-control	21 AMD *(66.6 years)* 11 Controls *(65.8 years)*	Pre-AMD: ≥6/6; AMD: ≤6/7.5 Controls: ≥6/6	Study eye: hard drusen ± pigmentation (10 AMD, 11 pre-AMD)	500W floodlight for 10s	Contrast discrimination	PSRT significantly longer in both pre-AMD and AMD compared with controls.
(Cheng and Vingrys 1993)	Case-control	11 AMD 11 Pre-AMD 8 Controls *(60-85 yrs)*	6/7.5 to 6/15 ≥6/7.5 ≥6/6	Early AMD: confluent drusen ± pigmentation Pre-AMD: no/hard drusen ± pigmentation	QI light (60,000cd/m^2) for 20s at 40cm	VA	AMD had longer PSRT compared with pre-AMD and controls. No significant difference between PRST of pre-AMD and controls.
(Sandberg and Gaudio 1995)	Cross-sectional	133 AMD *(74.4±0.6 yrs)*	≥ 20/60	Study eye: drusen only Fellow eye: nAMD	Welch Allyn Finnoff ocular transilluminator in trial frame for 10s at retinal illuminace 6logTd (94% cone bleach)	VA	Delayed PSRT in 62% of fellow eyes of patients with nAMD. PSRT increased with decreasing VA and foveal RPE atrophy.
(Sandberg et al. 1998)	Prospective (4.5 years)	127 AMD *(58-89 yrs)*	20/20 to 20/60	Study eye: fellow eye of unilateral nAMD pts with drusen (hard or soft), pig changes and RPE atrophy	Welch Allyn transilluminator for 10s	VA	Slow PSRT appears to be an independent risk factor for progression to nAMD. The relative risk increased by 30% for every minute of PSRT.
(Midena et al. 1997)	Case-control	47 AMD *(mean 65yrs)* 36 Controls *(mean 64yrs)*	≥20/25	Early AMD: soft drusen ≥ 63µm ± pig. changes ± RPE atrophy. Bilateral ARM: 34 pts Fellow eye nAMD: 13 pts	Registriert Nyktometer (3 mins bleach at 2200cd/m^2)	VA	PSRT significantly lower in early AMD compared to normal eyes but no difference in PSRT between bilateral AMD and fellow eyes with nAMD.
(Schmitt et al. 2003)	Cross-sectional	30 AMD *(73.3±9.7yrs)*	≥ 20/80	AMD severity graded using AREDS scale (G1: 1pt; G2: 6pts; G3: 11pts; G4: 12pts)	Eger Macular Stressometer (EMS)	VA	No significant difference in PSRT between patients with AMD, cataracts, glaucoma or diabetic retinopathy,

							perhaps due to EMS not creating enough photostress.
(Bartlett et al. 2004)	Case-control	29 AMD *(55-82, 70.2yr*s) 49 Controls *(18-76, 44.6yrs)*	≥ 0.1 ≥ 0.1	Early AMD: Soft drusen and pig. changes (17pts) AMD: GA/CNV (12pts)	EMS	VA	The EMS had a sensitivity of 29% in early AMD and 50% in late AMD. Direct illumination of greater intensity and longer duration may reduce variability.
(Wolffsohn et al. 2006)	Prospective (1 year)	156 AMD *(78.96 ±6.64yrs)*	0.60 (0.39) 0.08 (0.39) 0.07 (0.38)	nAMD: 90 pts GA: 19 pts GA + nAMD: 47 pts	EMS	VA	PSRT was normal in AMD pts and did not correlate with visual function measures (contrast sensitivity and VF defects) or subjective problems with light. PSRT did not predict those whose vision decreased over time.
(Binns and Margrain 2007)	Case-control	31 AMD *(72.4±8.0yrs)* 27 Controls *(71.7±7.0yrs)*	0.04 ± 0.07 0.20 ± 0.15	Early AMD: soft drusen ≥ 63µm ± pig. changes	Bright white background (5.6log phot Td) for 2 mins (86% cone bleach)	41Hz and 5Hz focal cone ERGs	Rate of recovery of the ERG photostress test was reduced in early AMD, and provided a sensitivity and specificity of 77% and 85% respectively.
(Dhalla et al. 2007)	Case-control	15 AMD *(65-84 years)* 50 Young Controls *(30-49 years*) 5 Old Controls *(65-84 years)*	Mild: >20/40; Moderate: 20/40 to 20/200 Severe: <20/200	Mild AMD: ≤5 drusen <64µm Moderate AMD: drusen≥ 63µm ± pig. changes Severe AMD: Foveal GA	Macular Automated Photostress (MAP) test	Foveal threshold using Humphrey perimeter	All 3 AMD groups had decreased foveal sensitivity and a delayed recovery time. Increasing AMD severity resulted in greater depression of foveal threshold after photostress of 17%, 22% and 39% for mild, moderate and severe AMD.

* Data unavailable. AMD: Age-related macular degeneration. EMS: Eger Macular Stressometer. nAMD: neovascular AMD. PSRT: Photostress Recovery Time. RPE: Retinal Pigment Epithelium. VA: Visual Acuity.

Table 3. Studies Investigating Photostress Recovery and Age-Related Macular Degeneration.

Study	Study Design	Participants	Visual Acuity	AMD Classification	Functional Test	Results
(Bowman 1978)	Case-Control	15 AMD *(mean 66.5 years)* 10 Control *(mean 64 years)*	6/6 -6/12: 8pts 6/12-6/30: 7pts	*	FM 100 Hue	AMD patients had a blue-yellow chromatic deficiency, which improved when illumination was increased.
(Bowman 1980)	Case-Control	15 AMD *(mean 66.5 yrs)* 10 Control *(mean 64 yrs)*	6/6 -6/12: 8pts 6/12-6/30: 7pts	*	FM 100 Hue Panel D-15	Colour discrimination deteriorated with decreasing luminance in AMD. FM 100 more sensitive than Panel D-15 in early AMD.
(Bowman et al. 1984)	Case-Control	10 AMD *(mean 74.3yrs)* 10 Old Control *(mean 73.2yrs)* 10 Young Control *(mean 21.3yrs)*	6/18-6/60	*	Panel D-15 Desaturated D-15 H- 16 Panel	With decreasing luminance, colour discrimination deteriorated more in AMD compared with both age-matched and young controls. Desaturated D-15 most sensitive in assessing chromatic deficiency.
(Collins 1986)	Case-Control	10AMD *(mean 67.2yrs)* 11 Pre-AMD *(mean 66.0yrs)* 11 Control *(mean 65.8 yrs)*	6/7.5 to 6/9.5 ≥6/6 ≥6/6	Pre-AMD and AMD: drusen ± pigmentary disturbance at macula	Desaturated D-15	Colour discrimination equally diminished in pre-AMD (VA ≥6/6) and AMD, with a tendency towards tritan deficiency.
(Applegate et al. 1987)	Prospective *(>2 years)*	3 AMD (4 eyes) *(53-73, mean 64yrs)*	≥ 20/25	Bilateral drusen Fellow eye CNV: 2pts	FM 100 Hue Panel D-15	Prior to VA loss, BY sensitivity is progressively reduced in AMD. RG sensitivity loss occurs later in the disease, when clinically manifest signs are seen.
(Smith et al. 1988)	Cross-Sectional	10 AMD *(50-78, mean 61yrs)*	6/6 to 6/18	Sarks Classification: Gd II (3pts); Gd III (4pts); Gd IV (3pts)	Colour matching and Stiles Crawford Effect using Moreland anomaloscope	Colour matching abnormalities increased with AMD severity. Stiles-Crawford effect abnormal in 9/10 eyes.

(Atchison and Lovie-Kitchin 1990)	Case-Control	15 AMD *(58-68, mean 63.5yrs)* 15 Control *(59-67, mean 63.3yrs)*	≥6/6 ≥6/6	AMD: Hard drusen ± pig. changes	Desaturated D-15	No significant difference in colour discrimination between patients with AMD and age-matched controls.
(Eisner et al. 1991)	Cross sectional	41 AMD *(≥ 60 yrs)*	≥ 20/25	Fellow eyes of unilateral nAMD: 32 high risk, 9 low risk (hyperpig ± drusen ± atrophy)	Farnsworth Panel D-15, Rayleigh colour matching	High-risk eyes (large confluent drusen + hyperpig) had abnormal colour matching and failed the D-15 test
(Eisner et al. 1992)	Prospective *(18 months)*	47 AMD *(55-86 yrs)*	≥ 20/25	Fellow eyes of unilateral nAMD (hyperpig ± drusen ± atrophy)	Farnsworth Panel D-15, Rayleigh colour matching	A combination of colour matching and dark adaptation was most effective at distinguishing the eyes which developed CNV after 18 months
(Cheng and Vingrys 1993))	Case-Control	11 AMD 11 Pre-AMD 8 Control *(60-85 yrs)*	6/7.5 to 6/15 ≥6/7.5 ≥6/6	Early AMD: confluent drusen ± pigmentation Pre-AMD: no/hard drusen ± pigmentation	Ishihara Plates Panel D-15 Desaturated panel	Only AMD pts had YB defects in Panel D-15. Desaturated panel produced many false positives. Positive correlation between confluent drusen and losses in colour saturation and hue discrimination.
(Frennesson et al. 1995)	Case-Control	27 AMD *(57-80, mean 69.7yrs)* 29 Control *(51-79, mean 67.7yrs)*	0.96±0.05 0.98±0.04	AMD: Soft drusen (some confluent) ± pig. changes (no pig. clumping) Fellow eye CNV: 8pts	Colour contrast sensitivity using computer graphics technique D-15	Mean colour contrast sensitivity significantly lower in early AMD for tritan, protan and deutan axis. Correlation between tritan threshold and FA. D-15 not significantly abnormal in AMD group.
(Holz et al. 1995)	Prospective *(2 years)*	47 AMD *(55-84, mean 69yrs)*	6/9	Unilateral or bilateral drusen	Colour contrast sensitivity using computer graphics technique	Tritan thresholds significantly elevated at fovea compared with parafovea, and increased with disease progression
(Midena et al. 1997)	Case-Control	47 AMD *(mean 65yrs)* 36 Control *(mean 64yrs)*	≥20/25	Early AMD: soft drusen ≥ 63µm ± pig. changes ± RPE atrophy. Bilateral AMD: 34 pts Fellow eye nAMD: 13 pts	FM-100 Hue	No colour vision defect was observed in any AMD pt using FM-100.

(Arden and Wolf 2004)	Case-Control	24 AMD *(mean 76 yrs)* 109 Control *(57-82, mean 71.5yrs)*	≥ 0.6 *	Early and late AMD grading using Bird's classification (Bird et al. 1995)	Colour contrast sensitivity (Computer graphics system)	Elevated threshold for tritan optotypes in unaffected eyes of AMD patients. Tritan thresholds in AMD eyes were correlated with disease severity.
(Feigl et al. 2004)	Prospective *(1 year)*	13 AMD *(mean 72yrs)* 13 Control *(mean 70yrs)*	≥ 6/12 ≥ 6/12	Early AMD: hard/ soft distinct and indistinct drusen >63µm ± RPE abnormalities	Desaturated D-15 and Panel D-15	Desaturated CV significantly impaired in AMD (mainly Tritan defect) but did not change over time.
(O'Neill-Biba et al. 2010)	Cross-sectional	18 AMD pts *(47-85, mean 68yrs)*	6/4.8 to 6/60	No drusen/small drusen: 2 eyes; Extensive small, inter drusen± pigmentation: 21 eyes; Large, extensive inter drusen, non-central GA: 5 eyes; Central GA: 1 eye; nAMD: 5 eyes	CAD test	All 18 AMD pts had acquired CV defects. Mean YB loss increases linearly with disease severity and is greater than RG loss for all AMD groups.

* Data unavailable. AMD: Age-related macular degeneration. FM-100 Hue: Farnsworth Munsell 100 Hue. RG: red-green. YB: yellow-blue.

Table 4. Studies investing colour vision and AMD.

Study	Study Design	Participants	Visual Acuity	AMD Classification	Methods	Results
(Brown and Lovie-Kitchin 1987b)	Case-control	9 AMD *(60-85,mean 70.9yrs)* 8 Pre-AMD *(61-72, mean 65.4yrs)* 10 Control *(57-74, mean 65.5yrs)*	≥ 6/30 ≥ 6/6 ≥ 6/6	AMD: Drusen ± pig. change (2pts), GA (3pts), pig. change only (3pts), CNV (1pt) Pre-AMD: Drusen ± pig. change (7pts), pig.change only (1pt)	Temporal modulation sensitivity and critical flicker frequency measured across frequencies of 0.5–30Hz.	Temporal function not significantly depressed in patients with drusen and pig. changes and normal VA.
(Applegate et al. 1987)	Prospective *(>2 years)*	3 AMD (4 eyes) *(53-73, mean 64yrs)*	≥ 20/25	Bilateral drusen Fellow eye CNV: 2pts	Flicker sensitivity	Flicker sensitivity was reduced by 0.5 log units in patients with early AMD and normal L-M cone sensitivities.
(Brown and Lovie-Kitchen 1989)	Case-control	8 AMD *(mean 71 years)* 8 Control *(mean 69.6 years)*	≥ 6/24	AMD: Hard drusen ± pig. change	Temporal summation measured using a red LED presented for durations between 4 and 1024ms.	Although patients with AMD had longer critical durations than controls, they were not statistically significant.
(Haegerstrom-Portney and Brown 1989)	Case-control	10 AMD *(72 years)* 8 Pre-AMD *(67 years)* 9 Control *(63 years)*	20/32 $20/20^{-1}$ 20/20	AMD: Drusen ± pig. change (10 pts)	Flicker sensitivity measured using a 2^{o} central target flickering at 25Hz presented on yellow, magenta and blue adaptation backgrounds.	S-cone sensitivity depressed in 80% of AMD patients only. Both AMD and pre-AMD patients showed a small reduction in M-cone sensitivity, but no significant loss in L-cone pathways.

(Mayer et al. 1992a)	Case-control	13 AMD *(71.7 years)* 19 Control *(70.3 years)*	≥ 20/30 ≥ 20/30	Test eye: fellow eye of unilateral CNV.	Foveal flicker frequency measured at frequencies of 10 and 14Hz.	Eyes at risk of developing AMD could be distinguished from healthy eyes with 78% accuracy on the basis of foveal flicker sensitivity at 10 and 14Hz.
(Mayer et al. 1992b)	Case-control	13 AMD *(60-82, mean 71.7yrs)* 19 Control *(65-88, mean 70.3yrs)*	≥ 20/30 ≥ 20/30	Test eye: fellow eye of unilateral CNV.	Temporal contrast sensitivity measured using foveal long-wavelength circle flickering between 1.8 and 50Hz.	Eyes at risk of developing AMD had less sensitivity to flicker contrast, especially at a frequency of 14Hz.
(Mayer et al. 1994)	Prospective *(1.5-4 years)*	16 AMD *(71.9 years)* 20 Control *(70.2 years)*	≥ 20/30 ≥ 20/25	Test eye: fellow eye of unilateral CNV.	Flicker modulation sensitivity measured at 2.5 and 50Hz using a 2.8º, 660nm stimulus.	Foveal flicker sensitivity at low- to mid-temporal frequencies discriminated pre-exudative AMD from healthy eyes
(Phipps et al. 2004)	Case-control	25 AMD *(69.4 ± 6.2yrs)* 34 Control *(68.9 ± 5.4yrs)*	≥ 6/12 ≥6/12	Study eye: greater than 5 soft drusen (>63 µm) ± pig. change or end-stage CNV in fellow eye	Static and flickering stimuli presented with durations of 200ms (static) or 800ms (flicker)	Flickering targets expose functional deficits in early AMD better than static targets.
(Dimitrov et al. 2011)	Case-control	221 Early AMD *(72.86 ±9.94 yrs)* 109 Control *(73.07±10.32 yrs)*	≥20/60 ≥20/20	Study eye: soft (>125µm) or reticular drusen ± hyperpig. ± hypopig. Fellow eye: drusen± pig. changes (129pts), CNV (8pts), GA ± CNV (84pts)	Flicker thresholds measured with a foveal, 2º Gaussian blob at temporal frequencies of 4 and 14Hz.	A combination of 14Hz flicker and PSR (71%) was favoured due to test reproducibility and clinical applicability.
(Dimitrov et al. 2012)	Case -control	293 AMD *(72.64 ± 10.04yrs)* 64 Control *(69.16 ± 11.35yrs)*	20/10 to 20/60 ≥20/20	*AMD classified into 12 subgroups using ICGS.* Hard drusen only (59pts), inter drusen (12pts), soft drusen >125µm (121pts), noncentral GA study eye (14pts), late	Flicker thresholds measured with a foveal, 2º Gaussian blob at a temporal frequency of 14Hz.	14Hz flicker thresholds declined gradually across the spectrum of early AMD fundus changes.

			AMD fellow eye (87pts)				
(Luu et al. 2012)	Prospective	*(24 months)*	127 AMD 24 Control	*(72.6 ± 6.9yrs)*	≥ 0.29 ≥ 0.0	*AMD graded using ICGS:* 88 progressed within early AMD and were excluded; 18 had non-progressed early AMD; 16 developed GA; 5 developed CNV.	Flicker perimetry performed with an automated perimeter (M-700; Medmont International Pty Ltd) within the central 6º from fixation.	Eyes that went on to develop GA or CNV had significantly reduced mean flicker sensitivity before clinical detection of GA or CNV compared with control eyes. The rate of change of flicker sensitivity was increased in eyes with GA but not in eyes with CNV.
(Luu et al. 2013)	Case-control		279 AMD 24 Controls	*(66.6 years)* *(65.8 years)*	Pre-AMD: ≥6/6; AMD: ≤6/7.5 Controls: ≥6/6	*AMD classified into 10 subgroups using ICGS*	Static and flicker perimetry performed with an automated perimeter (M-700; Medmont International Pty Ltd) within the central 6º from fixation.	Static and flicker perimetry both show trends of reduced sensitivity with disease progression.

* Data unavailable. AMD: Age-related macular degeneration. CNV: choroidal neovascularization. nAMD: neovascular AMD. GA: Geographic atrophy. RPE: Retinal Pigment Epithelium. VA: Visual Acuity. ICGS: International Classification and Grading System

Table 5. Studies investing temporal sensitivity and AMD.

Appendix II. Matlab Code for Dark Adaptation

```
%DARK ADAPTATION EXPERIMENT

% First written 3/3/090
% This version written 6/12/100

% This version is specific to the 12deg annulus used in the Bleaching
study
%   To   use   other   sizes   need   to   alter   code   in   line   15
back to >9*17.5

clear all

 % Input co ordinates and sizes for cross and spot
   HorizontalLocation = input('Horizontal location in degrees? ');
   VerticalLocation = input('Vertical location in degrees? ');
   SpotSize = input('Spot size in degrees?')*17.5; % size of spot in
pixels
   RingThickness = input('Ring thickness in degrees?')*35; % thickness
of ring in pixels
   if SpotSize < 9*17.5; OutsideLineSize=100; InsideLineSize=100; end
   if SpotSize > 20*17.5; OutsideLineSize=0; InsideLineSize=200; end
   if SpotSize == 14*17.5; OutsideLineSize=0; InsideLineSize=100; end
   LineThickness = 50; % this it the thickness of the fixation cross
   LineSize = SpotSize+OutsideLineSize; % this is the length of the
cross line in pixels
   InnerLineSize = SpotSize-InsideLineSize;
   % NOTE assumes a 55 cm viewing distance!

KbName('UnifyKeyNames');
% The Try, Catch, End commands will respond to bugs / problems
try
    % First set up all the parameters
    whichScreen = 0;
    window = Screen(whichScreen, 'OpenWindow');
    white = WhiteIndex(window); % pixel value for white
    black = BlackIndex(window); % pixel value for black
    gray = (white+black)/2;
```

```
    inc = white-gray;

    % And, set the parameters of the spot, 1st and 3rd numbers give
the horizontal position
    % the 2nd and 4th give the vertical, the spot is streched inbetween.
    % SpotSize = 35/2; % This is the size of the spot in pixels
    offsetCenteredspotRect = [640-SpotSize  512-SpotSize  640+SpotSize
512+SpotSize]; % size and position of spot on screen
    offsetCenteredspotRect2   =   [640-SpotSize+RingThickness     512-
SpotSize+RingThickness    640+SpotSize-RingThickness    512+SpotSize-
RingThickness];
    SurroundRectInner    =    [640-SpotSize-10        512-SpotSize-10
640+SpotSize+10  512+SpotSize+10]; % size and position of anulus
    SurroundRectOuter = [496 368 784 656];

    % Set up the sounds for correct and incorrect responses and to
indicate
    % that a new neutral density filter is required
    correctSound = sin(2*pi*100*[0:0.00125:2.0]);
    incorrectSound = sin(2*pi*40*[0:0.00125:2.0]);
    NewFilterSound = sin (2*pi*200*[0:0.00125:10.0]);

    % Intial psychophysical increment step size
    incrementStep = 0.4;% good parameter =12 if not bleached
    SpotLuminance = 2.0;% good parameter = 5 if not bleached

    % Set up various flags
    response = 0;
    responseCounter = 0;
    reversalCounter = 1;%this counts reversals but is reset after each
threshold
    DarkAdptCounter = 0; % counts the number of times a dark adptn
threshold is recorded.
    presentationCounter=1; %counts all presentations, used in Humphrey
version
    dataCounter=1;%this  is  the  reversal  counter,  it  counts  all
reversals
    thresholdCounter = 1;% this counter is for the Humphrey version
i.e. it counts the no. of threshold points
```

```
    AdjustmentFilter1 = 1.2;% this is the optical density of the first
ND filter
    AdjustmentFilter2 = 0;% this is the optical density of the secondt
ND filter - which is not yet in place!!!
    % Clear arrays that contain data
    SecondNDFIlterFlag = 0; % this line is used as a flag to stop the
luminance being raised if the spot luminance hits it's lowest level a
second time i.e. after the 2.1 ND filter has been added
    resultTime = 1;
    resultThreshold = 1;
    BreakFlag=0;

    % Set keys up.
    rightKey = KbName('RightArrow');
    leftKey = KbName('LeftArrow');
    escapeKey = KbName('ESCAPE');

    % This screen can be used to write instructions
    Screen(window, 'FillRect', 0);
    Screen('DrawText', window, 'DARK ADAPTATION VERSION 6/5/10', 300,
200, white);
    Screen('DrawText', window, 'Hit any key to start experiment', 300,
400, white);
    Screen(window, 'Flip');
    Kbwait;% duration of instruction presentation

    % Set up the timer.
    startTime = now;
    durationInSeconds = 1500;
    durationEachThreshold = 1;
    numberOfSecondsRemaining = durationInSeconds;
    SecondsRemaining = durationEachThreshold;

    % Calibration variables
    MinScreenLum = 0.12; % Keep: contrast = 100 & brightness = 63
    GammaFunc = 2.15;
    MaxScreenLum = 122.5;

    % Now start the experiment loop.
    fprintf('Experiment started'),
```

```
    StartExptSecs = GetSecs; % this times the whole dark adaptation
expt

 while GetSecs - StartExptSecs < durationInSeconds% Keep experiment
running

            % Set up flags etc to re enter the threshold loop
            stopRule = 1;%keeps loop running till stop rules met, then
=0

      while stopRule > 0 % Keep looking for threshold i.e. expt
running.

            GammaCorrectSpotLum      =      255*(((10^SpotLuminance)-
MinScreenLum)/MaxScreenLum)^(1/GammaFunc)
            %This calculates the grey scale required for desired
luminance
            %SpotLuminance raised to power of 10 to 'un-log' the number

            Screen('DrawText',       window,       ['GammaCorr:       '
num2str(SpotLuminance,4)], 970, 940, [0,0,240]);
                if InnerLineSize <0 % this line stops the central cross
going ' funny' if we are presenting a small spot.
                    InnerLineSize = 0;
                end
            Screen('DrawLine',     window,     [GammaCorrectSpotLum*7
GammaCorrectSpotLum*7                          GammaCorrectSpotLum*7],
640+(HorizontalLocation*35),      512-(VerticalLocation*35)-LineSize,
640+(HorizontalLocation*35),                                      512-
(VerticalLocation*35)+LineSize,LineThickness); % presents peripheral
fixation markers
            Screen('DrawLine',     window,     [GammaCorrectSpotLum*7
GammaCorrectSpotLum*7                          GammaCorrectSpotLum*7],
640+(HorizontalLocation*35)-LineSize,      512-(VerticalLocation*35),
640+(HorizontalLocation*35)+LineSize,                             512-
(VerticalLocation*35),LineThickness);
            Screen('FillOval', window, [0 0 0], SurroundRectInner); %
draws invisible spot i.e. surround
            Screen('FillOval',      window,      [GammaCorrectSpotLum
GammaCorrectSpotLum 0], offsetCenteredspotRect); % draws white spot
```

```
            Screen('FillOval',       window,       [0       0       0],
offsetCenteredspotRect2); % draws black spot
            Screen('DrawLine',     window,     [GammaCorrectSpotLum*7
GammaCorrectSpotLum*7                          GammaCorrectSpotLum*7],
640+(HorizontalLocation*35), 512-(VerticalLocation*35)-InnerLineSize,
640+(HorizontalLocation*35),                                      512-
(VerticalLocation*35)+InnerLineSize,LineThickness);     %     presents
peripheral fixation markers
            Screen('DrawLine',     window,     [GammaCorrectSpotLum*7
GammaCorrectSpotLum*7                          GammaCorrectSpotLum*7],
640+(HorizontalLocation*35)-InnerLineSize, 512-(VerticalLocation*35),
640+(HorizontalLocation*35)+InnerLineSize,                        512-
(VerticalLocation*35),LineThickness);
            Screen(window, 'Flip'); % presents test
            WaitSecs (0.2); % presentation time

            %Remove stimulus
            %Screen('DrawText',     window,     sprintf('%i     seconds
remaining...', numberOfSecondsRemaining), 20, 60, white);
            Screen('DrawText',       window,       ['GammaCorr:       '
num2str(SpotLuminance,4)], 970, 940, [0,0,240]);
            Screen('DrawLine',     window,     [GammaCorrectSpotLum*7
GammaCorrectSpotLum*7                          GammaCorrectSpotLum*7],
640+(HorizontalLocation*35),      512-(VerticalLocation*35)-LineSize,
640+(HorizontalLocation*35),                                      512-
(VerticalLocation*35)+LineSize,LineThickness);
            Screen('DrawLine',     window,     [GammaCorrectSpotLum*7
GammaCorrectSpotLum*7                          GammaCorrectSpotLum*7],
640+(HorizontalLocation*35)-LineSize,      512-(VerticalLocation*35),
640+(HorizontalLocation*35)+LineSize,                             512-
(VerticalLocation*35),LineThickness);
            Screen('FillOval', window, [0 0 0], SurroundRectInner); %
draws large spot i.e. surround
            Screen('DrawLine',     window,     [GammaCorrectSpotLum*7
GammaCorrectSpotLum*7                          GammaCorrectSpotLum*7],
640+(HorizontalLocation*35), 512-(VerticalLocation*35)-InnerLineSize,
640+(HorizontalLocation*35),                                      512-
(VerticalLocation*35)+InnerLineSize,LineThickness);     %     presents
peripheral fixation markers
            Screen('DrawLine',     window,     [GammaCorrectSpotLum*7
GammaCorrectSpotLum*7                          GammaCorrectSpotLum*7],
```

```
640+(HorizontalLocation*35)-InnerLineSize, 512-(VerticalLocation*35),
640+(HorizontalLocation*35)+InnerLineSize,                          512-
(VerticalLocation*35),LineThickness);
            Screen(window, 'Flip'); % blanks out test
            ResponseSecs = GetSecs;% gets the time the stimulus was
flipped out

            % Wait for a response
            while 1
                [ keyIsDown, timeSecs, keyCode ] = KbCheck;
                if keyIsDown

                    if keyCode(escapeKey)% this small loop helps stop
the programme after the ESC key is pushed.
                        BreakFlag=1;
                        break
                    end
                   %fprintf('"%s" typed at time %.3f seconds\n',
KbName(keyCode), timeSecs - ResponseSecs);
                   if (timeSecs - ResponseSecs)<0.6;
                        response = 1; %this means the response was
correct
                        %responseCounter = responseCounter + 1;
                        sound(correctSound)
                   else
                        response = -1; %this means the response was
incorrect (in this case too slow)
                        %responseCounter = responseCounter - 1;
                        sound (incorrectSound)
                        break
                   end

                   while KbCheck; end % this avoids KbCheck reporting
multiple events
                   break
                end

                % Now, if no button push + long wait, time is up!
                SecsNow = GetSecs;
                timeSincePresentation = (SecsNow - ResponseSecs);
```

```
                if timeSincePresentation > 1;
                    response = -1; %this means the response was
incorrect (in this case completely missed)
                    %responseCounter = responseCounter - 1;
                    break
                end
            end % waiting for repsonse or time up

            if BreakFlag==1% this small loop helps stop the programme
after the ESC key is pushed.
            break
            end

            %Now record each presentation.
             presentationTime(presentationCounter)=     (GetSecs     -
StartExptSecs);
            presentationThreshold(presentationCounter)=
SpotLuminance-AdjustmentFilter1-AdjustmentFilter2;
            presentationCounter = presentationCounter + 1;

  %Now adjust next stimulus increment on the basis of the response
            if response > 0;% that is, correct

                if incrementStep > 0.0; % that is, threshold was
raised up on the last step, this must be a threshold
                resultTime    (thresholdCounter)    =    (GetSecs    -
StartExptSecs);
                resultThreshold (thresholdCounter) = SpotLuminance-
AdjustmentFilter1-AdjustmentFilter2;
                thresholdCounter = thresholdCounter + 1;
                stopRule = -1; % this should make the programme
realise that a threshold has been recorded
                end

              incrementStep = -0.3;% now ensure that the next step is
down 0.3 log units
              WaitSecs (0.5 + rand(1.5))
            end

            if response < 0;% that is, incorrect
```

```
                %sound(incorrectSound)
                incrementStep = 0.1;
                WaitSecs (rand(1.0))
            end

            % Now alter stimulus for next presentation
            %if thisFlag == 1;
                SpotLuminance = SpotLuminance + incrementStep;
                if SpotLuminance > 2
                SpotLuminance = 2;
                end

                % Now reset the stimulus intensity when the minimum
                % luminance is reached
                if SpotLuminance < -0.9;
                   SecondNDFIlterFlag = SecondNDFIlterFlag + 1; %This
is the counter that determines which adjustments are made for a ND
filter put on the screen
                   sound (NewFilterSound) % makes a beep to tell the
investigator to insert a new filter
                   if SecondNDFIlterFlag == 1 % This is the 1st loop
i.e. the 1st time the subject reaches -1log cd/m2
                        AdjustmentFilter2 = 2.1;
                        LineThickness = 10;
                        WaitSecs (5.0)
                        SpotLuminance = 1.1; % resets the stimulus
intensity to the maximum brightness
                   end
                   if SecondNDFIlterFlag == 2 % This is the 2nd loop
i.e. the 2nd time the subject reaches -1log cd/m2
                      AdjustmentFilter2 = 3.6;
                      WaitSecs (5.0)
                      SpotLuminance = 0.5; % increases spot lum by 0.6
ND
                   end
                end

      end % this ends the search for a threshold
      beep
```

```
      if BreakFlag==1 % this small loop helps stop the programme after
the ESC key is pushed.
          break
      end

 end % Now go back and collect data for the next threshold point

% Now display the results
        presentationTime = presentationTime (:);% converts row of
presentation time into column
        presentationThreshold = presentationThreshold (:); %converts
row of presentation threshold to column
        plot(presentationTime,       presentationThreshold,'b*')%this
should plot every presentation
        xlabel('Time(s)')
        ylabel('Log Threshold')
        AXIS ([0 300 -1.5 2.5])
        hold on

        resultTime = resultTime(:);% This changes format to column
vectors
        resultThreshold = resultThreshold(:);
        plot(resultTime, resultThreshold,':ko')% this should plot the
thresholds

   % Now fit the final exponential curve
        Starting = [1.2,5,40];
        options=optimset('Display','off');% if set 'off' to 'iter'
will see iterations
        %logFOCThreshold=log10(FOCThresholdNotLog);

Estimates=fminsearch(@myfitExp,Starting,options,resultTime,resultThre
shold);
        fT = Estimates(1)
        iT = Estimates(2)
        Tau =Estimates(3)
        % Now plot this curve
        ExpFitTime =0:2.0:300;% now create some x-axis data at 1.0
steps
```

```
        ExpFitThreshold         =         Estimates(1)+((Estimates(2)-
Estimates(1))*exp(-ExpFitTime./Estimates(3)));
        plot(ExpFitTime, ExpFitThreshold,'r-','LineWidth',2)



   Screen('CloseAll');

   %Now output all the data to Excel spreadsheet
    presentationData = [presentationTime, presentationThreshold]
    thresholdData = [resultTime, resultThreshold]
    ExpFitTime=ExpFitTime(:);
    ExpFitThreshold=ExpFitThreshold(:);
    curveFit = [ExpFitTime, ExpFitThreshold]
    xlswrite('d:\projects              2012\TopographyDAresults.xls',
presentationData,'Model','A14');
    xlswrite('d:\projects              2012\TopographyDAresults.xls',
thresholdData,'Model','D14');
catch
    Screen('CloseAll');
    rethrow(lasterror);
    psychrethrow(psychlasterror);
end
```

Appendix III. Gamma correction and Matlab code for 14-Hz flicker test

Gamma Correction

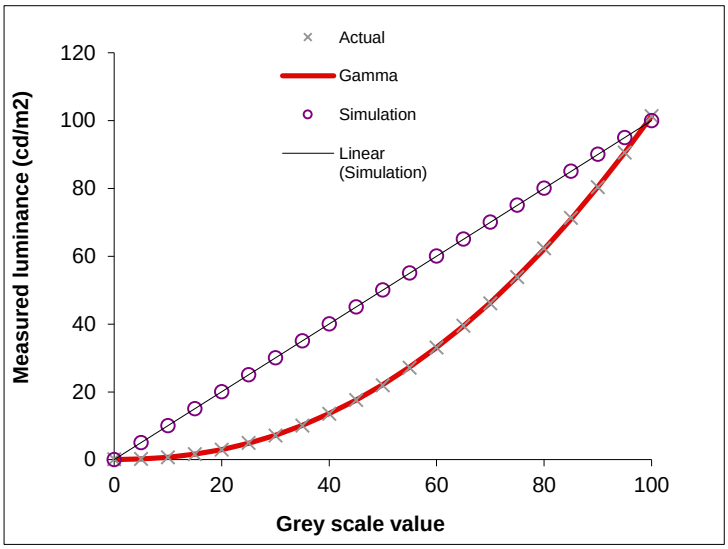

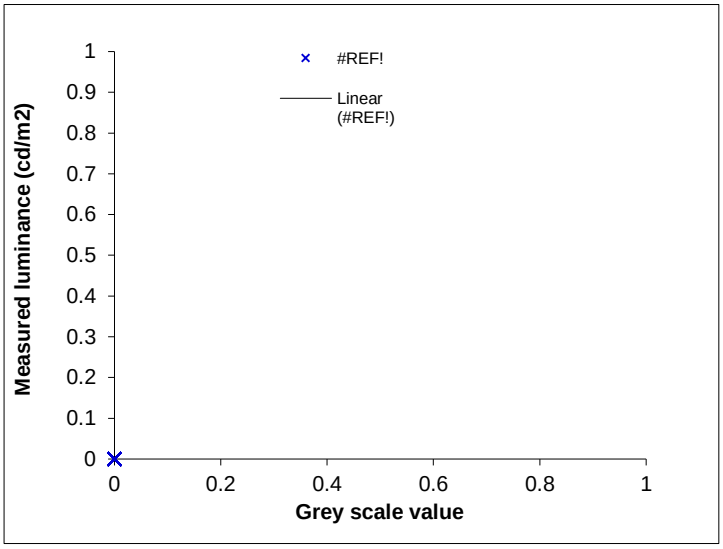

Matlab Code

```
% 14 Hz FLICKER THRESHOLD: YES/NO, QUEST
%
% This programme uses a YES/NO, QUEST driven staircase to determine
contrast
% thresholds for a flickering gaussian blob.
```

```
% The code is adapted from Gaboiumdemo, kbDemo and QuestDemo.
% Ver. 1: Tom Margrain on 28-11-12. This was a 2 IFC version.
% Issues: the frame refresh rate is 60Hz on the laptop but for some
reason
% it reduces significantly from time to time; I guess other programmes
% running the background are stealing resources. If this happens the
% stimulus will be flickering more slowly than expected. The main
problem
% seems to be for the first presentation, after that things are
generally
% better.
% Ver. 8 - Fully working 2 IFC programme. Only altered to Ver. 9
because 2
% IFC may be tricky for patients
% Ver. 9 - Here the programme is altered from 2 IFC to a Yes/No
% Ver. 10 - Now pushing the response key during the presentation should
% work too + keep track of false positives + improve the 'feel' by
altering
% the timing of presentations
% Ver. 11 - implements a 'simple gamma correction' using code from the
online
% AdditiveBlendingForLinearSuperpositionTutorial. The important lines
of
% code that were not used before include
% PsychImaging('AddTask', 'General', 'EnablePseudoGrayOutput') - this
line
% lets us call up all screen output in the range 0-1 (0-100%) rather
than
% grey scale.
%             PsychImaging('AddTask',             'FinalFormatting',
'DisplayColourCorrection', 'SimpleGamma');
% This line sets up simple gamma correction in the video output
'pipeline'
% PsychColourCorrection('SetEncodingGamma', win, gamma); So, all
output is
% gamma corrected automatically.
% This version also allows the 'blob' to occupy a 0-1 range rather
than
% 0-0.5 (line 130). It also changes the slightly misleading variable
% "contrast" to the more accurate "luminance" i.e. the output is
threshold
```

```
% luminance (lines 167, 173). The final output (threshold) is log
luminance
% as a fraction of the max screen luminance in cd/m2.
% This version saved as Trial14Hz Gaussian blob set for 2 degrees at
1.4m
% viewing distance.

% INSTRUCTIONS
% 1)This programme needs to write to an Excel file.
% 2)Tell subject the expt last 3.5 minutes (40 trials).
% 3)The task is to push any button when a flickering stimulus is seen.



% First, set up all the relevant parameters
clear all
trialsDesired = 40; % number of times a choise is offered
wrongRight={'wrong','right'}; % this is used at the end of each trail
to identify the response
stimFreq = 14; % temporal frequency of flickering gabor in Hz
KbName('UnifyKeyNames');
escapeKey = KbName('ESCAPE');
format compact
avgfps = [];
contrastPresent = [];
falsePositive = 0; % used to count false positive responses
%contrast = 1;
% PTB-3 correctly installed and functional? Abort otherwise.
AssertOpenGL;

% This programme uses Psychophysics QUEST routines to determine
threshold
% to get these to work it is necessary to provide information about
the
% threshold we are looking for in particular an initial guess at the
% treshold and the standard deviation
% Provide our prior knowledge to QuestCreate, and receive the data
struct "q".
participant=[];
while isempty(participant)
    participant=input('Subjects name please: ', 's');
```

```
end
tGuess=[];
while isempty(tGuess)
    tGuess=input('Estimate threshold (e.g. -1): ');
end
tGuessSd=[];
while isempty(tGuessSd)
    tGuessSd=input('Estimate the standard deviation of your guess,
above, (e.g. 2): ');
end
pThreshold=0.82;
beta=3.5;delta=0.01;gamma=0.5;% These values may not be right for yes
/no!!
% beta controls the steepness of the psychometric function. Typically
3.5.
% delta is the fraction of trials on which the observer presses blindly.
Typically 0.01.
% gamma is the fraction of trials that will generate response 1 when
intensity==-inf.
q=QuestCreate(tGuess,tGuessSd,pThreshold,beta,delta,gamma);
q.normalizePdf=1; % This adds a few ms per call to QuestUpdate, but
otherwise the pdf will underflow after about 1000 trials.

% Use try and catch to rescue code from a crash
try

% Select screen with maximum id for output window:
screenid = max(Screen('Screens'));

% Open a fullscreen, onscreen window with gray background. Enable 32bpc
% floating point framebuffer via imaging pipeline on it, if this is
possible
% on your hardware while alpha-blending is enabled. Otherwise use a
16bpc
% precision framebuffer together with alpha-blending. We need alpha-
blending
% here to superimpose the gabor blob on the background. The programme
will
% abort if your graphics hardware is not capable of any of this.
PsychImaging('PrepareConfiguration');
```

```
%PsychImaging('AddTask', 'General', 'FloatingPoint16Bit');
PsychImaging('AddTask', 'General', 'FloatingPoint32BitIfPossible');
% Enable bitstealing aka PseudoGray shader: This line is needed so
that
% subsequent screen output is in the range 0-1 i.e. up to 100% of
screen output. No need to call grey levels.
% It also increase the number of grey scales that can be generated
PsychImaging('AddTask', 'General', 'EnablePseudoGrayOutput');
% Sets up the final video output pipeline to include gamma correction
PsychImaging('AddTask', 'FinalFormatting', 'DisplayColourCorrection',
'SimpleGamma');
% Finally open a window according to the specs given with above
% PsychImaging calls, clear it to a background colour of 0.5 aka 50%
% luminance:
[win, winRect]=PsychImaging('OpenWindow',screenid, 0.5);
% This wait allow you to see the 'gamma correction' kick in! First its
not
% there, then,..
WaitSecs (0.5);
% OK, now apply the gamma correction to all outputs to the screen, so
% easy! The default value here is gamma = 2 but need to determine
exactly
% what it is for your screen
gamma = 1 / 2.196152819;
PsychColourCorrection('SetEncodingGamma', win, gamma);

WaitSecs (1);

% Enable alpha-blending, set it to a blend equation useable for linear
% superposition with alpha-weighted source. This allows to linearly
% superimpose gabor patches in the mathematically correct manner,
should
% they overlap. Alpha-weighted source means: The 'globalAlpha'
parameter in
% the 'DrawTextures' can be used to modulate the intensity of each
pixel of
% the drawn patch before it is superimposed to the framebuffer image,
ie.,
% it allows to specify a global per-patch contrast value:
Screen('BlendFunction', win, GL_SRC_ALPHA, GL_ONE);
```

```
% Query frame duration: We use it later on to time 'Flips' properly
for an
% animation with constant framerate:
ifi = Screen('GetFlipInterval', win);

% Create a gabor patch: This is 184x184 pixel matrix that has periperal
values
% around zero and a central value of 1. The gray scale range of the
monitor
% is 1 at the centre of the gabor.
[x,y] = meshgrid(-184:184, -184:184);
whiteBlob = (exp(-((x/92).^2)-((y/92).^2)));



% Create blob movie, first determine frame rate
rate = 1/ifi;

% Determine number of frames avaliable for a given stimulus frequency
framesAvaliable = rate/stimFreq;

% Determine the step size to get through 360 degrees (1 cycle) in the
% number of frames valiable
step = 360/framesAvaliable;

% Set up degrees, start a zero and increment in the loop according to
the
% step size
x=-180;

% Get the time at the very start to record the total experimental time
exptStart = Screen('Flip', win);

% Introduce experiment wait for signal to start
%Screen('FrameRect', win ,[0,128,0], [540,300,740,500],1);
Priority(2);% Uprate the priority for Matlab i.e. try to keep Windows
out!
Screen('DrawText', win, 'PUSH THE BUTTON WHEN YOU SEE THE BLOB', 350,
383, [1,1,1]);
```

```
Screen ('Flip', win);
WaitSecs (4);
Screen('HideCursorHelper', win);
Screen ('Flip', win); % Flipping removes the text from the screen

% NOW WE CAN IMPLEMENT THE MAIN EXPT LOOP
for k=1:trialsDesired;

    % First pick up the threshold recommened by QUEST
    tTest=QuestQuantile(q); % Recommended by Pelli (1987).

    % Unlog tTest, this controls the luminance of the stimulus
    luminance = 10^tTest;

    % Generate the textures to be displayed during each frame, assume
60Hz so
    % going from 1 to 120 will be a 2s presentation
    for i=1:120;
        %Need to change contrast to a fraction
        Blob = whiteBlob * (luminance) * sind(x);
        gabortex(i)=Screen('MakeTexture', win, Blob, [], [], 2);
        x=x+step;
    end;

    % Wait a random period of time before giving the presentation
    randomdelay = rand*6;
    StartSecs = GetSecs;
    timeNow=0;
    while timeNow <randomdelay
        SecsNow = GetSecs;
        timeNow = (SecsNow - StartSecs);
        [ keyIsDown, timeSecs, keyCode ] = KbCheck; % this command
checks the keyboard for an input
        if keyIsDown % if a key is pushed this is what to do
            falsePositive = falsePositive+1;% counts the incorrect
responses
            Beeper(400)
            while KbCheck; end % this avoids KbCheck reporting multiple
events
        end
```

```
    end



    % Clear the screen and wait a bit
    Screen ('Flip', win);
    %Screen('FrameRect', win, [200,200,200], [540,300,740,500]);

    response = 0; % This flag holds a record of if the stimulus is
seen or not, 0=not seen
    count = 0; % This is needed to count the number of presentations
    vbl = Screen('Flip', win);
    tstart = vbl; % records the time the main presentation loop started
    %lastTime=vbl;
    for i=1:120;
        Screen('DrawText', win, 1,0 ,0, [200,200,0]);
        Screen('DrawTexture', win, gabortex(i),[],[],45);
        % Check the frame presentation time, does it always match the
        % frame referesh rate?
        vbl = Screen('Flip', win, vbl + ifi/2);
        %frametime(i)=vbl-lastTime;% puts frame time (ms) into an
array
        lastTime = vbl;
        count = count+1; %Will count up to 120
        % check for keyboard response during presentation
        [ keyIsDown, timeSecs, keyCode ] = KbCheck; % this command
checks the keyboard for an input
        if keyIsDown % if a key is pushed this is what to do
            response=1;% flags a correct response
            break % breaks out of the presentation loop
        end
    end;

    % Clear the screen of any residual gabor and get time stamp
    tend = Screen ('Flip', win); % records the time the presentation
stopped

    % Check frames per second for this trial, store result in array
avgfps
    avgfps(k) = count / (tend - tstart);
```

```
    % Now get the participants response
    ResponseSecs = GetSecs;% gets the time the stimulus was flipped
out

    % Wait for a response for three seconds, if in the 1st second =
correct
    while 1
        [ keyIsDown, timeSecs, keyCode ] = KbCheck; % this command
checks the keyboard for an input
        if keyIsDown % This bit of code is only executed if a button
is pushed
            %fprintf('"%s"   typed   at   time   %.3f   seconds\n',
KbName(keyCode), timeSecs - ResponseSecs);
            if (timeSecs - ResponseSecs)<1; % checks that response was
within 1s of stimulus offset
                response = 1; %this 'flag' means the response was
correct
                Beeper (1000) % make a 'beep' sound

            else
                response = 0; %this means the response was incorrect
(in this case too slow)
                Beeper (600)
                falsePositive = falsePositive+1;% counts the incorrect
responses
                break
            end

            while KbCheck; end % this avoids KbCheck reporting multiple
events
            break
        end

        % Now, if no button push + long wait, time is up!
        SecsNow = GetSecs;
        timeSincePresentation = (SecsNow - ResponseSecs);
        if timeSincePresentation > 4; % If no response within 1s of
stimulus, its missed, get out of loop
            break
        end % waiting for repsonse or time up
```

```
    end

    % Print the results for this particular trial
    fprintf('Trial          %3d          at          %5.2f          is
%s\n',k,tTest,char(wrongRight(response+1)));
    LuminancePresent(k)=tTest;

    % Now update the QUEST routines with the last threshold value (this
is all
    % in logs) and let it know if the participant responded correctly
(1) or
    % incorrectly (0)
    q=QuestUpdate(q,tTest,response); % Add the new datum (actual test
intensity and observer response) to the database.

    % Close all the windows that were opened for this presentation
    Screen ('Close');

    % Now go back for the next trial
end

% Display cursor again now its all over
Priority(0);% Resest normal priority
Screen('ShowCursorHelper', win);

% Ask Quest for the final estimate of threshold.
t=QuestMean(q);      % Recommended by Pelli (1989) and King-Smith et
al. (1994). Still our favorite.
sd=QuestSd(q);

fprintf('Final threshold estimate (mean±sd) is %.2f ± %.2f\n',t,sd);

% Determine total experimental time and print this out
exptEnd = Screen('Flip', win);
exptTotal = exptEnd - exptStart

% Print out the frame per sec for each trial
%avgfps;
```

```
% Print out the number of false positives
falsePositive

% Close onscreen window, release all ressources:
Screen('CloseAll');

% The presentation rate has been a problem / variable so, these lines
are
% used to plot frame time.
figure(1)
k=1:trialsDesired;
plot (k,avgfps)
xlabel ('Trial')
ylabel ('Frames / sec')

% Plot the stimuli presented
figure(2)
k=1:trialsDesired;
plot (k,LuminancePresent, 'ob')
xlabel ('Trial')
ylabel ('Log luminance')

% Dump all the key data to Excel
LuminancePresent = LuminancePresent(:); % This (:) changes the vector
from a row to a column
trialNumber = k(:);
today = now; % this is a weird number that represents the current date
and time, Excel understands!
name ={participant};
xlswrite('c:\Users\CAD User\Documents\Excel\14Hz Flicker Data.xls',
today,'Sheet1','B3');
xlswrite('c:\Users\CAD User\Documents\Excel\14Hz Flicker Data.xls',
today,'Sheet1','B4');
xlswrite('c:\Users\CAD User\Documents\Excel\14Hz Flicker Data.xls',
name,'Sheet1','B5');
xlswrite('c:\Users\CAD User\Documents\Excel\14Hz Flicker Data.xls',
exptTotal,'Sheet1','E3');
xlswrite('c:\Users\CAD User\Documents\Excel\14Hz Flicker Data.xls',
trialNumber,'Sheet1','A8');
```

```
xlswrite('c:\Users\CAD User\Documents\Excel\14Hz Flicker Data.xls',
LuminancePresent,'Sheet1','B8');
xlswrite('c:\Users\CAD User\Documents\Excel\14Hz Flicker Data.xls',
t,'Sheet1','E4');
xlswrite('c:\Users\CAD User\Documents\Excel\14Hz Flicker Data.xls',
sd,'Sheet1','E5');
xlswrite('c:\Users\CAD User\Documents\Excel\14Hz Flicker Data.xls',
falsePositive,'Sheet1','E6');

% All done, phew!
catch % The following code is run if the experiment crashes
    Screen('CloseAll');
    rethrow(lasterror);
    psychrethrow(psychlasterror);
end
```

Appendix IV. Peer reviewed papers and supporting publications

An Evaluation of Two Candidate Functional Biomarkers for AMD

Miss Claire Mckeague BSc (Hons)[1]
Dr Alison M Binns PhD BSc (Hons)[2]
Dr Tom H Margrain PhD BSc (Hons)[1]

Affiliations:
1 School of Optometry and Vision Sciences, Cardiff University, UK
2 School of Health Sciences, City University London

Correspondence:
Tom H. Margrain
School of Optometry and Vision Sciences
Cardiff University
Maindy Road
Cathays, Cardiff, CF24 4HQ, United Kingdom
E-mail: margrainth@cf.ac.uk
Fax: +44 (0)29 2087 4859

Number of Tables and Figures: 5

Original Submission Date: 12th December 2013

Abstract

PURPOSE

To evaluate the inter-session repeatability of the Colour Assessment and Diagnosis (CAD) test and a novel 14-Hz flicker test in a population of healthy participants in order to provide benchmark data for their use as functional biomarkers for age-related macular degeneration (AMD).

METHODS

Visual function was assessed using both techniques in 30 healthy adults (mean age 36.3 ± 14.1 years) on 2 separate days. Inter-session repeatability of RG and YB CAD thresholds and 14-Hz flicker thresholds was assessed by determining their coefficient of repeatability (CoR).

RESULTS

The CoR was calculated to be 0.39 CAD units (17.0%) for RG thresholds, 0.43 CAD units (31.1%) for YB thresholds and 0.015 (53.4%) for 14-Hz flicker contrast thresholds. On average, thresholds improved by 4.72% (RG), 6.33% (YB) and 13.3% (14-Hz flicker) between visits 1 and 2, suggesting a small but consistent learning effect. The CoR for all parameters was relatively small compared to the mean thresholds obtained (RG: mean 2.27 ± 4.58, CoR 0.39; YB: mean 1.37 ± 0.55, CoR 0.43; 14-Hz flicker: mean 0.028 ± 0.01, CoR 0.015).

CONCLUSIONS

This study has described the repeatability of the CAD and 14-Hz flicker tests. The data can help clinicians decide if the results from repeated measures are of clinical significance. Despite pre-test training, there was some evidence of a learning effect. Therefore, clinical trials using these techniques should ensure training is sufficient to minimize these effects.

KEY WORDS: repeatability, age-related macular degeneration, biomarkers, colour vision, flicker

Age-related macular degeneration (AMD) is a disorder of the central retina that is characterized by progressive dysfunction and death of photoreceptor cells. It is thought

that 7.2 million people in the United States suffer from some form of AMD[1], whilst 56% of registrations as sight impaired in the United Kingdom are attributable to the condition[2], and over 50% of people aged over 65 in Europe are believed to have signs of AMD[3]. On a personal level, the condition is associated with an increased risk of falls, depression, and increased difficulty carrying out daily tasks[4-6]. The economic costs are also substantial, for example, AMD is estimated to cost the US economy $30 billion per annum[7]. Whilst anti vascular endothelial growth factor (anti VEGF) treatment provides a means of treating neovascular AMD (nAMD), it is both expensive and invasive. Giving up smoking, adopting healthy diets and consuming antioxidants can reduce AMD progression, but a treatment for early AMD and geographic atrophy is absent. It is not, therefore, surprising that a substantial research effort is being directed towards the development of new treatments for AMD.

Early AMD develops very slowly over time[8] and, therefore, it is not practicable to use end stage disease as an outcome measure for Phase II trials of new interventions. This necessitates the identification of biomarkers which may be used as surrogate outcome measures in clinical trials. The key requirements of these biomarkers are (i) that they must be sensitive to disease progression, and (ii) they must have a high level of inter-session repeatability. The development of tests sensitive to early AMD, and to disease progression is also a necessity in the early diagnosis and monitoring of patients with AMD in a primary care setting.

The standard psychophysical test of visual function used in clinical trials and in optometric practice is visual acuity. However, the high contrast visual acuity test does not meet either criterion for an optimal biomarker [9,10]. Whilst VA is substantially reduced by advanced AMD, during the earlier stages of the disease process it remains relatively unaffected[9]. This may be partially attributable to the relative sparing of the fovea in early stage disease[11], but is also likely to be due to the inherent variability in the test results (the between session coefficient of repeatability is around 0.15 logMAR / 1.5 lines for a standard logMAR test[10]). Hence, recent cross-sectional studies have evaluated a range of alternative functional biomarkers for AMD[12-16].

Numerous studies have found that temporal sensitivity is adversely affected by AMD[14,15,17-24], to a greater extent than the generalized loss which occurs due to normal

aging[25]. This is thought to be due to the compromised outer retinal oxygen supply in AMD being unable to meet the increased metabolic demand elicited by flickering stimuli[26,27]. Flicker frequencies of above 10Hz have been shown to increase the difference in oxygen tension between retinal arterial and venous blood substantially more than lower frequencies[28]. This indicates that the metabolic activity of the retinal tissue is upregulated in response to this high temporal frequency stimulation. Given the recent evidence to suggest that early functional changes in AMD are initiated by chronic retinal ischemia[29], a functional test which causes a greater demand on the retinal oxygen metabolism is more likely to detect the ischemic deficits in early AMD.
The threshold for flicker detection is a desirable test to use when monitoring functional changes in AMD as it can be performed quickly, is reproducible and diagnostically sensitive[14,22]. For this reason, Dimitrov et al. rated 14-Hz flicker threshold measurement as having the greatest potential clinical value out of a battery of functional tests in the diagnosis and monitoring of AMD[14]. Furthermore, flicker threshold has also been shown to increase gradually with disease progression[15].

An increase in chromatic thresholds, especially in the yellow-blue (YB or tritan) domain, is another functional change which has long been reported to occur in the early stages of AMD[12,30-36]. Tritan colour contrast thresholds are abnormal in patients with AMD and minimal lens opacities[36], and they also change significantly over time in patients with early AMD compared with age-matched controls[35]. However, for chromatic sensitivity to be employed as a functional biomarker of AMD, a means of accurately quantifying chromatic thresholds is required, which falls beyond the remit of standard clinical colour vision tests. A computer-based technology, known as the Colour Assessment and Diagnosis (CAD) test, has been developed which implements dynamic luminance contrast noise, in order to isolate red-green (RG) and YB thresholds[37-39]. This allows a rapid quantification of thresholds along 16 different directions in colour space[40]. Using the CAD test, YB thresholds in patients with AMD have been shown to increase linearly with disease severity[12]. O'Neill-Biba et al. reported evidence of an elevation in threshold, even when the retina appeared normal, in individuals whose fellow eye demonstrated signs of advanced AMD, indicating that impaired colour vision may be an early functional indicator of retinal dysfunction in AMD[12]. Barbur et al. evaluated an approach to maximizing the diagnostic sensitivity of the test through the calculation of an index representing chromatic threshold as a

function of light level in the low photopic, high mesopic range[41]. This resulted in a reduction in the substantial between subject variability in chromatic thresholds conferred by individual differences in factors such as media opacity, pupil diameter and macular pigment optical density, and removed the effect of age on colour vision in healthy individuals. However, to date, no data have been published regarding the between session variability of the CAD test.

It is clear that both the 14-Hz flicker and CAD chromatic sensitivity tests may be useful as functional biomarkers in future clinical trials, fulfilling the first requirement of showing a sensitivity to increased severity of funduscopic changes associated with AMD[12,14,15]. Repeatability data have recently been published for the assessment of cone dark adaptation[42], another potentially important biomarker for early AMD[13-16,33,43-47]. However, there is currently little published data regarding the inter-session repeatability of the flicker and chromatic threshold assessment techniques. This is crucial in determining the minimum change in each parameter which may be considered to be clinically significant – an important issue when powering trials and interpreting outcomes, as well as in the clinical management of patients with early AMD.

The aim of this study was to assess the inter-session repeatability of the colour assessment and diagnosis (CAD) test and the 14-Hz flicker test in a population of healthy participants.

METHODS

Participants

Adults with limited experience in psychophysical experiments were recruited to the study from the staff and students at the School of Optometry and Vision Sciences, Cardiff University. Thirty healthy adults (13 female), aged 22-72 years (mean 36.3 ± 14.1 years) took part in the study. This study was powered to detect within subject standard deviation to within 25% of the true population value[48]. All participants had corrected visual acuity of 20/20 or better (logMAR 0.0) in their test eye, age-normal lens clarity and a normal retinal appearance with no history of any ocular or systemic disease known to affect visual function. All participants had a LOCS score of 0 for all parameters, apart from RE, who had NO2 and NC2 (LOCS III)[49]. As a random sample

of the population was desired, subjects were not excluded on the basis of having a colour vision defect. The School's Research Ethics Committee approved the study and all procedures were carried out in accordance with the tenets of the Declaration of Helsinki. All participants provided written consent to taking part in the study, having received an information sheet prior to their appointment and having had the opportunity to ask any questions.

Experimental procedure

All participants attended the laboratory on two separate days within a period of two weeks. Screening data were obtained at the beginning of the first session to ensure that eligibility criteria were met. This included patient ocular and medical history, logMAR visual acuity (ETDRS chart), and fundus imaging (Optical Coherence Tomography and fundus photography; Topcon 3D OCT 1000). Lens clarity was assessed using a slit lamp biomicroscope, and graded according to the LOCS III system for nuclear opalescence (NO), nuclear colour (NC), cortical opacity (C) and posterior subcapsular opacity (P)[49].

Stimuli for both psychophysical tests were presented on a calibrated, high-resolution 24" widescreen LCD monitor (NEC MultiSync PA241W) with a frame rate of 60Hz, as depicted in Figure 1. The luminance of the monitor was Υ-corrected[50]. In a dimly illuminated room, participants were positioned 1.4 m away from the monitor, and any required refractive correction, appropriate for the viewing distance, was provided. The test eye was the eye with better visual acuity or, in the case of equal acuity, the right eye was selected. The fellow eye was occluded. The test order was randomized between subjects, but kept the same on both visits for each subject.

14-Hz flicker sensitivity

Flicker thresholds were determined using the well-established Bayesian adaptive psychometric method known as QUEST[51,52]. In this method, the strength of each successive stimulus presentation is set to match the current most probable estimate of threshold. In practice, QUEST was implemented in Matlab (The Math Works Inc.) using routines available within Psychophysics Toolbox to drive a yes / no adaptive staircase[53]. The results from a practice run that included 10 trials were used as the

starting point for a final threshold estimate that converged after 40 trials. False positive responses were deemed to be responses that occurred more than 1s after stimulus offset.

Subjects were asked to fixate the center of the screen where the test stimulus, a 4^{o} foveated Gaussian blob at a temporal frequency of 14Hz, was presented to the fovea for a duration of 2 seconds. The flickering stimulus was generated by modulating a luminance increment following a sinusoidal temporal profile. The mean luminance of the monitor was 51 cd/m^2 and the chromaticity co-ordinates were 0.305, 0.323. To ensure that participants could not anticipate the next presentation, the inter stimulus interval was varied randomly between 4 and 10 seconds. The participants received verbal instructions on how to perform the test before undertaking the familiarization trial. Their task was to press a button on a keypad as soon as they perceived a flickering stimulus in the center of the monitor. If more than one false positive response was made, the practice trial was repeated until they were able to complete the familiarization trial with a maximum of 1 false positive response.

Colour Contrast Sensitivity

Colour contrast sensitivity was assessed using the CAD test (v2.2.4, City Occupational Ltd). RG and YB colour detection thresholds were measured by employing coloured stimuli moving against an achromatic background. The background (chromaticity co-ordinates 0.305, 0.323; mean luminance 26 cd/m^2) comprised a checkerboard of 15x15 squares (total 3.3 degrees diameter), which fluctuated randomly in luminance above and below the average background level in order to generate dynamic luminance contrast noise. The check luminance was distributed with equal probability within +/- 55% of background luminance. This noise masked the detection of residual luminance contrast cues in the isoluminant coloured stimulus. The colour-defined stimulus comprised a checkerboard of 5 × 5 squares (total 1.1° diameter) moving diagonally across the checkerboard, in one of four directions. The stimulus duration was 600ms. A four-alternative forced choice procedure was used, whereby the participant was required to press a button indicating the direction of movement. Displacement thresholds were measured in 16 directions in colour space (6 red, 6 green, 2 blue, 2 yellow), with colour directions selected to correspond to the red / green colour confusion lines (140 to 175 degrees) and the S-cone isolating axes (58 to 68 degrees). Threshold was determined using a two-down, one-up staircase in which colour intensity

was reduced by an initial step size of 0.006 CD units until the coloured stimulus could not be distinguished from the background by the observer. This staircase procedure was repeated for nine reversals, at each of which the step size was reduced by 0.001 CD units until a final step size of 0.002 CD units was attained. Thresholds were obtained by averaging the chromatic distance in the CIE colour space during the last four staircase reversals.

The participant's task was to press one of four buttons on a keypad to indicate the perceived direction of motion of the coloured stimulus. Each stimulus presentation was followed by an audible 'bleep' to indicate when to respond. A response was required, even if the participant was uncertain of the direction of movement. Any trial could be presented for a second time at the participant's request. A familiarization trial lasting approximately 1 minute was performed prior to commencing the main trial. 100% correct response was required in the learning test to ensure that the subject understood the requirements of the test. The 'definitive' CAD program was then implemented and RG and YB thresholds were measured over a of 12 to 15 minute period.

Statistical Analysis

Flicker thresholds were transformed into Weber contrast values by dividing pedestal luminance ($I - I_b$) by the average luminance (I_b). The repeatability of the colour and flicker thresholds was assessed using established statistical techniques[55]. The coefficient of repeatability (CoR) was calculated by multiplying the standard deviation of the differences between the two visits by 1.96. Confidence intervals for the CoR were calculated according to the method described by Bland and Altman[55].

RESULTS

Chromatic sensitivity and flicker thresholds were successfully obtained from all 30 participants on two separate days. Data from the 2 visits were generally collected on successive days but always within two weeks. None of the participants required additional practice sessions for either test, which minimized potential inter-individual differences in any learning effect. An example of the flicker data obtained on both visits from a typical participant (AB) is shown in Figure 2. In each plot, the solid horizontal line represents the final threshold and the dashed horizontal lines denote the 95%

confidence intervals. Sample CAD results from the same observer are shown in Figure 3.

Only 1 subject (TM) with a congenital protanopic deficiency had a RG CAD threshold outside of the age-corrected statistically determined normal limits[56]. Similarly, only 1 subject (RE) had YB thresholds outside of the normal range. The lens opacities of this 72-year old participant had been graded as NO2 and NC2, so this YB defect is most likely due to the early stages of nuclear cataract. Both of these participants, whilst falling outside of the published limits of normality[56], showed repeatable results.

The difference in RG thresholds recorded at the first and second visits is plotted as a function of the mean RG threshold for all 30 participants in the Bland and Altman plots shown in Figure 4a, whereas Figure 4b shows the Bland Altman plot for RG thresholds with the protanopic individual's data point removed to aid visualization of the spread of the other data. Similar plots for all 30 individuals are shown for YB and 14-Hz flicker thresholds in Figure 4 c and d.

In each graph, the solid horizontal line depicts the bias, i.e. the mean difference between the two visits, and the dashed horizontal lines represent the 95% limits of agreement, i.e. the mean difference ± the coefficient of repeatability (CoR). These plots describe the between session repeatability for all 3 measures. There was no evidence of a systematic change in repeatability with increasing thresholds (i.e. no heteroscadicity). The bias line crosses the y-axis slightly above 0 in all cases. Relative to visit 1, thresholds improved by 4.72%, 6.33% and 13.3% for RG, YB and 14-Hz Flicker respectively, indicating the presence of a possible small learning effect.

The mean RG, YB chromatic thresholds and 14-Hz flicker thresholds for visits one and two are shown in Table 1, along with the CoR for each test. The expression of the CoR as a percentage of the group averaged test result (at visits 1 and 2) allows a direct comparison of the repeatability of parameters with different units. Although the RG thresholds were more repeatable than the YB thresholds, the difference in the CoR was not significant (95% confidence intervals did not overlap). There was also no significant difference in repeatability between the YB CAD thresholds and 14-Hz flicker. However, the CoR for the RG CAD thresholds was significantly better than that

of the 14-Hz flicker (see Table 1). Scatter plots showing the effect of age on the between visit variability are shown in Figure 5. There was no evidence of any systematic effect of age on variability for any parameter.

DISCUSSION

In order to monitor the progression of AMD and determine the efficacy of novel therapies, functional biomarkers must be identified that are reliable, repeatable and clinically applicable. This will allow candidate treatments to be assessed with maximum efficiency by minimizing the sample size and follow-up duration required to achieve a useful end point. The development of functional tests sensitive to subtle changes in AMD status is also important in the clinical diagnosis and management of the condition in clinical settings. Visual acuity, despite the common acknowledgement that it is a poor assay of early AMD, is still the standard functional vision test amongst both clinicians and researchers. It is therefore necessary that new functional tests are developed that are as quick to perform and have the same ease of use as VA, but with improved sensitivity to disease progression and better inter-session repeatability. Two such tests that have been shown to be sensitive to disease severity in AMD are the 14-Hz flicker and CAD chromatic sensitivity test[14,15]. The flicker test employs a stimulus which is bigger (4 degrees diameter) than the stimulus presented in the CAD test (1.1 degree diameter). However, the CAD stimulus moves out from a central fixation position to a location extending to 2.3 degrees into the parafovea. Hence both stimuli are assessing a region of the macula extending to around 2 degrees from fixation. This targets the parafoveal region in which functional deficits have been identified early in the AMD disease process[43].

The coefficient of repeatability (CoR) is an important statistical technique due to its potential to describe the smallest change that can be deemed clinically significant [55]. This is helpful in identifying those individuals who have shown a “clinically significant decline” in performance, and can therefore be used to determine the optimal sample size for a trial, i.e. it can be powered to detect a certain percentage who show this level of functional decline. The most repeatable test was found to be the RG CAD threshold test. This performed significantly better than the 14-Hz flicker test which produced the least repeatable results.

The Bland Altman plots all showed a mean difference between visits that was slightly above zero, suggesting a small learning effect for both the 14-Hz flicker test and the CAD parameters. This was confirmed by a post hoc paired samples *t*-test ($p < 0.05$) for all tests. This learning effect may have been limited by the familiarization trials which were carried out for the two techniques before both visits. If more than 1 false positive occurred on the 14-Hz flicker practice trial lasting 1 minute or if the subject did not score 100% in the CAD practice trial which also took 1 minute to complete, they were made to repeat it until they achieved the required standard and were deemed competent in task performance. However, the familiarization trials were clearly not sufficient to saturate learning.

A limitation of the study is that different repeatability values will need to be established if the tests are applied under different experimental conditions. A change in stimulus size, eccentricity, temporal frequency, retinal illuminance, or a change in the psychophysical procedure used, are all likely to affect the measured variability of the techniques. For example, in their recent evaluation of the effect of retinal illuminance on chromatic thresholds, Barbur et al. hypothesized that the assessment of colour vision at mesopic levels may increase the diagnostic sensitivity of the test, through the exacerbation of the effect of disease-related hypoxia [41]. Their 'healthy retina index' (HR_{index}) is a measure of the effect of retinal illuminance on chromatic thresholds. Additional repeatability data will be required to evaluate the clinical interpretation of mesopic chromatic thresholds and the HR_{index}. Inter-session repeatability is also likely to be influenced by the characteristics of the patient population. Hence, a further potential limitation of the repeatability data reported in this study is that the participant cohort was recruited from a University environment, and may not be generalizable to the population of patients with age-related macular degeneration. However, the age-range of participants extended to 72 years, and only 3 of the participants had previously taken part in psychophysical experiments hence, the group may be considered to be broadly representative of naïve participants in a clinical environment. Furthermore, we found no evidence of an effect of age on the between session variability, suggesting that the findings of this study will be broadly applicable across age groups.

One limitation of the yes / no adaptive staircase procedure used in the flicker sensitivity test is that results are dependent on stimulus strength and an individual's response

criterion i.e. their willingness to guess. Response criterion can vary between and within individuals. We attempted to minimize within subject changes in response criteria by providing identical instructions at each visit. However, we cannot rule out the possibility that the systematic difference between visits (i.e. the bias) was due to a change in response criterion. Many things, including instructions, can induce the observer to raise or lower his or her criterion, causing threshold to shift up or down. This unknown internal criterion of the observer typically differs among observers and may vary across populations and over time. The four alternative forced choice paradigm employed by the CAD test negates the effect of inter-individual differences in the response criterion.

The published limits of normality for the CAD test are based on data collected from 250 colour normal participants[56]. The majority of participants in this study produced thresholds which fell within these limits, apart from one protanope (TM), and one older participant with significant nuclear lens opacities (RE). Excluding these 2 participants, the mean (SD) RG thresholds for visit 1 were 1.45 (0.29) and for YB 1.34 (0.37). The RG threshold is very similar to that reported by O'Neill-Biba et al[12] but the YB value is somewhat lower than that reported previously 1.6 (0.15). Control participants in the O'Neill-Biba study were on average 20 years older than those studied here and increasing lens opacification may therefore, explain the difference. Barbur et al reported that chromatic thresholds, uncorrected for differences in media absorption and pupil diameter, increase significantly with increasing age in the healthy population[41].

In summary, this study has described the inter session repeatability of two tests that may be used in the diagnosis and monitoring of AMD. Both colour vision and flicker sensitivity tests have been shown to have excellent diagnostic capacity[12,14,15,17-24,30-36]. The results of this study will help clinicians to determine if changes observed over time are due to measurement imprecision or disease progression, provided that the experimental conditions and psychophysical procedures are kept constant. The observation that a small but significant learning effect exists highlights the need for control groups in clinical trials of new AMD therapies. These and other candidate biomarkers must now be validated in longitudinal studies to confirm their prognostic and predictive capabilities.

ACKNOWLEDGMENTS

This study was funded by a research grant from the College of Optometrists, United Kingdom.

REFERENCES

1. Klein R, Chou C-F, Klein BEK, Zhang X, Meuer SM, Saaddine JB. Prevalence of age-related macular degeneration in the US population. Arch Ophthalmol 2011;129:75–80.

2. Bunce C, Xing W, Wormald R. Causes of blind and partial sight certifications in England and Wales: April 2007-March 2008. Eye 2010;24:1692–1699.

3. Augood CA, Vingerling JR, de Jong PTVM, et al. Prevalence of age-related maculopathy in older Europeans: the European Eye Study (EUREYE). Arch Ophthalmol 2006;124:529–535.

4. Brody BL, Gamst AC, Williams RA, et al. Depression, visual acuity, comorbidity, and disability associated with age-related macular degeneration. Ophthalmology 2001;108:1893–9001.

5. Ivers RQ, Cumming RG, Mitchell P, Simpson JM, Peduto AJ. Visual risk factors for hip fracture in older people. J Am Geriatr Soc 2003;51:356–363.

6. Lamoureux EL, Hassell JB, Keeffe JE. The determinants of participation in activities of daily living in people with impaired vision. Am J Ophthalmol 2004;137:265–270.

7. Brown GC, Brown MM, Sharma S, et al. The burden of age-related macular degeneration: a value-based medicine analysis. Trans Am Ophthalmol Soc 2005;103:173–86

8. Davis MD, Gangnon RE, Lee L-Y, et al. The Age-Related Eye Disease Study severity scale for age-related macular degeneration: AREDS Report No. 17. Arch Ophthalmol 2005;123:1484–1498.

9. Klein R, Wang Q, Klein BE, Moss SE, Meuer SM. The relationship of age-related

maculopathy, cataract, and glaucoma to visual acuity. Invest Ophthalmol Vis Sci 1995;36:182–191.

10. Siderov J, Tiu AL. Variability of measurements of visual acuity in a large eye clinic. Acta Ophthalmol Scand 1999;77:673–676.

11. Sunness JS, Rubin GS, Zuckerbrod A, Applegate CA. Foveal-Sparing Scotomas in Advanced Dry Age-Related Macular Degeneration. J Vis Impair Blind 2008;102:600–610.

12. O'Neill-Biba M, Sivaprasad S, Rodriguez-Carmona M, Wolf JE, Barbur JL. Loss of chromatic sensitivity in AMD and diabetes: a comparative study. Ophthalmic Physiol Optic 2010;30:705–716.

13. Gaffney AJ, Binns AM, Margrain TH. The topography of cone mediated dark adaptation in age-related maculopathy. Optom Vis Sci 2011;88:1080–1087.

14. Dimitrov PN, Robman LD, Varsamidis M, et al. Visual function tests as potential biomarkers in age-related macular degeneration. Invest Ophthalmol Vis Sci 2011;52:9457–9469.

15. Dimitrov PN, Robman LD, Varsamidis M, et al. Relationship between clinical macular changes and retinal function in age-related macular degeneration Invest Ophthalmol Vis Sci 2012;53:5213–5220.

16. Gaffney AJ, Binns AM, Margrain TH. The effect of pre-adapting light intensity on dark adaptation in early age-related macular degeneration. Doc Ophthalmol 2013;127:191-199

17. Brown B, Lovie-Kitchin J.E. Temporal function in age-related maculopathy. Clinical and Experimental Optometry 1987;70:112-116.

18. Eisner A, Klein ML, Zilis JD, Watkins MD. Visual function and the subsequent development of exudative age-related macular degeneration. Invest Ophthalmol Vis Sci 1992;33:3091-3102.

19. Mayer MJ, Spiegler SJ, Ward B, Glucs A, Kim CB. Foveal flicker sensitivity discriminates ARM-risk from healthy eyes. Invest Ophthalmol Vis Sci 1992;33:3143–

3149.

20. Mayer MJ, Spiegler SJ, Ward B, Glucs A, Kim CB. Mid-frequency loss of foveal flicker sensitivity in early stages of age-related maculopathy. Invest Ophthalmol Vis Sci 1992;33:3136–3142.

21. Phipps JA, Guymer RH, Vingrys AJ. Loss of Cone Function in Age-Related Maculopathy. Invest Ophthalmol Vis Sci 2003;44:2277–2283.

22. Phipps JA, Dang TM, Vingrys AJ, Guymer RH. Flicker perimetry losses in age-related macular degeneration. Invest Ophthalmol Vis Sci 2004;45:3355–3360.

23. Luu CD, Dimitrov PN, Robman L, et al. Relationship between Clinical Macular Changes and Retinal Function in Age-Related Macular Degeneration. Invest Ophthalmol Vis Sci 2012;53:5213-5220

24. Luu CD, Dimitrov PN, Wu ZC, et al. Static and Flicker Perimetry in Age-Related Macular Degeneration. Invest Ophthalmol Vis Sci 2013;54:3560-3568

25. Kim CB, Mayer MJ. Foveal flicker sensitivity in healthy aging eyes. II. Cross-sectional aging trends from 18 through 77 years of age. J Opt Soc Am A Opt Image Sci Vis 1994;11:1958–1969.

26. Kiryu J, Asrani S, Shahidi M, Mori M, Zeimer R. Local response of the primate retinal microcirculation to increased metabolic demand induced by flicker. Invest Ophthalmol Vis Sci 1995;36:1240–1246.

27. Riva CE, Falsini B, Logean E. Flicker-evoked responses of human optic nerve head blood flow: luminance versus chromatic modulation. Invest Ophthalmol Vis Sci 2001;42:756–762.

28. Shakoor A, Blair NP, Mori M, Shahidi M. Chorioretinal vascular oxygen tension changes in response to light flicker. Invest Ophthalmol Vis Sci 2006;47:4962-4965

29. Feigl B, Brown B, Lovie-Kitchin J, Swann P. Functional loss in early age-related maculopathy: the ischaemia postreceptoral hypothesis. Eye 2007;21:689-696

30. Bowman KJ. The effect of illuminance on colour discrimination in senile macular

degeneration. Mod Probl Ophthalmol 1978;19:71–76.

31. Collins MJ. Pre-age related maculopathy and the desaturated D-15 colour vision test. Clin Exp Optom 1986;69:223–227.

32. Applegate RA, Adams AJ, Cavender JC, Zisman F. Early colour vision changes in age-related maculopathy. Appl Opt 1987;26:1458.

33. Eisner A, Stoumbos VD, Klein ML, Fleming S. Relations Between Fundus Appearance and Function. Invest Ophthalmol Vis Sci 1991;32:8–20.

34. Frennesson C, Nilsson UL, Nilsson S. Colour contrast sensitivity in patients with soft drusen, an early stage of ARM. Doc Ophthalmol 1995;90:377-386

35. Holz FG, Gross-Jendroska M, Eckstein A, Hogg CR, Arden GB, Bird AC. Colour contrast sensitivity in patients with age-related Bruch's membrane changes. Ger J Ophthalmol 1995;4:336–341.

36. Arden GB, Wolf JE. Colour vision testing as an aid to diagnosis and management of age related maculopathy. Br J Ophthalmol 2004;88:1180–1185.

37. Birch J, Barbur JL, Harlow AJ. New method based on random luminance masking for measuring isochromatic zones using high resolution colour displays. Ophthalmic Physiol Opt 1992;12:133–136.

38. Barbur JL, Harlow AJ, Plant GT. Insights into the different exploits of colour in the visual cortex. Proc R Soc Lond 1994;258:327–334.

39. Barbur JL. "Double-blindsight" revealed through the processing of colour and luminance contrast defined motion signals. Prog Brain Res 2004;144:243–259.

40. Barbur J, Rodriguez-Carmona M, Evans S, Milburn NJ. Minimum colour vision requirements for professional flight crew, part III: recommendations for new colour vision standards. FAA, 2009. Available at: http://www.caa.co.uk/docs/33/200904.pdf. Accessed November 6, 2013.

41. Barbur, JL, Konstantakopoulou E. Changes in colour vision with decreasing light level: separating the effects of normal aging from disease. J Opt Soc Am A Opt Image

Sci Vis 2012 29 (2):27-35.

42. Gaffney AJ, Binns AM, Margrain TH. Measurement of cone dark adaptation: a comparison of four psychophysical methods. Doc Ophthalmol 2014;128:33–41

43. Owsley C, Jackson GR, White M, Feist R, Edwards D. Delays in rod-mediated dark adaptation in early age- related maculopathy. Ophthalmology 2001;108:1196–1202

44. Binns AM, Margrain TH (2007) Evaluating retinal function in age-related maculopathy with the ERG photostress test. Invest Ophthalmol Vis Sci 2007;48:2806–2813

45. Owsley C, McGwin G Jr, Jackson GR, Kallies K, Clark M. Cone- and rod-mediated dark adaptation impairment in age-related maculopathy. Ophthalmology 2007;114:1728–1735

46. Brown B, Kitchin JL. Dark adaptation and the acuity/luminance response in senile macular degeneration (SMD). Am J Opt Physiol Opt 1983. 60:645–650

47. Eisner A, Fleming SA, Klein ML. Mauldin WM. Sensitivities in older eyes with good acuity: eyes whose fellow eye has exudative AMD.Invest Ophthalmol Vis Sci 1987;28:1832–1837

48. Bland M. How can I decide the sample size for a repeatability study? University of York, 2010. Available at: http://www-users.york.ac.uk/~mb55/meas/sizerep.htm. Accessed November 6, 2013.

49. Chylack LJ, Wolfe JK, Friend J, et al. Quantitating cataract and nuclear brunescence, the Harvard and LOCS systems. Optom Vis Sci 1993;70:886–895.

50. Metha AB, Vingrys AJ, Badcock DR. Calibration of a colour monitor for visual psychophysics. Behav Res Meth Instrum Comput 1993;25:371–383.

51. Watson AB, Pelli DG. Quest: A Bayesian adaptive psychometric method. Percept Psychophys 1983;33:113–120.

52. Pelli DG. The VideoToolbox software for visual psychophysics: transforming numbers into movies. Spat Vis 1997;10:437–442.

53. Brainard DH. The psychophysics toolbox. Spat Vis 1997;10:433–436.

54. King-Smith PE, Grigsby SS, Vingrys AJ, Benes SC, Supowit A. Efficient and unbiased modifications of the QUEST threshold method: theory, simulations, experimental evaluation and practical implementation. Vision Res 1994;34:885–912.

55. Bland JM, Altman DG. Statistical methods for assessing agreement between two methods of clinical measurement. Lancet 1986;1:307–310.

56. Barbur JL, Rodriguez-Carmona M. Establishing the statistical limits of “normal” chromatic sensitivity. CIE Proceedings Expert Symposium "75 Years of the CIE Standard Colourimetric Observer" (CIE x030) 2006.

FIGURES

Figure 1. Images showing the appearance of the moving coloured stimulus used in the CAD test [1] (left panel) and the flickering stimulus (right panel) used to determine flicker thresholds.

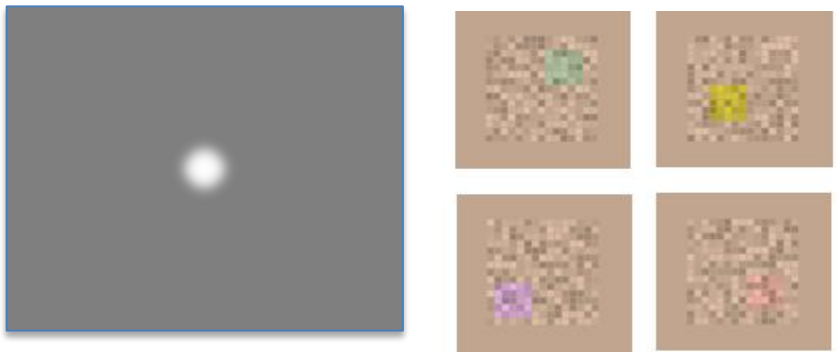

Figure 2. 14-Hz Flicker data for participant AB at visit 1 (left panel) and visit 2 (right panel), shown with the threshold in decibels. The dashed lines represent the 95% confidence intervals, with the solid line depicting the final threshold.

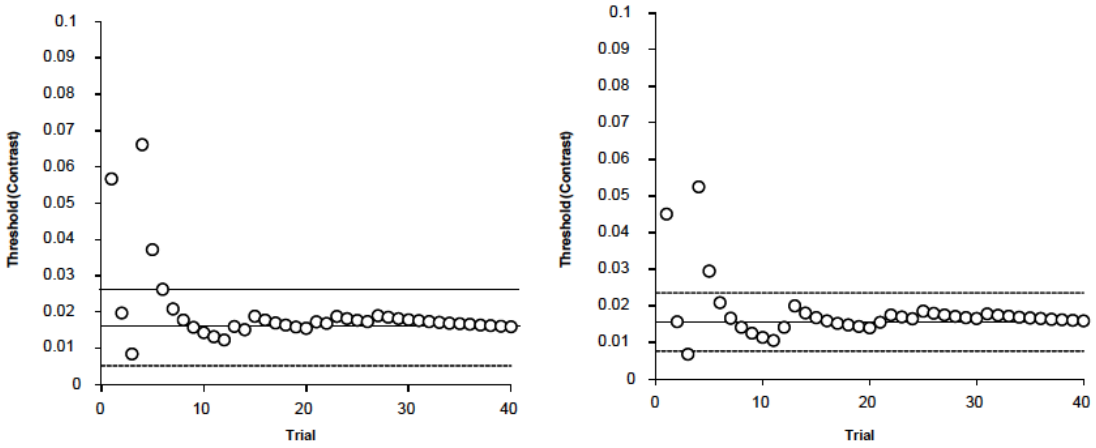

Figure 3. CAD data for participant AB at visit 1 (left panel) and visit 2 (right panel). The dotted black ellipse is based on the median RG and YB thresholds from 250 observers, with the grey shaded area representing the 95% limits of variability of these observers. The green, red and blue bands display the deuteranopic, protanopic and tritanopic confusion lines, respectively. The coloured symbols show the data measured for participant AB.

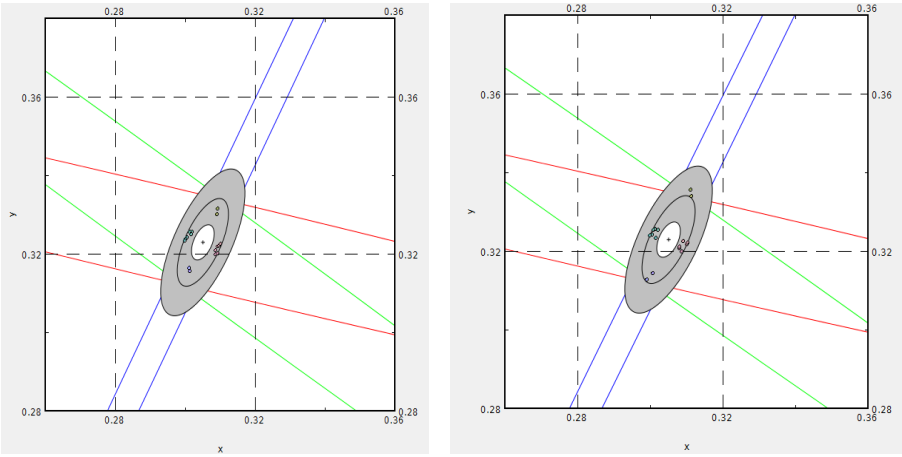

Figure 4. Bland Altman plots for RG chromatic thresholds (A), RG chromatic thresholds excluding participant TM (B), YB chromatic thresholds (C) and 14-Hz flicker thresholds (D). The difference between the measurements from visit 1 to visit 2 is plotted as a function of the mean value for all 30 participants, and is shown with the bias (solid line) and 95% limits of agreement (dashed lines).

a.

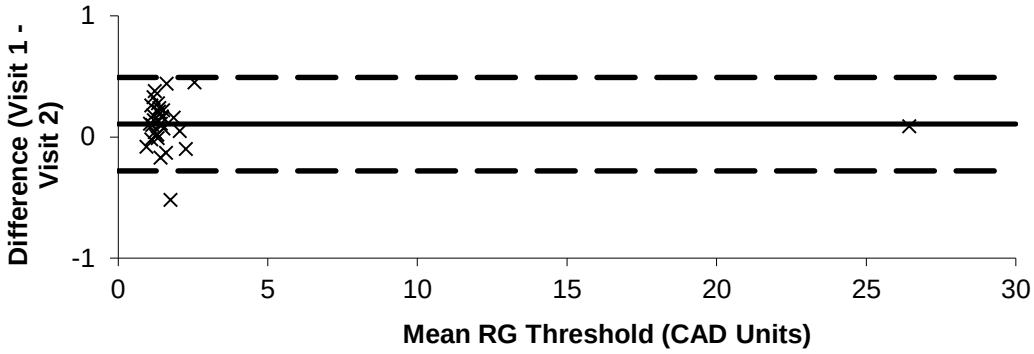
Difference (Visit 1 - Visit 2)
1
0
-1
0
5
10
15
20
25
30
Mean RG Threshold (CAD Units)

b.

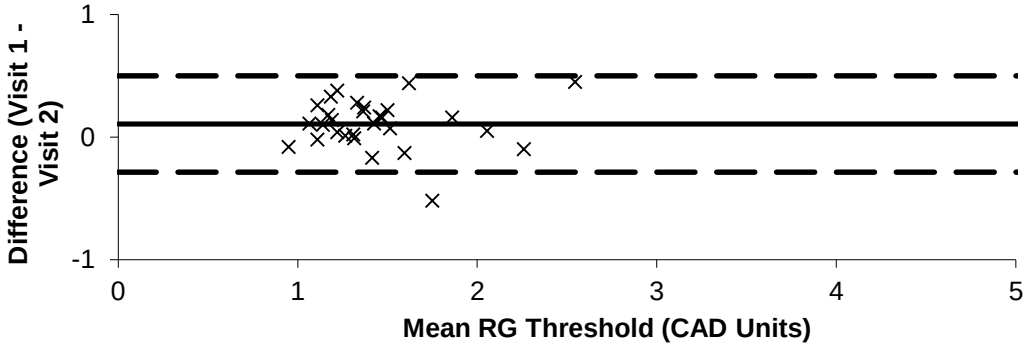
Difference (Visit 1 - Visit 2)
1
0
-1
0
1
2
3
4
5
Mean RG Threshold (CAD Units)

c.

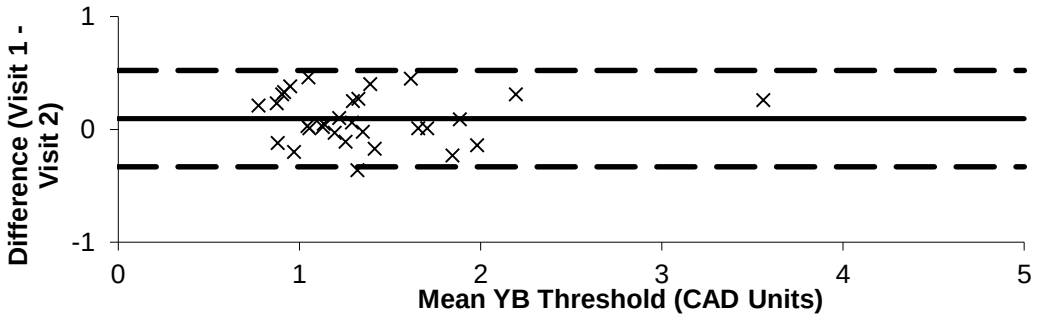
Difference (Visit 1 - Visit 2)
1
0
-1
0
1
2
3
4
5
Mean YB Threshold (CAD Units)

d.

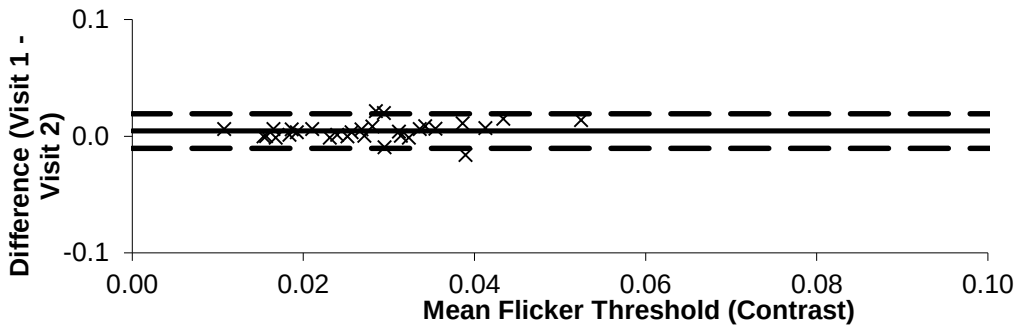
Difference (Visit 1 - Visit 2)
0.1
0.0
-0.1
0.00
0.02
0.04
0.06
0.08
0.10
Mean Flicker Threshold (Contrast)

Figure 5. Scatter plots demonstrating the relationship between age and between visit threshold variation for RG chromatic thresholds (A), YB chromatic thresholds (B) and 14-Hz flicker thresholds (C). Note the lack of a systematic relationship with age for any parameter.

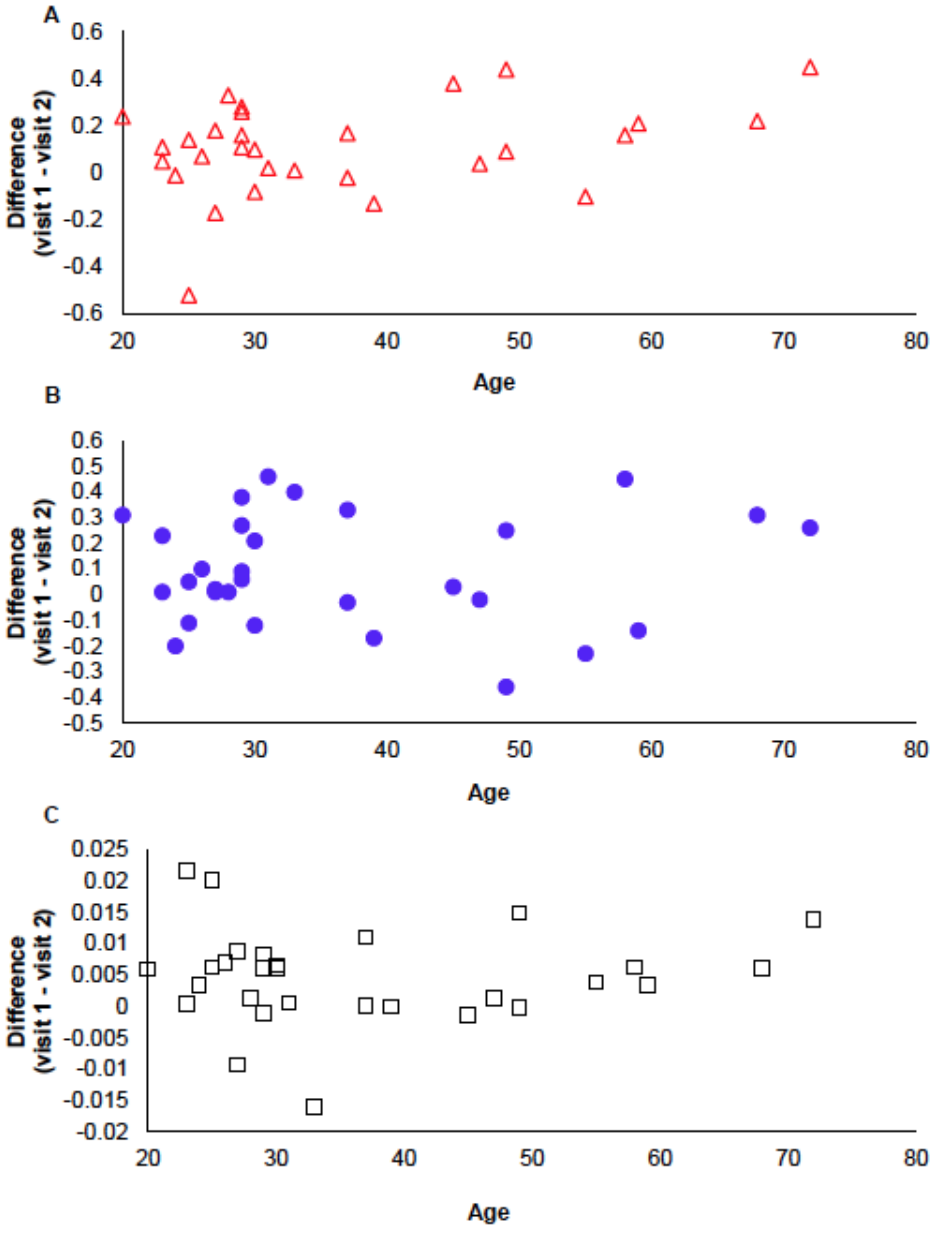

Table 1. Mean (± standard deviation) and coefficient of repeatability of all three parameters assessed at visit one and visit two.

	Mean (± standard deviation)		**CoR (95% CI)**	**CoR as % of mean threshold (95% CI)**
	Visit 1	**Visit 2**		
RG Threshold	2.33 (± 4.58)	2.22 (± 4.58)	0.39 (± 0.13)	17.1 (± 5.6%)
YB Threshold	1.42 (± 0.56)	1.33 (± 0.56)	0.43 (± 0.14)	31.1 (± 10.2%)
14-Hz Flicker Threshold	0.030 (± 0.01)	0.026 (± 0.009)	0.015 (± 0.005)	53.4 (± 17.6%)

Low-level night-time light therapy for Age-Related Macular Degeneration (ALight): study protocol for a randomised controlled trial

Claire McKeague[1], Tom H Margrain[1], Clare Bailey[3] and Alison M Binns[1,2*]

[1] School of Optometry and Vision Sciences, Cardiff University, Cardiff, CF24 4LU, UK

[2] Division of Optometry and Visual Science, City University, London, EC1V OHB, UK

[3] Bristol Eye Hospital, Lower Maudlin Street, Bristol, BS1 2LX, UK

[*] Corresponding author

Claire McKeague: mckeague@cf.ac.uk

Alison M Binns: alison.binns.1@city.ac.uk

Tom H Margrain: MargrainTH@cf.ac.uk

Claire Bailey: clare.bailey@bristol.ac.uk

Trial Sponsor: Cardiff University

Abstract

Background

Age-related macular degeneration (AMD) is the leading cause of blindness among older adults in the developed world. The only treatments currently available, such as Ranibizumab injections, are for neovascular AMD, which accounts for only 10-15% of people with the condition. Hypoxia has been implicated as one of the primary causes of AMD, and is most acute at night when the retina is most metabolically active. By increasing light levels at night, the metabolic requirements of the retina and hence the hypoxia will be considerably reduced. This trial seeks to determine if wearing a light mask that emits a dim, green light during the night can prevent the progression of early AMD.

Methods/Design

ALight is a phase I/IIa, multicentre, randomised controlled trial. Sixty participants (55-88 years) with early AMD in one eye and neovascular AMD (nAMD) in the fellow eye will be recruited from nAMD clinics. They will be randomised (in the ratio 1:1), to either receive the intervention or to be in the untreated, control group, stratified according to risk of disease progression. An additional 40 participants with healthy retinal appearance, or early AMD only will be recruited for a baseline cross-sectional analysis. The intervention is an eye mask which emits a dim green light which illuminates the retina through closed eyelids at night. This is designed to reduce the metabolic activity of the retina, thereby reducing the potential risk of hypoxia. Participants will wear the mask every night for 12 months. Ophthalmologists carrying

out monthly assessments will be masked to the treatment group, but participants will not be masked. The primary outcome measure is the proportion of people who show disease progression during the trial period in the eye with early AMD. A co-primary outcome measure is the rate of retinal adaptation. As this is a trial of a CE marked device for an off-label indication, a further main aim of this trial is to assess safety of the mask in the cohort of participants with AMD.

Trial Status

The present protocol aims to establish the therapeutic benefit of low-level light therapy on disease progression in AMD. Recruitment will begin in April 2014 and continue until February 2015. Data collection will take place from June 2014 to April 2016.

Trial Registration: Current Controlled Trials: ISRCTN82148651

Protocol : Version 14; 11th September 2013

Sponsor Contact Details:

Dr K Pittard Davies

Cardiff University Research, Innovation and Enterprise Services

Cardiff University

7th Floor, 30-36 Newport Rd

Cardiff CF24 0DE

Keywords

Age-related macular degeneration, randomised controlled trial, Light Mask, Hypoxia, Biomarker

Background

Age-related macular degeneration (AMD) is the leading cause of blindness in the developed world [1] and is responsible for 50% of visual impairment registrations in the UK [2]. For the majority of people with AMD, there is no treatment. The remaining 10-15% of people with the advanced, neovascular form of the disease (nAMD) are mainly treated with intra-ocular injections of Ranibizumab, an anti-vascular endothelial growth factor (VEGF) agent [3]. Follow up for these patients is long term and places a significant burden on the NHS. Indeed, advanced AMD currently costs the British economy £1.2B to £3.7B p.a [2, 4, 5]. Furthermore, the disease is associated with depression, falls and social isolation [6, 7]. Given this significant socioeconomic problem, there is a great need to evaluate potential therapeutic interventions which attempt to treat the disease at an early stage, to prevent vision loss from occurring.

Age-Related Macular Degeneration is characterised by the dysfunction and death of photoreceptors in the central retina. There is an increasing amount of evidence to suggest that hypoxia plays a major role in its pathogenesis [8, 9]. This has been attributed to factors including a disruption of choroidal circulation [10-13], and thickening and deposition of drusen at Bruch's membrane [9, 14]. The latter increases the distance over which oxygen must travel to reach the retinal pigment epithelium (RPE) from the choroidal circulation. Disease-related changes to Bruch's membrane also impair the diffusion of nutrients, which consequently exacerbates choroidal perfusion abnormalities, promoting further hypoxia [8, 15].

Even in the healthy retina, intra retinal oxygen profiles obtained from animals show that the oxygen tension at the proximal side of the photoreceptor inner segments is close

to zero in darkness [16, 17]. This is attributable to the metabolic demand of the 'dark current' in the approximately 120 million rods [18]. When this limited supply of oxygen to the outer retina is further compromised by the changes to the choroidal circulation and Bruch's membrane, which occur in AMD, hypoxia may result. This hypoxia could be the precursor for increased VEGF production and apoptosis [19, 20].

The fragile balance between metabolic demand and oxygenation is exemplified functionally by the adverse effects of hypoxia on colour vision [21-23], dark adaptation [21, 23-25], mesopic sensitivity [26] and the electroretinogram [12, 27-29]. To date, there is no direct evidence of the effect of hypoxia on visual function in AMD. However, there is evidence that scotopic threshold elevation and prolonged ERG implicit times are associated with areas of reduced choroidal blood flow in AMD [30, 31] and pilot data from our lab show a transient reduction in scotopic thresholds in an individual with early AMD whilst inhaling oxygen.

Environmental manipulation of light levels can substantially reduce the metabolic demands of the outer retina thereby reducing the need for oxygen, and potentially providing an intervention which would delay the progression of conditions with a hypoxic aetiology [32]. A pilot study by Arden et al. (2010) found no adverse effects from the provision of low-level night lighting over the course of 12 months in individuals with diabetic retinopathy [33]. Furthermore, a recent clinical trial in patients with diabetic macular oedema who wore a low-level light mask during the night for 6 months reported a reduction in oedema and an improvement in functional measures, which was attributed to the obviation of night time hypoxia [34]. In this trial, we will be using the same intervention (low level light therapy) to determine its ability to prevent the development of AMD.

Methods/Design

Trial objectives

The primary aim of this study is to collect preliminary Phase I/IIa proof of concept trial data from people with early Age-Related Macular Degeneration (AMD) in one eye and advanced neovascular AMD (nAMD) in the fellow eye, recruited from a hospital nAMD clinic, in order to assess the impact of low-level night-time light therapy, compared with no intervention, on disease progression in the eye with early AMD. A further main aim of this trial is to assess safety of the mask in the cohort of participants with AMD.

The secondary aims of the study are to:

1) Establish the effect of low-level night-time light therapy, compared with no treatment control, on secondary outcome measures, including: change in drusen volume from baseline in the eye with early AMD; Ranibizumab retreatment rates in the fellow eye with nAMD; progression of early AMD on the basis of change in functional outcome measures; change in health related QoL (assessed using the EuroQol EQ-5D instrument); change in self reported visual function assessed using the 48-item Veterans Affairs Low Vision Visual Functioning Questionnaire (VA LV VFQ-48).

2) Establish the acceptability of low-level night-time light therapy in people with AMD by monthly qualitative interviews.

3) Determine the effect of low-level night-time light therapy on sleep patterns by conducting the Pittsburgh Sleep Quality Index (PSQI) questionnaire every month with both intervention arms by interview with the study investigator.

4) Establish the relationship between baseline functional biomarker outcomes and the severity of AMD (assessed using simplified AREDS grading scale and initial drusen volume).

5) Evaluate the ability of all clinical tests to act as prognostic biomarkers for AMD progression.

6) Evaluate the ability of all clinical tests to act as predictive biomarkers for low-level night-time light therapy in people with AMD.

7) Compare the sensitivity of all clinical tests to disease progression over 12 months.

Study Design and Setting

ALight is a Phase I/IIa prospective proof of concept randomised controlled trial, consisting of two parallel groups. Trial recruitment and data collection will take place at the Medical Retina Clinic, Bristol Eye Hospital. Additional cross-sectional data will be collected from people with healthy eyes, or only early signs of AMD at Cardiff University School of Optometry and Vision Sciences.

Eligibility criteria

Inclusion criteria

- Between the ages of 55-88 years
- ETDRS visual acuity 40 letters or better in the test eye
- Early AMD in the study eye
- nAMD in the fellow eye, within a month of 3rd Ranibizumab injection (trial only)
- Willing to adhere to allocated treatment for duration of trial

Exclusion criteria

- Ocular pathology other than macular disease
- Significant systemic disease or medication known to affect visual function
- Systemic disease that would compromise participation in a 1 year study (trial

only)

- Insufficient English language comprehension
- Cognitive impairment as determined using an abridged Mini Mental State Examination (MMSE) [7]
- Oxygen mask worn at night

Suspension criteria for the Trial

- Participant wishes to discontinue the study
- Serious adverse events (e.g. conversion of nAMD in the test eye) or unexpected changes in clinical status

Interventions

Participants allocated to the treatment group will be given a 12 weekly disposable light mask (Polyphotonix Medical, UK) that presents organic light emitting diode (OLED) illumination (peak output 502 nm) to both eyes, overnight, for 12 weeks. Light masks will be replaced every 12 weeks at the participant's routine appointment at the nAMD clinic so that the total duration of mask usage is 12 months.

The mask provides a luminance of 75 photopic cd/m^2. When adjusted for the spectral sensitivity of rod photoreceptors, this equates to 186 scotopic cd/m^2 [35]. Light transmission by the human eyelid has been found to range between 0.3%-2% for light in the region of 500-505nm [36-38]. Under these conditions, pupil diameter in people in the age group 60-85 years is approximately 4mm [39]. This will result in a retinal illuminance in the order of 23 scotopic Td (assuming an eyelid transmission of 1%).

The masks will be pre-programmed to function only between specific hours i.e. 8pm to 8am, to prevent misuse. Outside of these hours they will not illuminate if worn. The mask is activated when a touch sensor on the device is gently covered with a finger for

3 seconds. It will deactivate if not worn continuously for the first 15 minutes, and after that, the light will remain on for the remainder of the 8 hour period.

Treatment acceptability will be evaluated during a monthly interview with the study investigator. Compliance data will be obtained at the monthly visit from the treatment group i) through evaluation of a diary of mask usage, ii) objectively through data collected on a chip in the mask itself (based on a sensor which logs when the mask is in contact with the face). This provides precise data on the hours the mask is worn each night by each participant. As each mask is programmed with the unique participant identification code, compliance data stored on-chip will be non-identifiable except via the password protected electronic database.

The current management of patients with early AMD involves advising on lifestyle factors, such as stopping smoking and improving diet. The only other intervention which is based on evidence from a robust RCT is the provision of a nutritional supplement consisting of high dose antioxidants plus zinc. This AREDS formula (vitamin C, 500 mg; vitamin E, 400 IU; beta carotene, 15 mg and zinc, 80 mg) has been shown to reduce risk of progression from early to advanced AMD by around 20% over 5 years in people with specific features of AMD [40]. However, a recent systematic review by the Cochrane Collaboration indicated that there may be an increased risk of mortality in individuals taking vitamin E and beta carotene supplementation [41]. As this is a recently published document, it is not reflected in the current guidelines for the management of AMD. For this reason, the low level light therapy will be compared to a no-treatment control, rather than to the AREDS formula as the best current intervention.

Participants in both groups will receive routine ophthalmological care for the eye with nAMD (i.e. Ranibizumab injections). If the eye with early AMD converts to nAMD,

they will proceed to Ranibizumab treatment for this eye also, and will be withdrawn from the study.

Outcome Measures

This study includes two co-primary outcome measures, one reflecting structural status, and one functional status.

i) The proportion of people who show 'disease progression' in the eye with early AMD during the 12 months of the study based on an increase in drusen volume beyond test-retest repeatability limits or a progression to advanced AMD. Software available for the Cirrus Optical Coherence Tomography (OCT) system allows automated assessment of drusen volume. Irrespective of initial drusen volume, approximately 50% of people with AMD show a significant increase in drusen volume over the 12 month study period i.e. beyond test-retest 95% confidence intervals (Yehoshua et al. 2011). Conversion to advanced disease will also be considered to be an indicator of disease progression in this analysis. Data from a trial on a similar group indicates about 10% of people meeting our inclusion criteria will develop advanced AMD within 12 months (Neelam et al. 2009). Hence 60% of participants might be expected to show progression based on increased drusen volume or progression to late AMD. The development of advanced AMD will be determined on the basis of ophthalmologist diagnosis at the monthly follow-up appointments at the nAMD clinic.

ii) The rate of retinal adaptation (time taken for photoreceptors to recover their sensitivity after being exposed to a bright adapting light).

Secondary outcome measures include: the change in drusen volume over the 12 month follow-up period; the number of Ranibizumab retreatments required during the year in the fellow eye with nAMD (assessed through review of medical records at the end of

12 months); changes in visual function including chromatic thresholds, visual acuity and psychophysical 14 Hz flicker thresholds; self-report outcome measures including health related quality-of-life (EQ-5D) and visual function (VFQ-48) [42]; a sleep quality questionnaire (Pittsburgh Sleep Quality Index, PSQI) and a semi structured interview (conducted monthly by interview) to determine intervention acceptability.

To obtain detailed information about the time-course of any therapeutic action, the primary and the first of the secondary outcome measures (based on drusen volume) will be assessed at baseline and then at monthly intervals (using OCT images obtained at the regular nAMD clinic follow up appointments).

Participant Timeline

The study flow diagram (Figure 1) outlines the appointment schedule. In brief, potential participants are identified at their first visit to the nAMD clinic. At the second visit (1 month later), informed consent will be obtained, and screening tests and baseline questionnaires will be carried out. At the third monthly visit, baseline functional tests will be carried out, and participants will be randomly assigned to either the treatment or intervention group. Participants in both intervention groups will attend a short, monthly follow-up appointment following their routine appointment at the nAMD clinic throughout the year. Final outcome data will be collected from control and intervention groups at a 12 month follow up appointment, scheduled to follow a regular visit to the nAMD clinic.

Participants in the cross-sectional baseline study will attend Cardiff University for one visit only.

Recruitment

Sixty participants will be recruited to the trial. Ophthalmologists will identify potential

trial participants who are attending for their first appointment at the nAMD clinic at Bristol Eye Hospital, and will provide them with an information sheet and ask for their permission to be contacted by the study investigators. The potential participants will be contacted at least 2 days after their receipt of the information sheet, and invited to meet the study investigator at their next visit to the nAMD clinic (approximately 1 month later) to discuss the trial, provide consent if they choose to participate, and carry out some basic screening tests. Participants will be informed after this screening visit whether they are eligible to take part in the study. Due to the low number of patients required to participate in the study it is planned for the trial and data collection to take place principally at a single NHS centre i.e. Bristol Eye Hospital. If needed, additional participants will be recruited from supplementary recruitment centres to ensure that targets are met.

Forty control participants and participants with grade 1 AMD (AREDS simplified scale [43] for the baseline cross-sectional analysis will be recruited by local Optometrists in Bristol and Cardiff, from a database of elderly volunteers, from Bristol Eye Hospital, from the list of research volunteers at the Cardiff University Eye Clinic and from staff and students of Cardiff University.

Randomisation

Participants will be stratified according to risk of AMD progression (using the AREDS simplified scale [43]), and randomly allocated to receive either light mask or no intervention in a 1:1 ratio using computer generated random permuted blocks (both groups will continue to receive Ranibizumab injections as required for the fellow eye). The study investigator will be provided with three piles of envelopes by the chief investigator in order to randomise the participant to either the intervention or control

arm of the study. Each pile relates to a different stratum of randomisation i.e. grade 2, 3 or 4 of AMD, according to the AREDS simplified scale. The envelopes in each pile will be numbered, and will contain the randomisation allocation for each participant.

Masking

It is not appropriate in this study to use a sham treatment since a non-illuminated mask may have a physiological effect on the retina and patients would be aware that they weren't perceiving light and so would be unmasked to their intervention group. The study investigator who collects the outcome data will also be providing the masks and instructions on its usage; hence, will not be masked to the intervention group. However, the potential for experimenter bias is limited as the primary outcome measure, disease progression, is an objective measurement carried out by automated computer software. The Ophthalmologists who are seeing the participants for their regular Ranibizumab injections will be masked, which will prevent any bias in their retreatment decisions for the fellow eye.

Data Collection Methods

Screening Visit

Following a discussion of the study, and the obtaining of informed consent, the study investigator will question the participant regarding their ocular and medical history. Retinal photographs will be taken if they have not already been acquired, and repeated if image quality is insufficient to allow evaluation. OCT and fundus photographs will be assessed to check for eligibility. Van Herick angle of drainage will be measured, and media clarity will be assessed for each eye and the lens graded according to the LOCS III grading scale[44]. Visual acuity will be assessed in each eye using the Early

Treatment of Diabetic Retinopathy Study (EDTRS) chart, following a brief refraction, if necessary. An abridged version of the MMSE test will be used to assess for cognitive impairment (5 mins;[7]).

Those still deemed eligible for inclusion in the study will also undertake several questionnaires, completed through verbal interview with the investigator: Visual function (VA LV VFQ-48) [42]; Health related quality-of-life (EQ-5D); Pittsburgh Sleep Quality Index (PSQI) [45]; Smoking history (pack years); Vitamin supplementation; Ethnic origin.

Baseline Assessment

Optical coherence tomography images and fundus photographs obtained during the participant's routine visit to the Ranibizumab clinic will be obtained and analysed to assess drusen volume and AMD grade, according to AREDS simplified scale [43]. If the images are of insufficient quality, additional images will be captured.

EDTRS visual acuity will be assessed in each eye. Chromatic thresholds will be measured for the eye with early AMD using the Colour Assessment and Diagnosis (CAD) test [46] (City Occupational Ltd). Contrast thresholds to a 14 Hz flickering stimulus will be measured for the eye with early AMD using the procedure outlined by [47]. The rate of parafoveal cone dark adaptation will be determined for the eye with early AMD using a psychophysical procedure described previously [48]. Thresholds will be determined using a psychophysical method, based on a '3 down, 1 up' staircase paradigm [48]. A Maxwellian View optical system will be used to light adapt photoreceptors in the central 43.6º of the test eye (the output of a white LED will be modified by a Lee filter, HT015, to provide a retinal illuminance of 5.20 log phot $Td.s^{-1}$, providing a bleach of 85% cone photopigment and 74% rhodopsin). All light levels

fall within the safety guidelines set out in British Standard BS EN 15004-2 (2007). There will be an initial training phase, of around 5 minutes, then the adapting light will be presented, and finally recovery of visual thresholds will be monitored for 25 minutes after exposure to the adapting light.

Those individuals who are assigned to the treatment group will then be given a light mask, and provided with written and oral instructions on its use. There will also be a reprise of the key information provided in the participant information letter about follow-up appointments. Participants will be given written copies to take home of the PSQI questionnaire that will be used in the monthly interview.

Monthly Assessment

The investigator will access the OCT images and medical records of all participants after they have attended the Ranibizumab clinic for each monthly follow up appointment. This will allow measurement of drusen volume on a monthly basis, which will allow the final analysis to include an assessment of the time course of any therapeutic action. Additionally, reviewing medical records will facilitate monitoring of the conversion rate to advanced AMD in the control and intervention groups in the eye with early AMD at baseline, and of Ranibizumab retreatment rates in the eye with nAMD, for adverse event reporting purposes.

Participants in both intervention groups will attend a short, monthly follow-up appointment following their routine Ranibizumab clinic appointment, during which both groups will undertake the PSQI sleep quality questionnaire. In addition, the treatment group will bring their mask along to each monthly visit to allow objective compliance data (nightly hours of use) to be exported from the device, retraining in mask use if required, functionality of the mask to be checked, masks to be replaced

every 12 weeks, and a semi-structured interview to be carried out to determine the acceptability of the intervention. These data will be used to address secondary objectives 2 and 3.

Final 12 month visit

This visit will be the same as the baseline visit with the addition of a final semi-structured interview assessing the acceptability of the intervention, and the questionnaires (PSQI, VA LV VFQ-48, Euroqol).

Baseline cross-sectional study

The 40 participants recruited only to the cross-sectional part of the study will undergo the tests outlined in the baseline assessment visit of the trial.

Statistical Methods

It should be noted that, as a Phase I/IIa proof of concept study, this research is designed to assess the acceptability of this therapy for the participants, and to provide preliminary data to support a larger Phase III randomised controlled trial (RCT) in the future, and so is not powered to detect small effect sizes. In order to maximise retention, all follow up visits will be timed to coincide with scheduled appointments at the nAMD clinic. We will aim to recruit 60 people, which, allowing for 15% dropout through the year, will leave a final cohort of 51. This will be sufficient to detect a 50% reduction in people showing progression at a probability level of 0.2, with a power of 80%, and a change in the time constant of cone adaptation of 1 minute to be detected at a probability level of 0.05, with a power of 80%. The additional 40 participants enrolled into the cross-sectional part of the study will allow a total cohort of n=100 to address secondary aim 4.

Analysis will be carried out on an intention to treat basis. There will be no interim analysis, but conversions to nAMD in the eye with early AMD at baseline, and Ranibizumab retreatments for the fellow eye, will be recorded at each participant visit to the nAMD clinic for safety monitoring purposes.

This trial will primarily be concerned with providing information about the safety of the device in the treatment of AMD, and the magnitude of any treatment effect. On this basis, descriptive statistics will be carried out to summarise the demographic characteristics of the two groups, as well as the proportion of individuals showing disease progression in each group, the magnitude of changes in secondary outcome measures including drusen volume, measures of visual function, and the self-report tests, and the fellow eye retreatment rates.

The primary outcome measure will be the proportion of patients demonstrating disease progression at 12 months. Comparisons will be performed using stratified Mantel-Haenszel tests and presented as Forest plots.

Formal statistical analysis will also include linear regression analysis to investigate changes in drusen volume controlling for intervention arm, baseline drusen volume and patient characteristics (such as age, vitamin supplement intake, and history of smoking). Analysis of covariance (ANCOVA) will be carried out to compare the change in secondary outcome measures (e.g. drusen volume, functional tests, self-report measures) and the Ranibizumab retreatment rates over 12 months between the two intervention arms, controlling for the characteristics listed above. Note that all analysis except for the Ranibizumab retreatment rate pertains to the eye with early AMD. This will address secondary aim 1. To meet our fourth secondary aim, which is to establish the relationship between baseline functional biomarker outcomes and the severity of

AMD, we will carry out a one way analysis of variance (ANOVA) to compare the mean results at baseline between participants with grades of AMD in each group on the AREDS simplified scale. This analysis will take place when the baseline data collection is complete. To assess the ability of the clinical tests to act as prognostic and predictive biomarkers, Receiver Operating Characteristics (ROC) curves will be constructed to plot the sensitivity and specificity of the baseline measures in predicting outcomes within the control and intervention arms, respectively. This will address secondary aims 5 and 6. When the trial is completed, linear regression analysis will be carried out to determine how well the change in the functional measures relate to the change in our primary outcome measure (drusen volume), which is a validated biomarker for disease progression. This will address the seventh secondary aim.

Trial Management

The Chief Investigator has ultimate responsibility for the trial management, assisted by the Trial Management Group. Any important protocol modifications will be communicated to all relevant parties (investigators, research ethics committee, NIHR CRN Portfolio, trial registry, journals, NHS Research and Development, Device Manufacturer, funding body) by the Chief Investigator.

A Trial Steering Committee has been established which will also act as a Data Monitoring Committee. In addition to annual meetings, they will be issued with information about any adverse events throughout the course of the study, so that they can decide whether it is appropriate for the study to be terminated. A 3 monthly newsletter will be issued to all investigators and the steering committee, updating on recruitment and other issues, throughout the trial.

Safety Monitoring

All Adverse Events (AEs) and Serious Adverse Events (SAEs) will be recorded. The chief investigator (AB) will be provided with an update of AEs every month and all SAEs within two working days. This trial does not involve a medicinal product or life-threatening procedure. Hence, the risk of a SAE is low. However, one potential SAE is an increased rate of progression to nAMD in the eye with early AMD at baseline. Although this is at odds with the literature it is not an impossible outcome. Another potential SAE would be an increased rate of recurrence of nAMD in the fellow eye (resulting in increased Ranibizumab retreatment rates). Conversion to nAMD and Ranibizumab retreatment requirement in the fellow eye will be determined by ophthalmologists at the monthly Ranibizumab clinic, and recorded by the study investigator through assessment of medical records after each monthly Ranibizumab appointment.

Wong et al (2008) carried out a meta-analysis of studies which had looked at the progression to choroidal neovascularization in the fellow eye when free of advanced disease at study inception. They reported that the cumulative 1 year incidence of nAMD in the 426 patients enrolled in the 5 studies which evaluated this outcome was 12.2% (CI 1.7%–30.6%). Therefore, we have placed an upper limit on the number of people expected to convert to nAMD per month of; n x (30.6% / 12 months), where n is the number of people in the trial who are using the light therapy light mask.

The chief investigator will assess the nature of the AEs and SAEs for seriousness, causality and expectedness. Following the initial report, follow up data may be requested by the chief investigator. Where the SAE is both related and unexpected the chief investigator will notify the Device Manufacturer, who will notify the MHRA, the National Research Ethics Service North West and the Trial Steering Committee within

15 days of receiving notification of the SAE.

Data Management

Any trial data will be recorded on spreadsheets using the numerical identifier for each patient. This data will be non-identifiable. All paper records will also use the unique numerical identifier, which will be non-identifiable. The only identifiable personal data will be the paper and electronic copies of the patient database. The paper copy will not be transferred between Cardiff and Bristol Eye Hospital, and will be kept in a locked filing cabinet at all times. The electronic database will be stored on a secure, Cardiff University computer drive, which is accessible from Bristol and Cardiff via a password protected connection. The study database will be checked for integrity every month by the chief investigator. At the end of the trial, the data will belong to Cardiff University. At this time, Polyphotonix Medical Ltd (the manufacturer) will have access to the results. Anonymised data will be available for verification at any time by the funding body, the College of Optometrists, on request. Neither the College of Optometrists, nor Polyphotonix Medical Ltd. will influence the data collection or analysis. All data will be kept for 15 years in line with Cardiff University's Research Governance Framework Regulations for clinical research.

Dissemination

A summary of the trial protocol is available to the public through the ISCTRN database. Any interested individuals may contact the Chief Investigator for further information. Results will be published in peer reviewed journals and at International Conferences. The Chief Investigator has ultimate responsibility for the scientific content of any

publications. Dissemination of results to trial participants will take place through a summary of findings newsletter sent at the end of the trial to those individuals who indicate a desire to receive an update. Dissemination to the wider community of people with AMD will take place through publication in the Macular Society's 'Digest' members' magazine, and through presentations at events such as the Macular Society 'Top Doctors' conference. Neither the funding body (the College of Optometrists), the light mask manufacturer (Polyphotonix Medical Ltd), or the Sponsor (Cardiff University) will influence the presentation or the publication of the research.

Ethical Considerations

The study has been approved by the National Research Ethics Service North West, and is registered with the International Standardised Clinical Trials Register. A notice of no objection has been obtained from the Medicines and Healthcare Regulatory Agency (MHRA). The trial will be conducted in adherence with the Declaration of Helsinki and the Good Clinical Practice guidelines. The Chief Investigator and the research team will preserve the confidentiality of participants in accordance with the Data Protection Act 1998.

Audits & inspections

The trial is liable to inspection by the College of Optometrists as the funding organisation. The study may also be liable to inspection and audit by Cardiff University under their remit as Sponsor.

Discussion

In this article, we present a clinical trial protocol to evaluate the effect of low-level night-time light therapy in patients with early AMD. To our knowledge, this is the first

randomised controlled trial of its kind in AMD. This study will provide the foundation for future large-scale clinical trials. With the prediction of longer life expectancy in the future, the prevalence of AMD and its associated social and economic problems will continue to increase unless a treatment is developed that will stop its progression.

Trial status

Patient recruitment to begin 1st April 2014.

List of abbreviations

AMD: Age-Related Macular Degeneration; nAMD: Neovascular Age-Related Macular Degeneration; MHRA: Medicines and Healthcare Regulatory Agency; VEGF: Vascular Endothelial Growth Factor; VA LV VFQ-48: 48-item Veterans Affairs Low Vision Visual Functioning Questionnaire; AREDS: Age-Related Eye Disease Scale

Authors' contributions

CM: design, manuscript writing, final approval of the manuscript; TM: conception and design, critical revision and final approval of manuscript; CB: design, critical revision and final approval of manuscript; AB: conception and design, manuscript writing and final approval of the manuscript. All authors read and approved the final manuscript.

Funding

This trial is funded by a research grant from the College of Optometrists, UK. The device manufacturer, Polyphotonix Medical Ltd, is providing the light masks and technical support for the trial free of charge. Both the College of Optometrists and Polyphotonix have the right to review manuscripts bearing their name before publication, but the Chief Investigator has ultimate authority over the protocol, trial

conduct and content of any publications.

Declarations of Interest

None of the authors have any financial interest in the device, or any other aspect of this trial.

Figure Legend

Figure 1. Study flow diagram showing participant timeline.

References

1. Resnikoff S, Pascolini D, Etya'ale D, Kocur I, Pararajasegaram R, Pokharel GP, Mariotti SP: **Global data on visual impairment in the year 2002**. *Bulletin of the World Health Organization* 2004, **82**:844–851.

2. Bunce C, Xing W, Wormald R: **Causes of blind and partial sight certifications in England and Wales: April 2007-March 2008.** *Eye (London, England)* 2010, **24**:1692–1699.

3. Bhutto I, Lutty G: **Molecular Aspects of Medicine Understanding age-related macular degeneration (AMD): Relationships between the photoreceptor / retinal pigment epithelium / Bruch ' s membrane / choriocapillaris complex**. *Molecular Aspects of Medicine* 2012, **33**:295–317.

4. Access Economics: *Future Sight Loss UK (1): the Economic Impact of Partial Sight and Blindness in the UK Adult Population Full Report Report Prepared for RNIB by Access Economics Pty Limited*. London: RNIB; 2009(July).

5. Cruess AF, Zlateva G, Xu X, Pauleikhoff D, Lotery A, Mones J, Buggage R, Schaefer C, Knight T, Goss TF: **Economic Burden of Bilateral Macular Degeneration Multi-Country Observational Study**. *Pharmacoeconomics* 2008, **26**:57–73.

6. Dargent-Molina P, Favier F, Grandjean H, Baudoin C, Schott AM, Hausherr E,

Meunier PJ, Br e art G: **Fall-related factors and risk of hip fracture: the EPIDOS prospective study.** *Lancet* 1996, **348**:145–149.

7. Margrain TH, Nollett C, Shearn J, Stanford M, Edwards RT, Ryan B, Bunce C, Casten R, Hegel MT, Smith DJ: **The Depression in Visual Impairment Trial (DEPVIT): trial design and protocol.** *BMC Psychiatry* 2012, **12**:57.

8. Feigl B: **Age-related maculopathy - linking aetiology and pathophysiological changes to the ischaemia hypothesis.** *Progress in Retinal and Eye Research* 2009, **28**:63–86.

9. Stefánsson E, Geirsdóttir A, Sigurdsson H: **Metabolic physiology in age related macular degeneration.** *Progress in Retinal and Eye Research* 2011, **30**:72–80.

10. Ciulla TA, Harris A, Martin BJ: **Ocular perfusion and age-related macular degeneration.** *Acta Ophthalmologica Scandinavica* 2001, **79**:108–115.

11. Ciulla TA, Harris A, Kagemann L, Danis RP, Pratt LM, Chung HS, Weinberger D, Garzozi HJ: **Choroidal perfusion perturbations in non-neovascular age related macular degeneration**. *British Journal of Ophthalmology* 2002, **86**:209–213.

12. Feigl B: **Age-related maculopathy in the light of ischaemia.** *Clinical & Experimental Optometry* 2007, **90**:263–271.

13. Metelitsina TI, Grunwald JE, DuPont JC, Ying G-S, Brucker AJ, Dunaief JL: **Foveolar choroidal circulation and choroidal neovascularization in age-related macular degeneration.** *Investigative Ophthalmology & Visual Science* 2008, **49**:358–363.

14. Sarks S, Cherepanoff S, Killingsworth M, Sarks J: **Relationship of Basal laminar deposit and membranous debris to the clinical presentation of early age-related macular degeneration.** *Investigative Ophthalmology & Visual Science* 2007, **48**:968–977.

15. Ciulla TA, Harris A, Chung HS, Danis RP, L K, L M, LM P, Martin BJ: **Colour Doppler Imaging Discloses Reduced Ocular Blood Flow Velocities in Nonexudative Age-related Macular Degeneration**. *American Journal of*

Ophthalmology 1999, **128**:75–80.

16. Ahmed J, Braun RD, Dunn R, Linsenmeier RA: **Oxygen distribution in the macaque retina.** *Investigative Ophthalmology & Visual Science* 1993, **34**:516–521.

17. Wangsa-Wirawan ND, Linsenmeier RA: **Retinal oxygen: fundamental and clinical aspects**. *Archives of Ophthalmology* 2003, **121**:547–557.

18. Hagins WA, Ross PD, Tate RL, Yoshikami S: **Transduction heats in retinal rods: tests of the role of cGMP by pyroelectric calorimetry.** *Proceedings of the National Academy of Sciences of the United States of America* 1989, **86**:1224–1228.

19. Witmer AN, Vrensen GFJM, Van Noorden CJF, Schlingemann RO: **Vascular endothelial growth factors and angiogenesis in eye disease.** *Progress in Retinal and Eye Research* 2003, **22**:1–29.

20. Dunaief JL, Dentchev T, Ying G-S, Milam AH: **The role of apoptosis in age-related macular degeneration.** *Archives of Ophthalmology* 2002, **120**:1435–1442.

21. Karakucuk S, Oner AO, Goktas S, Siki E, Kose O: **Colour vision changes in young subjects acutely exposed to 3,000 m altitude.** *Aviation Space and Environmental Medicine* 2004, **75**:364–366.

22. Connolly DM, Barbur JL, Hosking SL, Moorhead IR: **Mild hypoxia impairs chromatic sensitivity in the mesopic range.** *Investigative Ophthalmology & Visual Science* 2008, **49**:820–827.

23. Vingrys AJ, Garner LF: **The effect of a moderate level of hypoxia on human colour vision.** *Documenta Ophthalmologica* 1987, **66**:171–185.

24. Connolly DM, Hosking SL: **Aviation-related respiratory gas disturbances affect dark adaptation: a reappraisal.** *Vision Research* 2006, **46**:1784–1793.

25. Brinchmann-Hansen O, Myhre K: **The effect of hypoxia upon macular recovery time in normal humans.** *Aviation Space and Environmental Medicine* 1989, **60**:1183–1186.

26. Connolly DM, Hosking SL: **Oxygenation state and mesopic sensitivity to**

dynamic contrast stimuli. *Optometry and Vision Science* 2009, **86**:1368–1375.

27. Tinjust D, Kergoat s, Lovasik JV: **Neuroretinal function during mild systemic hypoxia.** *Aviation Space and Environmental Medicine* 2002, **73**:1189–1194.

28. Feigl B, Stewart IB, Brown B, Zele AJ: **Local neuroretinal function during acute hypoxia in healthy older people.** *Investigative Ophthalmology & Visual Science* 2008, **49**:807–813.

29. Pavlidis M, Stupp T, Georgalas I, Georgiadou E, Moschos M, Thanos S: *Multifocal Electroretinography Changes in the Macula at High Altitude: a Report of Three Cases. Volume 219*; 2005:404–412.

30. Chen JC, Firzke FW, Pauleikhoff D, Bird AC: **Functional Loss in Age-Related Bruch' s Membrane Change With Choroidal Perfusion Defect**. *Investigative Ophthalmology & Visual Science* 1992, **33**:334–340.

31. Remulla JF, Gaudio AR, Miller S, Sandberg MA: **Foveal electroretinograms and choroidal perfusion characteristics in fellow eyes of patients with unilateral neovascular age-related macular degeneration.** *The British Journal of Ophthalmology* 1995, **79**:558–561.

32. Arden GB: **The absence of diabetic retinopathy in patients with retinitis pigmentosa: implications for pathophysiology and possible treatment.** *The British Journal of Ophthalmology* 2001, **85**:366–370.

33. Arden GB, G u nd u z MK, Kurtenbach A, V o lker M, Zrenner E, G u nd u z SB, Kamis U, Ozt u rk BT, Okudan S: **A preliminary trial to determine whether prevention of dark adaptation affects the course of early diabetic retinopathy.** *Eye (London, England)* 2010, **24**:1149–1155.

34. Arden GB, Jyothi S, Hogg CH, Lee YF, Sivaprasad S: **Regression of early diabetic macular oedema is associated with prevention of dark adaptation.** *Eye (London, England)* 2011, **25**:1546–1554.

35. Wyszechki G, Stiles WS: *Colour Science: Concepts and Methods, Quantitative Data and Formulae.* New York: John Wiley; 1982.

36. Moseley MJ, Bayliss SC, Fielder AR: **Light transmission through the human eyelid: in vivo measurement.** *Ophthalmic & Physiological Optics* 1988, **8**:229–230.

37. Robinson J, Bayliss SC, Fielder AR: **Transmission of light across the adult and neonatal eyelid in vivo**. *Vision Research* 1991, **31**:1837-1840.

38. Ando K, Kripke DF: **Light attenuation by the human eyelid.** *Biological Psychiatry* 1996, **39**:22–25.

39. Winn B, Whitaker D, Elliott DB, Phillips NJ: **Factors affecting light-adapted pupil size in normal human subjects.** *Investigative Ophthalmology & Visual Science* 1994, **35**:1132–1137.

40. AREDS: **A Randomized, Placebo-Controlled, Clinical Trial of High-Dose Supplementation with Vitamins C and E, Beta Carotene, and Zinc for Age-Related Macular Degeneration and Vision Loss: AREDS Report No. 8.** *Archives of Ophthalmology* 2001, **119**:1417–1436.

41. Evans JR, Lawrenson JG: **Antioxidant vitamin and mineral supplements for slowing the progression of age-related macular degeneration**. *Cochrane Database of Systematic Reviews* 2012, **11**.

42. Stelmack JA, Szlyk JP, Stelmack TR, Demers-Turco P, Williams RT, Moran D, Massof RW: **Psychometric properties of the Veterans Affairs Low-Vision Visual Functioning Questionnaire.** *Investigative Ophthalmology & Visual Science* 2004, **45**:3919–3928.

43. Ferris FL, Davis MD, Clemons TE: **A simplified severity scale for age-related macular degeneration: AREDS Report No. 18**. *Archives of Ophthalmology* 2005, **123**:1570–1574.

44. Chylack LJ, Wolfe JK, Friend J, Khu PM, Singer DM, McCarthy D, del Carmen J, Rosner B: **Quantitating cataract and nuclear brunescence, the Harvard and LOCS systems**. *Optometry and Vision Science* 1993, **70**:886–895.

45. Buysse DJ, Reynolds CF, Monk TH, Berman SR, Kupfer DJ: **The Pittsburgh Sleep Quality Index: a new instrument for psychiatric practice and research.** *Psychiatry*

Research 1989, **28**:193–213.

46. O'Neill-Biba M, Sivaprasad S, Rodriguez-Carmona M, Wolf JE, Barbur JL: **Loss of chromatic sensitivity in AMD and diabetes: a comparative study**. *Ophthalmic and Physiological Optics* 2010, **30**:705–716.

47. Dimitrov PN, Robman LD, Varsamidis M, Aung K-Z, Makeyeva GA, Guymer RH, Vingrys AJ: **Visual function tests as potential biomarkers in age-related macular degeneration.** *Investigative Ophthalmology & Visual Science* 2011, **52**:9457–9469.

48. Gaffney AJ, Binns AM, Margrain TH: **The topography of cone mediated dark adaptation in age-related maculopathy**. *Optometry and Vision Science* 2011, **88**:1080–1087.